Evaluation de la durée de vie des structures en béton armé soumises à la diffusion des ions chlorure

Charbel Aoun

UNIVERSITE CLERMONT AUVERGNE

ECOLE DOCTORALE

SCIENCES POUR L'INGENIEUR DE CLERMONT-FERRAND

THESE

Présenté par

Charbel R. AOUN

Ingénieur & Msc en Génie Civil

Pour obtenir le grade de :

DOCTEUR D'UNIVERSITE

SPECIALITE : GENIE CIVIL

EVALUATION DE LA DUREE DE VIE DES STRUCTURES EN BETON ARME SOUMISES A LA DIFFUSION DES IONS CHLORURE

Soutenue Publiquement le 18 Décembre, 2019 devant le jury compose de:

PR	ANDRADE Carmen	Rapporteur
PR	DUPRAT Frédéric	Rapporteur
PR	AMZIANE Sofiane	Membre de Jury
DR	BONNET Stéphanie	Membre de Jury
DR	TORRENTI Jean-Michel	Président de Jury
PR	CHATEAUNEUF Alaa	Directeur de thèse

Ecole Doctorale :« Ecole Doctorale des Sciences Pour l'ingénieur »
Formation Doctorale « Mécanique, Génie mécanique, Génie civil, Génie industriel »
Laboratoire d'accueil : Institut Pascal (IP) – Polytech Clermont Ferrand – Université Clermont Auvergne

Table of Contents

Liste des Figures (Version Française)

List of Figures

List des Tableaux (Version Française)

List of Tables

List of Appendices

Tableau des Symboles (Version Française)

Symbole	Définition
D_{28}	Coefficient de diffusion des ions chlorure à 28 jours
w_c	Rapport eau-ciment
D_{SF}	Coefficient de diffusion des ions chlorure du béton à base de ciment et de fumée de silice, en tant que matériau cimentaire
D_{PC}	Coefficient de diffusion des ions chlorure du béton à base de ciment en tant que matériau cimentaire, sans addition d'autre matériau cimentaire
SF	Percentage de fumée de silice remplaçant le ciment
t	Temps
t_{ref}	Temps de référence égal à 28 jours
D_{ref}	Coefficient de diffusion des ions chlorure pris comme référence, à 28 jours et à une température de 293K
m	Indice de décroissance
PC	Contenu de ciment (kg/m^3)
FA	Percentage de cendre volante remplaçant le ciment
SG	Percentage de ciment à base de laitiers remplaçant le ciment
$UFFA$	Percentage de cendre volante ultrafin remplaçant le ciment
MA	Percentage d'addition minéral comme la fumée de silice, cendre volante, et le ciment à base de laitiers
T	Température absolue (K)
U	Energie d'activation du processus de diffusion (35000 J/mol)
R	Constante universelle des gaz parfaits
T_{ref}	Température de référence 293K
D_{ult}	Coefficient de diffusion ultime
t_e	Temps d'hydratation
t_c	Temps de cure du béton
$D(t)$	Coefficient de diffusion au temps t
$D(T)$	Coefficient de diffusion à une température T
D_{FA}	Coefficient de diffusion des ions chlorure du béton fabriqué avec du ciment et du cendre volante, comme matériau cimentaire
D_{UFFA}	Coefficient de diffusion des ions chlorure du béton fabriqué avec du ciment et du cendre volante ultrafin, comme matériau cimentaire.
D_{SG}	Coefficient de diffusion des ions chlorure du béton fabriqué avec du ciment et du ciment à base de laitiers, comme matériau cimentaire
RH	Humidité relative
D	Coefficient de diffusion des ions chlorure dans le béton
D_{H_2O}	Coefficient de diffusion des ions chlorures dans une solution infini égal à 1,6 x10^{-9} m^2/s pour le NaCl et 1,3 x10^{-9} m^2/s pour le CaCl2).
ρ_c	Densité du ciment
ρ_a	Densité des granulats

A	Masse totale des granulats (kg)
g_i	Fraction de volume des granulats dans le béton
D_{paste}	Coefficient de diffusion des ions chlorure dans la pâte cimentaire
D_{agg}	Coefficient de diffusion des ions chlorure dans les granulats
C_f	Concentration des ions Chlorure
h	Humidité relative des pores dans le béton
h_c	L'humidité à laquelle la diffusion de chlorure tombe à son mi-chemin entre le minimum et le maximum. Cette valeur a été démontré expérimentalement égale à 0,75
φ	Le rapport de la diffusivité de surface sur la diffusivité apparente du béton, ce qui est démontré expérimentalement à la gamme entre 0,21 à 0,53.
x_s	L'épaisseur de la zone de surface de l'élément qui varie de 20 mm à 40 mm
c	Concentration de la dissolution des chlorures (libre) dans la solution des pores
c_s	Concentration des chlorures à la surface de béton
D_a	Coefficient de diffusion apparent des chlorures
x	Distance de la surface
D_0	Coefficient de diffusion des chlorures à l'âge t_0'
n	Facteur d'âge, et t_{ex}' est l'âge du béton au début de l'exposition aux chlorures.
t_{ex}'	Age du béton au début de l'exposition aux chlorures.
D_{6m}	Coefficient de diffusion des chlorures mesuré à l'âge de 6 mois en utilisant l'essai de migration rapide du Standard Nordic NT 492
K_{TD}	Facteur de température
c_b	Concentration des chlorures lies
$\frac{\partial c_b}{\partial c}$	Capacité de liaison des ions chlorures
$6m$	Ce terme désigne le temps de 6 mois
T_0	Température dans le laboratoire
W_{gel6m}	Teneur en gel (kg/m$^{3)}$
ε_{6m}	Porosité accessible à l'eau
$p_{dep.}$	Probabilité que la dépassivation se produit
C_{crit}	Teneur en chlorure critique
$C(x, \mathrm{t})$	Teneur en chlorure à une profondeur x et un temps t
a	Enrobage du béton en mm
t_{SL}	Durée de vie en nombres d'années
p_0	Probabilité de défaillance cible
c_0	Concentration initiale des chlorures
$c_{S,\Delta x}$	Concentration des chlorures a une profondeur Δx et au temps t
erf	Fonction d'erreur
k_e	Coefficient de transfert de l'environnement
$D_{RCM,0}$	Coefficient de migration des chlorures

t_0	Temps de référence en année
a	Exposant de vieillissement
k_t	Paramètre de transfert
b_e	Paramètre de régression
T_{real}	Température réelle en Kelvin
Mf	Pourcentage de matières plus fines que 75 microns
Ab	Absorption des granulats (%)
Clf	Pourcentage d'argile et de particules friables
$V_{aggregate}$	Volume de la fraction de granulats dans le béton
$D_{bulk\ cement\ paste}$	Coefficient de diffusion des ions chlorures dans la pâte cimentaire
$(C3A)$	Teneur en aluminate tricalcique
λ	Libre parcours moyen de diffusion de particules
d	Diamètre des ions chlorure
N_A	Nombre d'Avogadro
P	Pression
ξ	Ouverture de la fissure

Table of Symbols

Symbol	Definition
D_{28}	Chloride Diffusion Coefficient at the age of 28 days
D_{ref}	Reference chloride diffusion coefficient
w_c	Water-cement ratio
t	Time
t_{ref}	Reference time for the diffusion coefficient, equal to 28 days
t_e	Hydration time
t_c	Curing time
T_{ref}	Reference temperature for the diffusion coefficient, equal to 293K
$D(t)$	Diffusion coefficient at time *t*
D_{ref}	Diffusion coefficient at time (equal to 28 days in Life-365) and temperature (equal 293K in Life-365)
m	Diffusion decay index, a constant.
$D(T)$	Diffusion coefficient at time t and temperature T
U	Activation energy of the diffusion process (35000 J/mol),
R	Gas constant
T	Absolute temperature (K)
RH	Relative Humidity
D_{ult}	Ultimate Diffusion Coefficient
D_{PC}	Chloride diffusion coefficient of concrete made with cement as cementitious material
D_{SF}	Chloride diffusion coefficient of concrete made with cement and silica fume as cementitious material
D_{UFFA}	Chloride diffusion coefficient of concrete made with cement and ultrafine fly ash as cementitious material
D_{SG}	Chloride diffusion coefficient of concrete made with cement and slag as cementitious material
D_{FA}	Chloride diffusion coefficient of concrete made with cement and fly ash as cementitious material
PC	Cementitious materials content (kg/m^3)
SF	Percentage of Silica fume replacing cement
FA	Percentage of Fly Ash replacing cement
SG	Percentage of Slag replacing cement
UFFA	Percentage of ultra fine fly ash replacing cement
MA	Percentage of mineral addition similar to Fly Ash, Micro Silica, and Slag.
D_{H_2O}	Diffusion coefficient of chloride ion in infinite solution (equal to 1.6 x10^{-9} m^2/s for NaCl and 1.3 x10^{-9} m^2/s for CaCl2).
ρ_c	Specific gravity of cement,
ρ_a	Specific gravity of aggregate,
A	Aggregate content (kg)

g_i	Volume fraction of the aggregate in concrete
D_{paste}	Chloride diffusion in the cement paste, and is
D_{agg}	Chloride diffusion in aggregate.
C_f	Free chloride concentration
h	Relative humidity in the pores and
h_c	Humidity at which the chloride diffusion drops to its halfway between the minimum and the maximum. This value was experimentally demonstrated to be equal to 0.75
φ	Ratio of the surface diffusivity over the bulk diffusivity of concrete, which is experimentally demonstrated to range between 0.21 to 0.53.
x_s	Factor is the thickness of the member's surface zone that ranges from 20 mm to 40 mm
$C_{RCPT,t}$	Rapid Chloride Penetration Test value at an age t
Cem	Cement content
$f'_{c,28}$	Concrete compressive strength at 28 days
D_c	Chloride diffusion coefficient
c	Chloride concentration
erf	Error function
c_0	Initial chloride concentration
c_{max}	Maximum chloride surface concentration
k	Coefficient of linear increase
τ	Factor that accounts for the variation of the chloride diffusion coefficient
c_s	Concentration of the chloride at the exposed concrete surface
D_0	Diffusion coefficient at the concrete age t'_0
n	Age factor
t'_{ex}	Age of concrete at the start of exposure
D_{6m}	Coefficient measured at an age of 6 months using the Nordic Standard Rapid Migration test NT BUILD 492
K_{TD}	Temperature factor for the diffusion coefficient
c_b	Bound chloride
$\frac{\partial c_b}{\partial c}$	Chloride binding capacity
T_0	Temperature in the laboratory condition
W_{gel6m}	Gel content in kg/m^3
ε_{6m}	Water accessible porosity
6m	Term that denotes the time at 6 months
$p_{dep.}$	Probability that depassivation occurs
c_{crit}	Critical chloride content
$c(x,t)$	Chloride content at depth x and time t
t_{SL}	Design service in years
p_0	Target failure probability
k_e	Environmental transfer variable
$D_{RCM,0}$	Chloride migration coefficient
k_t	Transfer parameter

t_0	Reference point of time in years
a	Aging exponent
b_e	Regression variable
T_{real}	Actual temperature
c_i^b	Binded chloride concentration
c_i	Free chloride concentration
z_i	Valence of the ionic species
F	Faraday's constant
w	Moisture capacity
φ	Electrodiffusion coupling
γ_i	Chemical activity
$D_{c,ref}$	Reference chloride diffusion coefficient
$f_1(T)$	Temperature influence function
$f_2(t_e)$	Time of hydration influence function
$f_3(h)$	Relative humidity influence function
$f_4(x)$	Depth influence function
D_p	Predicted chloride diffusion coefficient
V_p	Porosity
S	Surface area
V_p^C	Critical porosity (the porosity at which the pore space is first percolated)
c_f	Free chloride concentration
Q_c	Density of concrete
C_q	Concrete specific heat capacity

Résumé

Le béton est un matériau non-homogène, comprenant des granulats, un liant et des pores. Au cours des premières années de sa durée de service, le béton n'a pas besoin de maintenance particulière ; ceci ne sera plus le cas avec le vieillissement. Au cours du temps, de nombreuses substances transportées à travers le béton contribuent à sa détérioration, qui peut être d'origine chimique, physique, électrochimique, ou même couplée. La capacité à laquelle le béton peut résister à cette détérioration est appelée durabilité. Cette propriété est difficile à quantifier ; c'est la raison pour laquelle le terme « durée de vie » vient en lumière. La durée de vie peut être quantifiée en termes d'aptitude en service, plus précisément combien d'années le béton peut remplir sa fonction prévue sans maintenance corrective importante, mais seulement avec une politique de maintenance courante. Plusieurs formes de dégradation définissent la durée de vie des ouvrages en béton armé ; elles comprennent la corrosion des armatures, la dégradation chimico-physique du liant et les dégradations liées aux propriétés des granulats. La corrosion des armatures dans des environnement riches en chlorure est la principale cause de dégradation du béton armé à travers le monde. La corrosion des armatures conduit à une réduction de la section d'acier suivie d'une fissuration progressive, d'écaillage et de perte de capacite portante.

Plusieurs modèles existent pour décrire la pénétration des ions chlorure dans le béton. Des différences significatives ont été trouvées dans ces modèles provisionnels. Il est donc important d'étudier la raison de ces différences, qui est attribué aux paramètres d'entrée pris en considération. La littérature sur les paramètres qui influent sur la pénétration des ions chlorure identifie au total une trentaine de paramètres. Le nombre de paramètres qui ne sont pas pris en compte dans les modèles actuels est important. Ce qui explique les différences considérables dans les valeurs de la durée de service donnée par les différents modèles. L'objectif de cette thèse est d'atteindre un modèle plus complet de la diffusion des ions chlorure dans le béton en considérant divers paramètres affectants. Les paramètres sont mis en évidence par la littérature et confirmés par le programme d'essais à long-terme. Afin d'aboutir à ce modèle, une campagne d'essais à grande échelle a été conçue et réalisée. Le nombre total d'essais de laboratoire nécessaires pour cette étude et établir le modèle complet est égal à 2221 essais, avec un total de 39 mélanges de béton.

En terme de résultat final, ce travail aboutit à des conclusions globales concernant les paramètres affectants la durée de vie du béton dans des environnements riches en chlorure, avec des formules empiriques définissant quantitativement leurs effets. Un modèle complet est développé pour la diffusion des ions chlorure dans le béton est ensuite appliqué numériquement. Ce modèle tient compte des propriétés du béton, de l'environnement, de la mise-en-œuvre et de fissures. Une comparaison entre les modèles existants et le modèle proposé obtenu est également présentée.

Mots clés : Coefficient de diffusion des ions chlorure, corrosion, durabilité, durée de vie, rapport eau-ciment, granulats, Aluminate Tricalcique, dégrée de compactage, temps de gâchage, fissures, ciment, ciment a base de laitier, cendre volante, fumée de silice.

Abstract

Concrete end-product is a non-homogeneous material including aggregate, binder and pores. During its early service life, concrete needs no repair or maintenance; this will no longer be true with time. Along the time, many substances transported in or out of concrete contribute to its deterioration. The deterioration can be from chemical, physical or electrochemical origins, or even coupled. The rate at which the concrete can withstand this deterioration is called durability. This property is hard to quantify, and this is the reason why another term known a "service life" comes into light. Consequently, durability can be quantified in terms of service live, more specifically how many years the concrete can fulfill its intended use without serious need of maintenance, or either with a given maintenance policy. Several forms of degradation define the concrete service life, these forms include the reinforcement corrosion, chemical/physical paste degradation, and degradation mechanism related to the aggregate properties. Reinforcement Corrosion in chloride environments is responsible of the majority of reinforced concrete degradation across the world. The corrosion of reinforcement leads ultimately to a reduction of the reinforcing steel section followed by a progressive cracking and spalling. The steel corrosion in this environment is initiated as the chloride ions diffuse in concrete and reaches a critical threshold at the vicinity of the steel reinforcement.

Several models exist to describe the ingress of chloride in concrete. Large differences have been found in predictive models. It was thus important to investigate the reason of these differences, that is found attributed to the input parameters originally taken into consideration. A further literature review of the parameters that affect the chloride ingress result in identifying a total of thirty parameters that directly affect this mechanism. They particularly affect the chloride diffusion that is considered as the primary mode of chloride transportation. The number of parameters that are not taken into consideration in the available models is thus significant. This fact explains the root cause of the considerable differences in the service life values given by different models.

The aim of this thesis is to reach a tailored model for chloride diffusion in concrete taking into consideration various affecting parameters. These affecting parameters are demonstrated through the literature review and confirmed by the actual long-term testing program. In order to reach a complete model for chloride diffusion that includes these thirty influencing parameters, a large-scale testing protocol has been designed and carried out. The total number of laboratory tests needed to complete this study and reach the complete model is equal to 2221 tests and a total of 39 concrete mixes. As a final outcome, the present work reaches comprehensive conclusions regarding the parameters affecting the concrete service life in chloride environment, with empirical formulas quantitively defining their effects. A complete updated model for chloride diffusion in concrete is then obtained and applied through a numerical application. This model includes environmental, concrete properties, workmanship, and post-placing parameters, that directly affect the chloride diffusion in concrete. A comparison between the existing models and the obtained complete one is also presented.

Key words: Chloride diffusion coefficient, corrosion, durability, service life, water-cement ratio, cement, aggregate, tricalcium aluminate, consolidation, mixing time, cracks, cementitious materials.

Acknowledgments

I would like to thank first all the jury members for their participation in the thesis defense. The amount of added value, questions, suggestions and comments, have developed furthermore my vision for the thesis' subject. With all the knowledge and skills that I got from the thesis work years, I could benefit additionally for a future development, not only in this subject but also in the different relevant approaches. I want also to appreciate all the efforts that the jury has spent to attend this defense, traveling from Toulouse (France), Spain, and Lebanon. Sparing this time and efforts, in addition to the sincerely profound review/analysis of thesis, have made immensely grateful and indebted. It was a pleasure and a remarkable enlightening sharing this defense with you.

I can't describe enough acknowledgements is this manuscript for my Thesis Supervisor, Professor Chateauneuf Alaa, for being the extraordinary advisor/supervisor that he is. First for showing me a dimension in sincere tutoring and teaching that I didn't know existed, for all the patience he showed during these years, for all the heartily review and thorough comments on the work, and for all the dedication that he had for the successful completion of the subject. I also thank him for teaching me how to be a good autonomous researcher and for all the technical skills I learned from him during these years. Working with him was a lifechanging experience in technical, academic, and professional aspects.

This thesis wasn't possible without the personal encouragement of Mr. Khaled W. Awad, Advanced Construction Technology Services (ACTS)'s Founder and Chairman. Believing in me beyond my personal believe, pushing me to the maximum, motivating me, and showing me the right path, were the pillars of the person that I become after this thesis, and the reasons of its success. I want to thank him and ACTS for accepting the finance of this thesis with all its expenses and associated risks. The believe and vision they had for this work were immense and beyond any recognition.

In the end, I want to thank my friends and family for all the support that I got from them, and for selflessly understanding the time that I had to spare for the thesis away from them, missing eventually valuable moments, where they needed me. I can't be grateful enough for having each and everyone of them by my side during these years and on the day of thesis, noting preciously my two Doctors, Dr. Patricia Al Alam, and Dr. Chantal Aoun.

Synthèse des Travaux

1. Introduction

La conception de la durée de vie du béton armé présente l'un des principaux aspects de l'économie et la durabilité des constructions. La conception des structures en béton armé pour une période adéquate permet d'éviter les coûts de réparation précoce ainsi que les coûts fonctionnels associés. Les grands projets d'infrastructure sont conçus et construit pour être entretenus régulièrement, avec un coût total optimisé. Les modèles d'optimisation des coûts de maintenance sont basés sur l'identification adéquate de la durée de vie des ouvrages ; d'où l'importance de la précision de la durée de vie utile.

La définition de la durée de vie prend plusieurs significations en fonction de la nature de la structure et sa fonction. Alors que la durabilité est définie comme une description qualitative de l'aptitude en service du béton, la durée de vie est une durée quantitative, en nombres d'années, pour maintenir certaines caractéristiques du béton. La durée de vie doit prendre en considération les différents processus de dégradation qui peuvent affecter le béton, ainsi que leurs interactions. Compte tenu des différentes dégradations, le calcul de la durée de vie doit inclure les interactions nécessaires de dégradation. Ces mécanismes dépendent de l'environnement et des matériaux constitutifs du béton, dont certains peuvent être pris en compte lors des étapes de conception. Sur cette base, la durée de vie du béton est le plus souvent définie en prenant en compte de deux à trois types de dégradations principaux.

La corrosion des armatures a été largement rapportée dans la littérature au cours des trois dernières décennies comme le principal problème de durabilité du béton. Ce phénomène se produit principalement lorsque la barre d'armature dans le béton est exposée aux chlorures venant, soit des ingrédients du béton, soit de l'environnement. Le coût annuel mondial de la corrosion est estimé à 2,2 milliards de dollars qui représente plus de 3% du Produit Intérieur Brut (PIB) du monde. Le coût total de la corrosion pour l'année 2011 aux Etats-Unis seul a dépassé 1 milliard de dollars, ce qui représente 6,38% du PIB. L'Inde et la Chine ont enregistré des charges similaires, étant 2,4% et 5,2% de leur PIB, respectivement.

Il existe plusieurs modèles pour définir la durée de vie du béton dans un environnement riche en chlorure, vis-à-vis de la corrosion des armatures du béton. Les travaux récents ont conclu la nécessité de développer davantage des modèles de durée de vie des structures en béton armées qui seront plus précis et convenables. Cela est particulièrement vrai pour le béton fissuré comme la plupart des modèles traitent un béton non-fissuré. Cette thèse vise à trouver un nouveau modèle pour la diffusion des chlorures dans le béton prenant en compte des différents paramètres impliqués qui ne sont pas pris dans les modelés existants.

2. Modélisation de la durée de vie du béton dans des environnements riches en chlorure

La corrosion des aciers dans le béton exposé à des environnements riches en chlorure se divise en deux phases : phase d'initiation et phase de propagation. La phase d'initiation correspond au temps nécessaire pour que les ions chlorure se diffusent dans le béton et atteignent un seuil critique au voisinage des armatures. Le seuil critique est le taux de concentration de chlorure au-dessus duquel la corrosion de l'acier commence. La phase de propagation correspond au temps nécessaire pour que les aciers corrodent jusqu'à ce que le moment résistant ne soit plus suffisant. En conséquence, la corrosion de l'acier dans un environnement agressif est fortement dépendante de la vitesse de diffusion des ions chlorure dans le béton.

Trois approches sont disponibles pour définir la durée de vie du béton :

1. Spécifications prescriptives : il s'agit du cas où des limites sont imposés sur la contrainte de compression du béton, le rapport eau-ciment, la teneur en ciment, le type de matériau à base de ciment, et la classe de résistance, pour atteindre une durée de vie spécifique (généralement entre 50 et 100 ans). Dans cette catégorie, la durée de vie est d'abord définie, et les critères pour y parvenir sont ensuite imposées.

2. Méthode performantielle, comprend un total de dix types de tests de laboratoire. Dans cette catégorie, la durée de vie est d'abord définie, et les critères des essaies de performance (résultats d'essais) sont ensuite imposés. Les essais qui sont pertinents pour la pénétration des chlorures sont : l'essai de pénétration rapide de chlorure (RCPT), l'essai de migration de chlorure accéléré, et l'essai du coefficient de diffusion apparent de chlorure. Bien que moins couramment utilisé, sept autres méthodes expérimentales ont été développées pour tester la résistance aux chlorures du béton.

3. Modèles de dégradation : ces modèles simulent les phénomènes de dégradation (mécanismes physiques) en fonction des propriétés du béton et de l'environnement correspondant. La majorité de ces modèles simule la diffusion de chlorures dans le béton et calcule la durée de vie qui en résulte. La durée de vie dans ces modèles est définie comme la durée à la fin de la phase d'initiation décrite précédemment. Dans cette catégorie, l'entrée des modèles se compose des propriétés du béton et de l'environnement tandis que le résultat est la durée de vie de l'ouvrage.

La figure suivante illustre les différents types de conception de la durée de vie.

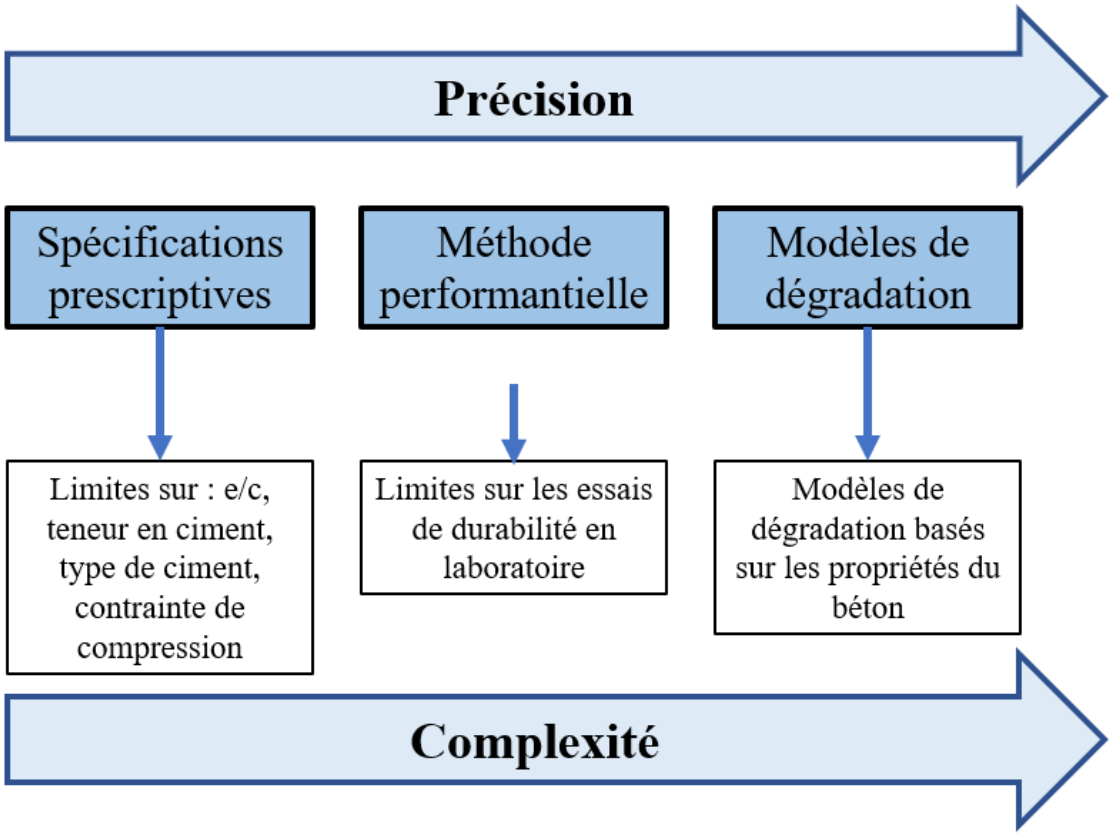

Figure X 1 - Différents types de conception de la durée de vie

Il existe plusieurs modèles pour calculer la diffusion des chlorures en fonction des propriétés du béton. Certains de ces modèles ont été implémentés dans des logiciels commerciaux alors que d'autres ont été développés par de nombreux chercheurs travaillant sur ce sujet.

Quatre grandes catégories de modèles ont été identifiées dans de la littérature :

- Les modèles basés sur la définition du coefficient de diffusion de chlorure en fonction des propriétés du béton. Les principaux modèles dans la revue de la littérature sont résumés dans le tableau 1, dont les symboles sont définis dans le tableau au début du manuscrit.

- Modèle physique utilisé par ClinConc [1,2,3].

- Approche probabiliste utilisée par le modèle DuraCrete [1,4].

- Modèle de pénétration des chlorures basé sur les lois de transport dans les matériaux cimentaires, utilisé par le logiciel STADIUM [1].

Tableau 1 - Principaux modèles du coefficient de diffusion de chlorure

Modèle	Equation
LIFE 365 [1][5]	$D_{28} = 1 \times 10^{(-12,06 + 2,40w_c)}$ $D_{SF} = D_{PC} e^{-0,165SF}$ $D(t) = D_{ref} \left(\frac{t_{ref}}{t}\right)^m$ $m = 0,2 + 0,4(\frac{\%FA}{50} + \frac{\%SG}{70})$ $D(T) = D_{ref}.\exp\left[\frac{U}{R}\left(\frac{1}{T_{ref}} - \frac{1}{T}\right)\right]$
ConcreteWorks [1][6]	$D_{28} = 2,17 \times 10^{-12} \times e^{\frac{w_c}{0,279}}$ $D(t) = D_{28} \times \left(\frac{28}{t}\right)^m + D_{ult} \times \left(1 - \left(\frac{28}{t}\right)^m\right)$ $D_{ult} = D_{28} \times \left(\frac{28}{36500}\right)^m$ $D(t,T) = D(t) \exp\left[\frac{U}{R} \times \left(\frac{1}{T_{ref}} - \frac{1}{T}\right)\right]$ $m = 0,26 + 0,4\left(\frac{FA}{50} + \frac{SG}{70}\right)$ $\frac{D_{UFFA}}{D_{PC}} = 0,170 + 0,829e^{-UFFA/6,07}$ $\frac{D_{SF}}{D_{PC}} = 0,260 + 0,794e^{-SF/2,51}$
4SIGHT [7]	$log_{10}D = 6,0w_c - 13,84$
CHLODIF++ [1][8][9]	$D = D_{w_c} \times f_{int}(SF, SG, FA, SP, Cu, Cr) \times f_{ext}(t, T, RH, W_s, C_s)$ $D_{w_c} = 5 \times 10^{-13} \times e^{4,8708w_c}$ $f_{ext}(t, T, RH, W_s, C_s) = \left(\frac{t_{ref}}{t}\right)^m \times exp\left[\frac{U}{R} \times \left(\frac{1}{T_{ref}} - \frac{1}{T}\right)\right]\left[1 + 256\left(1 - \frac{RH}{100}\right)^4\right]^{-1}$ $m = 0,0075 \times MA(\%) + 0,30$
Hektek [1][10]	$D_{28} = 50000 \times e^{-\sqrt{10/w_c}}$ $(mm^2/year)$
Luciano and Miltenberger [11]	$D_p = (5,760 + 5,810x_1 - 0,567x_2 - 1,323x_3 + 0,740x_4 - 2,117x_5 - 2,780x_6 + 0,254x_7 - 0,368x_8 + 1,071x_1x_4 - 2,891x_1x_6 - 1,503x_4x_6)^2$ (m^2/s) $x_1 = (w_c - 0,45)/0,2;\ x_2 = (PC - 425)/175;\ x_3 = (SF - 5)/5$ $x_4 = (FA - 22,5)/22,5;\ x_5 = (SG - 35)/35;$

	$x_6 = Log10(t_c - 2)/3;\ \ x_7 = (T(℃) - 24)/14$
Riding [12][13][14][15][16][17][18][19][20][21][22]	$D_{28} = 2{,}17 \times 10^{-12} e^{w_c/0{,}279} \qquad (m^2/s)$
Hobbs and Mattew [23]	$D_{28} = 0{,}04 \times 1166 \times w_c \times 10^{-12}$
Sague and Crank [24]	$D_{28} = 3 \times \left(\left(1 + \frac{w_c - 0{,}32}{0{,}09}\right)\left(1 + \frac{446 - 1{,}69PC}{56}\right)\right)$ (in²/year)
Malikakkal [25]	$D_{28} = (82{,}7 - 426 \times w_c + 568{,}4(w_c)^2 + 4{,}26\,(PC/350)^{-6}) \times 10^{-12}$
Papadakis [26]	$D_{ref} = D_{H_2O} \times 0{,}15 \times \frac{1 + \rho_c w_c}{1 + \rho_c w_c + \frac{\rho_c}{\rho_a}\frac{A}{PC}} \left(\frac{\rho_c w_c - 0{,}85}{1 + \rho_c w_c}\right)^3$
Xi and Bazant [27]	$D_{cl} = f_1{}'(w_c, t_c) f_2{}'(g_i) f_3{}'(H) f_4{}'(T) f_5(C_f)$ $f_1{}'(w_c, t_c) = \left(\frac{28 - t_c}{62500}\right) + \left(\frac{1}{4} + \frac{(28 - t_c)}{300}\right)(w_c)^{6{,}55}$ $f_2{}'(g_i) = D_{paste}\left(1 + \frac{g_i}{\frac{[1 - g_i]}{3} + \frac{1}{\left[\left(\frac{D_{agg}}{D_{paste}}\right) - 1\right]}}\right)$ $f_3(h) = \left[1 + \frac{(1-h)^4}{(1-h_c)^4}\right]^{-1}$ $f_4{}'(T) = \exp\left[\frac{U}{R}.\left(\frac{1}{T_{ref}} - \frac{1}{T}\right)\right]$ $f_5{}'(C_f) = 1 - 8{,}333(C_f)^{0.5}$

Ces modèles sont souvent calibrés pour tenir compte de la variation de température, de la maturation du béton, de l'humidité et de la distance de la surface à l'aide des fonctions suivantes :

Tableau 2 - Fonctions de Calibration

Fonction	**Equation**	
Effet de la température [28][29]	$f_{1a}(T) = \exp\left[\frac{U}{R}.\left(\frac{1}{T_{ref}} - \frac{1}{T}\right)\right]$	(X.1)
	$f_{1b}(T) = \frac{T}{T_{ref}} \exp\left[\frac{U}{R}.\left(\frac{1}{T_{ref}} - \frac{1}{T}\right)\right]$	(X.2)

Effet de la maturation du béton [29][30][31]	$f_2(t) = \left[\frac{t_{ref}}{t}\right]^n$ avec $n = 2.5 \times (w_c) - 0.6$	(X.3)
	$f_2(t) = \frac{1}{1-n}\left[\frac{t_{ref}}{t}\right]^n$ avec $n = 2.5 \times (w_c) - 0.6$	(X.4)
	$f_2(t) = \frac{1}{1-n}\left[\left(1+\frac{t_c}{t}\right)^{(1-n)} - \left(\frac{t_c}{t}\right)^{(1-n)}\right]\left[\frac{t_{ref}}{t}\right]^n$ avec $n = 2.5 \times (w_c) - 0.6$	(X.5)
	$f_2(t) = \left[\frac{t_{ref}}{t}\right]^n + \left(\frac{28}{36500}\right)^n \left(1 - \left[\frac{t_{ref}}{t}\right]^n\right)$ avec $n = 2.5 \times (w_c) - 0.6$	(X.6)
	$f_2(t) = \begin{bmatrix} \left(\frac{180}{t}\right)^\beta & for\ t < 180\ days \\ 1 & for\ t > 180\ days \end{bmatrix}$	(X.7)
Effet de l'humidité [32][33]	$f_3(h) = \left[1 + \frac{(1-h)^4}{(1-h_c)^4}\right]^{-1}$	(X.8)
Effet de la variation des propriétés du béton avec la profondeur [29][34]	$f_4(x) = \begin{bmatrix} \varphi + (1-\varphi)\left(\frac{x}{x_s}\right)^\beta & for\ x < x_s \\ 1 & for\ x \geq x_s \end{bmatrix}$	(X.9)

- Modèle ClinConc

ClinConc [1][2][3] est un modèle de diffusion des chlorures dans le béton. Il prend comme entrée, la valeur de la diffusion des chlorures résultant de l'essai de migration rapide à 6 mois (Nordic Standard NT 492). Les autres facteurs sont le potentiel de liaison de chlorures au C3A, le temps et la température. ClinCon repose ainsi sur un essai de durabilité basé sur la performance du béton réalisée à l'âge de 6 mois et donne le coefficient de diffusion des chlorures réel. La principale équation de diffusion de ClinCon est définie comme suit :

$$\frac{c}{c_s} = 1 - \mathrm{erf}\left(\frac{x}{2\sqrt{D_a t}}\right) \quad \text{X.10}$$

où c est la concentration de la dissolution des chlorures (libre) dans la solution des pores, c_s est la concentration des chlorures à la surface de béton, x est la distance, t est la durée d'exposition aux chlorures et D_a est le coefficient de diffusion apparent, donné par :

$$D_a = \frac{D_0}{1-n}\left(\frac{t_0'}{t}\right)^n \left[\left(1+\frac{t_{ex}'}{t}\right)^{1-n} - \left(\frac{t_{ex}'}{t}\right)^{1-n}\right] \quad \text{(X.11)}$$

où D_0 le coefficient de diffusion des chlorures à l'âge t_0', t est la durée d'exposition aux chlorures, n est le facteur d'âge, et t_{ex}' est l'âge du béton au début de l'exposition aux chlorures.

Le facteur d'âge est attribué à l'augmentation de la capacité de liaison des ions chlorures, comme suit :

$$n = -0{,}45a_t^2 + 0{,}66a_t + 0{,}02 \quad \text{(X.12)}$$

où a_t est une constante avec une valeur typique de 0,36, mais peut varier entre 0,1 et 0,6. Le coefficient de diffusion à l'âge t_0' est calculé comme suit :

$$D_0 = \frac{1+0{,}59K_{b6m}}{1+\frac{\partial c_b}{\partial c}} . D_{6m} . k_{TD} \quad \text{(X.13)}$$

où D_{6m} est le coefficient mesuré à l'âge de 6 mois en utilisant l'essai de migration rapide du Standard Nordic NT 492, K_{TD} est le facteur de température, c_b est la concentration des chlorures lié et $\frac{\partial c_b}{\partial c}$ est la capacité de liaison des ions chlorures. Le terme $6m$ désigne le temps de 6 mois. K_{TD} est donné par la formule suivante:

$$K_{TD} = e^{\frac{E}{R}\left(\frac{1}{T_0}-\frac{1}{T}\right)} \quad \text{(X.14)}$$

où E est l'énergie d'activation du coefficient de diffusion, T_0 est la température dans le laboratoire, T est la température d'exposition in-situ, et R est la constante universelle du gaz parfait. K_{b6m} est donné par :

$$K_{b6m} = \frac{W_{gel6m}}{1000\varepsilon_{6m}} \quad \text{(X.15)}$$

où W_{gel6m} est la teneur en gel en kg/m^3 et ε_{6m} est la porosité accessible à l'eau.

Modèle DuraCrete

DuraCrete [1][4] est une méthode d'évaluation de la durabilité fondée sur la deuxième loi de Fick. C'est un modèle de conception de durabilité basée sur la performance probabiliste qui implique des exigences de performance, le niveau de fiabilité, et le temps d'initiation à la corrosion. L'état limite de service, donné par l'équation ci-dessous, doit être satisfait :

$$p_{dep.} = p\{C_{crit} - C(a, t_{SL}) < 0\} < p_0 \quad \text{(X.16)}$$

où $p_{dep.}$ est la probabilité que la dépassivation se produit, C_{crit} est la teneur en chlorure critique [-% / teneur en liant en poids], $C(a, t_{SL})$ est la teneur en chlorure à une profondeur a et un temps t

[-% / teneur en liant en poids], a est l'enrobage du béton en mm, t_{SL} est la durée de vie en nombres d'années, et p_0 est la probabilité de défaillance cible donnée dans le Tableau 3 :

Tableau 3 - probabilité de défaillance - p_0

Class d'exposition – Eurocode 2	Description	Class de fiabilité	SLS	ULS
			Dépassivation	Défaillance
XD	Sel Dégivrant	RC1	0,1	10^{-4}
		RC2	0,1	10^{-5}
		RC3	0,1	10^{-6}
XS	Eau de mer	RC1	0,1	10^{-4}
		RC2	0,1	10^{-5}
		RC3	0,1	10^{-6}

La concentration de chlorure à une profondeur x est donnée au temps t par :

$$c(x,t) = c_0 + \left(c_{S,\Delta x} - c_0\right)[1 - erf\,\frac{a-\Delta x}{2\sqrt{D_a.t}}] \qquad \text{(X.17)}$$

où $c(x,t)$ est la concentration de chlorure dans le béton, c_0 est la concentration initiale des chlorures, $c_{S,\Delta x}$ est la concentration de chlorure a une profondeur Δx et au temps t, Δx est la zone de convection qui est la couche de béton à laquelle le processus de pénétration des ions chlorure diffère de la deuxième loi de diffusion (en mm), erf la fonction d'erreur, t est le temps en nombres d'années, et D_a est le coefficient de diffusion apparent des chlorures en mm^2/an.

Le coefficient de diffusion des chlorures dans DuraCrete est donné par l'équation suivante :

$$D_a = k_e D_{RCM,0} k_t \left(\frac{t_0}{t}\right)^a \qquad \text{(X.18)}$$

où k_e est le coefficient de transfert de l'environnement, $D_{RCM,0}$ est le coefficient de migration des chlorures, k_t est le paramètre de transfert, t est le temps en années, t_0 est le temps de référence en année, et a est l'exposant de vieillissement. Le coefficient environnemental k_e est donnée par :

$$k_e = \exp\left(b_e\left(\frac{1}{T_{ref}} - \frac{1}{T_{real}}\right)\right) \qquad \text{(X.19)}$$

où b_e est le paramètre de régression qui varie entre 3500K et 5500K; il peut être décrit par une distribution normale où la valeur moyenne est de 4800 et l'écart-type est de 700. T_{ref} est la

température de référence de 283K et T_{real} est la température réelle en Kelvin ; T_{real} peut être décrit par une distribution normale avec une moyenne et un écart-type obtenus par les données météorologiques. Le coefficient de migration des chlorures est une variable normale avec un écart-type égal à 0,2 fois la valeur moyenne qui doit être mesuré selon la norme NT 92 (Essai de performance de durabilité).

La variable de transfert k_t est mise à 1 pour la quantification de l'exposant de vieillissement a selon le tableau 4. La variable a est aussi une distribution normale avec des troncatures supérieure et inférieure.

Tableau 4 - Quantification de l'exposant de vieillissement

Type de béton	Exposant de vieillissement a			
	Valeur Moyenne	Ecart-Type	Limite Inferieur	Limite Supérieur
Béton à base de ciment Portland CEM I; 0,4≤w_c≤0,6	0,3	0,12	0,0	1,0
Béton à base de ciment Portland et de la cendre volante f≥0,2.z; k=0,5; 0,4≤w_c≤0,62	0,6	0,15	0,0	1,0
Béton à base de ciment Portland et du ciment à base de laitiers CEM III/B; 0,4≤w_c≤0,6	0,45	0,20	0,0	1,0

3. Comparaison des modèles du coefficient de diffusion des chlorures

Nous avons comparé quinze modèles de calcul de la pénétration des chlorures dans le béton, afin d'identifier les durées de vie correspondantes. A l'exception du modèle de STADIUM, les différents modèles utilisent un coefficient de diffusion de référence et corrigent cette valeur en fonction de la température réelle, de l'humidité, de la maturation et de la profondeur de béton. Le tableau 5 résume les caractéristiques des différents modèles.

Les modèles ont également été classés selon leur nature : empirique, physique, déterministe ou probabiliste. Le tableau 5 montre aussi les écarts dans le choix des paramètres dans les différents modèles. Le rapport eau-ciment est cependant le seul paramètre commun entre ces modèles. En adoptant les mêmes compositions du béton et conditions environnementales, les coefficients de diffusion des chlorures obtenus des différents modèles sont comparés sur la figure X2. Cette figure a été construite en gardant tous les paramètres d'entrée constantes, tout en faisant varier seulement le rapport eau-ciment. Les coefficients de diffusion des chlorures dans cette figure ont été ainsi calculés en fonction du rapport eau-ciment. La teneur en ciment considérée est de 425 kg/m^3.

Tableau 5 - Caractéristiques des modèles de dégradation

Caractéristiques	LIFE 365	ConcreteWorks	4SIGHT	CHLODIF++	ClinConc	Duracrete	HEKTEK	Stadium	Luciano and Miltenberger	Riding	Hobbs and Matthews	Sangue and Crank	Malikakkal	Papadaki et al.	Xi and Basant
Equation basé sur la deuxième loi de Fick	X	X	-	X	X	X	X	-	X	X	X	X	X	X	X
Approche de modélisation empirique	X	X	X	X	-	X	X	-	X	X	X	X	X	X	X
Approche de modélisation physique	-	-	-	-	X	-	-	X	-	-	-	-	-	-	-
Approche de calcul déterministes	X	X	X	X	X	-	X	X	X	X	X	X	X	X	X
Approche de calcul probabiliste	X	-	-	-	-	X	-	-	-	-	-	-	-	-	-
Basée sur le test de performance de durabilité selon la nome NT 492	-	-	-	-	X	X	-	-	-	-	-	-	-	-	-
Effet des adjuvant sur le béton	X	-	-	X	X	X	-	-	-	-	-	-	-	-	-
Effet Porosité	-	-	X	-	X	-	-	X	-	-	-	-	-	-	-
Effet de liaison de chlorure	-	-	-	-	X	-	-	X	-	-	-	-	-	-	X
Effet du rapport eau-ciment	X	X	X	X	X	X	X	Inconnue	X	X	X	X	X	X	X
Effet de la teneur en ciment	-	-	-	-	-	-	-		X	-	-	X	X	X	-
Effet du type du ciment	X	X	-	X	X	X	-		X	-	-	-	-	-	-
Effet de la teneur en granulats	-	-	-	-	-	-	-		-	-	-	-	-	X	X
Effet de la forme des granulats	-	-	-	-	-	-	-		X	-	-	-	-	-	-
Effet des fissures	-	-	X	X	-	-	-	-	-	-	-	-	-	-	-
Effet du type de chlorure	-	-	-	-	-	-	-	Inconnue	-	-	-	-	-	X	-
Effet de la densité du ciment	-	-	-	-	-	-	-		-	-	-	-	-	X	-
Effet de la densité des granulats	-	-	-	-	-	-	-		-	-	-	-	-	X	-
Effet du temps d'arrosage initial du béton	-	-	-	X	-	-	-		X	-	-	-	-	-	X
Effet de la teneur en aluminate tricalcique	-	-	-	X	-	-	-		-	-	-	-	-	-	-

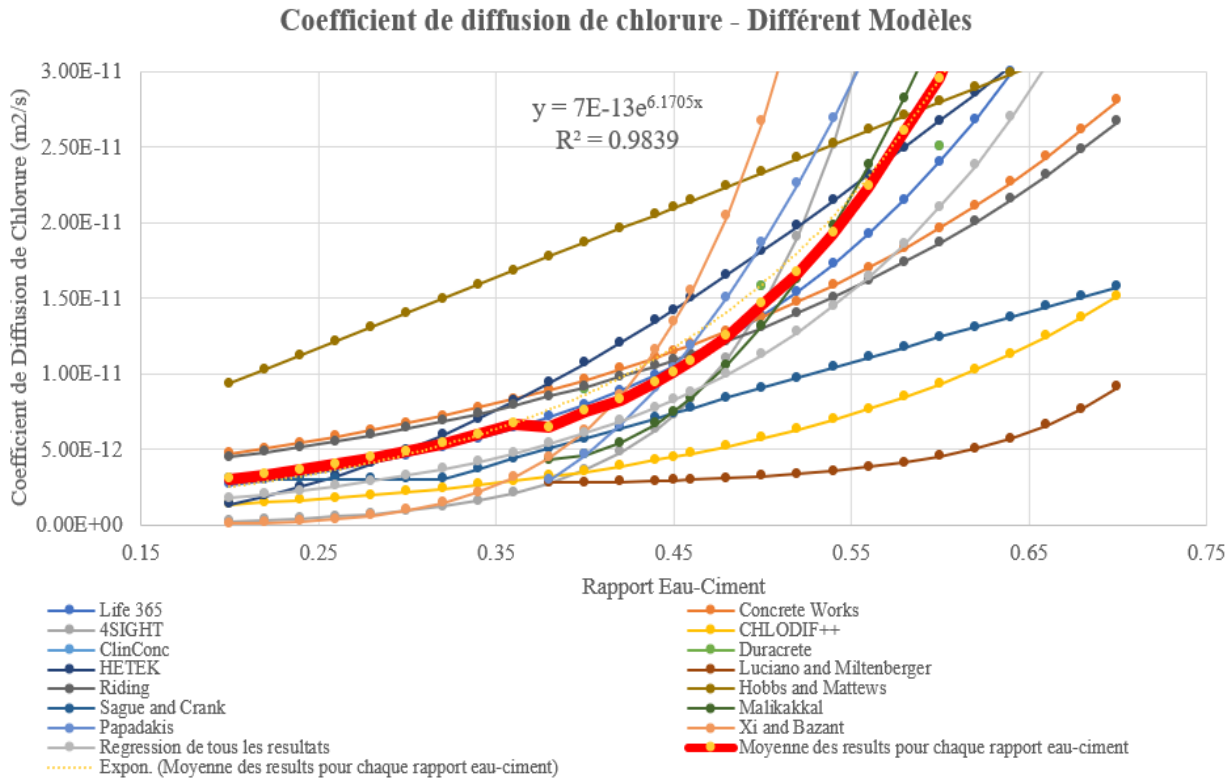

Figure X2 - Coefficient de diffusion de chlorure (différents modèles, teneur en ciment = 425 kg / m3)

Les résultats présentés sur la figure X2 montrent la dispersion des coefficients de diffusion de chlorure calculés par les différents modèles. Cela montre clairement que ce coefficient de diffusion dépend de nombreux paramètres autres que ceux présentés dans chaque modèle. Une analyse de régression pour tous les résultats en fonction du rapport eau-ciment conduit à l'équation suivante :

$$D_c = 5 \times 10^{-13} e^{6{,}2291 w_c} \qquad R^2 = 0{,}570 \tag{X.20}$$

où D_c est le coefficient de diffusion de chlorure et w_c est le rapport eau-ciment.

L'équation X.20 a été obtenue en prenant les valeurs individuelles à chaque niveau du rapport eau-ciment. Dans le même contexte, la valeur moyenne des coefficients de diffusion calculés par les différents modèles à chaque niveau de rapport eau-ciment a été calculée. Ce calcul donne par conséquent une valeur de coefficient de diffusion pour chaque niveau de rapport eau-ciment (moyenne des résultats). Une analyse de régression a ensuite été effectuée et a abouti à la relation suivante :

$$D_c = 7 \times 10^{-13} e^{6{,}1705 w_c} \qquad R^2 = 0{,}984 \tag{X.21}$$

4. Paramètres d'influence supplémentaires à considérer

L'étude des travaux dans la littérature porte sur divers modèles pour identifier le coefficient de diffusion de chlorure dans le béton. Ces travaux ont montré que le coefficient dépend des paramètres suivants :

- Paramètres environnementaux :
    - Température
    - Age du béton
    - Humidité relative
- Propriétés du béton
    - Rapport eau-ciment
    - Teneur en matières cimentaires
    - Pourcentage de matières cimentaires (fumée de silice, cendre volant, cendre volant ultrafin, ciment à base de laitiers)
    - Forme des granulats
    - Volume des granulats
- Paramètres de mise en œuvre
    - Temps de cure

En outre, cette étude bibliographique suggère que d'autres paramètres peuvent avoir une influence sur le coefficient de diffusion des chlorures. Ces paramètres sont décrits dans les paragraphes suivants :

- Propriétés des granulats : les granulats constituent un volume important dans le béton. Leurs propriétés et en particulier leur coefficient de diffusion, peuvent donc avoir une influence significative sur le coefficient de diffusion du béton. Les propriétés a prendre en compte sont la densité, l'absorption, l'abrasion, les matériaux délétères et la granulométrie.

- Teneur en aluminate tricalcique (C3A) : certains types de chlorures réagissent chimiquement avec les composants du ciment, tels que l'aluminate tricalcique pour former le chloroaluminate de calcium, et sont effectivement retirés de la solution dans les pores. Ce type de chlorure est appelé chlorure lié. La présence du C3A dans le ciment semble donc être bénéfique à la réduction de la pénétration de chlorure. L'étude bibliographique indique l'importance de ce paramètre dans notre étude.

- Degré de compactage, temps de gâchage initial et temps de cure initial : Ces trois paramètres sont liés à la mise en œuvre qui affecte directement la qualité du béton. Le degré de compactage peut augmenter ou diminuer la quantité d'air piégé à l'intérieur du béton. Ces pores ont normalement un diamètre supérieur à celui des pores initialement disponibles dans la pâte cimentaire. Leur présence peut donc influer sur la pénétration des ions chlorure. Le temps de gâchage initial peut également modifier la répartition des pores dans le béton. Le temps de cure affecte l'hydratation

du ciment, ce qui modifie la répartition des pores dans la pâte cimentaire et influe sur la diffusion des chlorures dans le béton.

- Ouverture des fissures : les fissures offrent un chemin sans obstacle aux agents agressifs pour s'infiltrer à travers la masse de béton ; ceci est également applicable à la pénétration des ions chlorure. La corrosion des armatures est en général plus sévère et commence plus tôt au droit des fissures et les endroits où l'eau peut pénétrer facilement. Plusieurs normes internationales, codes et directives ont limité l'ouverture des fissures à des valeurs spécifiques selon les conditions environnementales. La quantification de l'effet de l'ouverture des fissures sur le coefficient de diffusion est essentielle pour le calcul de la pénétration des chlorures dans le béton.

5. Approche adoptée

L'approche adoptée dans cette étude consiste à réaliser une campagne d'essais à grand échelle pour identifier les effets et quantifier les paramètres énumérés ci-dessus. Le protocole d'essai dans cette étude a été conçu pour isoler chacun des paramètres à partir d'une formulation de référence, en modifiant un paramètre à la fois. En réalité, les différents paramètres peuvent être liés comme ils caractérisent la même formulation de référence. A partir d'une formulation de référence, nous définissions les séries suivantes :

- Série AGG : cette série vise à identifier l'effet des propriétés des granulats. La formulation de référence a été reproduite en utilisant cinq types de granulats avec des propriétés différentes. Etant donné que le granulat est considéré comme un matériau inerte, l'interdépendance avec d'autres paramètres du béton a été exclue. Le seul paramètre modifié dans les cinq formulations de la série AGG est donc exclusivement le type de granulat. En parallèle, des échantillons pris des roches de granulats ont été collectés pour évaluer le coefficient de diffusion des chlorures dans les granulats.

- Série C3A : cette série vise à identifier l'effet de la teneur en Aluminate Tricalcique. La formulation de référence a été reproduite en utilisant cinq types de ciment avec cinq différentes teneurs en C3A. Selon la littérature, l'indépendance de ce paramètre nous a permis de faire varier le type de ciment seul.

- Série CONS : cette série vise à identifier l'influence du degré de compactage, considéré indépendant des autres propriétés du béton vis-à-vis de la diffusion des ions chlorure. La formulation de référence a été reproduite dans six lots différents, où les échantillons ont été placés dans des moules à l'aide de différents niveaux de vibration du béton.

- Série MIX : cette série vise à identifier l'effet du temps de gâchage initial, considéré indépendant des autres propriétés du béton vis-à-vis de la diffusion des ions chlorure. La formulation de référence a été reproduite dans cinq lots différents où le temps de gâchage a été modifié.

- Série CW : cette série a pour but d'identifier l'effet de l'ouverture des fissures. L'indépendance de l'ouverture des fissures et le rapport eau-ciment par rapport au coefficient de diffusion des chlorure n'est pas évidente. La dépendance de ces deux paramètres a ainsi été étudiée. La

formulation de référence a été reproduite avec cinq rapports eau-ciment. Pour chaque rapport eau-ciment, cinq ouvertures de fissure ont été intentionnellement créées dans le béton. Cette série a conduit à 25 combinaisons d'ouverture de fissure et de rapports eau-ciment.

En résumé, un total de 46 mélanges de béton a été réalisé aux laboratoires de Advanced Construction Technology Services (ACTS) situés à Jeddah en Arabie Saoudite selon le schéma de dépendance illustrée sur la figure X3 ci-dessous.

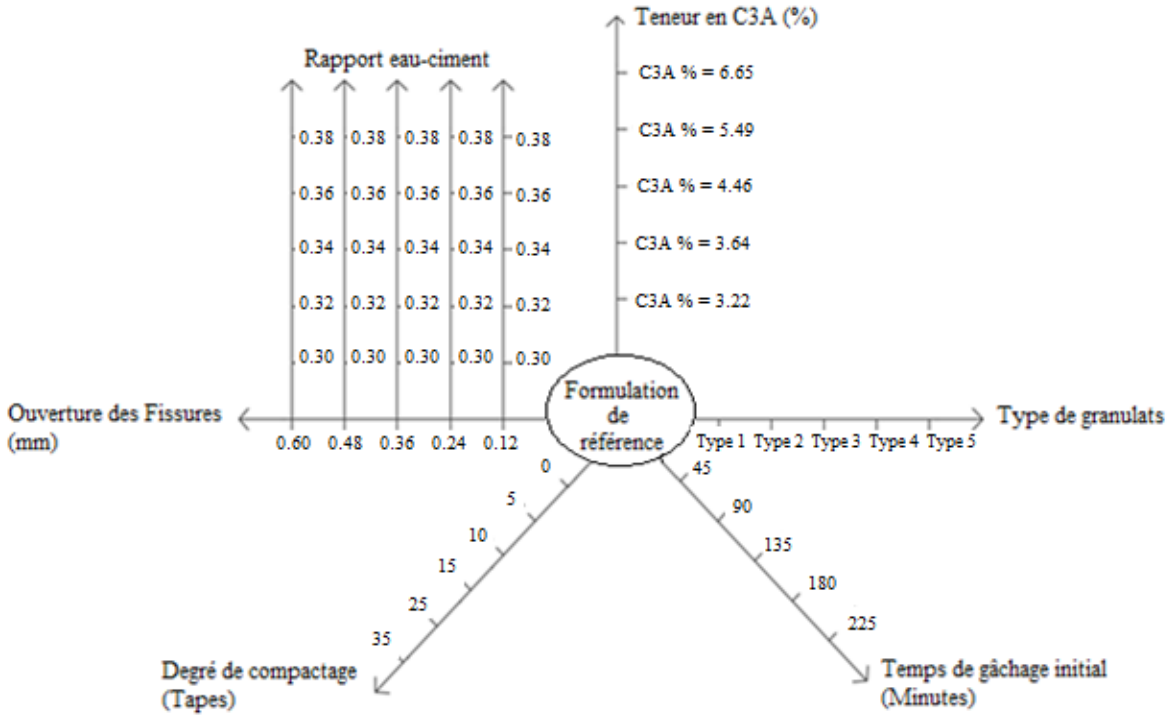

Figure X 3 - Illustration de la campagne expérimentale

Des éprouvettes de béton cylindriques standards ont été préparées selon la norme ASTM C31 / 31M pour chaque formulation. Le diamètre et la longueur de l'éprouvette sont de 150 mm et 300 mm respectivement. Les éprouvettes cylindriques ont été démoulées 24 heures après leur confection. Ces éprouvettes ont ensuite été placés dans un réservoir d'eau pendant 28 jours. Après la période de durcissement, des carottes avec un diamètre de 94 mm ont été forées dans l'éprouvette cylindrique afin d'éviter les effets de bord. Les carottes ont été nettoyés dans l'eau avec une brosse de nylon rigide, puis sécher pendant 24 heures à une température de 23 degrés et une humidité relative de 50%. Les échantillons ont été ensuite scellés de tous les côtés, avec un kit de silicium résistant à l'eau a l'exception de la surface supérieure.

Les échantillons ont été ensuite saturés avec de l'hydroxyde de calcium en utilisant une chambre à vide. Après 48 heures, les éprouvettes ont été retirées du vide et placées dans la solution de NaCl pour l'essai de diffusion de chlorure. La concentration de NaCl est de 165 g/l. Toutes les boîtes (contenant les solutions et les échantillons) sont stockées dans des salles à une température de

23^{O}C. Les échantillons ont été immergés dans la solution de NaCl pendant la durée spécifiée dans chaque essai. À la fin de la période d'immersion, les échantillons ont été retirés de la solution, rincés avec de l'eau et laissés sécher pendant 24 heures. Après séchage des éprouvettes, le coefficient de diffusion de chlorure est mesuré en utilisant les directives fournies dans la norme ASTM C1556 : Méthode d'essai standard pour déterminer le coefficient de diffusion de chlorure apparent.

6. Effet des propriétés des granulats

Plusieurs études dans la littérature ont étudié le rôle des granulats vis-à-vis du coefficient de diffusion des chlorures. Certains travaux ont considéré la loi des mélanges pour définir le coefficient de diffusion du béton à partir de ceux des granulats et de la pâte cimentaire. Certains travaux ont montré que la diffusion augmente proportionnellement à la teneur en granulats (en particulier entre 35% et 60%) en raison de l'augmentation de la diffusivité apparente (interconnexion de la zone de transition interfaciale ITZ) du béton : l'inclusion de granulats provoque la formation d'une ITZ autour des agrégats, ce qui est la principale voie de diffusion des chlorures. Zheng et al. [35] ont modélisé le béton en tant que trois matériaux : l'agrégat, l'ITZ et la pâte cimentaire, avec des coefficients de diffusion correspondants. Par rapport à la pâte cimentaire, les granulats sont considérés comme très dense et par conséquent le transport des chlorures dans l'agrégat peut être négligé. Ceci est en accord avec les travaux effectués par Zheng et al. qui considèrent l'ensemble comme formant un obstacle au mouvement des ions chlorure. Une étude récente par Titi et Tabatabai [36] a montré l'effet des granulats sur la résistance du béton aux ions de chlorure en reproduisant la même formulation avec 12 types de granulats selon l'essai de pénétration rapide des chlorures, à différents âges du béton. Les résultats de cette étude ont conduit aux conclusions suivantes :

- Variation significative des résultats d'essais de résistance aux chlorures pour les différents échantillons fabriqués avec différents types de granulats.

- Forte dépendance de la résistance mesurée par l'essai de pénétration rapide des ions chlorures, en fonction du type de granulats.

Ces constats suggèrent que, non seulement les granulats participent eux-mêmes à la diffusion des chlorures, mais aussi la zone de transition interfaciale entre les granulats et la pâte cimentaire joue un rôle important dans la diffusion. Ainsi ces trois paramètres doivent être étudiés de manière simultanée pour une représentation précise du rôle des granulats dans la diffusion.

Les propriétés des granulats utilisés dans la série AGG sont indiquées dans les tableaux 6 et 7, la formulation du béton de référence est indiquée dans le tableau 8 et les résultats des coefficients de diffusion correspondant sont illustrés sur la figure X4.

Tableau 6 - Propriétés des granulats

Résultats d'essaies											
Carrières d' extraction	Matériaux plus petits que 75 microns (%)	Densité à sec (kg / m^3)	Densité à surface saturée (kg / m^3)	Densité apparente (kg/m^3)	Absorption d' eau (%)	Pourcentage de morceaux d' argile et du particules friables (%)	Effritement (%)	Elongation (%)	Abrasion du type Los Angeles (500 Rev.) (%)	Solidité (%)	Eléments légers (%)
Bin Laheej	0,50	2660	2670	2700	0,50	0,10	28,00	21,00	22,90	1,80	0,00
Madinah	0,40	2800	2820	2880	1,00	0,30	13,00	18,00	12,20	5,60	0,00
Stevin Rock - Ghail	0,20	2700	2720	2750	0,60	0,10	16,00	21,00	20,80	3,10	0,00
Gabro	1,10	2820	2840	2890	0,80	0,20	20,00	26,00	16,50	4,10	0,00
Makah	0,20	2950	2960	2990	0,40	0,20	16,00	20,00	12,40	6,20	0,00

Tableau 7 - Analyse granulométrique des granulats

Analyse Granulométrique – pourcentage passant						
Diamètre d'ouverture	Numéro du tamis	Bin Laheej	Madinah	Stevin Rock - Ghail	Gabro	Makah
9,50 mm	3/8"	93,20	98,30	92,10	94,50	97,70
4,75 mm	No 4	10,10	25,20	8,30	24,00	27,60
2,36 mm	No 8	0,70	1,40	0,50	1,50	0,60
1,18 mm	No 16	0,60	0,70	0,40	1,30	0,40
0,075 mm	No 200	0,50	0,40	0,20	1,10	0,20

Tableau 8 - Formulation du béton

Ingrédients	Mass (kg)
Ciment (Type I)	400
Fumée de silice (ELKEM)	25
Eau	161,5
Granulats	1000
Granulats fin (sable)	865
Adjuvant	4

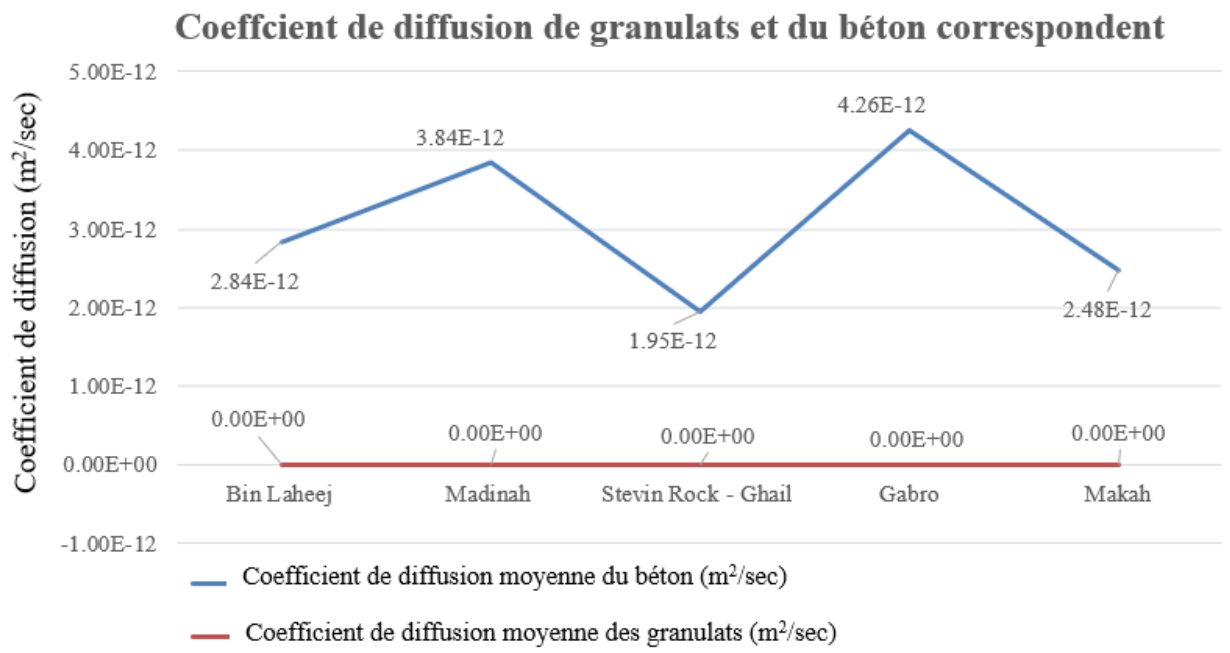

Figure X 4 - Coefficient de diffusion de granulats et du béton correspondent

Au niveau de la structure, les ions chlorure se diffusent dans le béton à travers trois volumes : les granulats, le volume de la pâte cimentaire, et la zone de transition interfaciale entre les granulats et la pâte cimentaire. La porosité de la zone entourant les granulats (ITZ) est plus élevée et plus faible en teneur de ciment par rapport aux zones de la pâte cimentaire plus éloigné. La campagne d'essais réalisée dans cette série vise à déterminer l'effet des propriétés des granulats sur le coefficient de diffusion des chlorures et sur la concentration en surface des chlorures. Cette compagne d'essais montre que plusieurs paramètres, autre que la présence des trois volumes de diffusion, affectent la diffusion des ions chlorure dans le béton. Ce fait indique la nécessité de mettre à jour le modèle des trois phases de diffusion des chlorures. Nous avons ainsi proposé de définir cinq zones de diffusion. Deux zones ont été ajoutées : la première comprend les impuretés

en faibles qualités dans les granulats qui ont tendance à avoir un impact significatif. Ces impuretés sont quantifiées par la quantité d'argile et de particules friables des granulats. La seconde affecte le transport de chlorure dans le béton et inclut l'état de surface de ces granulats. Ce paramètre peut être quantifié par l'absorption d'eau en plus de la quantité de matières fines en dessous de 75 micromètres agrippées sur la surface des granulats. L'absorption d'eau est identifiée en tant que paramètre qui contribue à des conditions de surface en considérant que, seuls les pores qui sont ouverts à la surface peuvent absorber l'eau. Les cinq zones de diffusion de chlorures dans le béton, permettant de considérer l'effet des granulats, sont ainsi illustrés sur la figure X5.

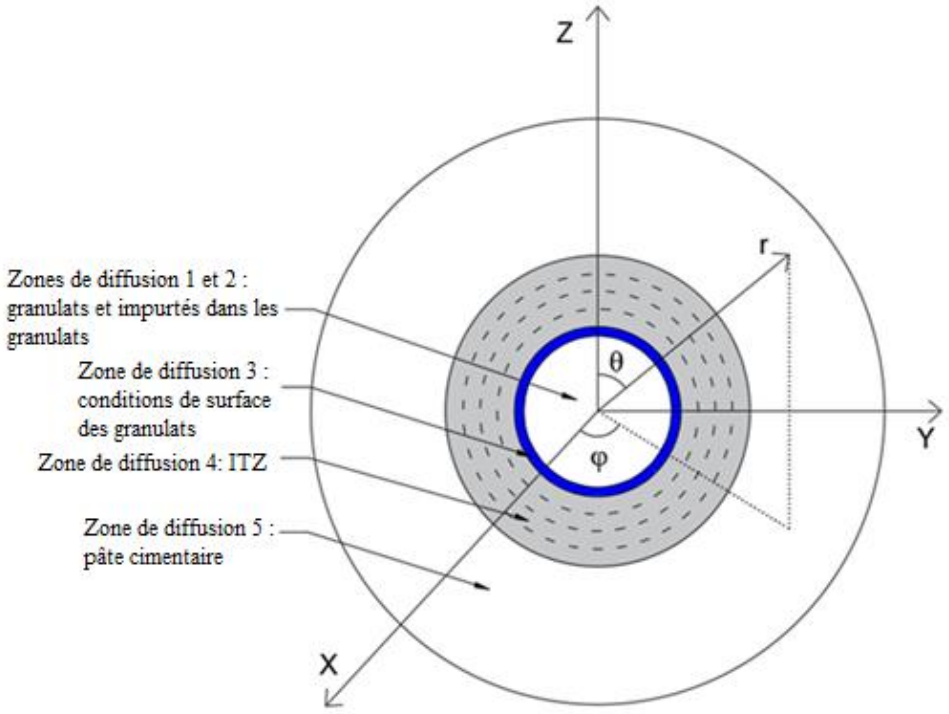

Figure X5 - Modèle de Volume de Diffusion suggéré

Une méthode numérique a été développée pour l'évaluation du coefficient de diffusion dans les cinq zones :

- Etape 1 : Identification du volume et le poids totaux des différents constituants tel que défini dans la formulation du béton.

- Etape 2 : Identification de la granulométrie des granulats selon la norme ASTM C136, pour une représentation précise.

- Etape 3 : Identification du coefficient de diffusion des granulats qui est démontré comme étant égale à zéro dans la gamme de propriétés mesurées.

- Etape 4 : Définition de l'épaisseur ITZ (ou mesurée à travers SEM).

- Etape 5 : Calcul du volume total de l'ITZ et la pâte cimentaire à partir de la largeur ITZ et la distribution granulométrique des granulats

- Etape 6 : calcul de la distribution des particules de ciment dans l'ITZ et la pâte cimentaire, en plus du rapport eau-ciment en fonction de la distance de la surface des granulats.

- Etape 7 : Simulation d'un modèle d'hydratation afin de déterminer le degré d'hydratation en fonction de la distance de la surface des granulats.

- Etape 8 : Calcul de la fraction volumique de pores capillaires, des pores de gel et des pores totaux en fonction de la distance de la surface des granulats.

- Etape 9 : Calcul de la valeur de diffusion relative en fonction de la porosité et la diffusivité des ions chlorure dans la solution des pores, dans la pâte cimentaire, et l'ITZ.

- Etape 10 : Développement du modèle de diffusion pour obtenir une diffusion du béton en fonction de la diffusion des granulats, la diffusion dans l'ITZ, la diffusion dans la pâte cimentaire, les propriétés de surface des granulats, et le pourcentage d'argile et de particules friables.

L'équation générale du coefficient de diffusion des chlorures dans le béton en fonction des propriétés des granulats est obtenue par :

$$D_c = (1{,}7258Mf + 0{,}0963Ab + 3{,}9165Clf + 1) \times \frac{\left(1 - V_{aggregate}\right) D_{bulk\ cement\ paste}}{\left[0{,}6265\left[\frac{1}{\sum_{i=1}^{i=n} V_i A_i}\right] + \left(0{,}3735\left[\sum_{i=1}^{i=n} \frac{V_i}{A_i}\right]\right)\right]} \quad \text{(X.22)}$$

où Mf est le pourcentage de matières plus fines que 75 microns, Ab est l'absorption des granulats (%), Clf est le pourcentage d'argile et de particules friables, $V_{aggregate}$ est la fraction volumique de granulats dans le béton, $D_{bulk\ cement\ paste}$ est le coefficient de diffusion des ions chlorure dans la pâte cimentaire, et les fonctions $\sum_{i=1}^{i=n} V_i A_i$ et $\left[\sum_{i=1}^{i=n} \frac{V_i}{A_i}\right]$ sont calculées à selon les procédures décrites dans ce manuscrit.

La fonction qui décrit l'effet des granulats sur le coefficient de diffusion des chlorures obtenue par :

$$f(Granulats) = (1{,}7258Mf + 0{,}0963Ab + 3{,}9165Clf + 1) \times \frac{\left(1 - V_{aggregate}\right)}{\left[0{,}6265\left[\frac{1}{\sum_{i=1}^{i=n} V_i A_i}\right] + \left(0{,}3735\left[\sum_{i=1}^{i=n} \frac{V_i}{A_i}\right]\right)\right]} \quad \text{(X.23)}$$

7. Effet de la teneur en Aluminate Tricalcique

L'aluminate tricalcique réagit avec les chlorures pour produire le chloroaluminate. Le rôle de l'aluminate tricalcique dans le mécanisme de diffusion des chlorures a été largement discuté dans la littérature. Rasheeduzzafar et al. [37] ont montré que le temps de corrosion, ainsi que la quantité de chlorures lié, sont directement proportionnels à la teneur en aluminate tricalcique comme illustré dans le tableau 9. Cette publication montre en outre que, en l'absence d'aluminate tricalcique, la formation de chloroaluminate de calcium est absente.

Tableau 9 - Effet de la teneur en Aluminate Tricalcique sur le temps de corrosion et le taux de chlorure liés

Teneur en C3A (%)	Temps de commencement de la corrosion (années)	Pourcentage de chlorure non-liés (libre) en termes de concentration	Pourcentage de chlorure liés en termes de concentration
2	93	86%	14%
9	163	58%	42%
11	180	51%	49%
14	228	33%	67%
Temps de corrosion = 1088,5 x (Teneur en C3A) + 68,038			(R^2 = 0,9854)
Pourcentage de Chlorure libre = -4,2949 x (Teneur en C3A) + 0,9565			(R^2 = 0,9895)
Pourcentage de chlorure liés = 4,2949 x (Teneur en C3A) + 0,9565			(R^2 = 0,9895)

Dans le même contexte, Glass et Buenfled [38] ont conclu que la liaison des chlorures avec l'aluminate tricalcique réduit la concentration en chlorure libre et donc la quantité de chlorure mobile partout dans le béton. Cependant, il maintient des gradients de concentration plus élevées pendant des périodes plus longues dans la zone proche de la surface, augmentant ainsi la vitesse moyenne et la quantité des ions chlorure introduits dans le béton par diffusion. L'effet total est une augmentation de la teneur totale en chlorure (lié et libre) près de la surface et une diminution de la teneur totale en chlorure en profondeur. Le travail de Sang-Hun Han [39] conduit à des conclusions similaires : plus la teneur en C3A augmente, plus la concentration totale en ions chlorure augmente à la surface. La différence de concentration totale en ions chlorure diminue avec la profondeur. De nombreux autres travaux ont conclu que la liaison de chlorure avec l'aluminate tricalcique enlève les ions chlorure de la solution des pores et ralentit le taux de pénétration. L'étude menée par Paul Sandberg [40] a également démontré que la liaison des chlorures affecte à la fois la vitesse de transport dans le béton et la concentration nécessaire pour amorcer la corrosion active.

Sur la base de ces études de littérature, les conclusions suivantes peuvent être établis :

- la quantité de chlorure liés est directement proportionnelle à la teneur en aluminate tricalcique (C3A) contenu.

- la résistance à la corrosion augmente avec l'augmentation de la teneur en aluminate tricalcique (C3A).

- les profils de chlorure varient avec la teneur en C3A, résultant en une augmentation de la concentration en surface et une diminution de la teneur en chlorure en profondeur. Il est donc clair que la teneur en aluminate tricalcique est l'un des paramètres qui influent sur le coefficient de

diffusion des chlorures. La série C3A comprend cinq mélanges identiques avec different teneurs en aluminate tricalcique. Le coefficient de diffusion des chlorures était ensuite obtenu comme le montre le graph sur la figure X.6.

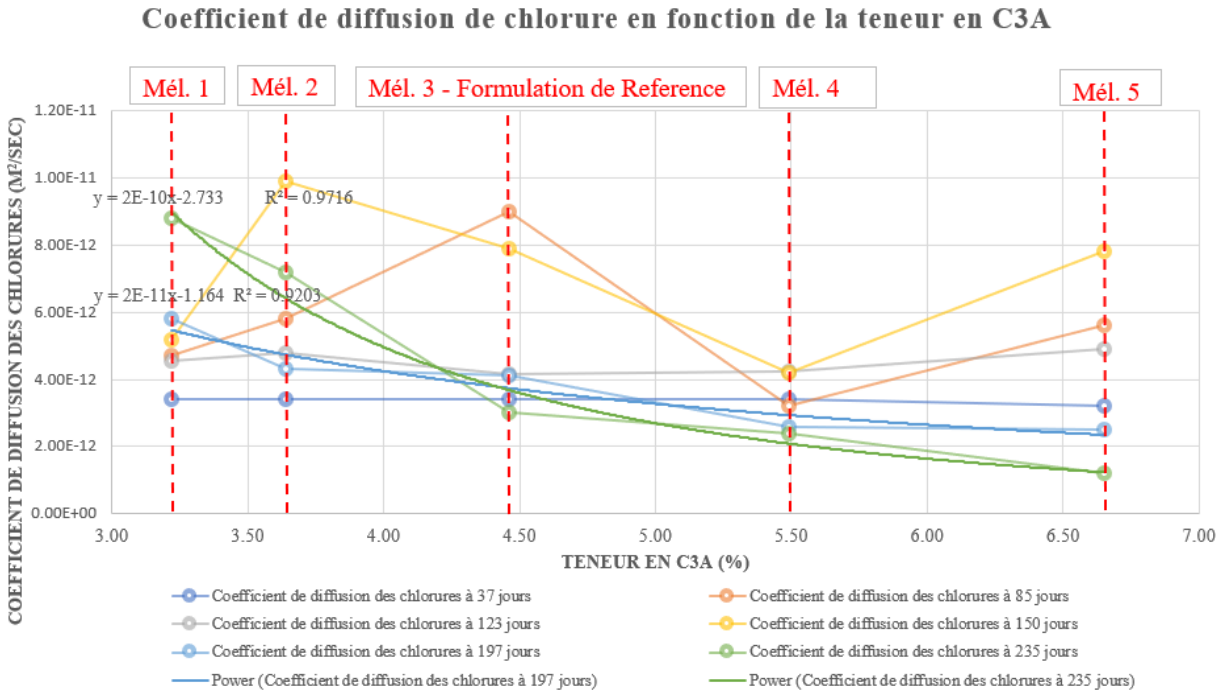

Figure X6 - Coefficient de diffusion des chlorures en fonction de la teneur en C3A

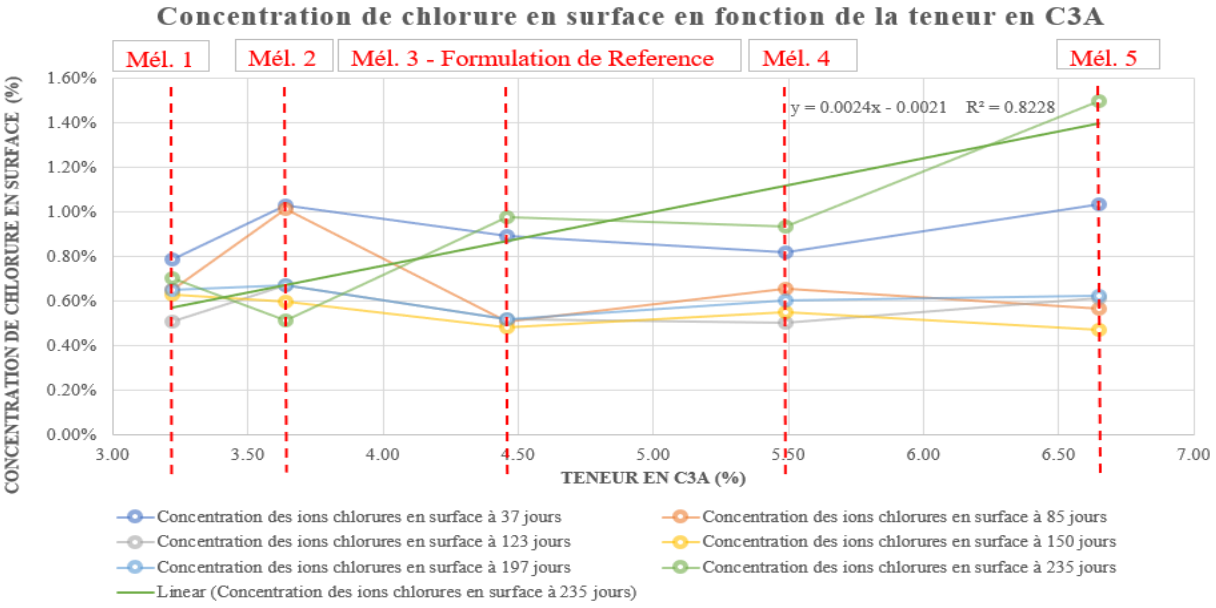

Figure X7 - Concentration des chlorures en surface en fonction de la teneur en C3A

Sur la base de cette étude expérimentale, la fonction traduisant l'effet de la teneur en C3A sur le coefficient de diffusion de chlorure est la suivante :

$$f(C3A) = 26{,}644 \times (C3A)^{-2{,}552} \qquad \text{(X.24)}$$

8. Effet du degré de compactage et du temps de gâchage

Le béton est un matériau poreux, la distribution et la taille des pores affecte de manière significative ses performances, surtout en ce qui concerne la durabilité, y compris le coefficient de diffusion des chlorures. Les sections passées ont conclu que plusieurs facteurs influent le coefficient de diffusion des chlorures. Ces facteurs modifient la distribution des pores et leur taille dans le béton. Plusieurs codes et normes de construction ont souligné l'importance d'un produit final en béton uniforme et bien compacté pour assurer la durabilité attendue du béton. Les pores dans le béton proviennent de plusieurs facteurs et peuvent être divisés en quatre catégories principales :

- les pores capillaires, sont généralement moins de 5-10 μm, sont induits par le rapport eau-ciment, le degré d'hydratation et le type de matériau cimentaire.

- les pores d'air entraînées, causés par l'ajout d'un agent entraîneur d'air, sont plus grands que les vides capillaires mais généralement inférieurs à 1 mm.

- les pores d'air piégées et les pores d'eau sont tous des pores dans le béton qui ont un diamètre supérieur à 1 mm et sont formés en piégeant l'air ou l'eau dans le béton. Les pores d'eau se trouvent généralement dans des mélanges de béton avec un rapport élevé, entre l'eau et les matériaux cimentaires.

La figure ci-dessous illustre la répartition de la taille des pores dans le béton.

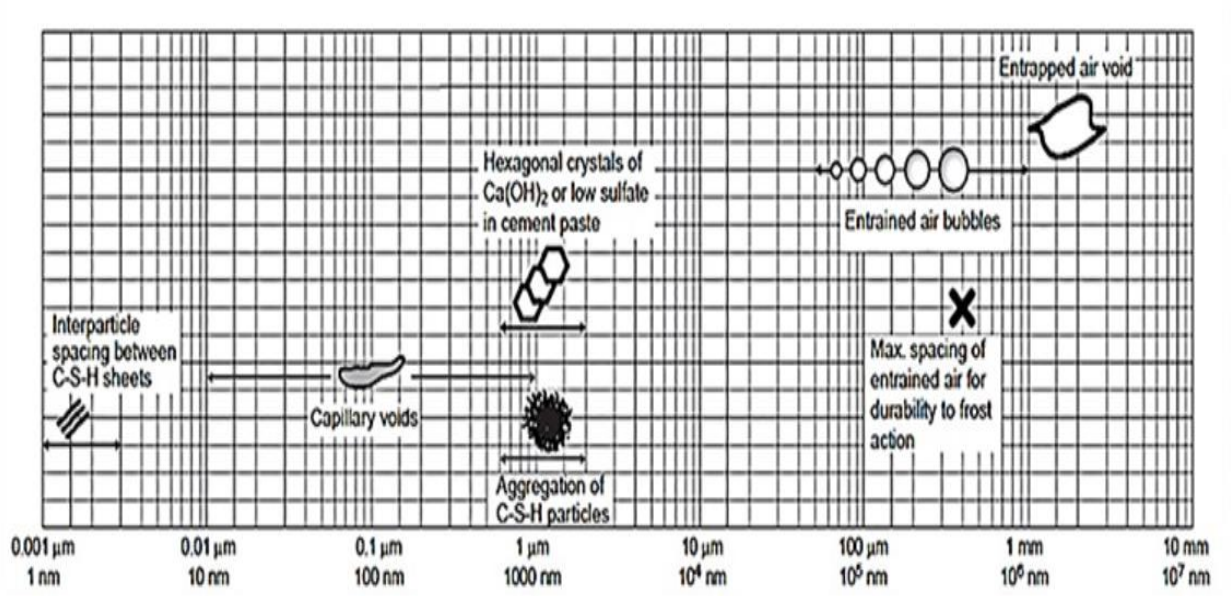

Figure X8 - Distribution de la taille de pore dans le béton

L'étude bibliographique indique que le dégrée de compactage et le temps de gâchage initial modifient la distribution des pores dont la taille est supérieure à 1mm. La formulation de référence a été reproduite avec six différent degrés de compactage et six différents temps de gâchage.

La diffusion de chlorure a été trouvée indépendante du niveau de compactage et le temps gachage et donc indépendante des pores causés par ces deux phénomènes. Par conséquent aucun effet des deux paramètres étudiés n'a été trouvé sur le coefficient de diffusion des chlorures. Cette diffusion a été démontrée à prendre place dans les pores inférieurs à 1 µm de diamètre par la notion de « Libre Parcours Moyen de Diffusion de Particules » calculé par l'équation suivante :

$$\lambda = \frac{RT}{\sqrt{2}\pi d^2 N_A P} = 0{,}917\ \mu m \qquad (X.25)$$

où λ est le libre parcours moyen de diffusion de particules, R est la constante de gaz parfait (égal à 8,3145 m^3.Pa.mol^{-1}.K^{-1}) , T est la températures en Kelvin, d le diamètre des ions chlorure, N_A est le nombre d'Avogadro (égal à 6,0221.10^{23} mol^{-1}), and P est la pression en Pa.

Cette gamme de diamètres est inférieure à la taille de l'air piégé. La diffusion ne se fera donc pas en dehors des pores capillaires (pores de tailles inférieures à 1 µm). Cette démonstration a confirmé la conclusion de la campagne d'essais.

Cependant, la perméabilité expérimentée par les essais de durabilité a été dépendante du degré de compactage. L'effet négatif du manque de consolidation ou de temps de gâchage initial sur la durabilité du béton évoqué dans la littérature provient de mécanismes de transport autres que la diffusion, à savoir la perméabilité et l'absorption.

9. Effet de l'ouverture des fissures

La fissuration dans le béton est un phénomène normal et se produit lors de la phase plastique et la vie du béton durcis. Deux types de fissures se produisent principalement au stade plastique : fissures de tassement plastique et fissures de retrait plastique. Les fissures de tassement plastique se produit dans les bétons ayant une haute teneur en eau dans des éléments où l'enrobage de l'acier est faible. Les fissures de retrait plastic se produit lorsque le taux d'évaporation dans un environnement dépasse le taux de saignement de béton. Dans la phase durcie, les fissures se produisent lorsque l'amplitude de la contrainte de traction dans le béton dépasse sa résistance. La présence de fissures est dans certains cas sensiblement préjudiciable à l'entretien du béton. Du point de vue de la durabilité, la présence de fissures diminue la durabilité du béton. En plus des spécifications normatives qui limitent l'ouverture des fissures pour diminuer leur effet négative sur la durabilité, l'effet de la fissuration sur le transport de chlorure a été étudié par plusieurs chercheurs. Plusieurs enquêtes ont été également menées pour identifier l'effet de l'ouverture des fissures sur la diffusion des chlorures. Dans la littérature, les travaux de recherche effectués à cet égard sont principalement divisés en quatre grands axes :

- étude qualitative de l'effet des fissures sur la pénétration et la diffusion des chlorures ;
- essais accélérés de pénétration des chlorures pour élaborer des modèles de simulation ;
- essais de longue durée pour évaluer l'effet de la fissuration sur le transport des chlorures ;

- Evaluation du coefficient de diffusion des chlorures dans les structures existantes fissurées

Ces axes de recherches ne permettent pas de quantifier de façon précise l'effet des fissures sur la migration des chlorures. Afin d'aboutir à une meilleure quantification, les éléments suivants doivent être considérés :

- Géométrie et propriétés des fissures : les fissures initiées dans les essais doivent avoir une largeur fixe sur toute la longueur de l'échantillon. Bien que cette géométrie ne corresponde pas au cas réel dans le béton, son utilisation est essentielle pour quantifier l'effet en fonction de l'ouverture maîtrisée de la fissure. La modélisation des structures réelles en béton peut être effectuée en prenant plusieurs couches avec différentes ouvertures de fissure. La tortuosité des fissures initiées et les propriétés surfaciques doivent également simuler les propriétés réelles des fissures.

- Type d'essais en laboratoire adopté pour la migration des chlorures : Alors que la collecte de données réelles sur le terrain de plusieurs structures fissurées soumises à un environnement de chlorure peut paraître plus précise, le nombre de paramètres inconnus rends l'exploitation imprécise. Ces inconnues peuvent comprendre des variations dans les formulations du béton, l'absence de données précises, l'exposition aux agents agressifs avec d'autres mécanismes de dégradation. Les essais en laboratoire doivent donc simuler plus précisément la véritable migration des chlorures. L'essai de long durée selon la norme ASTM C1556 semble être le plus proche de la migration réelle des chlorures.

- Réparation autogène des fissures : La réparation autogène des fissures peut être prise en compte par immersion des échantillons pendant une longue durée dans la solution de chlorure. Au cours de cette période, la réparation autogène aura lieu et l'effet ultérieur sur la diffusion des chlorures peut être évalué.

- Composition du béton : Etant donné que le taux de chlorure et le rapport eau-ciment affectent également le transport des chlorures dans le béton, l'effet couplé de ces deux paramètres doit être étudié en même temps que la géométrie des fissures. Plusieurs rapports eau-ciment doivent être envisagés.

- Taille de l'échantillon : ainsi en présence de fissures, les ions chlorure peuvent se diffuser dans les deux sens. Par conséquent, plus le diamètre de l'échantillon est petit, plus la différence de gradient est grande. En conséquence, l'échantillon doit avoir un diamètre fixe avec l'approche de modélisation qui sera utilisée. Par exemple, si une discrétisation supplémentaire est prévue pour l'élément en béton pour identifier la diffusion des chlorures, le maillage doit être compatible avec la taille de l'échantillon sur la base de laquelle les équations de coefficient de diffusion des chlorures ont été établies.

Par conséquent, la campagne expérimentale nécessaire pour quantifier l'effet de l'ouverture de la fissure doit envisager différents rapports eau-ciment et ouvertures de fissure. Un essai de longue durée doit aussi être utilisé.

La campagne CW d'essais tient compte des points ci-dessus, en considérant cinq rapports eau-ciment et cinq ouvertures de fissure. La forme finale de la fonction d'influence est comme suit :

$$f_{10}(w_c, \xi) = 2{,}1 \times 10^{-3} e^{9{,}31 w_c \xi + 14{,}64 w_c} \quad \text{(X.26)}$$

où ξ est l'ouverture de la fissure et w_c le rapport eu-ciment.

10. Modèle proposé

Le modèle final du coefficient de diffusion des ions chlorures est décrit par l'équation suivante :

$$D_c = f_1(T).f_2(h).f_3(x).f_4(CA, Hy).f_5(C3A).f_6(Cs).f_7(Mi).f_8(CW, w_c).D_{c,ref} \quad \text{(X.27)}$$

Les fonctions ci-dessus sont définies dans le tableau 10. Ce modèle est fonction des paramètres suivants :

- Paramètres Environnementaux :
    - Température
    - Age du béton
    - Humidité relative
- Propriétés du béton :
    - Rapport eau-ciment
    - Teneur en matières cimentaires
    - Pourcentage de matières cimentaires (fumée de silice, cendre volant, cendre volant ultrafin, ciment à base de laitiers)
    - Densité du Ciment
    - Finesse du ciment
    - Composition chimique du ciment
    - Coefficient d'hydratation
    - Forme des granulats
    - Volume des granulats
    - Propriétés des granulats
- Paramètres de mise en œuvre
    - Temps de cure
    - Dégrée de compactage
    - Temps de gâchage initial
- Ouvertures des fissures

Tableau 10 - Fonctions d'influence

Fonction	Terminologie
D_c	Coefficient de diffusion des chlorures
$f_1(T)$	Influence de la température : $f_1(T) = \frac{T}{296,15} \exp\left[\frac{U}{R}.\left(\frac{1}{296,15} - \frac{1}{T}\right)\right]$
$f_2(h)$	Effet de l'humidité relative : $f_2(h) = \left[1 + \frac{(1-h)^4}{(1-0,75)^4}\right]^{-1}$
$f_3(x)$	Effet de la profondeur : $f_3(x) = \begin{bmatrix} 0,53 + (1-0,53)\left(\frac{x}{20}\right)^{\beta} & for\ x < 20mm \\ 1 & for\ x \geq 20mm \end{bmatrix}$
$f_4(CA, Hy)$	Effet du volume et des propriétés des granulats : $f_4(CA, Hy) = (1,7258Mf + 0,0963Ab + 3,9165Clf + 1) \times \frac{(1 - V_{aggregate})}{\left[0,6265\left[\frac{1}{\sum_{i=1}^{i=n} V_i A_i}\right] + \left(0,3735\left[\sum_{i=1}^{i=n} \frac{V_i}{A_i}\right]\right)\right]}$
$f_5(C3A)$	Effet de la teneur en aluminate tricalcique : $f_5(C3A) = 26,644 \times (C3A)^{-2,552}$
$f_6(Cs)$	Effet du dégrée de compactage : $f_6(Cs) = 1$
$f_7(Mi)$	Effet du temps de gâchage initiale : $f_7(Mi) = 1$
$f_8(CW, w_c)$	Effet de l'ouverture des fissures : $f_8(w_c, \xi) = 2,1 \times 10^{-3} e^{9,31 w_c \xi + 14,64 w_c}$

$D_{c,ref}$	Coefficient de diffusion de référence à 28 jours, 23 °C, et 100% humidité relative. Ce paramètre est une fonction du rapport eau-ciment, la teneur en ciment, et le pourcentage de matières cimentaire (fumée de silice, cendre volant, cendre volant ultrafin, ciment à base de laitiers). Ce coefficient de diffusion de référence est basé sur une analyse de régression des valeurs moyennes données par les différents modèles de la littérature. Les valeurs moyennes sont prises pour des différents teneurs en ciment et rapports eau-ciment. Le facteur de corrélation de cette méthode est de 0,99 : $D_{c,ref} = (-(1{,}55 \times 10^{-14})e^{1{,}834 w_c} \times w_c \times PC + 1{,}50 \times 10^{-12} e^{5{,}52 w_c}) \times e^{-0{,}165.SF} \times (\frac{28}{t})^{(0{,}2 + 0{,}4(\frac{FA}{50} + \frac{SG}{70}))}$

Une analyse paramétrique est réalisée pour identifier l'influence de chaque paramètre sur la durée de vie des structures en béton armé. Les tableaux ci-dessous résument les effets correspondants. L'analyse paramétrique a été faite en changeant un seul paramètre à la fois, pour une même formulation de béton, tout en laissant les autres constants. On peut conclure que la prise en compte des paramètres supplémentaires affecte d'une façon significative la durée de vie des structures en béton armé.

Tableau 11 - Influence de température

Température annuelle moyenne (°C)	Coefficient de diffusion des chlorures après 50 années (m^2/s)	Durée de vie résultante (Années)
20	$1{,}10 \times 10^{-14}$	107
25	$1{,}41 \times 10^{-14}$	94
30	$1{,}81 \times 10^{-14}$	82
35	$2{,}29 \times 10^{-14}$	73
40	$2{,}88 \times 10^{-14}$	65
45	$3{,}60 \times 10^{-14}$	58

Tableau 12 - Influence de l'humidité relative

Humidité relative annuelle moyenne (%)	Coefficient de diffusion des chlorures après 50 années (m^2/s)	Durée de vie résultante (Années)
50	$6{,}29 \times 10^{-15}$	144
60	$1{,}41 \times 10^{-14}$	94
70	$3{,}48 \times 10^{-14}$	59
80	$7{,}58 \times 10^{-14}$	40
90	$1{,}04 \times 10^{-13}$	34
100	$1{,}07 \times 10^{-13}$	34

Tableau 13 - Influence de la quantité des granulats

Quantité de ciment (kg/m^3)	Quantité de fumée de silice (kg/m^3)	Quantité totale de granulats (kg/m^3)	Coefficient de diffusion des chlorures après 50 années (m^2/s)	Durée de vie résultante (Années)
300	25	1982	$1{,}16 \times 10^{-14}$	104
350	25	1892	$1{,}36 \times 10^{-14}$	96
400	25	1797	$1{,}55 \times 10^{-14}$	89
450	25	1707	$1{,}69 \times 10^{-14}$	85
500	25	1612	$1{,}82 \times 10^{-13}$	82
550	25	1517	$1{,}07 \times 10^{-13}$	80

Tableau 14 - Influence des propriétés des granulats

Pourcentage de matières plus fines que 75 microns (%)	Absorption d'eau des granulats (%)	Pourcentage d'argile et de particules friables (%)	Coefficient de diffusion des chlorures après 50 années (m^2/s)	Durée de vie résultante (Années)
1	1	1	$1{,}46 \times 10^{-14}$	92
3	3	3	$1{,}62 \times 10^{-14}$	87
5	5	5	$1{,}78 \times 10^{-14}$	83
7	7	7	$1{,}93 \times 10^{-14}$	79
9	9	9	$2{,}09 \times 10^{-14}$	76
11	11	11	$2{,}25 \times 10^{-14}$	73

Tableau 15 - Influence de l'aluminate tricalcique

Teneur en aluminate tricalcique (%)	Coefficient de diffusion des chlorures après 50 années (m^2/s)	Durée de vie résultante (Années)
4	$2{,}00 \times 10^{-13}$	25
6	$6{,}80 \times 10^{-14}$	42
8	$3{,}11 \times 10^{-14}$	62
10	$1{,}68 \times 10^{-14}$	85
12	$1{,}00 \times 10^{-14}$	112
14	$6{,}46 \times 10^{-15}$	142

Tableau 16 - Influence de l'ouverture des fissures

Ouverture des fissures (mm)	Coefficient de diffusion des chlorures après 50 années (m^2/s)	Durée de vie résultante (Années)
0.0	$3{,}64 \times 10^{-14}$	57
0.1	$4{,}32 \times 10^{-14}$	53
0.2	$5{,}68 \times 10^{-14}$	48
0.3	$6{,}25 \times 10^{-14}$	44
0.4	$7{,}60 \times 10^{-14}$	40
0.6	$1{,}16 \times 10^{-13}$	32
0.8	$1{,}82 \times 10^{-13}$	26
1.0	$2{,}94 \times 10^{-13}$	21
1.2	$4{,}85 \times 10^{-13}$	17
1.4	$8{,}18 \times 10^{-13}$	14
1.6	$1{,}40 \times 10^{-12}$	12
1.8	$2{,}43 \times 10^{-12}$	10
2.0	$4{,}26 \times 10^{-12}$	9

Afin de comparer le modèle proposé aux modèles existants, trois formulations de béton ont été choisis comme le montre le tableau 17. Ces formulations sont considérées dans des états non-fissurés et fissurés respectivement. Comme les modèles existants ne prennent pas tous les paramètres en considération, le coefficient de diffusion des chlorures était presque constant pour les six combinaisons, pour le même rapport eau-ciment. Le modèle proposé montre en-outre la différence entre les coefficients de diffusion des chlorures dans les six formulations d'une façon plus précise. La comparaison des diffèrent modèles est montre dans la figure X9.

Tableau 17 - Formulations de Béton Considérés

Paramètre	**Formulation 1 – Béton non-fissuré Mix 1 U**	**Formulation 2 – Béton Non-fissuré Mix 2 U**	**Formulation 3 – Béton Non-fissuré Mix 3 U**	**Formulation 1 – Béton fissuré Mix 1 C**	**Formulation 2 – Béton fissuré Mix 2 C**	**Formulation 3 – Béton fissuré Mix 3 C**
Ouverture de fissure (mm)	0.0	0.0	0.0	0.5	0.5	0.5
Quantité de ciment (kg/m^3)	350	425	305	350	425	305
Quantité de fumée de silice (kg/m^3)	0	0	45	0	0	45
Quantité de cendre volante (kg/m^3)	0	0	100	0	0	100

Quantité de ciment a base de laitiers (kg/m^3)	0	0	150	0	0	150
Quantité de granulats (kg/m^3)	1947	1810	1365	1947	1810	1365
Quantité d'eau (kg/m^3)	133	161.5	228	133	161.5	228
Rapport eau-ciment	0.38	0.38	0.38	0.38	0.38	0.38
Matériaux plus petits que 75 microns (%)	1	3	10	1	3	10
Absorption d'eau des granulats (%)	1	2	10	1	2	10
Pourcentage d'argile et de particules friables (%)	1	1	10	1	1	10
Teneur en aluminate tricalcique (%)	12	8	5	12	8	5

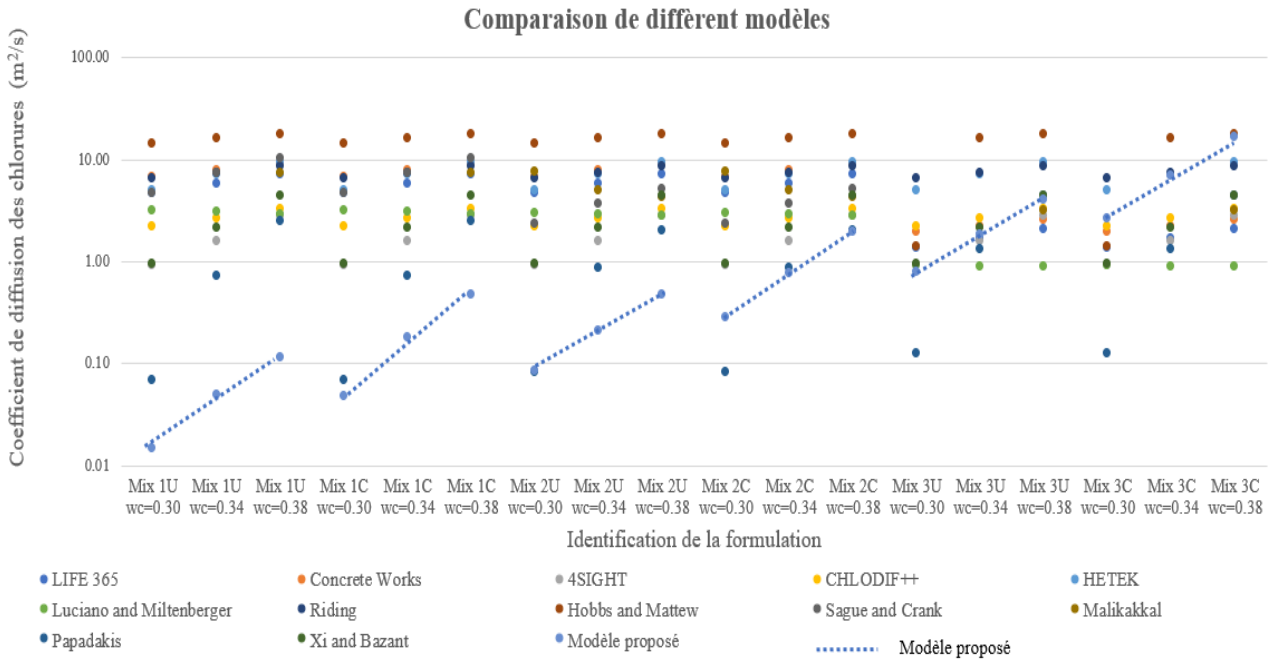

Figure X 9 - Comparaison de diffèrent modèles

11. Conclusion

La durée de vie des structures en béton dans un environnement riche en chlorure est obtenue par le temps auquel la corrosion des aciers devient inacceptable. Ce mécanisme est divisé en deux phases : phase d'initiation et phase de propagation. Il est contrôlé dans la plupart des cas par la première phase, en raison de sa durée significative par rapport à la phase de propagation. La phase

d'initiation est la durée où les ions chlorure diffusés dans le béton atteignent un seuil critique au voisinage des armatures.

La modélisation de cette durée de vie est essentiellement gouvernée par la valeur du coefficient de diffusion de chlorures dans le béton. La modélisation de ce coefficient en fonction des propriétés du béton a fait l'objet de plusieurs travaux de recherches au cours des dernières décennies. Les modèles disponibles dans la littérature considèrent principalement le rapport eau-ciment, avec quelques autres propriétés du béton et de l'environnement. L'étude de la littérature a également identifiée beaucoup d'autres paramètres affectent le coefficient de diffusion. Parmi ces paramètres, nous trouvons les propriétés et le volume des granulats, la teneur en aluminate tricalcique, le degré de compactage, le temps de gâchage et l'ouverture des fissures. L'influence de ces propriétés a été étudié dans cette thèse.

L'influence des propriétés des agrégats a été présenté dans le chapitre 2. L'étude montre que la diffusion des chlorures dans le béton peut théoriquement être divisée en trois phases de diffusion : une diffusion qui a lieu dans les granulats, une diffusion qui a lieu dans la zone de transition interfaciale entre les granulats et la pâte cimentaires, et la diffusion qui a lieu dans la pâte cimentaire. Le modèle proposé comprend deux autres zones de diffusion : l'état de surface totale et les impuretés dans les granulats. Ces deux zones peuvent être quantifiés à l'aide d'essais en laboratoire, contenu de Matériaux plus fines que 75 microns, essai d'absorption d'eau et l'essai du contenu d'argile et de particules friables. Il est également à noter que les propriétés des granulats n'affectent pas directement le coefficient de diffusion des chlorures. Ces propriétés sont plutôt dépendantes, et travaillent en combinaison avec les propriétés du béton pour influer sur la diffusion de chlorure dans le béton. Il est donc nécessaire de considérer ces entités lors de la quantification de l'effet des propriétés des granulats.

Le rôle de l'aluminate tricalcique a été étudié dans le chapitre 3, où la fonction d'influence a été obtenue. Le principal mécanisme concerne la liaison entre l'aluminate tricalcique et les chlorures, affectent par conséquent la valeur du coefficient de diffusion.

L'étude dans le chapitre 4 a montré que le temps de gâchage de béton et le degré de compactage sont indépendants du mécanisme de diffusion. La principale raison est attribuée à la taille des pores créés par ces deux paramètres. Ce fait révèle le rôle de la perméabilité important dans le transport des chlorures. Les deux mécanismes de transport (diffusion et pénétration) doivent être considérés en même temps pour une meilleure simulation de la transportation des ions chlorure. La quantité de chlorure dans le béton mis en œuvre avec différents niveaux de compactage variait considérablement, même pour la même valeur du coefficient de diffusion. Ceci est un élément qui doit être considéré lors de l'évaluation du seuil de chlorure provoquant la corrosion des armatures.

Les effets néfastes des fissures dans le béton sur la durabilité globale ont été analysés dans de nombreux travaux dans la littérature. Les fissures diminuent la durabilité du béton et augmentent la diffusion de chlorure. Le chapitre 5 étudie la quantification de cet effet par une campagne d'essais à grande échelle qui simule la forme précise et la largeur des fissures. L'étude prend en

considération l'effet du rapport eau-ciment et la cicatrisation autogène du béton, en plus de l’ouverture des fissures.

Le modèle final est présenté dans le chapitre 6, avec les paramètres supplémentaires affectant le coefficient de diffusion des chlorures. Le calcul de la pénétration des chlorures est effectué en calculant le coefficient de diffusion à chaque incrément de temps. La deuxième loi de Fick est ensuite appliquée pour calculer la pénétration des chlorures dans le béton en utilisant la méthode de différences finies. Le coefficient de diffusion de référence dans cette formule est basé sur la littérature disponible en fonction du rapport eau-ciment, teneur et type de ciment.

Au final, un modèle complet du coefficient de diffusion des chlorures a été obtenu en fonction de huit fonctions d’influence et un coefficient de diffusion de référence. Ces fonctions comprennent un total de trente paramètres. Ce modèle permet une représentation précise, par rapport aux modèles existants.

Introduction

Construction and life cycle costs minimization has pressed engineers in finding more tailored models for concrete service life assessment. Several models to estimate the concrete service life were developed till this day with the attempt of finding the most suitable real-life prediction. The models varied significantly in results and can reach ten times difference in some instances. This variation has caused confusion and ambiguity in concrete design, especially that the validation of these models requires a considerable long duration. The reinforcing steel corrosion was proved to be the major cause of concrete degradation. The financial survey associated with concrete repairs supported furthermore this fact whereby the majority of the repair applications were made for concrete degraded further to reinforcing steel corrosion. While this corrosion can originate from carbonation as well as chloride ingress, this later rules over the former and governs most of the corrosion occurrences and consequent repairs. Concrete resistance to chloride ingress is thus one of the primary factors defining the life-cycle cost of concrete structures. The available researches demonstrated that the chloride diffusion is the principal transportation method of chloride ingress whereas the permeation and absorption play a less prominent role, with the absorption being the least contributive. It is therefore essential to thoroughly study the diffusion mechanism and to determine the time for the onset of reinforcing steel corrosion in concrete. Consequently, the proper determination of chloride diffusion values including the different affecting parameters and how they change with time, is essential for service life modeling.

Three approaches to identify the concrete service life in chloride environment are discussed. The first approach includes a set of prescriptive based specification, which if followed, will result a predefined service life. These prescriptive based specifications are sets by national/international standards, codes, and construction guidelines. The second approach includes a set of laboratory durability test result ranges that will similarly result in a predefined concrete service life, if justified. A total of ten types of durability testing was identified. The limitation on the test results ranges are included in guidelines and specific project specifications. The third approach includes service life assessment models. These models take two major types of inputs, the first group of input includes the environmental parameters whereas the second set of input includes the concrete properties. Apart from the chloride surface concentration, that is considered as an environmental input in these models, the two sets of input parameters (environmental and concrete properties) yield a chloride diffusion coefficient. On the contrast of the former two approaches mentioned, the models output a specific service life, in “years”, rather than having a predefined service life that dictate concrete properties.

Large differences have been found in diffusion predictive models. It is thus important to investigate the reason of these differences, that is found attributed to the input parameters originally taken into consideration. Combining the list of the parameters in these models result in more than ten parameters that affect the chloride diffusion coefficient, not all the parameters were considered in various models. A further literature review of the parameters that affect the chloride diffusion

coefficient result in identifying a total of thirty parameters that directly affect the chloride diffusion coefficient. The number of parameters that are not taken into consideration in the available models is thus significant. This fact explains the root cause of the considerable difference in the service life values given by the different models.

The aim of this thesis is to reach a tailored model for chloride diffusion in concrete taking into consideration various affecting parameters. It includes a detailed survey of the available approaches and models for service life calculation versus chloride ingress. The affecting parameters are demonstrated through the literature review and confirmed by actual long-term testing program. It has been noticed that the literature works provide mainly qualitative information on the affecting parameters. This limitation makes it difficult to use this knowledge in service life prediction. In our work, a large-scale testing campaign was initiated to transform this qualitative effect into quantitative and measurable effect, the parameter dependence is also carefully considered. Once this combination of literature review and test results is identified, the functions describing the influence of each parameter is defined. As a final outcome, the present thesis reaches comprehensive conclusions regarding the parameters affecting the concrete service life in chloride environment, with empirical formulas quantitively defining their effects. A complete updated model for chloride diffusion in concrete is then obtained and applied through a numerical application.

Having defined in chapter 1, a list of affecting parameters, the grouping of the parameters discussed in chapter 1 to 5 can be done following four major groups:

- Environmental parameters: Temperature, relative humidity, and age.
- Concrete properties parameters
- Workmanship parameters: Concrete initial mixing time, consolidation level, and curing time.
- Post placing parameters: cracks (including the different types of cracks)

In order to reach a complete model for chloride diffusion coefficient that includes these influencing parameters, a large-scale testing protocol has been designed and carried out. The total number of laboratory tests needed to complete this study and reach the complete model is equal to 2221 tests and a total of 39 concrete mixes. The various concrete mixes and laboratory tests are made at Advanced Construction Technology Services Laboratories (ACTS) in Lebanon and Saudi Arabia, which financially supported this work. The company ACTS has also provided two chemists for a period of two years to support the testing works.

The testing protocol is constructed in a way to reflect the right method of long-term testing, associated with the most suitable number of tests and the combination of parameters selected in each testing series. The literature review concluded that five series of parameters should be selected: the aggregate properties, the tricalcium aluminate content, the initial mixing time, the degree of concrete consolidation, and the crack width. Since the crack width effect on chloride diffusion is associated with the autogenous healing of the cracks that will reduce the chloride ingress, a coupling effect of the crack width with the concrete water-cement ratio was necessary,

and integrated in the testing protocol. The linking point between the different testing series is one crossing reference concrete mix design. The five series of the parameter variations are as follows:

- AGG Series for mixes with various types of aggregate.
- C3A Series for mixes with various content of tricalcium aluminate.
- MIXT Series for mixes with different initial mixing time.
- CONS Series for mixes with different consolidation efforts.
- CW Series for mixes with different water-cement ratio and different crack widths.

A literature review is conducted in chapter 1 in order to identify the various methods available for the service life assessment of reinforced concrete structures in chloride environments. A total of fifteen models for service life assessment in chloride environment are discussed in this chapter. These models are compared for various concrete mix designs and result in significant difference in the resulting service life. The difference in service life given by various models reaches in some instances, a value exceeding ten times.

The second chapter is dedicated to AGG series and starts by reviewing the available literature related to this topic. The test results related to AGG series were in line with the literature review made in his chapter suggesting that the diffusion takes place in three volumes, namely, the aggregate, the interfacial zone between the aggregate and the bulk cement paste, and the bulk cement paste. The test results also identified other aggregate properties that affect the diffusion coefficient. These properties include the aggregate surface condition and the impurities found in the aggregate. The diffusion volumes are thus updated to a suggested model of five volumes and a method to calculate the apparent diffusion coefficient is developed.

While identifying the tricalcium aluminate as an important parameter affecting the chloride diffusion coefficient, chapter 3 is dedicated to C3A series. The literature review agrees that the higher the tricalcium aluminate content, the higher the corrosion resistance. In addition to this fact, with higher tricalcium aluminate content, lower chloride diffusion coefficients are expected. The results of the testing protocol agree well with these assumptions. The analysis and interpretation of the test results yield an additional function describing the effect of the tricalcium aluminate on the chloride diffusion coefficient.

The workmanship parameters are discussed in chapter 4 including the results of MIXT and CONS series. The aim is to quantify the effect of the initial mixing time and consolidation on the chloride diffusion coefficient. This chapter reaches important conclusions on the role of these parameters in chloride diffusion whereas the corresponding effects seems to be more pronounced on other chloride transportation mechanism like the permeation and absorption.

The post-placing parameters that includes crack effects on chloride diffusion coefficient is presented in chapter 5. The key element in the successful completion of CW series includes the method of crack initiation and the type of required testing. The literature review was grouped

following the type of testing, methods of cracks initiation, and used evaluation approach. A critical review is made for each category justifying the choice of the testing protocol adopted in CW series. The various methods of purposely initiating cracks in concrete samples were also discussed and evaluated reaching the best method to initiate cracks in CW series. Long term testing was preferable over accelerated testing used in some previous works and was therefore selected for CW series. The autogenous healing that may affect the chloride ingress mechanism and consequently overestimate cracks effect on chloride diffusion coefficient is thoroughly discussed. High correlation is obtained suggesting an exponential increase of the chloride diffusion coefficient with the crack width at different water-cement ratios.

Each of the above chapters ends by defining the functions describing the effect of these parameters on the chloride diffusion coefficient.

The last chapter groups the different functions identified in the previous chapters into one complete model. As these chapters mainly describe the variation of the chloride diffusion coefficient with the selected parameters, the reference chloride diffusion coefficient is concluded from the available literature. The method of two-dimensional finite difference to be used to simulate the chloride diffusion in concrete, is presented and explained along with the input and output parameters. Chapter 6 ends by a numerical application where the results of the complete model are compared to the output of other existing models. A parametric analysis to evaluate the relative effect of each parameter is also presented.

The thesis ends by the conclusions made from this study along with future works needed to complete the concrete service life assessment under different combinations of exposures. The proposed future works thus include a road map to study the chloride diffusion in combination with other degradation models.

Chapter 1: Service Life of Concrete Structures

1. Introduction

The design of concrete service life presents one of the main aspects of construction economy and sustainability. Designing concrete structures for an adequate period prevents early repair costs along with the associated functional costs. Concrete repair, in addition to being costly and avoidable in some cases, may be impossible to conduct in extreme cases. Large infrastructure projects for instance are designed to be constructed once and maintained regularly with optimized total cost. Existing models, developed to optimize maintenance costs, have to start with adequate identification of the structure's initially projected service life.

The definition of service life takes several meanings and terminologies depending on the nature of the structure and its function. Several references have defined these terminologies and will be presented later in this report. Concrete durability is also different from the concrete service life; the durability is set as a qualitative description of the concrete to serve successfully its intended use whereas the service life is a quantitative duration, in "years", for the concrete to maintain a certain characterization.

The concrete service life needs to take into consideration the different degradation processes that can affect the concrete, along with their interactions. Considering the different concrete degradations, an adequate service life calculation will need to include indefinite degradations interactions. Concrete degradations are luckily dependent on the surrounding environment which makes few degradations governing the concrete service life. Limited other degradation processes are related to the concrete constituent materials and can be mainly taken into account at the design stages, by specifying the right material. Based on this, the concrete service life is most often defined by taking into consideration two to three governing concrete degradation processes. Reinforcement corrosion has been widely reported in the literature over the last three decades as one of the major durability problems [41]. It mainly occurs when the rebar in the concrete is exposed to the chlorides either contributed from the concrete ingredients or penetrated from the surrounding chloride-bearing environment. The worldwide annual cost of corrosion is estimated to be 2.2 trillion USD which is over 3% of the world's Gross Domestic Product (GDP) [42]. The total cost of corrosion for the year 2011 in the US alone has exceeded 1 trillion USD, accounting for 6.38% of the GDP. India and China suffered similar expenses recording values of 2.4%, and 5.2% of their GDP respectively [43,44].

Several models exist to define the concrete service life in chloride environment, more specifically versus the chloride induced concrete reinforcement corrosion. Even with this advancement, recent works [45] have concluded the need for further development in service life modelling of concrete structures in chloride environment. This is especially true for cracked concrete as most of the models deal with uncracked concrete.

2. Concrete service life definition

The description of concrete durability and concrete service life was defined from several points of view in various references. The two terms (durability and service life) were always differentiated. The American Concrete Institute committee 365.1 [46] for example defines the durability as "*the ability of maintaining the serviceability of a product, component, assembly, or construction over a specified time*" and the service life as "*the period of time after placement during which all the properties exceed the minimum acceptable values when routinely maintained*". Seven general types of service life descriptions were found in the literature:

a) Technical Service life: Time until a defined un-acceptable state is reached [46].

b) Physical Service Life: The physical service life of a structure is the period from construction to when its collapse occurs [47].

c) Functional Service Life: Time until the structure no more fulfills the functional requirements [46].

d) Economic Service life: Time until replacement of the structure is economically more advantageous than keeping it in service [46].

e) Technological Obsolescence: This period is defined from the construction to the time where it is no longer technologically superior to alternatives [47].

f) Social and Legal Obsolescence: This is the period from construction to when the human desires dictate replacement for non-economic reasons [47].

g) Design working life: assumed period for which a structure or a part of it is to be used for its intended purpose with anticipated maintenance but without major repair being necessary [48].

The above service life definitions agree that the service life of a concrete structure is the period outside which the structure no longer fulfill its intended use or needs major action to conserve it. In chloride environments, the service life is mostly defined as the time in “years” where the initiation phase is completed or the time in years where the level of corrosion is no longer acceptable. This definition road-crosses the definitions above in the different aspects.

3. Concrete reinforcing steel corrosion

Concrete reinforcing steel corrosion is due to the chemical composition of steel whereby this later tends to regain its natural form: iron oxide. The steel corrosion results, at a certain level, in concrete spalling reducing thus the structure durability, then in reduction of steel cross-section which jeopardizes the structural adequacy of the reinforced concrete member. When embedded in concrete, the steel is kept in a passive state which prevents it from corrosion. The passive state is due to the highly alkaline medium provided by the concrete properties. The protection is pronounced furthermore by the additional cover normally provided by the concrete to the steel reinforcement. This cover tends to significantly delay the ingress of deleterious materials that break the protective film around the reinforcement and initiate corrosion.

The protective layer surrounding the steel reinforcement and provided by the sound concrete can be destroyed following two main occurrences. The first occurrence consists in concrete carbonation, starting from the portion exposed to the environment inwards. This carbonation is due to the naturalization of the cement by the carbon dioxide available in the atmosphere. As the carbonation proceeds, the concrete pH is lowered significantly reaching values close to 9. At that level, the concrete can no longer provide the high alkaline ambiance necessary for steel passivation, and corrosion will be initiated.

Another occurrence of rescinding the protective film consists in the chloride ingress through the concrete cover. This corrosion type initiates as soon as the concentration of chloride ions in the pores adjacent to the reinforcement reaches a critical level that causes a localized breakdown in the protective film and steel corrosion. Chloride diffuses in concrete going from an initial concentration at the surface. The diffusion is proportional to the concrete chloride diffusion coefficient. The concrete diffusion coefficient depends on several factors including the concrete properties. Calculating the chloride diffusion coefficient was reported in several international publications and literature as discussed later in this manuscript.

In addition to the chloride diffusion, the chloride in concrete can originate as a consequence of several mechanisms. These mechanisms include the chloride initially present in the concrete constituent materials similar to the aggregate, cement, water, or admixtures. Other forms include the water absorption, water flow and wick action. These mechanisms are described as following:

- Inherent Chloride: Concrete constituent materials may include chloride before being mixed into an homogeneous concrete. This chloride may be available in large quantities in the aggregate at the time of manufacturing, especially aggregate that are dredged from marine environment. The water used in concrete may also include a percentage of chloride that will be eventually included in the concrete mix. Several admixtures, similarly to the calcium chloride, include a percentage of chloride that will be summed to the total chloride in the mix.

- Chloride ingress by water absorption: Concrete that is not saturated absorbs water by capillary action. This water can include a percentage of chloride that increases the chloride content in hardened concrete. An example of this mechanism includes the reinforced concrete elements that are exposed to deicing salt and seawater while partly saturated.

- Water flow in concrete: Water rich in chloride may flow in concrete due to a pressure gradient, known as permeation. This mechanism is more pronounced in marine structures where the water pressure gradient increases with depth.

- Wick action is the movement of water in a reinforced concrete section that is exposed to water from one side and dry from the side. This water may as well be rich in chloride that is added to the total chloride content in the concrete.

Chloride ions destroy the protective film developed by the steel, and in the presence of water and oxygen, corrosion occurs [49]. This phenomenon is however localized; the chloride ions activate the surface of the steel making it the anode and the passive surface being the cathode [49]. Therefore, during the concrete reinforcing steel corrosion, one portion of the bar will work as an anode and another portion will be working as cathode. The anode and cathode are electrically linked together by the reinforcing bar itself, and both are immersed in the concrete which contains dissolved ions. When the passive layer is destroyed, the electrolyte mechanism will be launched as follows [50]:

Step 1: At anodes, iron atoms loose electrons:

$$Fe \text{ ----> } Fe2+ + 2e- \quad (1.1)$$

Step 2: Electrons will combine with water and oxygen

$$H_2O + 1/2\ O_2 + 2e^- \text{ ----> } 2OH^- \quad (1.2)$$

Step 3: The ferrous ions will combine with the OH^- forming iron oxide or rust

$$Fe^{2+} + 2OH^- \text{ ----> } Fe(2OH) \quad (1.3)$$

Thus, the corrosion reaction mechanism is triggered between one portion of the steel as anode and another portion as cathode with presence of a destroyed passive film, oxygen and water. The absence or shortage in any of the above-mentioned parameters can halt or decrease the rate of the corrosion reaction. In this connection, chloride-induced corrosion is highly concentrated at a small anode with pitting of the steel taking place [49]. It is to note that corrosion of steel by chloride attack is considered as the most critical form of embedded steel corrosion. This mechanism can occur without disruption of the cover concrete and almost total corrosion of section can occur before problems become apparent at the surface [51]. The initiation period, t_i, defines the time it takes for sufficient chlorides to penetrate the concrete cover and accumulate in sufficient quantity at the depth of the embedded steel to initiate corrosion of steel [28]. In another term, it is the time needed for the chloride to reach a critical concentration at the steel level to initiate the corrosion. The subsequent period further to the trigger of the corrosion is called the propagation period.

The propagation period is the beginning of the reinforcing steel corrosion, it starts as soon as the chloride level at the vicinity of the steel reaches the critical threshold level. It is the stage where the steel regains its original form of iron oxide. This phenomenon is expected to last few years. LIFE 365 model [28] defines this value as 6 years and 20 years for carbon steel and epoxy coated steel respectively. The propagation phase is accompanied with an increase in the steel reinforcement volume. Concrete cracking and ultimately concrete cover spalling.

4. Concrete service life in chloride environment

The calculation/identification of the concrete service life in chloride environment can be categorized into three groups as illustrated in Figure 1.1:

1. Prescriptive-based specifications where limits on strength, water-cement ratio, cement content, cementitious materials type, and strength grade are imposed to achieve a specific service life (usually between 50 and 100 years). In this category, the service life is initially defined, and the criteria to achieve it are imposed. This category is discussed more in details in section 5.
2. Performance-based testing, including a total of ten types of tests. In this category, the service life is initially defined, and the durability performance tests criteria (Test results range) are then dictated. The tests that are relevant directly to the chloride ingress include three tests, i.e. the Rapid Chloride Penetration Test, the Chloride Migration Test, and the Apparent Chloride Diffusion Coefficient Test. Although less commonly used, another seven testing methods were developed to test the concrete chloride resistance [52]. The performance-based durability testing is discussed more in details in section 6.
3. Degradation models to simulate physical mechanisms according to effective concrete properties. The majority of these models simulates the chloride diffusion in concrete and calculates the service life accordingly. The service life in these models is defined mostly as the end of the initiation phase described earlier. These models are discussed more in details in section 7. In this category, the input consists of the concrete and environment properties whereas the output will be the resulting service life.

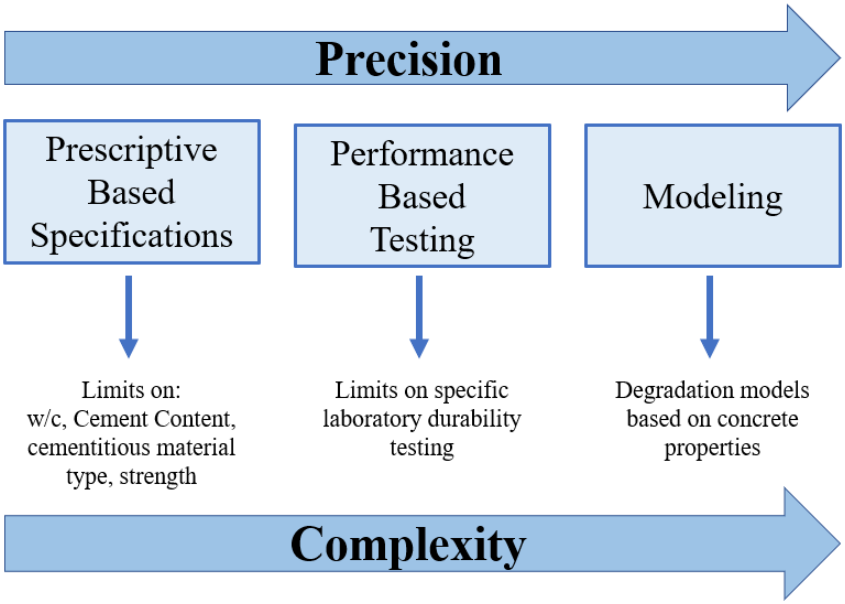

Figure 1.1 - Categories for Service Life Prediction

The two categories discussed formerly were based on comparable performance rather than actual calculations. In the prescriptive and performance-based methods in defining a service life, internationally monitored reinforced concrete structures that have endured a specific environment while inhering specific properties are taken as benchmark. This means that subsequent reinforced concrete elements should have similar properties to yield similar service life in the same environment.

5. Prescriptive-based durability specifications

This section discusses the majority of the prescriptive based durability references available in the concrete construction industry. A survey of the most commonly used references for prescriptive based durability specifications is included in appendix 1.1. This list was extracted from the concrete durability reports that were developed for several large-scale reinforced concrete projects where prescriptive based durability specifications were used.

The study of various documents allowed us to divide the durability deficiencies into three categories:

- Category 1: Durability deficiency due to **corrosion of steel reinforcement**, induced by chloride and carbonation.
- Category 2: Durability deficiency by **deterioration of the cement paste**: Freeze and thaw, Leaching, Delayed Ettringite formation, Sulfate attack, Acid and Base Attack, Salt Crystalisation, Abrasion, erosion, and Cavitation.
- Category 3: Durability deficiency due to **aggregate deterioration**: Alkali-Silica Reactivity and Alkali-Carbonate reactivity.

In addition, the recommendations and standards relate the concrete durability and inherent service life to the above-mentioned deterioration mechanism through the following factors:

- Type 1: water-cement ratio specifications.
- Type 2: cement content specifications.
- Type 3: cement type usage specifications.
- Type 4: concrete strength prescriptions.
- Type 5: constituent materials test results range specifications.
- Type 6: concrete practices that can affect concrete durability.

As a consequence, in prescriptive based specification, the concrete resistance towards chloride ingress is not defined in terms of chloride diffusion. It is rather a defined range of properties that will ensure the intended service life. Additional information regarding each type and category of prescriptive based specifications is available in appendix 1.1.

The information thus concluded from the prescriptive-based specifications can yield a workflow for concrete durability assessment towards chloride ingress. The following five steps summarizes the workflow.

- Step 1: Definition of the environment from references in section A.1.
- Step 2: Definition of the maximum water-cement ratio, minimum cement content and type from references in section A.1.
- Step 3: Definition of constituent material properties from the references in section A.2.
- Step 4: Limit of concrete durability test result specifications for paragraph A.5.

- Step 5: Generation of concrete practice recommendations checklists relevant to the structure along with the permissible crack widths from references in paragraph A.3 and A.6.

While the different prescriptive standards link the concrete durability to the concrete compressive strength, water-cement ratio, cementitious materials type and quantity, several other parameters that may affect the concrete durability, were mentioned in these references. These parameters include the effect of tricalcium aluminate (C3A) content, crack width, compaction degree, concrete mixing time, aggregate chloride diffusion coefficient variation and others. These parameters do not however enter in the concrete durability design or service life assessment in prescriptive-based specifications. This fact indicates that the water-cement ratio, cementitious material content/type, and strength grade are not exclusive in defining the concrete durability neither in the service life.

In order to illustrate the application of prescriptive-based specifications use in large-scale projects, three case studies are presented below, where data are drawn from the corresponding durability reports:

- Case Study 1: Riyadh Metro Project Lines 1 and 2 (Kingdom of Saudi Arabia) – Concrete Durability Report:

A concrete durability report was prepared for Riyadh Metro Project Lines 1 and 2, one of the mega projects in Riyadh. This report has identified the environmental conditions in Riyadh area in the vicinity of the project. The main aim of this report was to identify the concrete mix designs needed to achieve a service life of 100 years. The following prescriptive based specifications were used:

- AASHTO-LRFD Design Specifications, 6th Ed. 2012.
- ACI 318M-11 Building Code Requirements for structural Concrete
- ACI 365.1R-00: Service Life Prediction – State-of-the-Art Guideline
- ACI 201.2R-01: Guide to Durable Concrete
- ACI 362.1R-97: Guide for the design of Durable Parking Structures
- ACI 304R-00: Guide for measuring, mixing, transporting and Placing Concrete
- ACI 305R-99: Hot Weather Concrete
- ACI 308.1-98: Specifications for Curing Concrete
- ACI 350-06 Requirements for concrete Exposed to Sulfate- Containing Solution
- SBC 304-07: Requirements for concrete Exposed to Sulfate-Bearing Soils or water
- Saudi Building Code
- BRE SD1-05 Concrete in Aggressive Environment

These documents included recommendations for the maximum water cement ratio, the minimum cement content, the cement type, the materials properties, the minimum concrete compressive strength, the minimum concrete cover, the maximum crack width, and construction practices that affect concrete durability. These guidelines were used as the basis of designing concrete mixes that ensure a service life exceeding 100 years.

The last sections of the report have conducted a service life calculation of the selected mix design based on the following software:

- LIFE 365 Software
- DuraCon Software

- Case Study 2: Riyadh Metro Project Lines 4, 5 and 6 (Kingdom of Saudi Arabia) – Concrete Durability Report:

This report was prepared by a completely different firm and for a different client, it is also related to the Riyadh Metro Project, but in different lines. It started in a similar way by defining the environmental conditions. A different set of prescriptive-based specifications was used in this project. These documents included also recommendations for the maximum water cement ratio, the minimum cement content, the cement type, the materials properties, the minimum concrete compressive strength, the minimum concrete cover, the maximum crack width, and construction practices that affect concrete durability. These guidelines were used as the basis of designing concrete mixes that ensure a service life exceeding 100 years. The documents used in this report are as follows:

- BRE SD1-05 'Concrete in Aggressive Environments';
- CIRIA C577-02 'Guide to the Construction of Reinforced Concrete in the Arabian Peninsula';
- CIRIA 31-84 'Guide to Concrete Construction in the Gulf Region';
- Concrete Society CS163, 'Guide to the Design of Concrete Structures in the Arabian Peninsula.' 2008.
- ACI 365.1R-00: Service-Life Prediction — State-of-the-Art Report;
- ACI 201.2R-01: Guide to Durable Concrete;
- BS 8500 / BS EN 206-1: Concrete Specification, Performance, Production and Conformity;
- BS 8110 Parts 1 to 3: Structural Use of Concrete;
- BS 5400 Parts 1 to 10: Steel, Concrete and Composite Bridges;
- BS 8007:1987: Code of Practice for Design of Concrete Structures for Retaining Aqueous Liquids;
- ACI 362.1R-97: Guide for the Design of Durable Parking Structures;
- ACI 304R-00: Guide for measuring, mixing, transporting and placing concrete;
- ACI 305R-99: Hot weathering concreting;
- ACI 308.1-98: Specification for curing concrete;
- SBC 304-07: Structural Concrete Structures

- Case Study 3: Lusail Plaza – Doha – Qatar – Concrete Durability Report:

This report used the similar approach as of the first two case studies where a list of prescriptive based specifications in terms of maximum water cement ratio, minimum cement content, cement type, materials properties, minimum concrete compressive strength, minimum concrete cover,

maximum crack width, and construction practices that affect concrete durability, was used to design the concrete mixes satisfying a service life exceeding 100 years. Additional limits on performance-based durability testing were also included in this report. This testing category is explained in more details in the next section.

As a summary, one primary form of defining the concrete service life include a set of prescriptive specifications based on international codes and standards. These prescriptions mainly include requirements for the water-cement ratio, cement content, cementitious materials type, concrete compressive strength, and materials properties. The same guidelines also include construction and detailing recommendations similarly to the minimum concrete cover.

6. Performance based durability specifications

Performance-based durability testing includes a total of ten durability tests that indicate the concrete chloride resistance. In addition to these tests, three other durability tests are frequently specified, these additional tests include Water Absorption Tests, Water Permeability and Initial Surface Absorption Tests. In this category, the service life is initially defined, and the durability performance test criteria are then dictated. The criteria of durability test results are set by the project specifications based on local and national experience. The ten tests are listed in Table 1.1.

Table 1.1 - Performance Based Durability Testing

Performance- Based Durability Testing		**Output/Indicator**
1	Rapid Chloride Penetration Tests	Amount of charge that passes through a concrete sample
2	Bulk Diffusion Test	Apparent Chloride Diffusion Coefficient
3	Electrical Chloride migration Test	Indicative Apparent Chloride Diffusion Coefficient
4	Rapid Migration Test	Indicative Apparent Chloride Diffusion Coefficient
5	Salt Ponding Test	Chloride Penetration
6	Resistivity Techniques	Concrete Resistivity
7	Pressure Penetration Techniques	Chloride Penetration
8	Indirect Measurement Techniques	Correlation between concrete permeability and concrete resistance to chloride
9	Sorptivity	Correlation between concrete Sorptivity and concrete resistance to chloride
10	Other Test Methods that relate to diffusion of specific gases in concrete to the diffusion of chloride in concrete.	Correlation between gases diffusion in concrete and chloride diffusion in concrete

Appendix 1.2 details the performance-based durability tests described above. There are no current international limits on the test results related to the tests above versus the concrete durability or inherent service life. The corresponding limitations on the test results are generally defined, if any, in the relevant project specifications and followed during the course of the project. ASTM C1202 [53] categorizes the results of the RCPT test following five categories: High, Moderate, Low, Very low, and Negligible. These categories can give an idea related to the chloride durability level of the concrete versus chloride ingress. The apparent chloride diffusion test simulates the chloride diffusion in concrete under saturated conditions and can be used directly to calculate the chloride ingress under these conditions. The remaining chloride resistance performance durability test can be used in a comparative way. Table 1.2 summarizes the above-mentioned techniques [52] and categorizes them. Although the performance-based durability test can identify the level of concrete durability, the apparent chloride diffusion test and the pressure penetration techniques seems to have the least disadvantages when compared to other methods, especially that the outcome is a diffusion coefficient value rather than a comparative parameter. The pressure penetration technique is not however covered by a widely used standard.

Table 1.2 - Summary of Performance Based Durability Tests Related to Chloride Ingress

Test Methods		**Considers Chloride Ion Movement**	**At a Constant Temperature**	**Unaffected by Conductors in Concrete**	**Outcome as a Direct Results or a Comparative one**
Long Term	Salt Ponding	YES	YES	YES	Comparative
	Apparent Chloride Diffusion	YES	YES	YES	Direct
Short Term	Rapid Chloride Penetration	NO	NO	NO	Comparative
	Electrical Chloride Migration	YES	YES	NO	Direct
	Rapid Chloride Migration Test	YES	YES	NO	Direct
	Resistivity Techniques	NO	YES	NO	Comparative
	Pressure Penetration Techniques	YES	YES	YES	Direct
	Other Methods	NO	YES	YES	Comparative

From the above tests, three tests are commonly used to identify the concrete resistance to chloride, namely the “Apparent Chloride Diffusion”, “Rapid Chloride Migration”, and the “Rapid Chloride Penetration Tests”. The later one’s use is even more pronounced due to its short time duration.

An attempt to link the Rapid Chloride Penetration Test, as a performance-based durability test with the prescriptive based durability specifications detailed in section 5, was made as part of our work. A total of thirteen mixes (13) were prepared by ACTS using the same materials but with different cement contents and water-cement ratios (yielding different concrete compressive strength). The testing protocol and the concrete mixes used are detailed in appendix 1.4. The thirteen mixes were tested for their Rapid Chloride Penetrations values at 28 days and 56 days. The following relationships were identified:

- RCPT versus Cement content and Water cement ratio at 28 days:

$$C_{RCPT,28\ days} = -1832.26 - 2.38 \times Cem + 17707.1 \times w_c \qquad (R^2 = 0.726) \qquad (1.4)$$

- RCPT versus Cement content and Water cement ratio at 56 days:

$$C_{RCPT,56\ days} = -4201.26 + 0.684 \times Cem + 18382.77 \times w_c \qquad (R^2 = 0.932) \qquad (1.5)$$

- RCPT (tested at 28 days) versus the 28 days concrete compressive strength:

$$C_{RCPT,28\ days} = 8651.55 - 101.64 \times f'_{c,28} \qquad (R^2 = 0.563) \qquad (1.6)$$

- RCPT (tested at 56 days) versus the 28 days concrete compressive strength:

$$C_{RCPT,56\ days} = 7691.9 - 96.778 \times f'_{c,28} \qquad (R^2 = 0.688) \qquad (1.7)$$

where $C_{RCPT,t}$ is the RCPT value that is defined as the charge that passes through a standard concrete sample at an age t, in coulombs, Cem is the cement content, w_c is the water-cement ratio, and $f'_{c,28}$ the concrete compressive strength at 28 days.

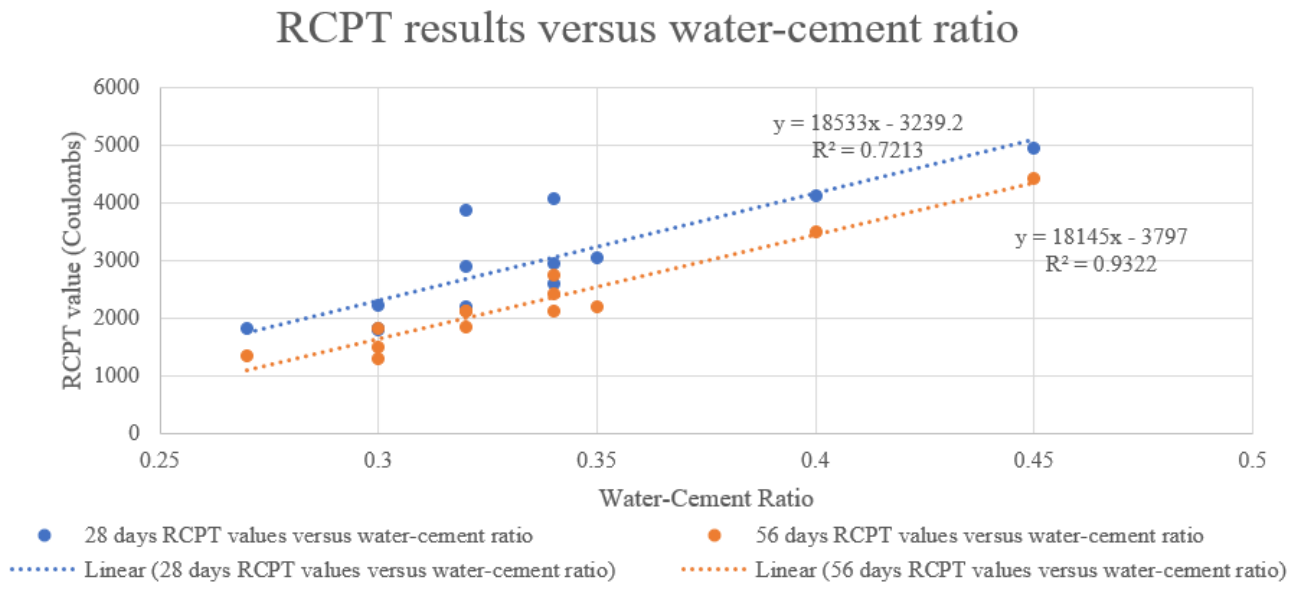

Figure 1.2 - RCPT values versus water-cement Ratio

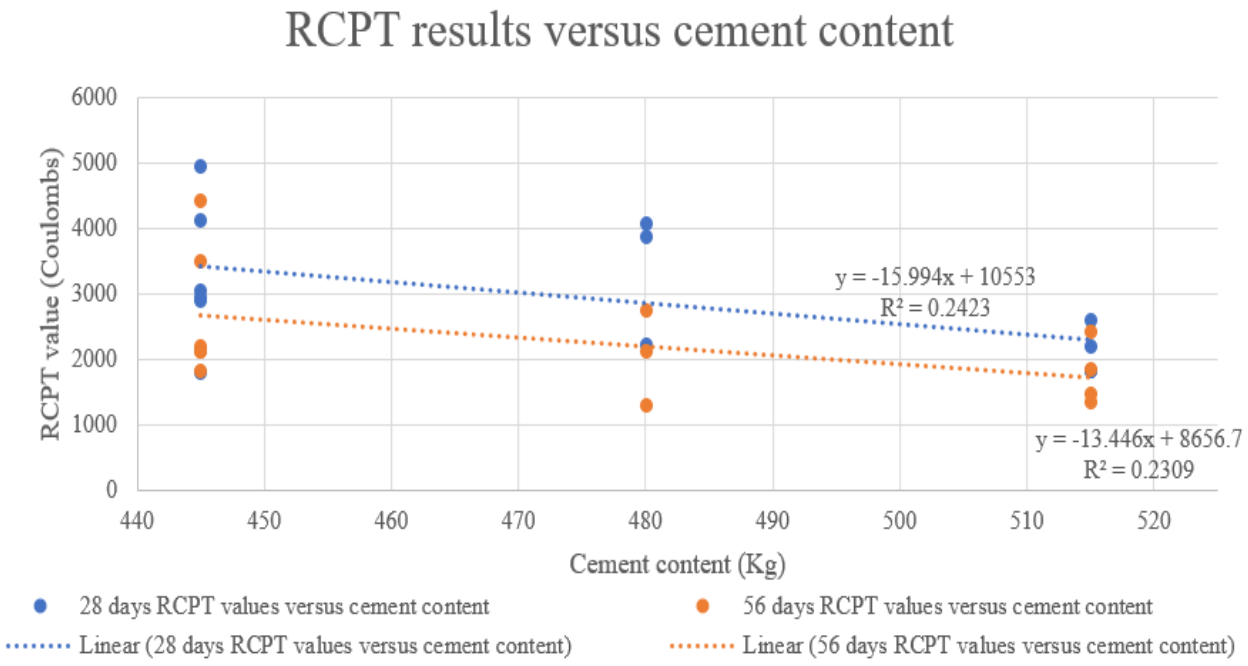

Figure 1.3 - RCPT values versus cement content

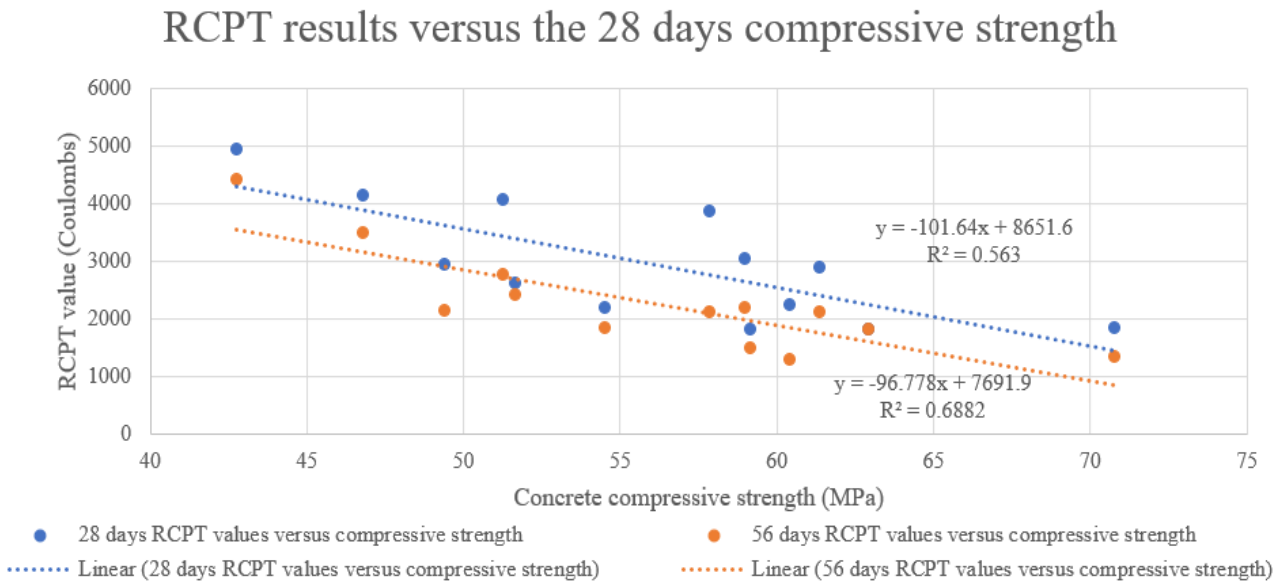

Figure 1.4 - RCPT versus the 28 Days Concrete Compressive Strength

The test results above show the concordance between the prescriptive-based specifications and the performance-based durability specifications in terms of concrete durability. In a similar context, FIB 34 [4] has included the following relationships between the rapid chloride migration test values and the water cement ratio:

Table 1.3 - Chloride Migration Coefficient as a function of the water-cement ratio

CEM I 42.5 R		CEM I 42.5 R + FA 22% Fly Ash (Fly ash percentage as cement replacement)		CEM I 42.5 R + SF 5% Silica Fume (Silica Fume percentage as cement replacement)		CEM III/B 42.5	
0.35	No Data	0.35	No Data	0.35	4.4×10^{-12}	0.35	No Data
0.40	8.9×10^{-12}	0.40	5.6×10^{-12}	0.40	4.8×10^{-12}	0.40	1.4×10^{-12}
0.45	10.0×10^{-12}	0.45	6.9×10^{-12}	0.45	No Data	0.45	1.9×10^{-12}
0.50	15.8×10^{-12}	0.50	9.0×10^{-12}	0.50	No Data	0.50	2.8×10^{-12}
0.55	19.7×10^{-12}	0.55	10.9×10^{-12}	0.55	5.3×10^{-12}	0.55	3.0×10^{-12}
0.60	25.0×10^{-12}	0.60	14.9×10^{-12}	0.60	No Data	0.60	3.4×10^{-12}

Titi and Tabatabai [36] have demonstrated the significant effect of the coarse aggregate properties on the Rapid Chloride Penetration. The below formula resulted from their research.

$$C_{RCPT,t} = (5076.2A + 6904.7) \times t^{-0.58} \tag{1.8}$$

where $C_{RCPT,t}$ is the RCPT value in coulombs, A is the aggregate water absorption, and t is the time of testing.

This research has shown that, factors other than the water-cement ratio, cement content, and concrete compressive strength, can affect the concrete service life.

As a summary to this section, the performance-based durability testing presents a more advanced approach compared to the prescriptive based durability specifications, based on the actual concrete samples rather than a set of mix design prescriptions. Aside of the apparent chloride diffusion, that can give direct chloride diffusion coefficient in saturated conditions, and in the absence of approved correlation models that relate the results of the performance-based durability testing to the concrete service life, this category of testing can be used as comparative method to qualify the concrete durability.

7. Service life assessment models for chloride ingress

A more precise method of assessing the chloride ingress in concrete consists of service life assessment modeling. As the phenomenon of chloride diffusion in concrete is similar to concentration diffusion in porous material, Fick's second law is among the most used model, yet not the most accurate to simulate the concentration of chloride in a concrete. This model has, at the initial time, a maximum concentration at the concrete surface. The concentration throughout the depth of concrete is defined as a function of surface concentration, time, and Chloride diffusion

coefficient. Although several models rely on Fick's second law, this model has presented several pitfalls as listed below [54]:

- Non-saturated conditions are not considered
- Cracks are not included,
- Absorption is neglected
- Chloride binding is neglected
- Surface chloride is not well defined
- Models for coating, sealers, inhibitors, coated reinforcement, etc. are not well implemented

In the past decades, several researches have been conducted to model chloride ingress in concrete. Some of the main models are discussed in the following sections.

7.1. LIFE 365 Model

LIFE 365 [1] is a software developed by concrete companies and available for free download on the internet, it is based on Fick's second law. The software includes several simplifications and takes into account the chloride ingress as sole type of deterioration. Validation is based on laboratory data only and the program uses standardized concrete properties.

The empirical equations for the diffusion coefficient were based on Toronto University report [5]. At reference temperature, the coefficient of diffusion is defined in LIFE365 as follows:

$$D(t) = D_{ref}\left(\frac{t_{ref}}{t}\right)^{m} \tag{1.9}$$

Where *D(t)* is the diffusion coefficient at time *t*, D_{ref} is the diffusion coefficient at time t_{ref} (equal to 28 days in Life-365), and *m* is the diffusion decay index, a constant.

Life 365 assumes that the diffusion coefficient reaches a constant value after 25 years. This assumption was taken into consideration to prevent the coefficient from excessive decrease. To take into consideration the temperature, LIFE 365 assumes the following equation:

$$D(T) = D_{ref}.\exp\left[\frac{U}{R}\left(\frac{1}{T_{ref}} - \frac{1}{T}\right)\right] \tag{1.10}$$

where $D(T)$ is the diffusion coefficient at time t and temperature T, D_{ref} is the diffusion coefficient at time t_{ref} and temperature T_{ref} which is equal 293K, U is the activation energy of the diffusion process (35000 J/mol), R is the gas constant, and T is the absolute temperature (K).

The solution for time to initiation of corrosion is carried out using a finite difference implementation of Fick's second law equation where the value of D is modified at every time step using equations (1.9) and (1.10). Two important parameters need to be defined in this case:

- The maximum surface concentration: It is either tested as per ASTM C1556 or input based on a known data base.

- The diffusion coefficient reference and Decay "m": It is a function of the cement content and the supplementary cementitious materials as follows:

$$D_{28} = 1 \times 10^{(-12.06 + 2.40w_c)} \quad (\text{m}^2/\text{s}) \tag{1.11}$$

$$D_{SF} = D_{PC} e^{-0.165SF} \tag{1.12}$$

$$m = 0.2 + 0.4\left(\frac{\%FA}{50} + \frac{\%SG}{70}\right) \tag{1.13}$$

where SF is the percentage of Silica Fume (Valid up to 15%), FA is the percentage of Fly Ash (valid up to 50%), and SG is the percentage of Slag (valid up to 70%)

7.2. ConcreteWorks

ConcreteWorks model [1] is based on Fick's second law and developed by Texas Department of Transportation. It considers the chloride ingress without any other deterioration phenomena. The model assumes standard properties based on the mix information and no approach was made to link the performance to neither validated laboratory tests nor to field test results.

The Fick's second law used in this model is as follows:

$$\frac{\partial}{\partial x}\left(D_c \frac{\partial c}{\partial x}\right) + \frac{\partial}{\partial y}\left(D_c \frac{\partial c}{\partial y}\right) + \frac{\partial}{\partial z}\left(D_c \frac{\partial c}{\partial z}\right) = \frac{\partial c}{\partial t} \tag{1.14}$$

where D_c is the diffusion coefficient and c is the concentration.

Equation (1.14) assumes that the concrete is uncracked, saturated, the density is constant, and that diffusion is the only mass transport mechanism, i.e. the mass transport from any temperature gradient or pressure gradient is negligible [6].

The diffusion coefficient is mainly based on the water to cementitious material ratio as follows:

$$D_{28} = 2.17 \times 10^{-12} \times e^{\frac{w_c}{0.279}} \tag{1.15}$$

where D_{28} is the chloride diffusion at 28 days and w_c is the water to cementitious material ratio. The following formulas should be taken into consideration to introduce the effect of time, cementitious materials, and temperature:

$$D(t) = D_{28} \times \left(\frac{28}{t}\right)^m + D_{ult} \times \left(1 - \left(\frac{28}{t}\right)^m\right) \tag{1.16}$$

$$D_{ult} = D_{28} \times \left(\frac{28}{36500}\right)^m \tag{1.17}$$

$$D(t,T) = D(t) \exp\left[\frac{U}{R} \times \left(\frac{1}{T_{ref}} - \frac{1}{T}\right)\right] \tag{1.18}$$

$$m = 0.26 + 0.4\left(\frac{FA}{50} + \frac{SG}{70}\right) \tag{1.19}$$

$$\frac{D_{UFFA}}{D_{PC}} = 0.170 + 0.829e^{-UFFA/6.07} \quad (1.20)$$

$$\frac{D_{SF}}{D_{PC}} = 0.260 + 0.794e^{-SF/2.51} \quad (1.21)$$

where $FA, SG, SF, and\ UFFA$ are respectively the fly ash replacement by weight of cement (%), the Slag replacement by weight of cement (%), the silica fume replacement by weight of cement (%), and the ultra-fine fly ash replacement by weight of cement (%).

7.3. 4SIGHT

The 4SIGHT model, published in 1995, was developed as a resource for estimating the service life of new underground concrete structures [7]. The model was the first to use combined numerical models for ion transport, chemical reaction, and subsequent changes to transport coefficients to model the response of a concrete structure to its environment. This model is specific in its concept as it models ions transportation.

The input in this software includes the material properties and the concentration of different ions in the nearby environment. The input are as follows:

- Ions: H, Ca, Na, K, OH, Cl, SO_4, and CO_3. These parameters are defined either as internal or external.
- Salts: NaCl, CaOH, and $NaSO_4$. These parameters are defined either as internal or external.
- The concrete water-cement ratio
- The degree of hydration α
- The concrete porosity, calculated as:

$$\emptyset = \frac{1+1.31\alpha}{1+3.2w_c} \quad (1.22)$$

- The concrete chloride diffusion coefficient, simply taken as a function of the water cement ratio as follows:

$$log_{10}D_{Cl-} = 6.0w_c - 13.84 \quad [\textbf{Error! Bookmark not defined.}] \quad (1.23)$$

- The concrete permeability is calculated as:

$$k = 10^{5.0w_c} \times 10^{-21}m^2 \quad (1.24)$$

- The concrete thickness
- The crack width, depth and spacing
- Joint width, spacing, life expectancy, and permeability

This model includes multiple degradation by relying of the ions transportation equation. At the core of the model is the advection-Diffusion equation as follows:

$$j = -D\nabla_c + cu \quad (1.25)$$

Where, j is the flux, c is the ion concentration, D is the effective diffusion coefficient, u is the average pore fluid velocity.

The rate of change in concentration is given as follows:

$$\frac{\partial c}{\partial t} = \nabla . D \nabla_c - u \nabla_c \tag{1.26}$$

The equation is solved by finite difference techniques. The ion transportation equation was verified through an inert ceramic rather than concrete to prevent any chemical reactions that mislead the findings.

7.4. CHLODIF++

CHLODIF++ [1] is created by the Engineering Institute of Croatia based on Fick's second law. The validation was made based on laboratory test results. The model used in CHLODIF++ follows the below equation [8]:

$$c(x,t) = [c_0 + k(t-1)]\left(1 - erf\frac{x}{2\sqrt{\tau}}\right) + k\left[\left(1 + \frac{x^2}{2\tau_1}\right)\left(1 - erf\frac{x}{2\sqrt{\tau_1}}\right) - \frac{x}{\sqrt{\pi\tau_1}}e^{\frac{-x^2}{4\tau_1}}\right] \tag{1.27}$$

When c_0 reaches the maximum concentration $c_0 = c_{max}$ the equation used is as follows:

$$C(x,t) = c_0\left(1 - erf\frac{x}{2\sqrt{\tau}}\right) \tag{1.28}$$

where c_0 is the initial chloride concentration, c_{max} is the maximum surface chloride concentration, k is the coefficient of linear increase in c_0, t is the time effect, erf is the error function, x is the clear cover depth, and τ is the factor that accounts for the variation of the chloride diffusion coefficient D. The factor τ is given by:

$$d\tau = D(t)dt \quad \text{thus} \quad \tau = \int_0^t D(s)ds \tag{1.29}$$

The chloride diffusion coefficient is given by:

$$D = D_{w_c} \times f_{int}(SF, SG, FA, SP, Cu, Cr) \times f_{ext}(t, T, RH, W_s, C_s) \tag{1.30}$$

where D_{w_c} is the chloride diffusion coefficient based on the water-cement ratio and given by the below formula:

$$D_{w_c} = 5 \times 10^{-13} \times e^{4.8708(w_c)} \tag{1.31}$$

$f_{int}(SF, SG, FA, SP, Curing, Crack)$ is the internal parameters function which depends on the silica fume content SF, slag content SG, fly ash content FA, super plasticizer in concrete SP, curing time Cu, and cracks Cr). f_{int} is given in Table 1.4:

Table 1.4 - Internal Parameters Function

f_{int}	**Influence**
1 - 1.35	Sulphates
0.5 - 1	Increase of C3A Quantity
0.4 – 0.9	Addition of Fly Ash
0.08 – 0.12	Addition of Silica Fume
0.3	Addition of Slag
0.8	Addition of Superplasticizer
1 – 1.3	Cracking of Concrete under Basic Loads
0.04	Embedding in Fabric Formwork

$f_{ext}(t, T, RH, W_s, C_s)$is the external parameters function that depends from the time t, temperature T, relative humidity RH, wind effects W_s, and the chloride surface concentration C_s. f_{ext} is given by the equation (1.32).

$$f_{ext}(t, T, RH, W_s, C_s) = \left(\frac{t_{ref}}{t}\right)^m \times exp\left[\frac{U}{R} \times \left(\frac{1}{T_{ref}} - \frac{1}{T}\right)\right]\left[1 + 256\left(1 - \frac{RH}{100}\right)^4\right]^{-1} \quad (1.32)$$

where t is the actual age of concrete in years, t_{ref} is the reference age from which the initial chloride diffusion coefficient is derived, U is the activation energy of the diffusion process in J/mol, R is the universal gas constant in J/mol.K, RH is the relative humidity, T_{ref} is the reference temperature in K, and T is the average temperature of each month in K. The coefficient m is given by equation (1.33):

$$m = 0.0075 \times MA(\%) + 0.30 \quad (1.33)$$

where MA is the percentage of mineral addition similar to Fly Ash, Micro Silica, and Slag.

According to Oslakovic et al. [9] CHLODIF gives greater differences in the results and an unrealistic range of the initiation period.

7.5. ClinConc

ClinConc [1] is another chloride diffusion model in concrete. It takes as a constant input, the chloride diffusion value resulting from the Nordic Standard Rapid Migration test NT BUILD 492 at 6 months. The other inputs are binding potential, time, and temperature. ClinCon is thus based on a performance-based durability testing conducted at an age of 6 months and yielding the actual concrete chloride diffusion coefficient. ClinCon's main diffusion equation is defined as follows [2]:

$$\frac{c}{c_s} = 1 - \text{erf}\left(\frac{x}{2\sqrt{D_a t}}\right) \quad (1.34)$$

where c is the concentration of dissolved (free) chloride in the pore solution within the concrete cover, c_s is the concentration of the chloride at the exposed concrete surface, x is the distance, t is the duration of chloride exposure and D_a is the apparent chloride diffusion coefficient, given by:

$$D_a = \frac{D_0}{1-n}\left(\frac{t_0'}{t}\right)^n \left[\left(1+\frac{t_{ex}'}{t}\right)^{1-n} - \left(\frac{t_{ex}'}{t}\right)^{1-n}\right] \quad (1.35)$$

where D_0 is the diffusion coefficient at the concrete age t_0', t is the duration of chloride exposure, n is the age factor, and t_{ex}' is the age of concrete at the start of exposure.

The age factor is attributed to the increase in chloride binding capacity as follows:

$$n = -0.45a_t^2 + 0.66a_t + 0.02 \quad (1.36)$$

where $a_t$is a constant. The typical value of a_t is 0.36 [3] but may vary between 0.1 and 0.6.
The diffusion coefficient at the concrete age t_0' is calculated as follows:

$$D_0 = \frac{1+0.59K_{b6m}}{1+\frac{\partial c_b}{\partial c}}.D_{6m}.k_{TD} \quad (1.37)$$

where D_{6m} is the coefficient measured at an age of 6 months using the Nordic Standard Rapid Migration test NT BUILD 492. This parameter is used an input constant value. K_{TD} is the temperature factor for the diffusion coefficient, c_b is the bound chloride and $\frac{\partial c_b}{\partial c}$ is the chloride binding capacity. K_{TD} is the given by the formula:

$$K_{TD} = e^{\frac{E}{R}\left(\frac{1}{T_0}-\frac{1}{T}\right)} \quad (1.38)$$

where E is the activation energy of the diffusion coefficient, T_0 is the temperature in the laboratory condition, T is the exposure condition, and R is the natural gas constant.

K_{b6m} is given by:

$$K_{b6m} = \frac{W_{gel6m}}{1000\varepsilon_{6m}} \quad (1.39)$$

where W_{gel6m} is the gel content in kg/m^3 and ε_{6m} is the water accessible porosity. The term 6m denotes the time at 6 months.

7.6. DuraCrete

DuraCrete [1][4] is a durability assessment methodology based on Fick's second law. It is a probabilistic performance-based durability design model that uses performance requirements, reliability index, and desired time of corrosion initiation. The service limit state, given by the below equation, should be satisfied [4]:

$$p_{dep.} = p\{c_{crit} - c(a, t_{SL}) < 0\} < p_0 \quad (1.40)$$

where $p_{dep.}$ is the probability that depassivation occurs, c_{crit} critical chloride content [wt. -%/binder content], $c(a, t_{SL})$ chloride content at depth a and time t [wt. -%/binder content], a is the concrete cover in mm, t_{SL} is the design service in years, and p_0 is the target failure probability given in Table 1.5:

Table 1.5 - Recommended Values for p_0

Exposure Class – Eurocode 2	Description	Reliability Class	SLS	ULS
			Depassivation	Collapse
XD	Deicing Salt	RC1	0.1	10^{-4}
		RC2	0.1	10^{-5}
		RC3	0.1	10^{-6}
XS	Seawater	RC1	0.1	10^{-4}
		RC2	0.1	10^{-5}
		RC3	0.1	10^{-6}

The function that defines the chloride content at a depth x, and a time t is given by:

$$c(x,t) = c_0 + \left(c_{S,\Delta x} - c_0\right)[1 - erf\,\frac{a-\Delta x}{2\sqrt{D_a.t}}] \tag{1.41}$$

where $c(x,t)$ is the chloride content in the concrete at depth x, and time t, c_0 is the initial chloride concentration, $c_{S,\Delta x}$is the chloride content at depth Δx and a certain point of time t, Δx is the convection zone which is the concrete layer up to which the process of chloride penetration differs from Fick's 2nd law of diffusion in mm, erf is the error function, t is the time in years, and D_a is the apparent chloride diffusion coefficient through concrete in mm^2/ year.

The chloride diffusion coefficient in DuraCrete is given by the below equation:

$$D_a = k_e D_{RCM,0} k_t \left(\frac{t_0}{t}\right)^a \tag{1.42}$$

where k_e is the environmental transfer variable, $D_{RCM,0}$ is the chloride migration coefficient, k_t is the transfer parameter, t is the time in years, t_0 is the reference point of time in years, and a is the aging exponent.

The environmental variable k_e is given by:

$$k_e = \exp\left(b_e\left(\frac{1}{T_{ref}} - \frac{1}{T_{real}}\right)\right) \tag{1.43}$$

where b_e is the regression variable, it varies between 3500K and 5500K; it can be described as a normal distribution curve where the mean value is 4800 and the standard deviation is 700. T_{ref} is the reference temperature of 283K and T_{real} is the actual temperature in Kelvin, T_{real} can be described as a normal distribution curve with an average and a standard deviation that are based on the weather station data.

The chloride migration coefficient is a normally distributed variable with a standard deviation equal to 0.2 times the mean value that should be tested in reference to NT Build 92 (Performance Based Durability testing) or quantified as per table 1.2 above.

The transfer variable k_t is set to 1 to carry out the quantification of the aging exponent a as per Table 1.6 [4]. The variable a is also a normal distribution curve with mean value, standard deviation, and upper and lower bounds.

Table 1.6 - Quantification of the Aging Exponent

Concrete	Aging Exponent a			
	Mean Value	Standard Deviation	Lower Bound	Upper Bound
Portland Cement Concrete CEM I; 0.4≤w/c≤0.6	0.3	0.12	0.0	1.0
Portland Fly Ash Cement Concrete f≥0.2.z; k=0.5; 0.4≤w/c≤0.62	0.6	0.15	0.0	1.0
Blast Furnace Slag Cement Concrete CEM III/B; 0.4≤w/c≤0.6	0.45	0.20	0.0	1.0

7.7. HETEK

HETEK [1] model was developed by the Danish Technological Institute and based on Fick's second law. The chloride diffusion coefficient was solely related to the water-cement ratio as developed by Frederisken et al [10]. Frederisken et al used a testing campaign that included the chloride diffusion test (NT Build 443) on an identical mix with seven different water cement ratios going from 0.3 to 0.6 with a 0.05 step. Figure 1.5 illustrates the results. The equation relating the chloride diffusion coefficient to the water-cement ratio is as follows:

$$D_{28} = 50000 \times e^{-\sqrt{10/(w_c)}} \qquad (mm^2/year) \qquad (1.44)$$

where D_{28} is the chloride diffusion at 28 days and w_c is the water-cement ratio.

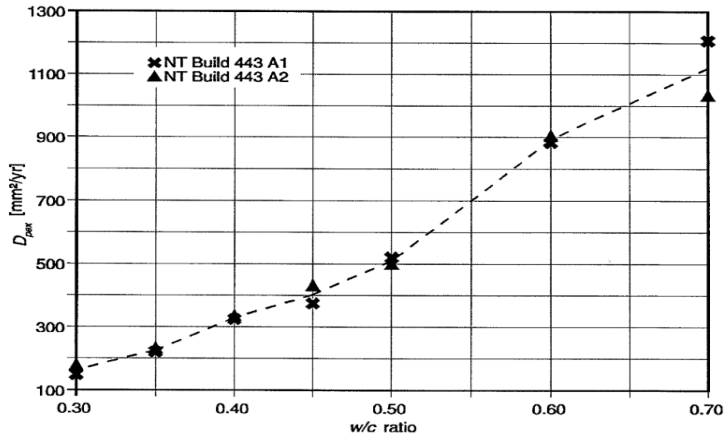

Figure 1.5 - Chloride diffusion coefficient as a function of W_c (Frederisken et al)

7.8. STADIUM Model

STADIUM [1] is a software for durability assessment developed by SIMCO, based on the transportation laws of chemical species in cementitious materials. The software takes into consideration the concrete properties and conducts three laboratory tests as a basis of analysis. The remaining analysis is made based on the concrete composition. The three laboratory tests include the Volume of Permeable Voids (ASTM C642), Migration Test for Ion transport properties (ASTM C1202), and drying test for moisture transport properties (ASTM C1792). The base equation in the model is as follows:

$$\frac{\partial c_i^b}{\partial t} + \frac{\partial w c_i}{\partial t} - div\left(D_i grad(c_i) + \frac{D_i z_i F}{RT} w c_i grad(\varphi) + D_i w c_i grad(ln\gamma_i) + \frac{D_i c_i ln(\gamma_i c_i)}{T} w grad(T) + c_i D_w grad(w)\right) = 0 \quad (1.45)$$

where c_i^b is the binded chloride, c_i is the free chloride, t is the time, D_i is the chloride diffusion coefficient, T is the temperature, z_i is the valence of the ionic species (chloride), F is Faraday's constant, R is the universal gas constant, w is the moisture capacity, φ is the electrodiffusion coupling, and γ_i is the chemical activity. The model does not take into consideration the cracking mechanism of concrete and the corresponding restraint strain. The accurate final Stadium model is not shared for public. The different calculation of the parameters taken in the service life calculation are not as well shared for public.

While Stadium's model takes into consideration all these transport mechanisms, the studies made by Luciano and Miltenberger states the following [11]: In certain situations (e.g., marine splash and tidal zones) the combined effects of diffusion, sorption, and convection can significantly increase the chloride content of the concrete and lead to a calculated value of the apparent chloride diffusion coefficient that is several times larger than the true (effective) diffusion coefficient. The relative influence of these alternate chloride transport modes depends largely on environmental factors and should be modeled separately. Steady-state diffusion tests eliminate the influences of the alternate chloride transport modes by maintaining saturation but still require multiyear

exposure periods to obtain reliable chloride diffusion coefficient estimates in high-quality concrete.

8. Literature Review of Chloride Diffusion Coefficient Calculation Models

In addition to the available models, explained in section 7, many research works were developed in an attempt to tailor the chloride diffusion coefficient. In a nutshell, most of the available literature works use Fick's Second law in a modified form to take into consideration the affecting parameters [34]: temperature, porosity, cementitious material types, cation type associated with the chloride ion Cl^-, moisture content, and curing conditions. The proposed diffusion coefficient is expressed by correcting the value $D_{c,ref}$ at a temperature of 23℃, an age of 28 days, and a relative humidity of 100% as per the following:

$$D_c = D_{c,ref}.f_1(T).f_2(t_e).f_3(h).f_4(x) \qquad (m^2/s) \qquad (1.46)$$

where, D_c is the Diffusion Coefficient, $D_{c,ref}$ is the reference diffusion coefficient at an age of 28 days, and a temperature of 23℃, and a 100% relative humidity, $f_1(T)$ considers the dependence of D_c on temperature, $f_2(t_e)$ considers the decrease of D_c on increasing degree of hydration, $f_3(h)$ relates the diffusion coefficient D_c on concrete pore relative humidity, and $f_4(x)$ relates the diffusion coefficient D_c on the distance from the surface. This parameter takes into consideration that the binder content on the surface is higher than the concrete binder in the concrete. Two other functions were introduced by Xi and Bazant [27] to take into consideration the effect of the aggregate content and the effect of the free chloride concentration as described in section 8.1.7.

At a certain time t, the chloride diffusion coefficient is calculated using this model, based on a reference chloride diffusion coefficient corrected by influence functions. These functions consider the temperature, humidity, maturity, and depth. Not all the tailoring function were defined in all the publication works, as can be seen in the following sections.

8.1. Reference Chloride Diffusion Coefficient

8.1.1. Model Proposed by Luciano and Miltenberger

The database used in the works of Luciano and Miltenberger [11] provides a representative sampling of commercial ready-mixed and laboratory concrete made throughout the United States. The samples populating this database were produced by several ready-mixed concrete producers using their materials in addition to concrete produced from three laboratories. All samples were cured under standard laboratory conditions and were saturated prior to testing. Luciano and Miltenberger used an accelerated method to correlate the chloride diffusion coefficient. The data included a total of 241 concrete mixes made using different water-cement ratios, cement contents, silica fume contents, fly ash contents, slag contents, curing times, concrete temperatures, and

aggregate types (angular or rounded). The details of the chloride diffusion values versus each mix design were not available in the publication. The following figure was however extracted:

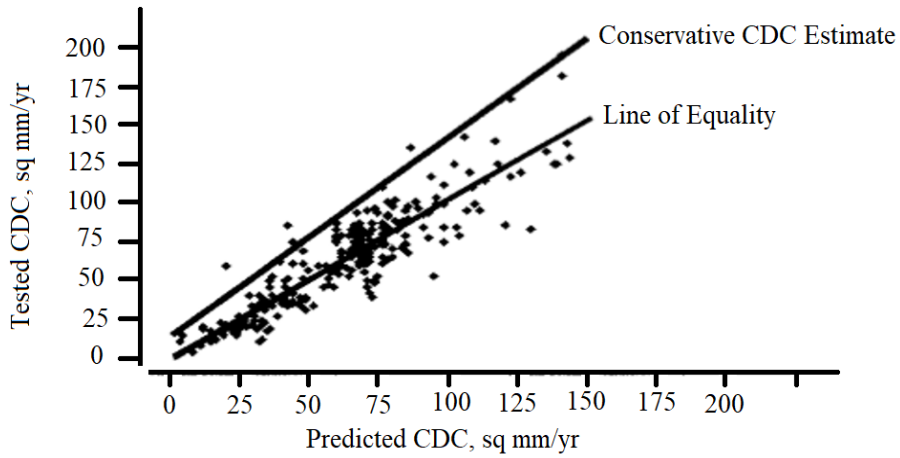

Figure 1.6 – Tested Versus Predicted Chloride Diffusion Coefficient [Error! Bookmark not defined.**]**

The resulting equation further to a multiple regression analysis is as following:

$$D_p = (5.760 + 5.810x_1 - 0.567x_2 - 1.323x_3 + 0.740x_4 - 2.117x_5 - 2.780x_6 + 0.254x_7 - 0.368x_8 + 1.071x_1x_4 - 2.891x_1x_6 - 1.503x_4x_6)^2 \quad (m^2/s) \quad (1.47)$$

where D_p is the predicted chloride diffusion coefficient, mm^2/yr, x_1 is the water cement ratio function define in equation (1.48), x_2 is the cementitious materials content function defined in equation (1.49), x_3 is the silica fume mass function defined in equation (1.50), x_4 is the fly ash mass function defined in equation (1.51), x_5 is the slag mass function defined in equation (1.52), x_6 is the curing time function defined in equation (1.53), x_7 is the concrete temperature function defined in equation (1.54), and x_8 is the aggregate shape function which is equal to 1 if angular aggregate is used and 0 if rounded aggregate is used.

$$x_1 = (w/cm - 0.45)/0.2 \quad (1.48)$$

$$x_2 = (cementitious\ materials\ content, kg/m3 - 425)/175 \quad (1.49)$$

$$x_3 = (Silica\ Fume\ mass\ \%\ of\ cementitious\ materials - 5)/5 \quad (1.50)$$

$$x_4 = (Fly\ ash\ mass\ \%\ of\ cementitious\ materials - 22.5)/22.5 \quad (1.51)$$

$$x_5 = (Slag\ mass\ \%\ of\ cementitious\ materials - 35)/35 \quad (1.52)$$

$$x_6 = Log10(Curing\ time\ in\ days - 2)/3 \quad (1.53)$$

$$x_7 = (Concrete\ temperature, C - 24)/14 \quad (1.54)$$

The range of application of this equation includes the limitations defined in Table 1.7:

Table 1.7 - Equation 26 Range of Application

Parameter	**Minimum Value**	**Maximum Value**
Water-Cementitious Material	0.25	0.65
Cementitious Materials Content	250 Kg/m^3	600kg/m^3
Silica Fume Percentage	0%	10%
Fly Ash Percentage	0%	45%
Slag Percentage	0%	70%
Curing Time	3 days	100 days
Concrete Mixture Temperature	10°C	38°C
Aggregate Shape	Binary: Angular or Rounded	

If the above equation is applied on the far end concrete mixes eventually considered in this study, as follows:

- The first concrete mix having a cement content of 250kg/m^3 and a water cement ratio of 0.7

- The second concrete mix with a cement content 500kg/m^3, a silica fume of 10%, and a fly ash content of 50%.

The results of the chloride diffusion coefficient will be equal to $9.71 \times 10^{-12}\, m^2/s$ and $1.3 \times 10^{-12} m^2/s$ respectively. The error considered in ASTM C1556 for measuring the chloride diffusion coefficient in a single laboratory is 39%. Therefore, an average value $of\ 5.41 \times 10^{-12}$ may be in reality varying between 3.3×10^{-12} and $7.5\ \times 10^{-12}$. The range of value given in this equation is thus very close to the deviation that may occur from a single test. The equation is therefore not adequately reliable to estimate the chloride diffusion coefficient since the range of chloride diffusion results is very narrow.

8.1.2. Model Proposed by Riding

Riding [12] has grouped different chloride diffusion calculations as a function of the water-cement ratio using a type I ordinary cement without any supplementary cementitious materials. Figure 1.7 shows the chloride diffusion coefficient according to the model proposed by Riding:

$$D_{28} = 2.17 \times 10^{-12} e^{(\frac{w}{c})/0.279} \qquad (m^2/s) \qquad (1.55)$$

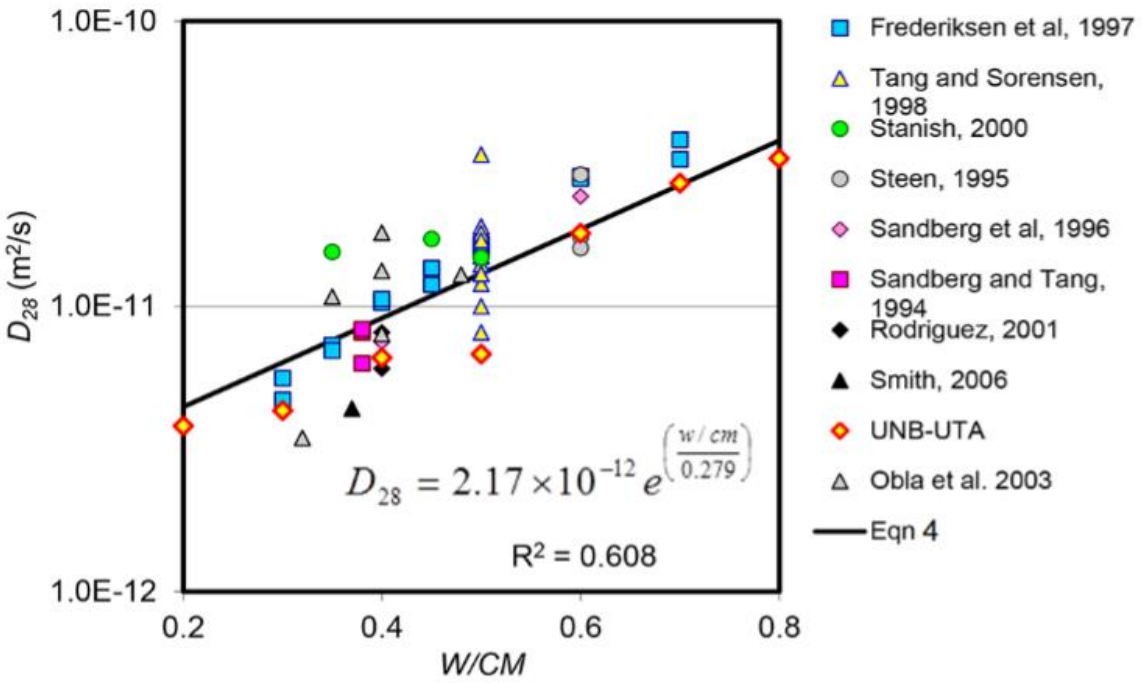

Figure 1.7 - Chloride diffusion coefficient as a function of the water-cement ratio

As seen from the graph above, the chloride diffusion equation was based on the work of ten different researchers. These ten researches are briefly presented below:

- The work conducted by Frederisken et al [13] was described in the previous section.
- The work conducted by Tang and Sorensen [14] where the chloride diffusion coefficient test (NT Build 443) was made on three mixes in five different laboratories in an attempt to calculate the precision of this test method. The cement used is CEM I with a C3A content below 5%.
- The chloride diffusion test results from the works conducted by Stanish and Thomas [15].
- The chloride diffusion test results from the works conducted by Steen [16].
- The data collected from the works conducted by Sandberg et al. [17] and shown in Riding model include a set of chloride diffusion test results. These test results were based on 13 concrete mix exposed to laboratory and field conditions for durations of 5 months, 1 year, and 2 years.
- The chloride diffusion test results from the works conducted by Sandberg and Tang [18].
- Some of the chloride diffusion test results were taken from the works conducted by Rodrigez [19], rather than a specific model.
- The grouping of the chloride diffusion test results from the works conducted by Smith [20].
- The test results noted as UNB-UTA were chloride diffusion test results collected from the University of New Brunswick and the University of Texas at Austin [12].

- The works conducted by Obla et al [22] and described in figure 1.7 included the chloride diffusion test results of several mixes with different cementitious material types. Excluding the ones with fly ash and micro silica, one mix included only Portland cement, was tested at 28 days, as described in the table below. The C3A in the cement used was equal to 11%.

8.1.3. Model Proposed by Hobbs and Mattews

Hobbs and Mattews [23] have developed the below formula for marine environment (Type 1 cement):

$$D = 0.04 \times 1166 \times w_c \times 10^{-12} \tag{1.56}$$

This formula was based on the chloride diffusion test results conducted by a group of researchers as illustrated in Figure 1.8:

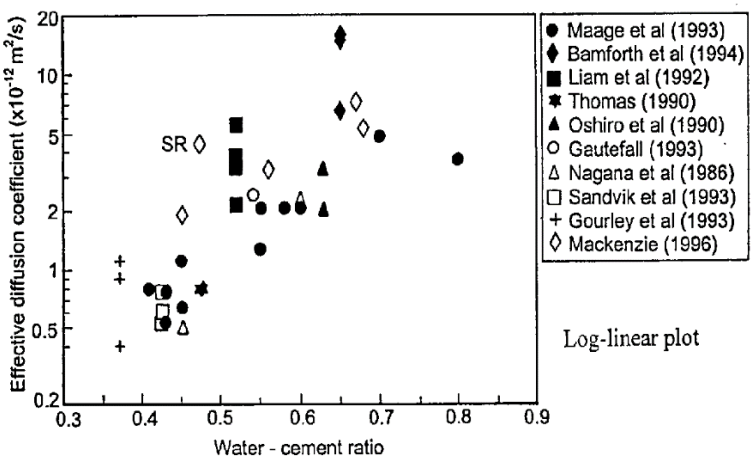

Figure 1.8 - Model proposed by Hobbs and Mattews

8.1.4. Model Proposed by Sague and Crank

Sague and Crank [24] have developed the below formula for marine environment, it was developed for decay old structures:

$$D = 3 \times \left(\left(1 + \frac{w_c - 0.32}{0.09}\right)\left(1 + \frac{446 - 1.69Cem}{56}\right)\right) \text{ (in}^2\text{/year)} \tag{1.57}$$

where w_c is the water-cement ratio and Cem is the cement content in kg/m^3.

8.1.5. Model Proposed by Malikakkal

Malikakkal [25] has published the below formula for general ordinary Portland cement concrete.

$$D = (82.7 - 426 \times w_c + 568.4(w_c)^2 + 4.26\,(Cem/350)^{-6}) \times 10^{-12} \tag{1.58}$$

where w_c is the water-cement ratio and Cem is the cement content in kg/m^3.

8.1.6. Model Proposed by Papadakis et al

Papadakis et al [26] have proposed a model based on a detailed testing campaign. This model has taken into consideration the type of chloride, i.e. sodium chloride or calcium chloride. It also took into consideration the density of cement, density of aggregate, aggregate content, and cement content. The cement's tricalcium aluminate used in this testing campaign was 8%. The diffusion coefficient is given by:

$$D_{ref} = D_{H_2O} \times 0.15 \times \frac{1+\rho_c w_c}{1+\rho_c w_c + \frac{\rho_c \ a}{\rho_a \ Cem}} \left(\frac{\rho_c w_c - 0.85}{1+\rho_c w_c}\right)^3 \quad (1.59)$$

where D_{H_2O} is the diffusion coefficient of chloride ion in infinite solution (equal to 1.6 x10^{-9} m^2/s for NaCl and 1.3 x10^{-9} m^2/s for CaCl2), ρ_c is the specific gravity of cement, ρ_a is the specific gravity of aggregate, a is the aggregate content (kg), Cem is the cement content (kg), and w_c is the water cement-ratio.

8.1.7. Model Proposed by Xi and Bazant

The model proposed by Xi and Bazant [27] is defined by the following formula based on the water-cement ratio and the curing time. The chloride diffusion coefficient is corrected for the aggregate volume, temperature, humidity, and dependence of the chloride diffusion coefficient on the free chloride concentration.

$$D_{cl} = f_{1'}(w_c\ , t_0) f_{2'}(g_i) f_{3'}(H) f_{4'}(T) f_5(C_f) \quad (1.60)$$

where $f_{1'}$, $f_{2'}$, $f_{3'}$, $f_{4'}$ and $f_{5'}$ are functions that depends on the water-cement ratio and time of curing, aggregate content, humidity, temperature, and dependence of the chloride diffusion coefficient on the free chloride concentration, respectively. The function $f_{3'}(H)$ is described in section 8.4 whereas the remaining functions are calculated as follow:

$$f_{1'}(w_c\ , t_0) = \left(\frac{28-t_0}{62500}\right) + \left(\frac{1}{4} + \frac{(28-t_0)}{300}\right)(w_c\ )^{6.55} \quad (1.61)$$

where w_c and t_0 are the water-cement ratio and curing time, respectively.

$$f_{2'}(g_i) = D_{cp}\left(1 + \frac{g_i}{\frac{[1-g_i]}{3} + \frac{1}{\left[\left(\frac{D_{agg}}{D_{cp}}\right)-1\right]}}\right) \quad (1.62)$$

where g_i is the volume fraction of the aggregate in concrete, D_{cp} is the chloride diffusion in the cement paste, and $D_{agg}$is the chloride diffusion in aggregate. Based on the literature [27], the cement paste chloride diffusion is either taken as 1.10^{-12} cm/s or evaluated based on the porosity,

surface area, and critical porosity using the below equation. The aggregate chloride diffusion is calculated using the same equation.

$$D = \frac{2(1-(V_p - V_p^C))}{S^2}(V_p - V_p^C)^{4.2} \tag{1.63}$$

where V_p is the porosity, S is the surface area, and V_p^C is the critical porosity (the porosity at which the pore space is first percolated).

$$f_{4'}(T) = \exp\left[\frac{U}{R}.\left(\frac{1}{T_{ref}} - \frac{1}{T}\right)\right] \tag{1.64}$$

where U is the activation energy of the chloride diffusion process (Kj/mol), R is the gas constant in (kJ/K·mol), T_{ref} is the reference absolute temperature at which the reference chloride diffusivity has been measured in (K), and T is the actual absolute temperature in the concrete (K).

$$f_{5'}(c_f) = 1 - 8.333(c_f)^{0.5} \tag{1.65}$$

where c_f is the free chloride concentration.

8.2. Temperature Effect

The term related to the temperature effect noted as $f_1(T)$ in equation (1.46), has two forms defined in the literature [28][29] as follows:

$$f_{1a}(T) = \exp\left[\frac{U}{R}.\left(\frac{1}{T_{ref}} - \frac{1}{T}\right)\right] \tag{1.66}$$

and

$$f_{1b}(T) = \frac{T}{T_{ref}}\exp\left[\frac{U}{R}.\left(\frac{1}{T_{ref}} - \frac{1}{T}\right)\right] \tag{1.67}$$

where U is the activation energy of the chloride diffusion process (Kj/mol), R is the gas constant in (kJ/K·mol), T_{ref} is the reference absolute temperature at which the reference chloride diffusivity has been measured in (K), and T is the actual absolute temperature of the concrete (K).

Page et al. [55] reported the activation energies for the chloride diffusion process in Portland cement pastes of 41.8, 44.6, and 32.0 kJ/mol for water-to-cementitious ratios as 0.4, 0.5, and 0.6, respectively.

In order to have an accurate representation of the diffusion dependence of temperature, the heat transfer across the concrete section should be modeled. This function depends on the concrete depth, ambient temperature and time. The temperature at any point (x, y) in concrete can be modeled using Fourier heat conduction law. The temperature profile is then determined by applying the energy conservation requirement:

$$Q_c C_q \frac{\partial T}{\partial t} = \frac{\partial}{\partial x}\left(-\gamma \frac{\partial T}{\partial x}\right) + \frac{\partial}{\partial y}\left(-\gamma \frac{\partial T}{\partial y}\right) \qquad (w/m^3) \tag{1.68}$$

where Q_c is the density of concrete (kg/m^3), C_q is the concrete specific heat capacity (J/kg.℃), and T is the temperature at depth (x, y) (℃) at time t.

8.3. Concrete maturity Effects

From reviewing experimental data mainly on marine structures, various researchers have proposed a similar mathematical description of the decay. The term related to the maturity effect noted as $f_2(t)$ in equation 1.46 is thus as follows [29][30][31]:

$$f_2(t) = \left[\frac{t_{ref}}{t}\right]^n \tag{1.69}$$

$$f_2(t) = \frac{1}{1-n}\left[\frac{t_{ref}}{t}\right]^n \tag{1.70}$$

$$f_2(t) = \frac{1}{1-n}\left[\left(1+\frac{t_c}{t}\right)^{(1-n)} - \left(\frac{t_c}{t}\right)^{(1-n)}\right]\left[\frac{t_{ref}}{t}\right]^n \tag{1.71}$$

$$f_2(t) = \left[\frac{t_{ref}}{t}\right]^n + \left(\frac{28}{36500}\right)^n \left(1 - \left[\frac{t_{ref}}{t}\right]^n\right) \tag{1.72}$$

$$f_2(t) = \begin{bmatrix} \left(\frac{180}{t}\right)^{\beta} & for\ t < 180\ days \\ 1 & for\ t > 180\ days \end{bmatrix} \tag{1.73}$$

where t_{ref} is the reference time, t is the time the factor t_c is the curing time, the term β range between 0.3 and 0.5, and the factor n is calculated as per equation (1.74):

$$n = 2.5 \times (w_c) - 0.6 \tag{1.74}$$

Bamforth [30] has proposed other values for "n" as follows:

n = 0.264 for ordinary Portland Cement
n = 0.699 for Fly Ash Concrete
n = 0.621 for Micro Silica Concrete

8.4. Concrete Humidity Effect

The relative humidity in the pores plays an important role on the chloride diffusion coefficient. The model therefore proposed by Saetta et al. [32] includes an empirical relationship wherein chloride diffusivity decreases with the decrease in the concrete pore relative humidity:

$$f_3(h) = \left[1 + \frac{(1-h)^4}{(1-h_c)^4}\right]^{-1} \tag{1.75}$$

where h is the relative humidity in the pores and h_c is the humidity at which the chloride diffusion drops to its halfway between the minimum and the maximum. This value was experimentally demonstrated to be equal to 0.75 by Bazant and Najjar [33].

8.5. Effect of the Concrete Properties Variation with Depth

As the concrete surface incudes a higher percentage of binder when compared to the remaining part of concrete, the model defined for the corresponding effect on the chloride diffusion coefficient is given by [34]:

$$f_4(x) = \begin{bmatrix} \varphi + (1-\varphi)\left(\frac{x}{x_s}\right)^{\beta} & for\ x < x_s \\ 1 & for\ x \geq x_s \end{bmatrix} \quad (1.76)$$

The factor φ is the ratio of the surface diffusivity over the bulk diffusivity of concrete, which is experimentally demonstrated [34] to range between 0.21 to 0.53. The factor x_s is the thickness of the member's surface zone that ranges from 20 mm to 40 mm. The factor β a constant equal to 0.68 [56].

9. Chloride diffusion coefficient models comparison

A total of fifteen models to calculate the chloride ingress in concrete and consequently identifying the corresponding concrete service life in chloride environment, were discussed in sections 7 and 8. Except for Stadium model, the different other models include the calculation of a chloride diffusion coefficient and correcting this value based on the actual temperature, humidity, maturity, and concrete depth, following Fick's second law. Different parameters were taken in each model. Table 1.8 summarized of the chloride ingress models. The models were also categorized based on whether they are empirical models or physical models, and whether the computational used is deterministic or probabilistic.

Table 1.8 shows the scatter in the influencing parameters that were taken among different models and researches. As the different models aims at calculating a chloride diffusion coefficient. A comparison between the different chloride diffusion coefficient yielded from the different models was made and presented in Figure 1.9. The different models discussed take as input different parameters. The water-cement ratio is however the only common parameters among these models. Figure 1.9 was thus built by keeping all the input parameters constant while varying only the water-cement ratio. The chloride diffusion coefficients in this figure was thus calculated as a function of the water-cement ratio. The cement content considered is 425 kg/m^3.

Table 1.8 - Chloride Ingress Models Properties Summary

Characteristics	LIFE 365	Concrete Works	4SIGHT	CHLODIF++	ClinConc	Duracrete	HEKTEK	Stadium	Luciano and Miltenberger	Riding	Hobbs and Matthews	Sangue and Crank	Malikakkal	Papadaki et al.	Xi and Basant
Equation Based on Fick's Second Law	X	X	-	X	X	X	X	-	X	X	X	X	X	X	X
Empirical Modeling Approach	X	X	X	X	-	X	X	-	X	X	X	X	X	X	X
Physical Modeling Approach	-	-	-	-	X	-	-	X	-	-	-	-	-	-	-
Deterministic Computational Approach	X	X	X	X	X	-	X	X	X	X	X	X	X	X	X
Probabilistic Computational Approach	X	-	-	-	-	X	-	-	-	-	-	-	-	-	-
Based on NT Build 492 Performance Test	-	-	-	-	X	X	-	-	-	-	-	-	-	-	-
Admixtures in Concrete	X	-	-	X	X	X	-	-	-	-	-	-	-	-	-
Porosity	-	-	X	-	X	-	-	X	-	-	-	-	-	-	-
Chloride Binding	-	-	-	-	X	-	-	X	-	-	-	-	-	-	X
Effect of W/C	X	X	X	X	X	X	X	Unknown	X	X	X	X	X	X	X
Effect of Cement Content	-	-	-	-	-	-	-		X	-	-	X	X	X	-
Effect of Cementitious Materials Type	X	X	-	X	X	X	-		X	-	-	-	-	-	-
Effect of Aggregate Volume	-	-	-	-	-	-	-		-	-	-	-	-	X	X
Effect of Aggregate Shape	-	-	-	-	-	-	-		X	-	-	-	-	-	-
Effects of Cracks	-	-	X	X	-	-	-	-	-	-	-	-	-	-	-
Chloride Type	-	-	-	-	-	-	-	Unknown	-	-	-	-	-	X	-
Specific Gravity of the Cement	-	-	-	-	-	-	-		-	-	-	-	-	X	-
Specific Gravity of the Aggregate	-	-	-	-	-	-	-		-	-	-	-	-	X	-
Initial Time of Curing	-	-	-	X	-	-	-		X	-	-	-	-	-	X
Effect of C3AContent	-	-	-	X	-	-	-		-	-	-	-	-	-	-

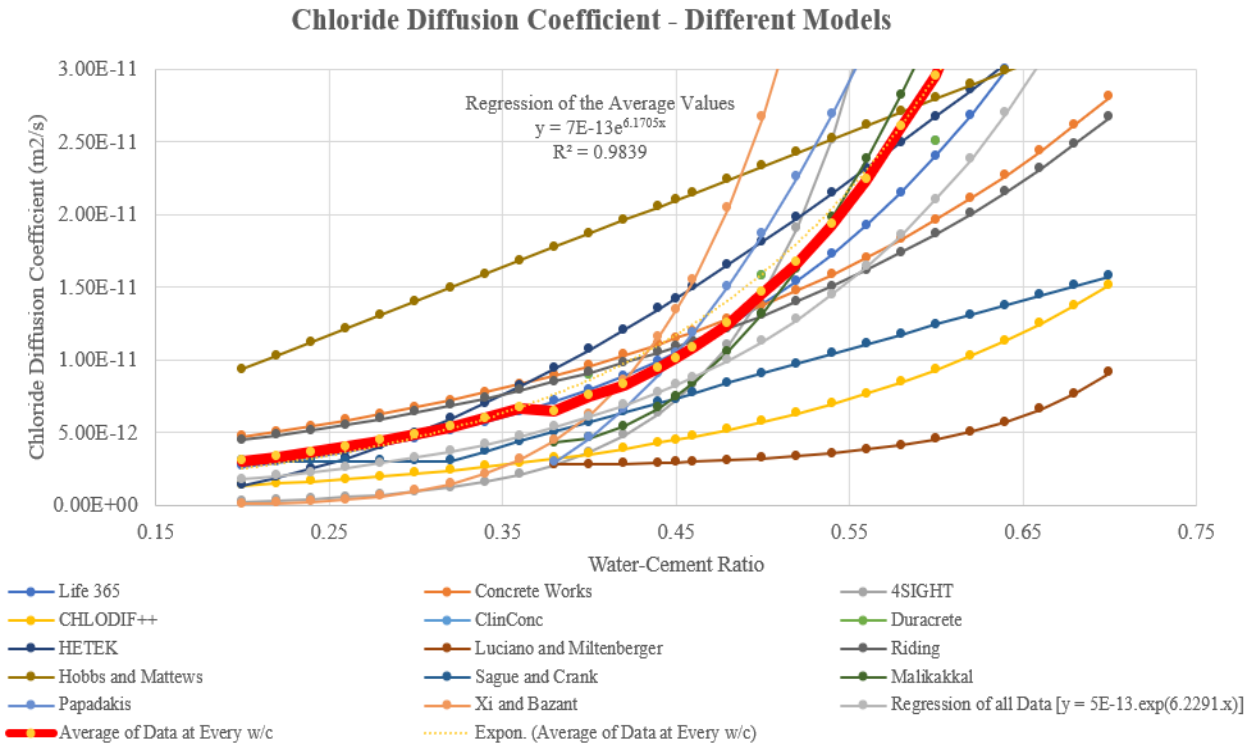

Figure 1.9 - Chloride Diffusion Coefficient (Different Models; Cement Content = 425kg/m3)

The data presented in Figure 1.9 show the chloride diffusion scatter in results of the various models available. This clearly shows that the chloride diffusion coefficient is dependent on many parameters other than the ones presented in each model. A regression analysis for all the data as a function of the water-cement ratio has yielded the following equation:

$$D_c = 5 \times 10^{-13} e^{6.2291(w_c)} \qquad R^2 = 0.570 \tag{1.77}$$

where D_c is the concrete chloride diffusion and w_c is the water-cement ratio.

Equation 1.77 was concluded while taking the individual data at each level of water-cement ratio for every model. In the same context, the average value, given by the various models, for the chloride diffusion coefficient calculated for every level of water-cement ratio was calculated. This calculation gives consequently one value of chloride diffusion coefficient for every level of water-cement ratio. A regression analysis was subsequently made and yielded the following relationship:

$$D_c = 7 \times 10^{-13} e^{6.1705(w_c)} \qquad R^2 = 0.984 \tag{1.78}$$

10. Needed additional influencing parameters

The above literature review discusses various models to identify the chloride diffusion coefficient in concrete. This coefficient is found to be dependent from the following influencing parameters:

- Water-cement ratio
- Cementitious materials content
- Cementious materials percentage (Fly ash, silica fume, slag, and ultrafine fly ash).
- Aggregate shape
- Volume of aggregate
- Curing time
- Curing temperature
- Age
- Relative humidity

The literature review suggests as well that other parameters may have an influence on the chloride diffusion coefficient. The works researching the effect of these parameters were grouped in the following chapters, where the relevant parameters was studied.

- Coarse aggregate properties: Aggregate constitutes a significant volume of the concrete. Their corresponding properties generally affect the concrete final properties. The aggregate properties and their corresponding chloride diffusion coefficient may thus have a significant influence on the chloride diffusion coefficient. These properties include the density, absorption, abrasion values, deleterious materials, size distribution and other properties. The relevant literature study is available in chapter 2.

- Tricalcium Aluminate content (C3A) Content: Some of the chlorides react chemically with the cement components, such as calcium aluminates to form calcium chloroaluminate, and are effectively removed from the pore solution [57]. The later type of chloride is called binded chloride. The presence of C3A in the cement appears thus to be beneficial to the reduction of chloride ingress [58]. The literature review, which is thoroughly discussed in chapter 3, has made this parameter an essential one in this study.

- Consolidation degree, initial mixing time, and initial curing time: These three parameters are related to the workmanship that generally affects the concrete quality. The degree of concrete consolidation may increase or decrease the quantity of entrapped air inside the concrete. These pores (entrapped air) have normally higher diameter than the pores originally available in the cement paste. The relevant presence may thus influence the chloride ingress. The initial concrete mixing time may equally alter the pore distribution in concrete and may contribute to the same phenomena. The initial curing time will decrease the cement hydration, changing thus the pores distribution in the cement paste and influencing the chloride diffusion in concrete. The relevant literature review is available in chapter 4.

- Crack width: Cracks provide an unobstructed path for the deleterious materials to infiltrate through the concrete mass. This is applicable also to chloride ingress. Reinforcement corrosion is generally more sever and begins earlier at cracks and places where water can easily penetrates [59]. Several international standards, codes, and guidelines have limited the crack widths to specific values under relevant environmental conditions. The models defined in this literature

consider the hypothesis of an uncracked concrete which is not always the case. Quantifying the effect of the crack width on the concrete chloride diffusion coefficient is advantageous is calculating the chloride ingress in cracked concrete. The relevant literature review is available in chapter 5.

11. Research Goals and Structure of the Study

The goal of this study is to identify the effect of the following parameters on the chloride diffusion coefficient: aggregate properties, Tricalcium Aluminate content (C3A), Consolidation degree, Initial mixing time, Initial curing time, and Crack width. The aim is to reach a final model that integrates these parameters, in addition to the known influencing ones. The target function for the chloride diffusion coefficient is written as follows:

$$D_c = D_{c,ref}.f_1(T).f_2(t_e).f_3(h).f_4(x).f_5(CA).f_6(C3A).f_7(Cs).f_8(Mi).f_9(Cu).f_{10}(CW) \quad (1.79)$$

The above functions are defined in table 1.9 below. The dependence of the functions f_1 to f_{10} was analyzed in the relevant chapters.

Table 1.9 - Influencing Functions

Function	Terminology
D_c	concrete diffusion coefficient
$D_{c,ref}$	reference diffusion coefficient at an age of 28 days, a temperature of 23°C, and a relative humidity of 100%
$f_1(T)$	dependence on the temperature
$f_2(t_e)$	dependence on the time and degree of hydration
$f_3(h)$	dependence on the concrete pores relative humidity
$f_4(x)$	dependence on the distance from the surface
$f_5(CA)$	dependence on the aggregate content and properties
$f_6(C3A)$	dependence on the tricalcium aluminate content
$f_7(Cs)$	dependence on the consolidation level
$f_8(Mi)$	dependence on the initial mixing time
$f_9(Cu)$	dependence on the curing time
$f_{10}(CW)$	dependence on the cracks width

12. Testing Protocol for this Study

The testing protocol for this study was designed to isolate each of the parameters listed above going from one reference mix and changing one parameter at a time. The different parameters can be finally related as they are initially crossing the same reference concrete mix. The mixes started from one reference mix and proceeded as follows:

- AGG Series: This series of mixes aims to identify the function f_5. The reference mix was replicated using five different types of aggregate with different properties. The different properties of the aggregate were thoroughly tested. Aggregate in concrete is considered as an inert material, the interdependence with other concrete parameters was thus ruled out. The changing parameter in the five mixes related to AGG series was therefore the aggregate type exclusively. The details of the five mixes are explained in chapter 2.

- C3A Series: This series of mixes aims to identify the function f_6. The reference mix was replicated using five different types of Portland cement with five different C3A contents. The literature review has identified the independence of this phenomenon from the water-cement ratio. Based on this, only the cement type has changed. The details of the five mixes are explained in chapter 3.

- CONS Series: This series aims to identify the function f_7. It takes into consideration that the consolidation level effect on the chloride diffusion is independent from other concrete properties. This hypothesis is then proved in chapter 4. The reference concrete mix was replicated in six different batches and the relevant samples were placed in the molds using different levels of concrete consolidation. The details of the six mixes are explained in chapter 4.

- MIX Series: This series aims to identify the function f_8. It takes into consideration that the mixing time effect on the chloride diffusion is independent from other concrete properties. This hypothesis is then proved in chapter 4. The reference concrete mix was replicated in five different batches where the initial mixing time used at the batching plant was different. Five different initial mixing times were used. The details of the five mixes are explained in chapter 4.

- CW Series: This series aims to identify the function f_{10}. The independence of the crack width from the concrete water-cement ratio versus the chloride diffusion coefficient was not obvious. The dependence of these parameters was also studied. The reference concrete mix was replicated using five different water-cement ratios. In each category of the water-cement ratios, five different crack widths were intentionally created in concrete. This series led to 25 combinations of crack widths and water-cement ratios.

As a summary, a total of 46 concrete mixes were made at Advanced Construction Technology Services Laboratories (ACTS) located in Jeddah Saudi Arabia as per the schematic of dependence illustrated in Figure 1.10 below.

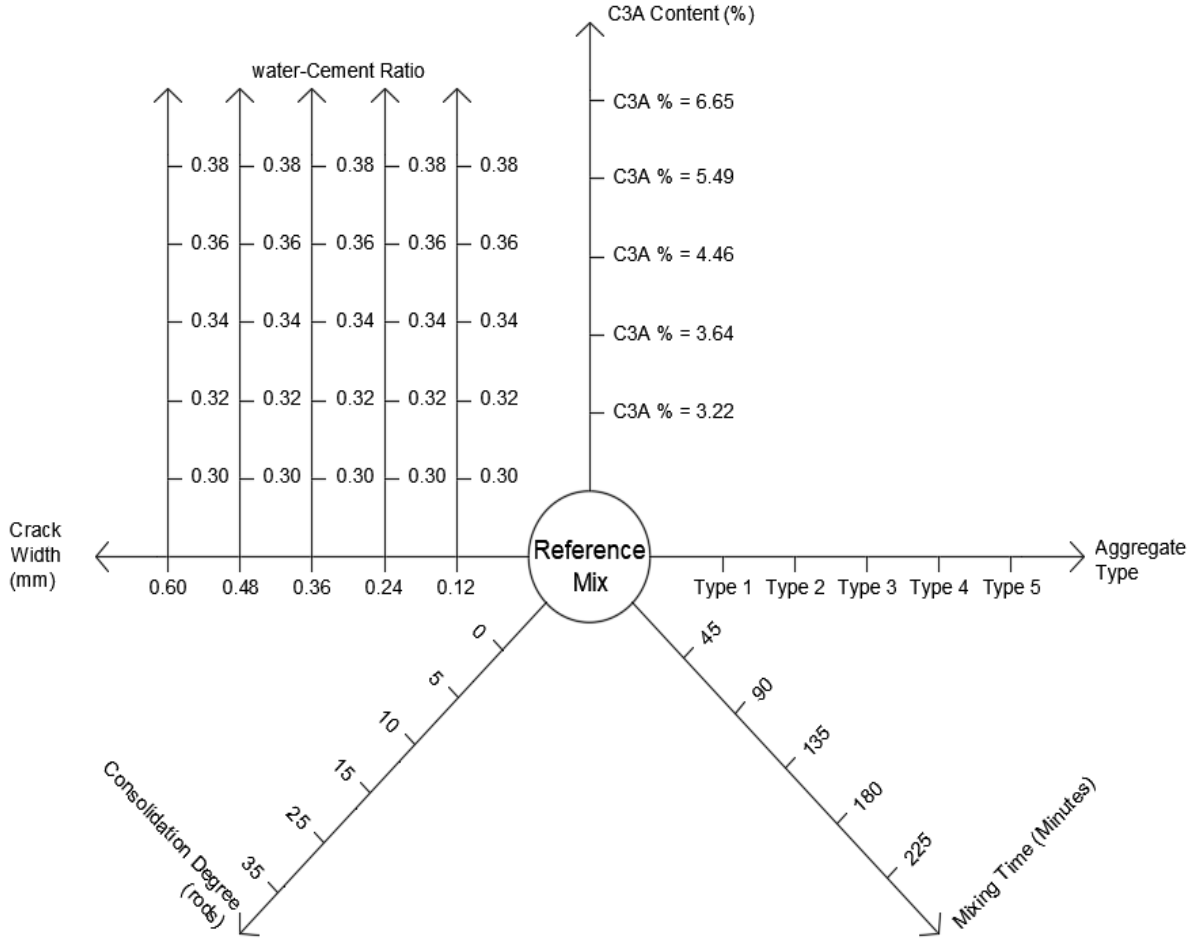

Figure 1.10 - Testing Protocol Scheme

Standard cylindrical concrete specimens were prepared as per ASTM C31/31M [60] for each mix. The diameter and length of the specimen are 150 mm and 300 mm respectively. The cylindrical specimens were demolded at 24 hours after casting. The number of cylindrical specimens placed for each series are detailed in the corresponding chapter. These specimens were then moved into the water tank for 28 days of curing. After the curing period, cores with the diameter of 94 mm were drilled from the cylindrical specimen. The cores were cleaned with water and a stiff nylon brush then allowed to dry for 24 hours at a temperature of 23 degrees with a relative humidity of 50%. The specimens were then sealed from all sides with a water-proof silicon kit with only top surface exposed. When the silicon kit dried, the specimens were afterwards vacuum saturated with saturated calcium hydroxide using a vacuum chamber for 48 hours.

After 48 hours, the test specimens were removed from the vacuum and moved into the NaCl solution for natural chloride diffusion test. Concentration of NaCl is 165 g/L. The volume of the

NaCl solution added is 1 L for each core. All the boxes were stored in curing rooms at 23^{O}C. The cores were immersed in the NaCl solution for the duration specified in the following chapters.

After completing the immersion period, the cores were moved out of the solution, rinsed with taped water and dried in the curing room for 24 hours. After drying the specimens, each specimen was divided into at least six increments, going from the exposed surface while discarding the first 1mm. The grinded/Sliced samples (increments) were then, tagged, placed in water tight plastic bags, and then placed in a freezer until the time of testing. The portions were placed in a freezer as the samples were not tested at the same time due to their excessive number.

Chloride diffusion rate is measured using the guidelines provided in ASTM C1556: Standard Test Method for Determining the Apparent Chloride Diffusion Coefficient of Cementitious Mixtures by Bulk Diffusion:

Summary of the test procedure:

A representative sample of the cementitious mixture is obtained prior to exposure to chloride ion. Each sample is separated into a test specimen and an initial chloride-ion content specimen. The initial chloride-ion content of the specimen is crush and the initial acid-soluble chloride-ion content is determined. All sides of the test specimen are then sealed, except the finished surface, with a suitable barrier coating. The sealed specimens are then saturated in a calcium hydroxide solution, rinsed with tap water, and then placed in a sodium chloride solution. After a specified exposure time, the test specimen is removed from the sodium chloride solution and thin layers are ground off parallel to the exposed face of the specimen. The acid-soluble chloride content of each layer is determined. The apparent chloride diffusion coefficient and the projected surface chloride-ion concentration are then calculated using the initial chloride-ion content, and at least six related values for chloride-ion content and depth below the exposed surface.

The apparent chloride diffusion coefficient is used in Fick's second law of diffusion to estimate chloride penetration into cementitious mixtures that are in a saturated condition. The chloride diffusion coefficient is given by the below formula.

$$\frac{1}{D_a} = 4 \times t \times \left(\frac{erf^{-1}(\frac{C_S - C(x,t)}{C_i - C_S})}{x} \right)^2 \quad (1.80)$$

The reagents used are as follows:

- Distilled Water.
- Calcium Hydroxide Solution, saturated, (approx. 3 g/L).
- An aqueous NaCl solution prepared with a concentration of 165 ± 1 g NaCl per L of solution.
- Silicon Kit capable of forming a barrier membrane that is resistant to chloride ion diffusion.

Each slice of the core was tested for Acid-Soluble Chloride at the specific age as per BS EN 1881 -124: 2015. The test is thoroughly explained in appendix 1.3.

13. Summary of Laboratory Testing Required

The below table includes the number of laboratory tests required to complete this study; they sum up to a total of 2221 tests. The different tests were conducted by Advanced Construction Technology Services (ACTS) who has financially sponsored this work. The company (ACTS) has additionally dedicated three chemists to conduct this large quantity of laboratory tests over a period of two years.

Table 1.10 - List of Laboratory Testing Required for this Study

Series	Reference Chapter	Test Description	Test Quantity
Correlation between RCPT value and Concrete Properties	1	RCPT Test	52
		Concrete Compressive Strength	39
AGG	2	Material Finer than 75 Microns	5
		Oven Dry Density	5
		SSD Density	5
		Apparent Density	5
		Water Absorption	5
		Clay Lumps and Friable Particles	5
		Flakiness	5
		Elongation	5
		Los Angeles Abrasion (500 Rev.)	5
		Soundness	5
		Lightweigth Pieces	5
		Aggregate Sieve Analysis	5
		Cylinder Preparation	66
		Cores Extraction	157
		Acid Soluble chloride Content Testing	215
C3A	3	Cement Chemical Analysis	5
		Cylinder Preparation	30
		Cores Extraction	60
		Water Soluble Chloride Testing	10
		Acid Soluble chloride Content Testing	436
MIXT	4	Absorption	10
		Apparent Density	10
		Volume of Permeable Pores	10
		Permeability	10
		Cylinder Preparation	30
		Cores Extraction	10
		Acid Soluble Chloride	70
CONS	4	Absorption	12

		Apparent Density	12
		Volume of Permeable Pores	12
		Permeability	12
		Cylinder Preparation	30
		Cores Extraction	12
		Acid Soluble Chloride	84
CW	5	Cylinder Preparation	30
		Cores Extraction	12
		Cracked Cores Preparation	175
		Crack Width Measurement by Microscope	175
		Acid Soluble Chloride	375
Total Number of Laboratory Tests			**2221**

Table 1.11 - Quantity of Concrete Mixes Made

Series	Reference Chapter	Quantity of Concrete Mixes Made
Correlation between RCPT value and Concrete Properties	1	13
AGG	2	5
C3A	3	5
MIXT	4	5
CONS	4	6
CW	5	5
Total Number of Concrete Mixes		**39**

14. Conclusion

The literature review in this chapter discusses the concrete service life taking into account that the reinforcing steel corrosion in chloride environment is the most critical concrete degradation phenomenon.

The different methods of identifying the concrete service life in chloride environment were described including the prescriptive-based specifications, performance-based testing and available models for chloride ingress in concrete.

The models in the literature were found dependent from several parameters such as the water-cement ratio, cement content, cement type, temperature, humidity, distance from the member's surface, curing time, maturity, aggregate content, cement density, aggregate density, and degree of hydration. Not all the models included all the listed parameters. A comparison of the chloride diffusion coefficient calculated using the various models yielded a significant difference in the

resulting values. This difference has suggested that other parameters are also influencing the chloride diffusion coefficient.

The literature review made in this chapter identified several other parameters that are affecting the chloride diffusion coefficient without any quantification for their role in this effect. These parameters are: the aggregate properties, tricalcium aluminate content, concrete consolidation degree, concrete initial mixing time, curing time, and crack width.

A tailored testing campaign was therefore prepared and explained. This testing protocol aimed at identifying and quantifying the effect of these additional parameters on the chloride diffusion. The testing campaign was defined to identify the effect of the influencing parameters while taking into consideration their eventual coupling effect. One reference concrete mix design was taken as a reference crossing mix design. Five different values of the influencing parameters were changing in every series of testing in order to identify the influence function.

Chapter 2: Effect of Aggregate Properties

1. Introduction

The main objective of this chapter is to assess the effect of the aggregate properties, on the chloride diffusion coefficient and the surface concentration. It starts by presenting the goal of this study, followed by the testing protocol, the raw materials properties and mix design. Details of the core specimens' preparations and chloride diffusion rate test plan are discussed as well. Further to the test procedures, the results are presented, and related calculations are performed. This chapter finally reaches comprehensive conclusions regarding the effect of aggregate properties, on the concrete chloride diffusion coefficient and surface concentration.

2. General effect of aggregate properties on the chloride resistance

Chloride penetrates concrete following three main transportation mechanism. These mechanisms include the diffusion, capillary absorption and hydrostatic pressure. The governing transportation mechanism is however the diffusion [61]. It is to note that among the three mechanisms, the capillary absorption tends to have the shallower penetration depth. This mechanism requires moisture gradient for chloride ions to penetrate the concrete [36]. Chloride ions in the water enter concrete pores through capillary suction that takes place when water encounters a dry concrete surface [36]. Capillary suction usually occurs at shallow depths and the chloride ions do not generally reach the vicinity of the reinforcing steel [36]. This phenomenon may not transport chloride ions to the steel level but will reduce the distance that chloride ions need to diffuse to reach the vicinity of the reinforcing steel [62].

It was eventually considered that the chloride diffusion in concrete is primary dependent on the quality of the cement paste. The volume of aggregate constitutes in average twice the volume of cementitious materials pastes, which conclude that the properties of aggregate in terms of chloride diffusion can greatly affect the overall performance. Assuming that the chloride transportation is solely through the cement paste, the use of low-quality aggregate will not impart the concrete resistance to chloride migration, which is not obviously the case. Hobbs [63] has concluded that the rate at which chloride ion ingress into saturated concrete occurs, depends on the chloride ion diffusion coefficient of the cement paste and aggregate fractions, and the aggregate volume. Additionally, the rate of ingress will be influenced by paste/aggregate interfacial effects and internal cracks.

The effect of aggregate, in terms of properties and volume was found in many studies affecting the general performance of concrete, noting the following two examples:

- Water permeability: Powers et al. [64] have tested the water permeability of different aggregate types where they demonstrated that the water permeability of a cement paste with a water cement ratio of 0.48 can range between 0.001 to 10 times the water permeability of the

aggregate used in concrete. That was as equivalent as changing the water cement ratio of the paste from 0.48 to 0.71.

- Concrete modulus of elasticity: The effect of the aggregate content on the modulus of elasticity was covered in several publications and testing protocols. Among the works, we can mention those of Z. Hanshin and S. Shtrikman [65], and Hobbs [63]. Both publications agree on the fact that the modulus of elasticity of concrete can be written in the following form:

$$\boldsymbol{E_{concrete}} = \frac{[(\boldsymbol{E_{Aggregate}} - \boldsymbol{E_{Paste}})\boldsymbol{V_{Aggregate}} + (\boldsymbol{E_{Paste}} + \boldsymbol{E_{Aggregate}})]\boldsymbol{E_{Paste}}}{(\boldsymbol{E_{Paste}} + \boldsymbol{E_{Aggregate}}) + (\boldsymbol{E_{Paste}} - \boldsymbol{E_{Aggregate}})\boldsymbol{V_{Aggregate}}} \quad (2.1)$$

where $E_{concrete}$ is the concrete modulus of elasticity, E_{paste} is the modulus of elasticity of the paste, $E_{Aggregate}$ is the modulus of elasticity of the aggregate, V_{Paste} is the volume fraction of the paste and $V_{Aggregate}$ is the volume fraction of the aggregate.

In an equivalent way, Hobbs included in a separate publication [63] that for a saturated concrete, the above equation may be used for the chloride diffusion while taking into consideration the assumption that the decrease in chloride ion concentration is the same in both the paste and aggregate, and the mass of chloride ions carried across a unit area is the same in both the paste and aggregate. The formula will thus be as follows:

$$D_{concrete} = \frac{[(D_{Aggregate} - D_{Paste})V_{Aggregate} + (D_{Paste} + D_{Aggregate})]D_{Paste}}{(D_{Paste} + D_{Aggregate}) + (D_{Paste} - D_{Aggregate})V_{Aggregate}} \quad (2.2)$$

where $D_{concrete}$ is the concrete chloride diffusion coefficient, D_{paste} is the chloride diffusion coefficient of the paste, and $D_{Aggregate}$ is the aggregate chloride diffusion coefficient.

The above formula does not consider the influence of paste/aggregate interface.

Several other publications have investigated the role of coarse aggregate in the chloride diffusion coefficient. Some papers have demonstrated that the diffusion increases proportionally with the aggregates content (especially between 35% and 60%) as a result of the increase in the bulk diffusivity (interconnection of Interfacial Transition Zone ITZ) of concretes [66][67]. The inclusion of aggregates into the cement paste results in the formation of an ITZ around the aggregates, which is the primary pathway for chloride diffusion. The suggested thickness of the Interfacial Transition Zone as reported by Bourdette et al. is 30 µm [68]. In the presence of microsilica however (10% as a replacement of cementitious materials), Baja et al. [69] found that the ITZ is insignificant and measures 3µm and considered to have a negligible effect on the chloride transportation. The porosity of the ITZ was also generally found to increase with an increase in the quantity of aggregate content [70] as reported by Winslow et al.

Given these results, the ITZ has a major effect on the chloride transportation. Zheng et al. [71] have modeled the concrete as three phase materials when it comes to chloride diffusion; the aggregate, the ITZ, and the bulk cement paste, with corresponding diffusion coefficients. Their

work has reached a theoretical apparent diffusion coefficient as function of the ITZ and bulk cement paste apparent diffusion. Going back to the assumption that the ITZ is proven to have very little effect when silica fume is added, this apparent diffusion coefficient may be obtained by the equation proposed by Hobbs.

On the other hand, Delagrave et al. [72] reported that, as the aggregate content increased, the chloride diffusivity decreased. As compared to the cement paste, the aggregate is considered to be relatively very dense, therefore, the transportation of the chloride within the aggregate could be neglected [73]. This is in agreement with the works done by Zheng et al [74][75] that considered the aggregate as forming an obstacle to the movement of chloride ions. He studied the effect of aggregate shape on the chloride diffusivity of concrete, reaching a conclusion suggesting that the chloride diffusivity decreases with an increasing aggregate aspect ratio.

A recent study published by the university of Wisconsin-Milwaukee [36] investigated the effect of coarse aggregate type effects on the chloride ions resistance by replicating the same concrete mix design using 12 different types of coarse aggregate and testing the corresponding samples, with Rapid Chloride Penetration Test, at different ages. The results of this study have reached the following conclusions:

- Significant change in chloride ion resistance test results was identified among different samples that are made with different coarse aggregate type.
- The chloride ion resistance as tested through the RCPT is strongly dependent on the aggregate type and corresponding coarse aggregate absorption. A formula accurate to 98% illustrated the value of the RCPT (coulombs) as a function of the coarse aggregate absorption; the formula is as follows:

$$C = [(5076.2 \times A) + 6904.7]\, t^{-0.58} \quad (2.3)$$

where C is the RCPT value in coulombs, A is the water absorption in (%), and t is the time in days.

The above have thus suggested that, not only the diffusion of the aggregate themselves participate in the total chloride diffusion coefficient, but also the interfacial transition zone between the aggregate and the cement paste. The three parameters should be equally investigated for an accurate representation of the role of coarse aggregate in the overall chloride diffusion. In another note, these studies qualitatively assess the effect of the aggregate on the chloride transportation in a general way and quantitatively when it comes to the correlation with the Rapid Chloride Penetration Test. It is thus of great interest to quantify the chloride diffusion coefficient of the concrete as a function of the aggregate chloride diffusion coefficient and the aggregate properties, when the same cement paste properties are used. For these reasons, the herein study aims at providing conclusions with practical importance in the calculation of the concrete services life when considering different types of aggregates.

3. Testing protocol

One reference concrete mix design was replicated using five different sources of aggregate. More than 6 concrete cylindrical specimens were taken from each trial mix as per ASTM C31. The concrete cylinders were then cured for 28 days in water. Further to the curing period, concrete cores were taken from the cylinders with a diameter of 94mm and a height of 80mm. Two sets of samples were crushed from each concrete mix design and the initial acid soluble chloride content is determined. All of the remaining sides were then sealed, except the finished surface, with a suitable barrier coating. The sealed specimens were then saturated in a calcium hydroxide solution, rinsed with tap water, and then placed in a sodium chloride solution.

In parallel, rock cores were taken from the source of the different aggregate after visiting the relevant crushers. Two set of samples were crushed from each rock source and the initial acid soluble chloride content is determined. All of the remaining sides were then sealed, except the finished surface, with a suitable barrier coating. The sealed specimens were then saturated in a calcium hydroxide solution, rinsed with tap water, and then placed in a sodium chloride solution.

After a duration of 149 days, sets of test specimens were removed from the sodium chloride solution and thin layers were ground off parallel to the exposed face of the specimen. The acid-soluble chloride content of each layer is determined. The apparent chloride diffusion coefficient and the projected surface chloride-ion concentration were then calculated using the initial chloride-ion content, and at least six related values for chloride-ion content and depth below the exposed surface. The different apparent chloride diffusion coefficients of the different samples, at different ages, were compared, analyzed and interpreted. The chloride profile testing protocol adopted in all the campaigns is thoroughly explained in chapter 1.

4. Concrete Mix Design and Materials Source

The reference concrete mix is given in Table 2.1 using northern region cement with a tricalcium aluminate content of 4.46%. Four other mixes were identically made with different types of coarse aggregate. The changing parameter among the five mixes is only the type of coarse aggregate. Five different types of aggregate are used in this study, which are: Madinah Rock, Shoaiba-Makkah Rock, UAE-Gabbro Rock, UAE-Al Ghail (Stevin) Rock and UAE-Binlahej Rock. In the different mixes, the volume of coarse aggregate remained unchanged (not the weight of the coarse aggregate). The properties of five types of aggregate used is listed in Table 2.2 and Table 2.3 and pictures from the rocks samples are included in Figure 2.1.

Table 2.1 - Reference Mix

Reference Mix							
Mix Ingredients	SSD Weight (kg)	Density (kg/m3)	Moisture (%)	Absorption (%)	Final Weight (kg)	Volume (m3)	Trial Weights (0.1m3) (kg)
Cement (NORTH REGION CEMENT Ordinary Portland Cement)	400	3150			400	0.127	40
Micro Silica (ELKEM)	25	2200			25	0.0114	2.5
Water	161.5	1000			171.8	0.1718	17.18
CA 3/8 (MAD Source)	1000	2820	0.5	1.1	994	0.3513	99.4
Washed Sand (MAD Source)	865	2660	0.4	0.9	860.68	0.3236	86.068
Admixture BASF Glenium Sky 504	4	1120			4	0.0036	0.4
Air Content						0.02	
Total Volume						1.0087	0.099

Table 2.2 - Properties of Aggregate

Coarse Aggregate Test Results											
Aggregate Source	Material Finer than 75 Microns (%)	Oven Dry Density (kg/m3)	SSD Density (kg/m3)	Apparent Density (kg/m3)	Water Absorption (%)	Clay Lumps and Friable Particles (%)	Flakiness (%)	Elongation (%)	Los Angeles Abrasion (500 Rev.) (%)	Soundness (%)	Lightweigth Pieces (%)
Bin Laheej	0.50	2660	2670	2700	0.50	0.10	28.00	21.00	22.90	1.80	0.00
Madinah	0.40	2800	2820	2880	1.00	0.30	13.00	18.00	12.20	5.60	0.00
Stevin Rock - Ghail	0.20	2700	2720	2750	0.60	0.10	16.00	21.00	20.80	3.10	0.00
Gabro	1.10	2820	2840	2890	0.80	0.20	20.00	26.00	16.50	4.10	0.00
Makah	0.20	2950	2960	2990	0.40	0.20	16.00	20.00	12.40	6.20	0.00

Table 2.3 - Aggregate Sieve Analysis

Coarse Aggregate Sieve Analysis Test Results						
Sieve Opening Diameter	Sieve Number	Bin Laheej (Percentage Particle Passing)	Madinah (Percentage Particle Passing)	Stevin Rock - Ghail (Percentage Particle Passing)	Gabro (Percentage Particle Passing)	Makah (Percentage Particle Passing)
9.50 mm	3/8"	93.20	98.30	92.10	94.50	97.70
4.75 mm	No. 4	10.10	25.20	8.30	24.00	27.60
2.36 mm	No.8	0.70	1.40	0.50	1.50	0.60
1.18 mm	No. 16	0.60	0.70	0.40	1.30	0.40
0.075 mm	No. 200	0.50	0.40	0.20	1.10	0.20

Figure 2.1 - Photos of Different Rocks

5. Trial experiment and core sample preparation

The core sample preparation detailed in chapter 1 was followed. A profile grinder was used resulting in grinding test samples with an increment of 3mm. The datasheet of the profile grinder in attached in appendix 2.7. For each mix, more than 18 cores were prepared, the corresponding details are listed in Table 2.4. The core identifications were as follows:

- Cores that originate from the mixes made with Madinah aggregate: MAD-01 to MAD-33.
- Cores that originate from the mixes made with Makah aggregate: MAK-01 to MAK-33
- Cores that originate from the mixes made with Al-Gail aggregate: GHA-01 to GHA-24
- Cores that originate from the mixes made with Bin Laheej aggregate: LAH-01 to LAH-24
- Cores that originate from the mixes made with Gabbro aggregate: GAB-01 to GAB-18

Table 2.4 - Details of Cores Drilled from Each Mix

Mix No.	Agg. Source	Core Nos.	Core Size	
			Diameter, mm	Length, mm
Trial-19	Madinah	33	100	75
Trial-20	Shoaiba-Makkah	33	100	75
Trial-21	UAE-Al Ghail (Stevin)	24	100	75
Trial-22	UAE-Binlahej	24	100	75
Trial-23	UAE-Gabbro	18	100	75

Five types of rock core samples were also drilled from the aggregate sources (quarries) studied in this report. The diameter of the rock cores is 100 mm and the length is 100 mm. The details of the rock cores are listed in Table 2.5. The rocks were coated with silicon kit and immersed in the NaCl solution. Additional rock slices were used to identify the initial acid chloride content.

Table 2.5 - Details of Rock Cores

Rock Source	Core Nos.	Core Size	
		Diameter, mm	Length, mm
Madinah	5	100	100
Shoaiba-Makkah	5	100	100
UAE-Al Ghail (Stevin)	5	100	100
UAE-Binlahej	5	100	100
UAE-Gabbro	5	100	100

Figure 2.2 - Cores Drilled for Chloride Diffusion Test

6. Chloride diffusion test results

6.1. Chloride diffusion coefficient in rocks

The rocks extracted from the aggregate quarries were immersed in companion sodium chloride solution as per Table 2.6. Two cores of rocks were removed after an immersion duration of 115 days and another two cores of rocks removed after an immersion duration of 202 days. The four cores of rocks were tested as per the mentioned requirements. The purpose of the tests is to determine the chloride content profile and eventually the chloride diffusion coefficient and chloride surface concentration. The increment of samples taken is 3mm while discarding the first 1mm. Whereas the results are summarized in the table below, it was obvious that the chloride did not diffuse in the rocks for the different types of used aggregate.

Table 2.6 - Rocks Chloride Profile Test Results after Immersion in NaCl Solution

Rocks chloride profile test results after immersion in NaCl solution				
Aggregate source	Testing depth	Initial chloride content	Aggregate profile chloride content after 115 Days of immersion	Aggregate profile chloride content after 202 days of immersion
Source 1: Bin Laheej Aggregate	2.5	0.01%	0.01%	0.02%
	5.5		0.01%	0.01%
	8.5		0.01%	0.01%
	11.5		0.01%	0.01%
	14.5		0.01%	0.01%
	17.5		0.01%	0.01%
	20.5		N/A	0.01%
Source 2: Madinah Aggregate	2.5	0.01%	0.01%	0.01%
	5.5		0.01%	0.01%
	8.5		0.01%	0.01%
	11.5		0.01%	0.01%
	14.5		0.01%	0.01%
	17.5		0.01%	0.01%
	20.5		0.01%	0.01%
Source 3: Stevin Rock - Ghail Aggregate	2.5	0.01%	0.02%	0.01%
	5.5		0.01%	0.01%
	8.5		0.02%	0.01%
	11.5		0.01%	0.01%
	14.5		0.01%	0.01%
	17.5		0.01%	0.01%
	20.5		0.01%	0.01%
Source 4: Gabro Aggregate	2.5	0.04%	0.05%	0.08%
	5.5		0.04%	0.07%
	8.5		0.04%	0.07%
	11.5		0.04%	0.07%
	14.5		0.04%	0.07%
	17.5		0.04%	0.07%
	20.5		N/A	0.07%

Source 5: Makah Aggregate	2.5	0.01%	0.01%	0.02%
	5.5		0.01%	0.01%
	8.5		0.01%	0.01%
	11.5		0.01%	0.01%
	14.5		0.01%	0.01%
	17.5		0.01%	0.01%
	20.5		0.01%	0.01%

6.2. Chloride Diffusion Coefficient in Concrete Made with Different Types of Aggregate

After an immersion duration of 150 days four concrete cores from every set of concrete mix (same concrete mix replicated with five different types of coarse aggregate) were removed from the sodium chloride solution and tested for their corresponding chloride profile, chloride diffusion coefficient and chloride surface concentration. The raw results are described in Table 2.7 whereas the chloride diffusion coefficient and the corresponding chloride surface concentration are available in Table 2.8.

Table 2.7 - Concrete Cores Chloride Profile Test Results after Immersion in NaCl Solution

Concrete cores chloride profile test results after immersion in NaCl solution						
Aggregate Source	Depth	Initial Chloride Content	Profile Chloride Content in Core 1 After 150 Days of Immersion	Profile Chloride Content in Core 2 After 150 Days of Immersion	Profile Chloride Content in Core 5 After 150 Days of Immersion	Profile Chloride Content in Core 9 After 150 Days of Immersion
Source 1: Bin Laheej Aggregate	2.5	0.01%	0.71%	0.67%	0.63%	0.73%
	5.5		0.54%	0.45%	0.45%	0.54%
	8.5		0.36%	0.30%	0.28%	0.38%
	11.5		0.18%	0.19%	0.13%	0.23%
	14.5		0.06%	0.02%	0.02%	0.09%
	17.5		0.01%	0.02%	0.01%	0.02%
	20.5		0.01%	0.01%	0.01%	0.01%
Source 2: Madinah Aggregate	2.5	0.01%	0.60%	0.66%	0.69%	0.74%
	5.5		0.53%	0.50%	0.45%	0.57%
	8.5		0.32%	0.24%	0.33%	0.37%
	11.5		0.23%	0.19%	0.20%	0.22%
	14.5		0.12%	0.09%	0.10%	0.15%
	17.5		0.06%	0.04%	0.04%	0.09%
	20.5		0.01%	0.01%	0.02%	0.02%
Source 3: Stevin Rock - Ghail Aggregate	2.5	0.01%	0.60%	0.60%	0.61%	0.71%
	5.5		0.42%	0.33%	0.43%	0.50%
	8.5		0.21%	0.15%	0.27%	0.24%
	11.5		0.08%	0.06%	0.16%	0.07%
	14.5		0.03%	0.02%	0.04%	0.01%

	17.5		0.02%	0.01%	0.02%	0.01%
	20.5		0.02%	0.01%	0.02%	0.01%
Source 4: Gabro Aggregate	2.5	0.06%	0.53%	0.63%	0.52%	0.77%
	5.5		0.48%	0.50%	0.49%	0.56%
	8.5		0.39%	0.37%	0.39%	0.38%
	11.5		0.18%	0.22%	0.31%	0.26%
	14.5		0.17%	0.12%	0.21%	0.19%
	17.5		0.11%	0.08%	0.14%	0.07%
	20.5		0.08%	0.04%	0.07%	0.05%
Source 5: Makah Aggregate	2.5	0.01%	0.46%	0.56%	0.51%	0.51%
	5.5		0.34%	0.42%	0.36%	0.42%
	8.5		0.21%	0.23%	0.22%	0.25%
	11.5		0.08%	0.09%	0.10%	0.12%
	14.5		0.02%	0.03%	0.04%	0.03%
	17.5		0.01%	0.01%	0.01%	0.01%
	20.5		0.01%	0.01%	0.01%	0.01%

Table 2.8 - ASTM C1556 Test Results Summary Concrete Cores Made with Different Coarse Aggregate Source

ASTM C1556 Test Results Summary Concrete Cores Made with Different Coarse Aggregate Source

Aggregate Source	Chloride Diffusion Coefficient for Test 1 [$\times 10^{-12} m^2/sec$]	Chloride Surface Concentration for Test 1 [%]	Chloride Diffusion Coefficient for Test 2 [$\times 10^{-12} m^2/sec$]	Chloride Surface Concentration for Test 2 [%]	Chloride Diffusion Coefficient for Test 3 [$\times 10^{-12} m^2/sec$]	Chloride Surface Concentration for Test 3 [%]	Chloride Diffusion Coefficient for Test 4 [$\times 10^{-12} m^2/sec$]	Chloride Surface Concentration for Test 4 [%]	Average Chloride Diffusion Coefficient [$\times 10^{-12} m^2/sec$]	Average Chloride Surface Concentration [%]
Source 1: Bin Laheej Aggregate	2.93	0.95	2.67	0.88	2.45	0.86	3.31	0.95	2.84	0.91
Source 2: Madinah Aggregate	4.09	0.79	2.86	0.87	3.20	0.87	3.78	0.94	3.48	0.87
Source 3: Stevin Rock - Ghail Aggregate	1.92	0.85	1.43	0.88	2.57	0.81	1.88	1.02	1.95	0.89
Source 4: Gabro Aggregate	3.95	0.69	3.67	0.81	6.02	0.66	3.40	0.97	4.26	0.78
Source 5: Makah Aggregate	2.40	0.64	2.30	0.78	2.45	0.69	2.78	0.71	2.48	0.70

7. Analysis of Results

The results discussed in section 6 indicates that the chloride diffusion coefficient for the rocks is equal to zero; the aggregate themselves thus have insignificant chloride diffusion mechanism. The whole chloride diffusion mechanism takes place thus in the paste fraction of the concrete and the Interfacial Transition Zone. On the other hand, the concrete cores extracted from the five concrete mixes resulted in different chloride diffusion coefficient values as well as different chloride surface concentration values. This fluctuation is illustrated in Figure 2.3. Noting that the five concrete mixes were identical except for the source of course aggregate, other coarse aggregate properties may have affected the chloride diffusion mechanism. Since the coarse aggregate were thoroughly tested prior to concrete mixing operation, relationships between the different coarse aggregate properties and the chloride diffusion properties were established as per the subsequent sections. These relationships were described accordingly.

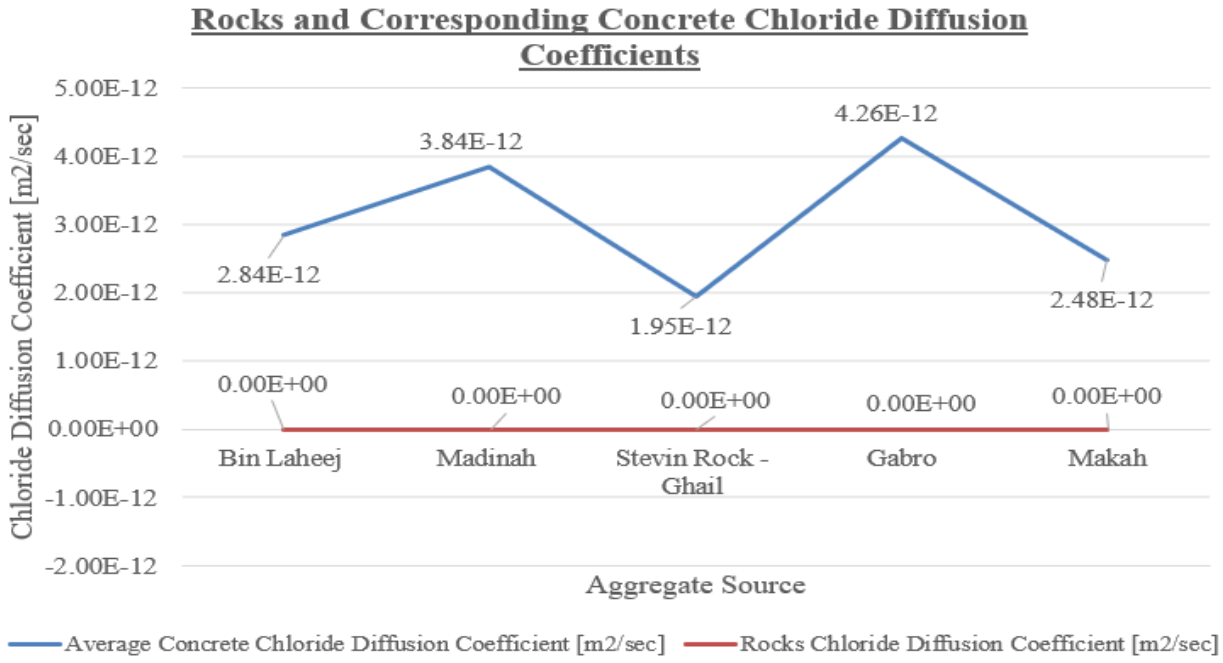

Figure 2.3 - Rocks and Corresponding Concrete Chloride Diffusion Coefficients

7.1. Effect of the coarse aggregate materials finer than 75 microns

Material finer than 75 µm covers clay particles and other aggregate particles that are dispersed by the wash water, as well as water-soluble materials. These materials cannot be separated from coarser material by normal dry sieving thus the need of wet sieving. Material finer than 75 µm found in natural sand are usually clay and harm particles. In manufactured fine aggregate, these particles are most likely smaller size fractions. ASTM C33 table 1 limits the percentage of material finer than 75µm to 5.0% and 3.0% depending on whether the concrete is subjected to abrasion or not (higher content of fine material lowers the abrasion resistance).

Figures 2.4 and 2.5 illustrate the change of chloride diffusion coefficient and surface chloride concentration for the concrete cores based on the value of the material finer than 75 microns found in the coarse aggregate. A high correlation was found between the chloride diffusion coefficient and the material finer than 75 microns content. This occurrence is mainly due to the change in the interface between the coarse aggregate and the paste that the fine materials can induce. This phenomenon is evaluated in more details in section 8. The surface chloride concentration is however not affected by the materials finer than 75 microns portion.

Chloride Diffusion Coefficient Versus Material Finer than 75 Microns

Aggregate Source	Material Finer than 75 Microns (%)	Average Chloride Diffusion Coefficient [m2/sec]
Bin Laheej	0.50	2.84E-12
Madinah	0.40	3.48E-12
Stevin Rock - Ghail	0.20	1.95E-12
Gabro	1.10	4.26E-12
Makah	0.20	2.48E-12

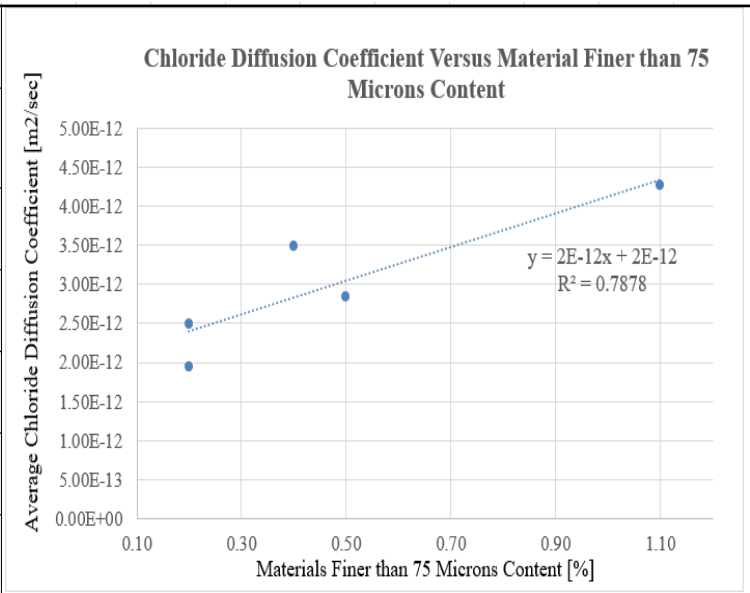

Figure 2.4 - Chloride Diffusion Coefficient Versus Coarse Aggregate Materials Finer than 75 Microns

Chloride Surface Concentration Versus Material Finer than 75 Microns

Aggregate Source	Material Finer than 75 Microns (%)	Average Chloride Surface Concentration [%]
Bin Laheej	0.50	0.91
Madinah	0.40	0.87
Stevin Rock - Ghail	0.20	0.89
Gabro	1.10	0.78
Makah	0.20	0.70

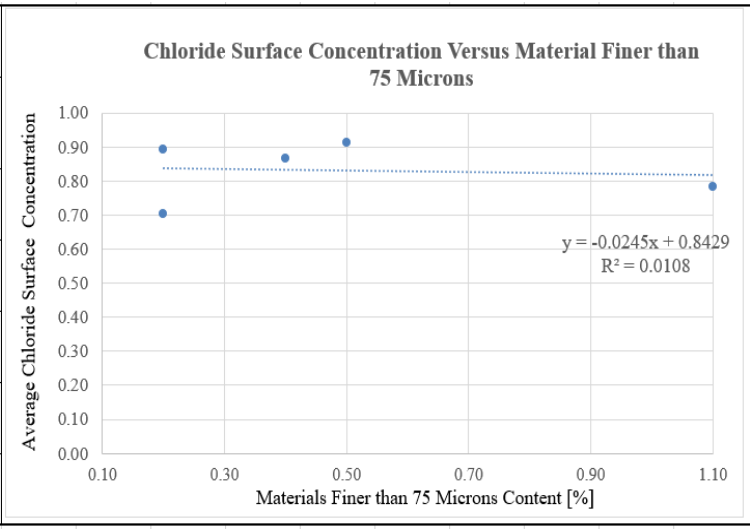

Figure 2.5 - Surface Chloride Concentration Versus Coarse Aggregate Materials Finer than 75 Microns

7.2. Effect of coarse aggregate density

Aggregate specific gravity or relative density is defined as the ratio of mass per unit volume of material to the density of distilled water at a stated temperature. Relative density is noted as OD (oven dry), SSD (surface-saturated-dry), and apparent. The OD and SSD relative densities are calculated according to the impermeable and permeable pores, dry and water-filled respectively. The apparent relative density includes only the impermeable portion of the aggregate. Relative density is used for calculating the volume occupied by the aggregate in various mixes. Relative density SSD is used if the aggregate is wet (absorption has been satisfied) and specific gravity OD is used when aggregate is dry.

The figures below show a good relationship between the coarse aggregate density and the chloride surface concentration with an R^2 factor exceeding 0.9. The effect of the density on the chloride diffusion is absent.

Chloride Diffusion Coefficient Versus Oven Dry Density		
Aggregate Source	Oven Dry Density [kg/m3]	Average Chloride Diffusion Coefficient [m2/sec]
Bin Laheej	2660	2.84E-12
Madinah	2800	3.48E-12
Stevin Rock - Ghail	2700	1.95E-12
Gabro	2820	4.26E-12
Makah	2950	2.48E-12

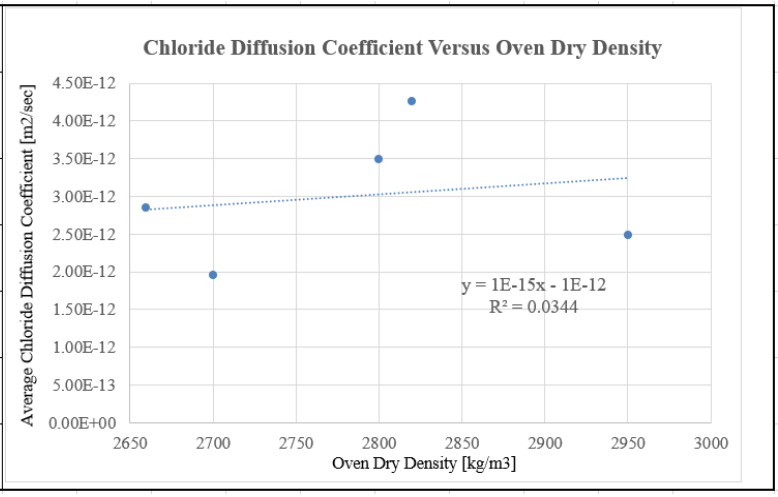

Figure 2.6 - Chloride Diffusion Coefficient Versus Oven Dry Density

Chloride Surface Concentration Versus Oven Dry Density		
Aggregate Source	Oven Dry Density [kg/m3]	Average Chloride Surface Concentration [%]
Bin Laheej	2660	0.91
Madinah	2800	0.87
Stevin Rock - Ghail	2700	0.89
Gabro	2820	0.78
Makah	2950	0.70

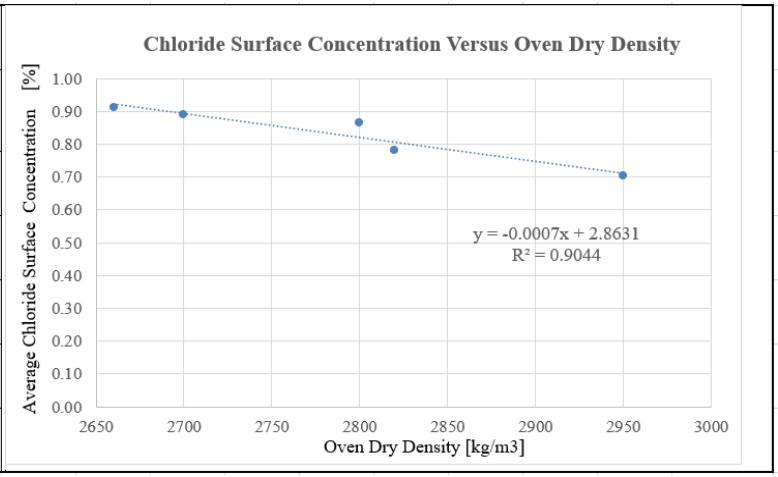

Figure 2.7 - Chloride Surface Concentration Versus Oven Dry Density

Chloride Diffusion Coeficient Versus SSD Density		
Aggregate Source	SSD Density [kg/m3]	Average Chloride Diffusion Coefficient [m2/sec]
Bin Laheej	2670	2.84E-12
Madinah	2820	3.48E-12
Stevin Rock - Ghail	2720	1.95E-12
Gabro	2840	4.26E-12
Makah	2960	2.48E-12

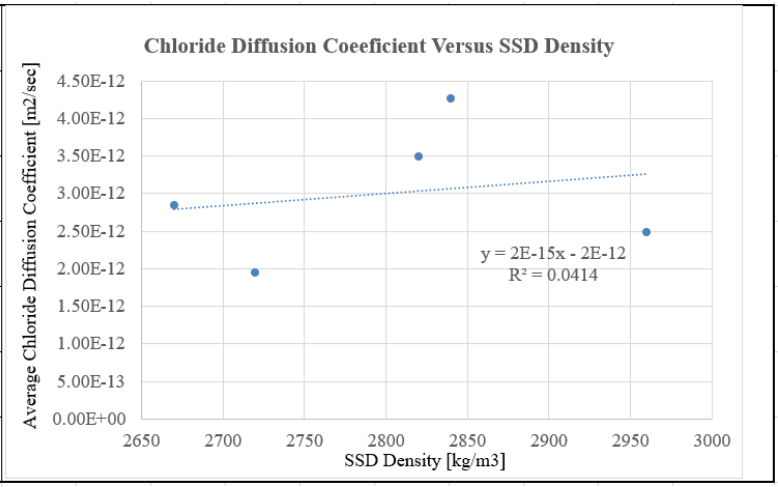

Figure 2.8 - Chloride Diffusion Coefficient Versus SSD Density

Chloride Surface Concentration Versus SSD Density		
Aggregate Source	SSD Density (kg/m3)	Average Chloride Surface Concentration [%]
Bin Laheej	2670	0.91
Madinah	2820	0.87
Stevin Rock - Ghail	2720	0.89
Gabro	2840	0.78
Makah	2960	0.70

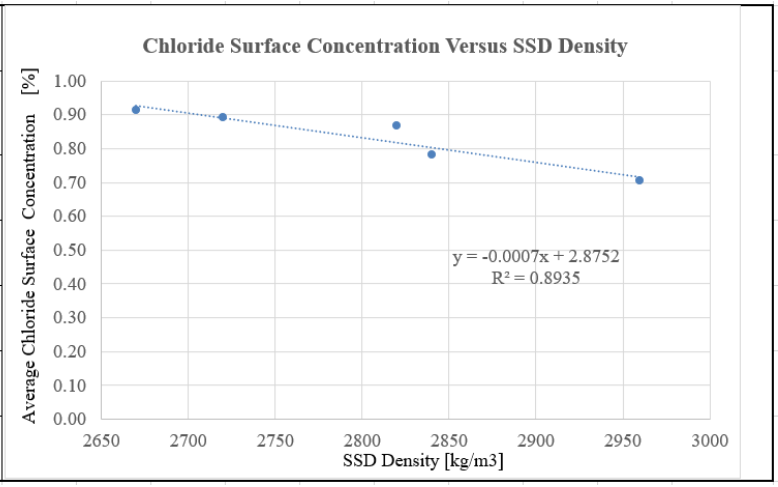

Figure 2.9 - Chloride Surface Concentration Versus SSD Density

Chloride Diffusion Coefficient Versus Apparent Density		
Aggregate Source	Apparent Density (kg/m3)	Average Chloride Diffusion Coefficient [m2/sec]
Bin Laheej	2700	2.84E-12
Madinah	2880	3.48E-12
Stevin Rock - Ghail	2750	1.95E-12
Gabro	2890	4.26E-12
Makah	2990	2.48E-12

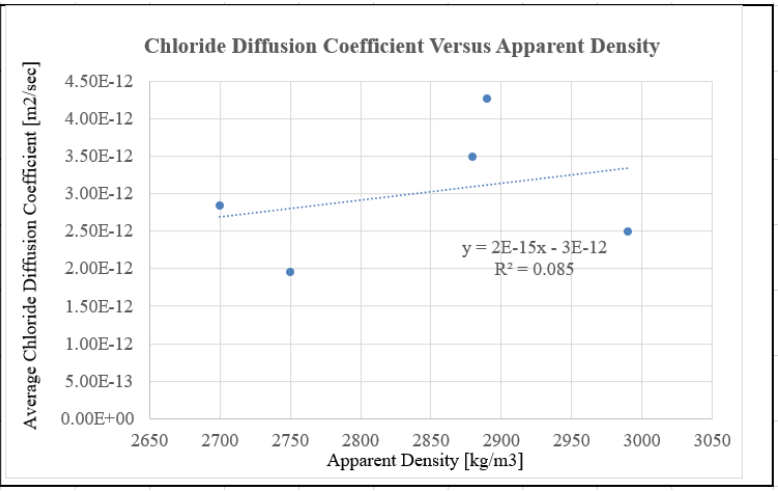

Figure 2.10 - Chloride Diffusion Coefficient Versus Apparent Density

Chloride Surface Concentration Versus Apparent Density		
Aggregate Source	Apparent Density (kg/m3)	Average Chloride Surface Concentration [%]
Bin Laheej	2700	0.91
Madinah	2880	0.87
Stevin Rock - Ghail	2750	0.89
Gabro	2890	0.78
Makah	2990	0.70

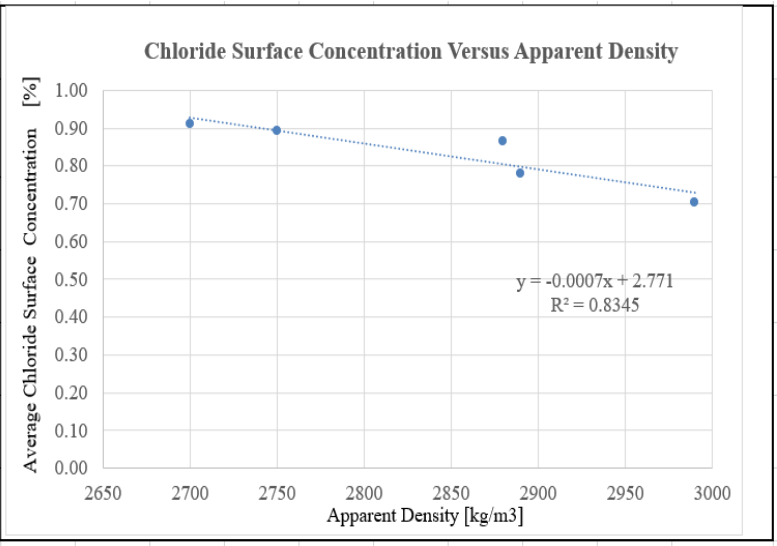

Figure 2.11 - Chloride Surface Concentration Versus Apparent Density

7.3. Effect of coarse aggregate water absorption

Absorption is defined as the increase in mass of aggregate due to water penetration into the pores of the particles (not including water adhering to the outside surface of the particles). A higher absorption value indicates a higher aggregate porosity. It worth mentioning that the pores that can be filled by water during the water absorption test are the pores that are opened to the surface. The graphs below show a fair relationship between the aggregate water absorption and chloride diffusion coefficient whereas the chloride surface concentration was independent from this property.

Chloride Diffusion Coefficient versus Water Absorption		
Aggregate Source	Water Absorption [%]	Average Chloride Diffusion Coefficient [m2/sec]
Bin Laheej	0.50	2.84E-12
Madinah	1.00	3.48E-12
Stevin Rock - Ghail	0.60	1.95E-12
Gabro	0.80	4.26E-12
Makah	0.40	2.48E-12

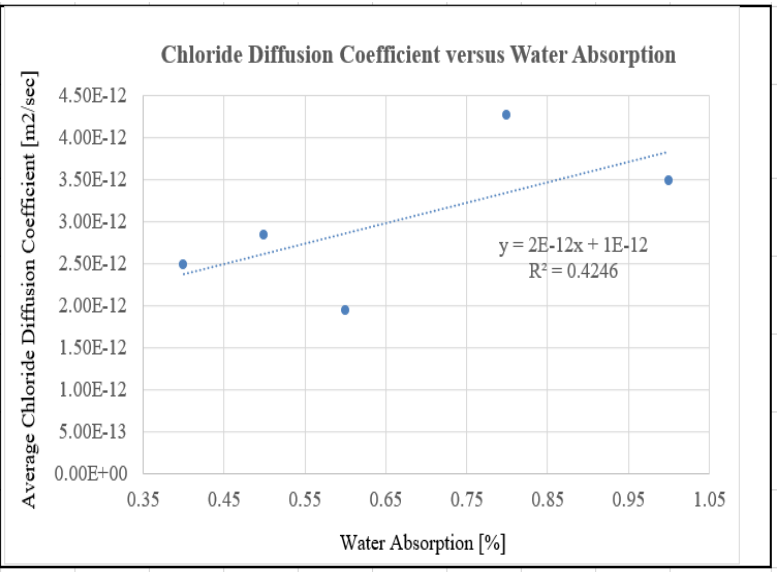

Figure 2.12 - Chloride Diffusion Coefficient versus Water Absorption

Chloride Surface Concentration Versus Water Absorption		
Aggregate Source	Water Absorption (%)	Average Chloride Surface Concentration [%]
Bin Laheej	0.50	0.91
Madinah	1.00	0.87
Stevin Rock - Ghail	0.60	0.89
Gabro	0.80	0.78
Makah	0.40	0.70

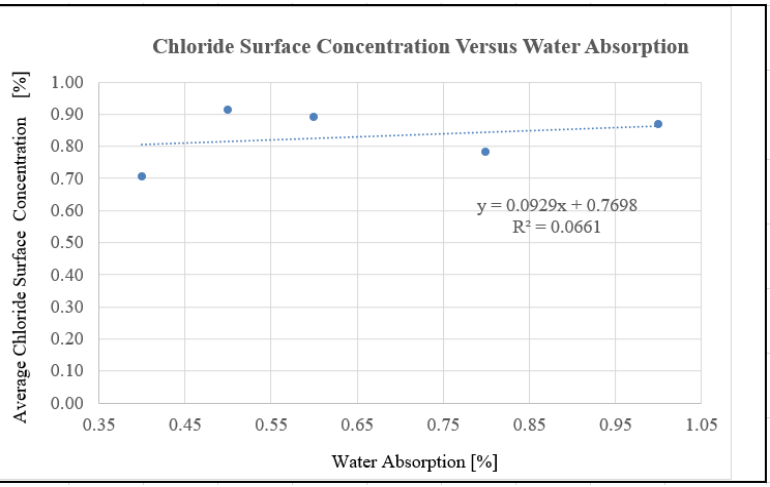

Figure 2.13 - Chloride Surface Concentration Versus Water Absorption

7.4. Effect of the coarse aggregate clay lumps and friable particles content

Clay lumps and friable particles in the aggregate are due to contamination at the time the deposit was formed, at the time of quarrying, or at the time of hauling and handling. Clay lumps in aggregate are defined as any particles or aggregation of particles which when thoroughly wet can be distorted when squeezed between the thumb and forefinger, or will disintegrate into individual grain sizes when immersed for a short period in water. This type of clay is different from lightweight pieces in aggregate (shert, shale, coal, lignite…) which have a relative density lower than 2.0 and are separated accordingly. ASTM C33 limits the amount of clays lumps and friable particles in fine aggregate to 3.0%, and in coarse aggregate, to a Maximum of 5.0% for concrete other than exposed architectural concrete. A relatively low effect was identified by this property on the chloride diffusion coefficient. The chloride surface concentration was however not affected by this property.

Chloride Diffusion Coefficient versus Clay Lumps and Friable Particles Content		
Aggregate Source	Clay Lumps and Friable Particles [%]	Average Chloride Diffusion Coefficient [m2/sec]
Bin Laheej	0.10	2.84E-12
Madinah	0.30	3.48E-12
Stevin Rock - Ghail	0.10	1.95E-12
Gabro	0.20	4.26E-12
Makah	0.20	2.48E-12

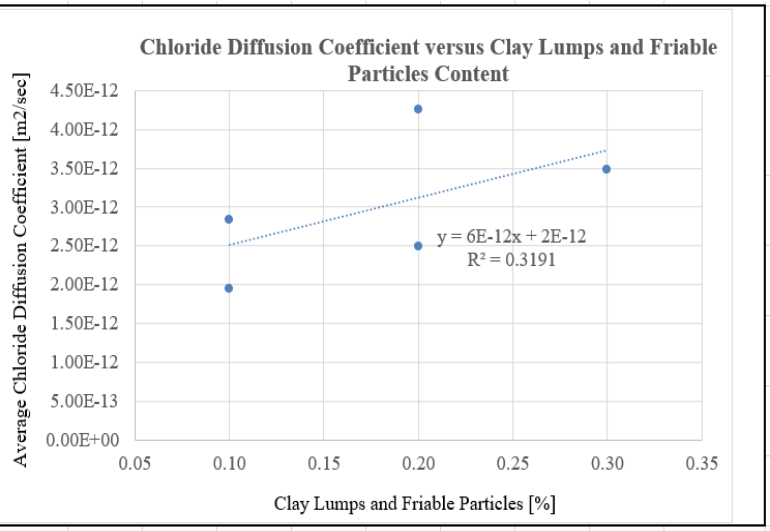

Figure 2.14 - Chloride Diffusion Coefficient versus Clay Lumps and Friable Particles Content

Chloride Surface Concentration Versus Clay Lumps and Friable Particles Content		
Aggregate Source	Clay Lumps and Friable Particles (%)	Average Chloride Surface Concentration [%]
Bin Laheej	0.10	0.91
Madinah	0.30	0.87
Stevin Rock - Ghail	0.10	0.89
Gabro	0.20	0.78
Makah	0.20	0.70

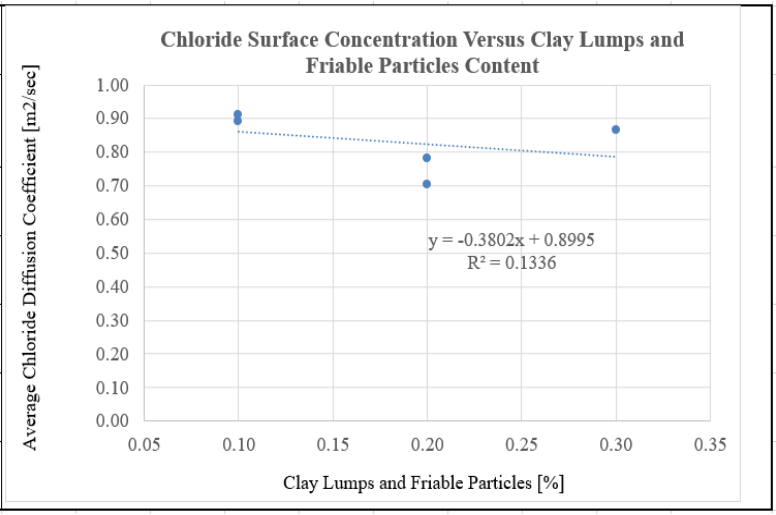

Figure 2.15 - Chloride Surface Concentration Versus Clay Lumps and Friable Particles Content

7.5. Effect of the coarse aggregate flakiness and elongation

The flakiness index is the percentage by weight of particles whose lowest dimension (thickness) is less than 0.6 of the mean size. The elongation index is the percentage by weight of particles whose highest dimension (length) is greater by 1.8 times its mean size. These tests are not applicable to sizes smaller than 6.5 mm (1/4 in). Flaky and elongated aggregate require more paste for coating which may eventually affect workability and strength (less economical mix). The graphs below show the variation of the chloride diffusion coefficient and the corresponding chloride surface concentration with the change of flakiness and elongation. Both properties seem to be unaffected by the aggregate flakiness and elongation.

Chloride Diffusion Coefficient versus Aggregate Flakiness		
Aggregate Source	Flakiness [%]	Average Chloride Diffusion Coefficient [m2/sec]
Bin Laheej	28.00	2.84E-12
Madinah	13.00	3.48E-12
Stevin Rock - Ghail	16.00	1.95E-12
Gabro	20.00	4.26E-12
Makah	16.00	2.48E-12

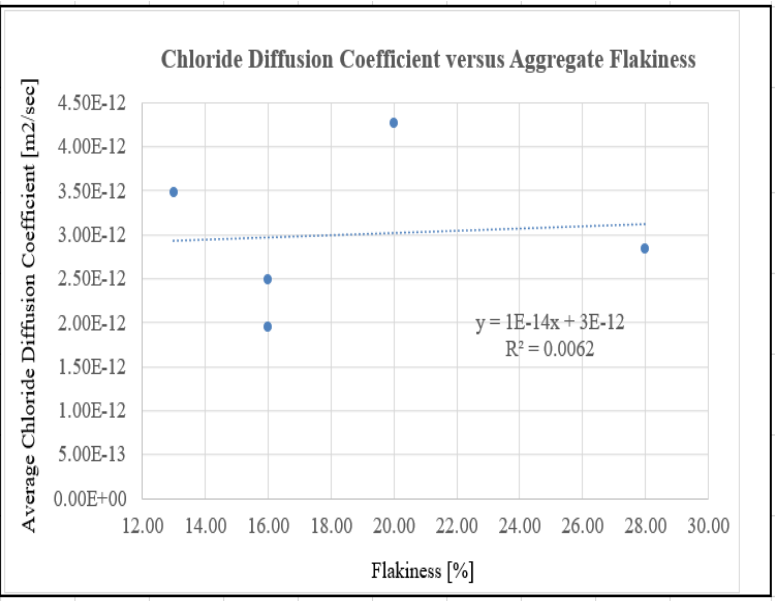

Figure 2.16 - Chloride Diffusion Coefficient versus Aggregate Flakiness

Chloride Surface Concentration Versus Aggregate Flakiness		
Aggregate Source	Flakiness (%)	Average Chloride Surface Concentration [%]
Bin Laheej	28.00	0.91
Madinah	13.00	0.87
Stevin Rock - Ghail	16.00	0.89
Gabro	20.00	0.78
Makah	16.00	0.70

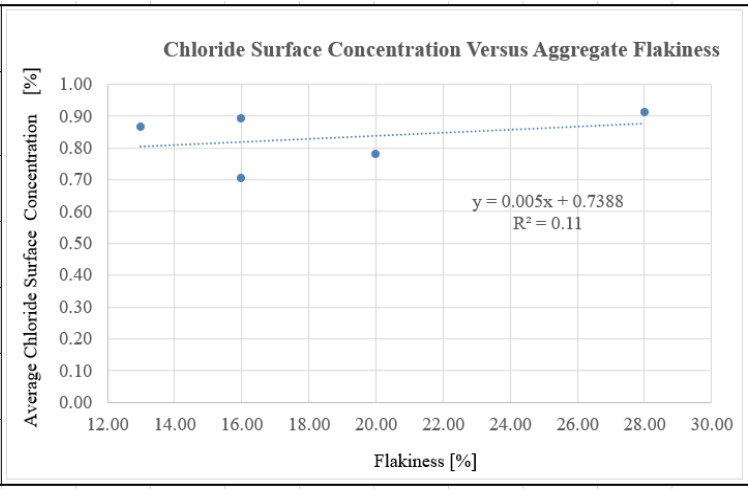

Figure 2.17 - Chloride Surface Concentration Versus Aggregate Flakiness

Chloride Diffusion Coefficient versus Aggregate Elongation		
Aggregate Source	Elongation [%]	Average Chloride Diffusion Coefficient [m2/sec]
Bin Laheej	21.00	2.84E-12
Madinah	18.00	3.48E-12
Stevin Rock - Ghail	21.00	1.95E-12
Gabro	26.00	4.26E-12
Makah	20.00	2.48E-12

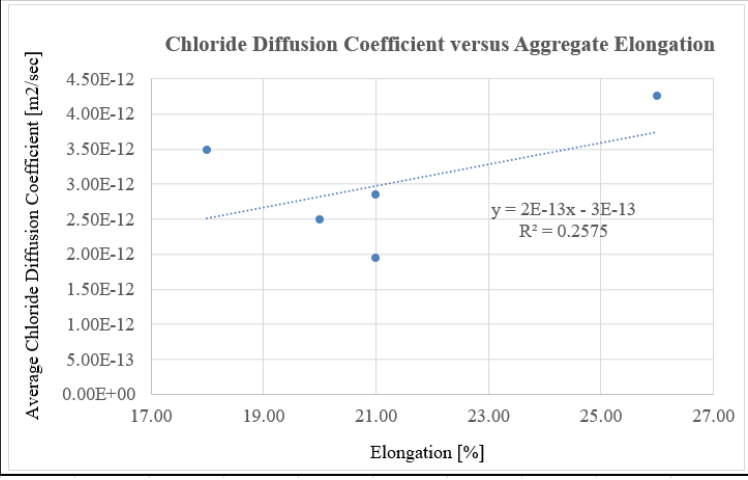

Figure 2.18 - Chloride Diffusion Coefficient versus Aggregate Elongation

Chloride Surface Concentration Versus Aggregate Elongation		
Aggregate Source	Elongation [%]	Average Chloride Surface Concentration [%]
Bin Laheej	21.00	0.91
Madinah	18.00	0.87
Stevin Rock - Ghail	21.00	0.89
Gabro	26.00	0.78
Makah	20.00	0.70

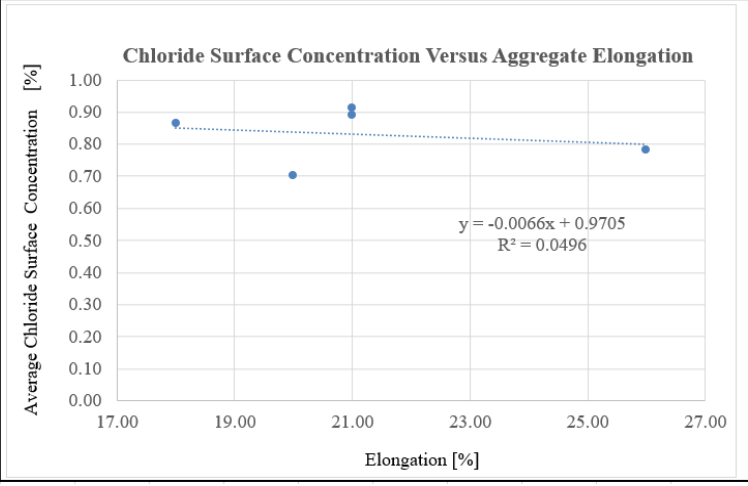

Figure 2.19 - Chloride Surface Concentration Versus Aggregate Elongation

7.6. Effect of coarse aggregate Los Angeles abrasion index

Los Angeles abrasion is usually used as an indicator of the relative quality or competence of various sources of aggregate. The test includes subjecting the coarse aggregate sample to a series of abrasive cycles in a drum containing steel balls and measuring the loss in aggregate weight. The lower the Los Angeles value, the tougher the aggregate and the less abrasive they are. Dense and non-weathered aggregates tend to have lower Los Angeles abrasion values. The below graphs show the variations in chloride diffusion coefficient and corresponding chloride surface concentration for different used Los Angeles Abrasion values; none of which seems to be related in any form.

Chloride Diffusion Coefficient versus Aggregate Los Angeles Abrasion

Aggregate Source	Los Angeles Abrasion (500 Rev.) [%]	Average Chloride Diffusion Coefficient [m2/sec]
Bin Laheej	22.90	2.84E-12
Madinah	12.20	3.48E-12
Stevin Rock - Ghail	20.80	1.95E-12
Gabro	16.50	4.26E-12
Makah	12.40	2.48E-12

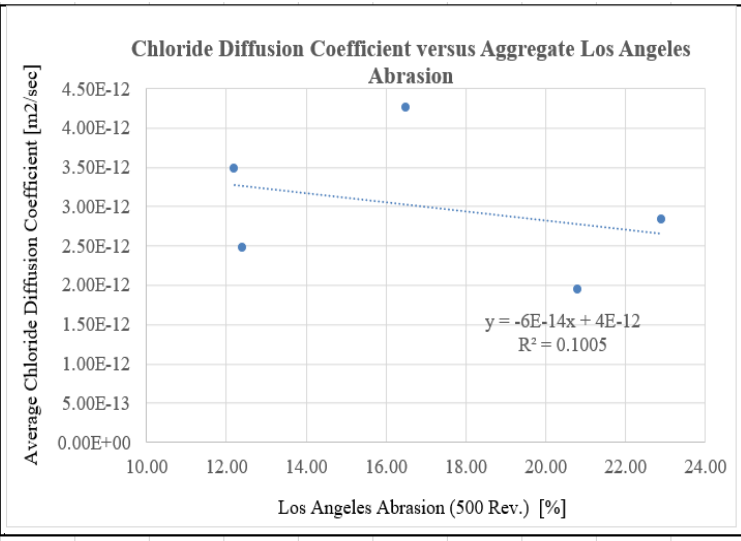

Figure 2.20 - Chloride Diffusion Coefficient versus Aggregate Los Angeles Abrasion

Chloride Surface Concentration Versus Aggregate Los Angeles Abrasion

Aggregate Source	Los Angeles Abrasion (500 Rev.) [%]	Average Chloride Surface Concentration [%]
Bin Laheej	22.90	0.91
Madinah	12.20	0.87
Stevin Rock - Ghail	20.80	0.89
Gabro	16.50	0.78
Makah	12.40	0.70

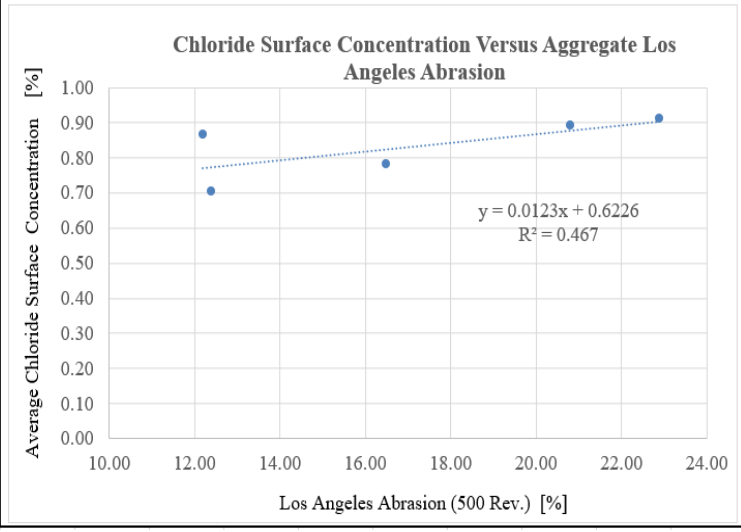

Figure 2.21 - Chloride Surface Concentration Versus Aggregate Los Angeles Abrasion

7.7. Effect of the coarse aggregate soundness

Soundness is the aggregate resistance to weathering that primarily includes resistance to freezing and thawing, and to a lesser extent, resistance to wetting and drying; heating and cooling. Durability problems such as pop-outs and D-cracking in pavements in some regions have been reported associated with unsound aggregates. ASTM C33 limits the aggregate soundness to Maximum 18.0% for coarse aggregate and 15.0% for fine aggregate. As seen from Figure 2.22 and 2.23, the aggregate soundness did not affect the chloride diffusion coefficient but have a fair influence on the chloride surface concentration.

Chloride Diffusion Coefficient versus Aggregate Soundness

Aggregate Source	Soundness [%]	Average Chloride Diffusion Coefficient [m2/sec]
Bin Laheej	1.80	2.84E-12
Madinah	5.60	3.48E-12
Stevin Rock - Ghail	3.10	1.95E-12
Gabro	4.10	4.26E-12
Makah	6.20	2.48E-12

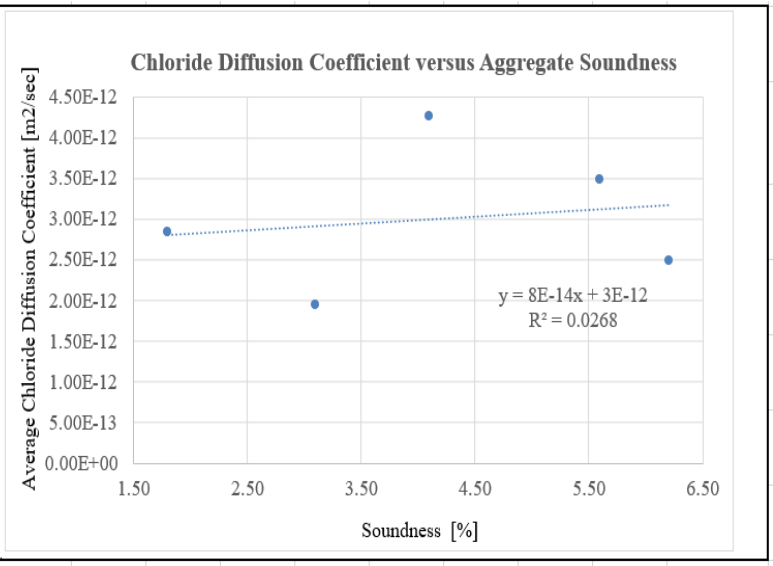

Figure 2.22 - Chloride Diffusion Coefficient versus Aggregate Soundness

Chloride Surface Concentration Versus Aggregate Soundness

Aggregate Source	Soundness [%]	Average Chloride Surface Concentration [%]
Bin Laheej	1.80	0.91
Madinah	5.60	0.87
Stevin Rock - Ghail	3.10	0.89
Gabro	4.10	0.78
Makah	6.20	0.70

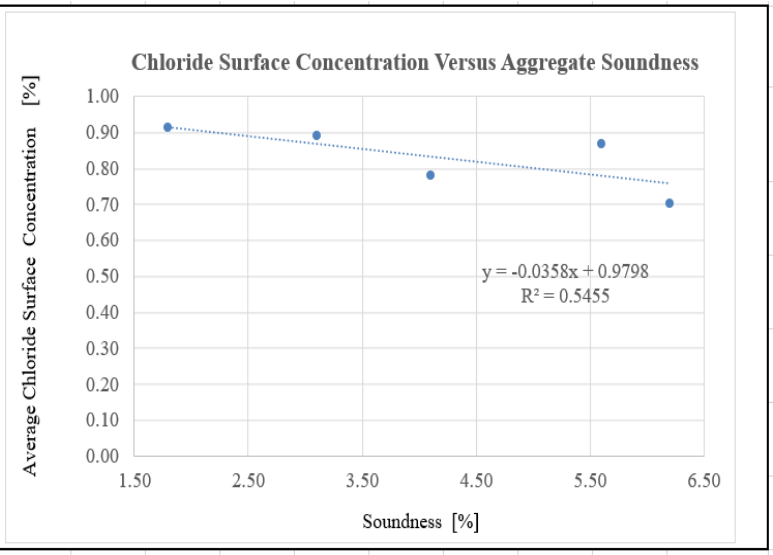

Figure 2.23 - Chloride Surface Concentration Versus Aggregate Soundness

7.8. Coupled effect of aggregate properties

A relatively good relation was identified between the following parameters:

- Chloride diffusion coefficient and Materials finer than 75 microns.
- Chloride diffusion coefficient and water absorption
- Chloride diffusion coefficient and Clay lumps – Friable particles
- Chloride surface concentration and density
- Chloride surface concentration and soundness
- Chloride surface concentration and loss Angeles Abrasion

The six relationships suspected above, suggested that the chloride diffusion coefficient was affected by the peripheral condition of the aggregate whereas the chloride surface concentration was affected by the type of the aggregate constituent material.

The relationships were however identified separately as a function of each aggregate property. As an indication of the coupled effect of the three former properties on the chloride diffusion coefficient, a linear multiple regression analysis was made, the input parameters for this multiple regression are defined in Table 2.9. Similarly, the three later aggregate properties defined in the list were found to individually affect the surface concentration. A linear multiple regression analysis was made to identify the coupled effect of these three parameters on the chloride surface concentration.

The main aim of the multiple regression analysis is not to identify he final influencing function affecting the chloride diffusion coefficient and the surface concentration. It rather indicates the coupling effect. The influencing functions, taking into account the mediums of chloride ingress are far more complex than a linear regression analysis and will be demonstrated in detail in the following sections.

Multiple regression 1:

Table 2.9 - Multiple Regression 1 - Chloride Diffusion Coefficient – Input Parameters

Aggregate source	Y	X1	X2	X3
	Average chloride diffusion coefficient $[\times 10^{-12} m^2/sec]$	Material finer than 75 microns (%)	Water absorption [%]	Clay lumps and friable particles [%]
Bin Laheej	2.84	0.50	0.50	0.10
Madinah	3.48	0.40	1.00	0.30
Stevin Rock - Ghail	1.95	0.20	0.60	0.10
Gabro	4.26	1.10	0.80	0.20
Makah	2.48	0.20	0.40	0.20

The multiple regression was made using excel where the results are summarized in Table 2.10:

Table 2.10 - Multiple Regression 1 - Chloride Diffusion Coefficient - Output Parameters

SUMMARY OUTPUT – Regression Analysis 1 – Chloride Diffusion Coefficient								
Regression Statistics								
Multiple R	0.99095385							
R Square	0.981989533							
Adjusted R Square	0.92795813							
Standard Error	2.40813E-13							
Observations	5							
ANOVA								
	df	*SS*	*MS*	*F*	*Significance F*			
Regression	3	3.16186E-24	1.05E-24	18.17442	0.170358			
Residual	1	5.7991E-26	5.8E-26					
Total	4	3.21985E-24						
	Coefficients	*Standard Error*	*t Stat*	*P-value*	*Lower 95%*	*Upper 95%*	*Lower 95.0%*	*Upper 95.0%*
Intercept	1.17655E-12	3.51079E-13	3.351252	0.18461	-3.3E-12	5.64E-12	-3.3E-12	5.64E-12
Material Finer than 75 Microns (%)	1.98504E-12	3.6487E-13	5.4404	0.115725	-2.7E-12	6.62E-12	-2.7E-12	6.62E-12
Water Absorption [%]	4.66055E-14	7.71443E-13	0.060413	0.961586	-9.8E-12	9.85E-12	-9.8E-12	9.85E-12
Clay Lumps and Friable Particles [%]	4.68847E-12	2.04764E-12	2.289698	0.262142	-2.1E-11	3.07E-11	-2.1E-11	3.07E-11

Multiple regression 2:

Table 2.11 - Multiple Regression 2 - Chloride Surface Concentration – Input Parameters

Average chloride surface concentration [%]	Oven dry density [kg/m3]	Soundness [%]
0.00913	2660	1.8000
0.00867	2800	5.6000
0.00892	2700	3.1000
0.00781	2820	4.1000
0.00704	2950	6.2000

The multiple regression was made using Microsoft Excel where the results are summarized in Table 2.12. The Los Angeles abrasion was omitted from the multiple regression as the attributed coefficient in the corresponding regression was negative. This finding contradicts the initial test result and no coupled effect was thus concluded including the Los Angeles Abrasion.

Table 2.12 - Multiple Regression 2 - Chloride Surface Concentration - Output Parameters

SUMMARY OUTPUT – Regression Analysis 2 – Chloride Surface Concentration								
Regression Statistics								
Multiple R	0.996719							
R Square	0.99345							
Adjusted R Square	0.986899							
Standard Error	9.96E-05							
Observations	5							
ANOVA								
	df	SS	MS	F	Significance F			
Regression	2	3.01074E-06	1.51E-06	151.6641	0.00655			
Residual	2	1.98513E-08	9.93E-09					
Total	4	3.03059E-06						
	Coefficients	Standard Error	t Stat	P-value	Lower 95%	Upper 95%	Lower 95.0%	Upper 95.0%
Intercept	0.041022	0.002672605	15.34918	0.004218	0.029523	0.052522	0.029523	0.052522
Oven Dry Density [kg/m3]	-1.2E-05	1.04796E-06	-11.6955	0.007232	-1.7E-05	-7.7E-06	-1.7E-05	-7.7E-06
Soundness [%]	0.000345	6.61453E-05	5.214963	0.034859	6.03E-05	0.00063	6.03E-05	0.00063

The correlation factors for the multiple regression where found higher than the ones concluded with single regression, and thus adopted.

When only the type of coarse aggregate is the varying parameter in the concrete mix, the chloride diffusion coefficient is found depended from the materials finer than 75 microns content, water absorption, and Clay lumps-Friable Particles content. The chloride surface concentration was found dependent from the density and soundness of the aggregate. The two R-squared values found in the corresponding regression analysis are above 0.98 which indicates a very high dependence.

8. Results discussion and evaluation

8.1. Chloride diffusion doefficient

At the structure level, chloride ions in concrete diffuse through three volumes. The aggregate volume, the bulk cement paste volume and the interfacial transition zone between the aggregate at the cement paste. The cement paste in the region surrounding each aggregate particle, i.e. the ITZ, contains higher porosity and lower cement content relatively to the bulk cement paste regions farther away. Therefore, this zone is attributed a separate diffusion volume. The concept of dividing the diffusion volumes into different volumes is analogous to the method developed by Zheng et al. [76] where the diffusion volume was divided into three: Aggregate, Interfacial Transit Zone, and cement paste. The idea of dividing the concrete into three zones instead of considering it as a two phases material (aggregate and matrix) was equally used in other publications. The main reason behind this concept is that the cement paste cannot be considered as a homogenous phase.

In fact, the microstructure of the cement paste is modified in the vicinity of the aggregate particles [77].

The testing campaign made in this chapter tends to reflect the effect of the coarse aggregate properties on the chloride diffusion coefficient and the corresponding chloride surface concentration. The results are thus expected to concern the diffusion through the coarse aggregate volume and the ITZ.

Since the test results indicate that there are several parameters that affects the chloride transportation in concrete, apart from the type of coarse aggregate, ITZ, and bulk cement paste, the need to update the model of a three-phases materials (for chloride diffusion) was essential.

8.2. Suggested diffusion phases

This model was updated into a five diffusion volumes/zones. Two volumes were added to the zones of chloride diffusion. The first volume added include the low-quality impurities in the coarse aggregate which tend to have a significant impact. These impurities are reflected by the amount of clay lumps and friable particles in concrete. Other impurities may have similar effects and should be investigated. The second parameter affecting the chloride transportation in the concrete (and related to the coarse aggregate quality) includes the coarse aggregate surface condition. This parameter can be reflected by the aggregate absorption in addition to the amount of materials finer than 75 microns caught on the coarse aggregate's surface. The coarse aggregate water absorption is selected as a parameter that contributes to the surface conditions considering that, only the pores that are opened to the surface can absorb water. The five zones of chloride diffusion in concrete, while taking into consideration the effect of coarse aggregate properties, are thus as follows:

Table 2.13 – Suggested Zones of Chloride Diffusion in Concrete

Zones/Volumes of Chloride Diffusion in Concrete (Taking in into consideration the effect of coarse aggregate properties)				
Zone 1: Coarse Aggregate Materials	Zone 2: Low Quality Impurities in Coarse Aggregate	Zone 3: Coarse Aggregate Surface Conditions	Zone 4: Interfacial Transition Zone	Zone 5: Bulk Cement paste

To illustrate the model for further analysis, the aggregates are considered as polydisperse spheres that includes a percentage of low-quality impurities. These spheres are considered to have a radius "r_a". These spheres are coated with a transition layer that represents the surface conditions, with a specific width, then enveloped by a multilayer area that illustrates the ITZ. The thickness of the ITZ and the aggregate spheres is noted as "r_b" (the width of the ITZ is thus equal (r_b - r_a). The

whole is embedded in the bulk cement paste so the total thickness of the aggregate sphere, ITZ and enveloping cement paste is equal to "r_c".

In order to take into account the varying properties of the ITZ, the ITZ was divided into N concentric shell element. Each element is considered to have specific consistent properties. The higher the N number the higher the accuracy of the model. The varying properties of the ITZ are the porosity and the cement content/hydration product as a function of the distance from the aggregate. The values of "r_a", "r_b", and "r_c", are calculated to meet the volumes of the aggregate, the ITZ, and the bulk cement paste.

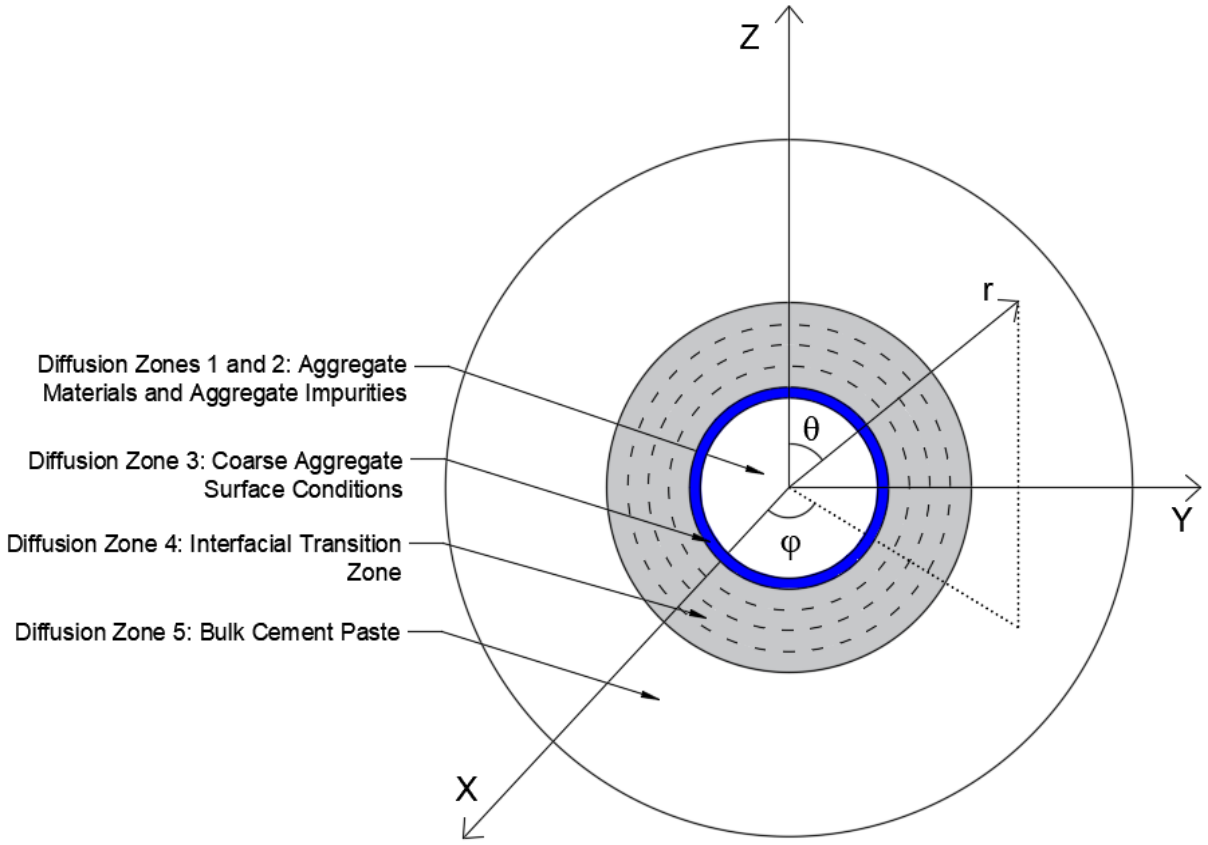

Figure 2.3 – Suggested new diffusion zones/volumes

8.1.1. Diffusion volume 1: chloride diffusion in the coarse aggregate material

The main finding observed in the testing campaign concludes that the chloride diffusion in the coarse aggregate portion itself is insignificant. This is valid for the range of properties tested. Considering the model proposed by Hobbs [63], the insignificant diffusion through the aggregate means that the concrete diffusion coefficient is solely in the paste portion. The results of the testing campaign suggest otherwise.

The chloride diffusion is thus taking place necessarily in the four remaining volumes, from which the coarse aggregate itself can be excluded due to the insignificant chloride diffusion coefficient.

Considering however this zone of diffusion, is essential due to the effect of its contribution, as a varying volume, on the total chloride diffusion.

8.1.2. Chloride diffusion coefficient dependence from the coarse aggregate properties – diffusions in volumes 2 and 3

The chloride diffusion coefficient was found to be highly dependent from the aggregate properties as follows: Materials Finer than 75 microns, water absorption, and clay lumps-friable particles. The former two parameters are relatively related to the surface condition of the aggregate and thus partially characterize the ITZ, whereas the third parameter is a clay and friable quantity of aggregate in the concrete, that would expect to reduce the concrete quality, and consequently reduce the durability, and increase the chloride diffusion.

Materials finer than 75 microns: Materials finer than 75 microns or also interchangeably known as "fines" is tested in reference to ASTM C117 [78]. This material may be very fine sand, silt, dust or clay [79]. Excessive fine increases the water demand and reduce the aggregate-cement bond [79]. ASTM C33 [80] limits the range of materials finer than 75 microns content generally to 3% due to its adverse effects on the concrete quality. This limit can be increased to 5% in crushed sand then increased by 2% if the concrete is not subjected to abrasion [80]. BS882 sets a similar limit where the maximum percentage can reach 2%, 4%, and 16% depending on the type of aggregate [81]. The effect on the concrete performance was assessed in several publications where up to 44% of the concrete compressive strength was found to be affected by this materials presence [82]. These publications identify the significant effect of this material portion on the concrete properties. The test results related to the campaign conducted in this chapter has quantitively identified the effect of this materials portion on the chloride diffusion. Going from the fact that this type of materials is usually stuck on the aggregate surface, the corresponding effect was subsequently considered as an aggregate surface effect that affects the concrete chloride diffusion.

Aggregate Water Absorption: Water absorption is defined as the change in the mass of an aggregate due to water absorbed in the pore spaces within the constituent particles [83]. It is directly related to the pores in the aggregate that are opened to the surface. These pores will be filled with water to an SSD (Saturated Surface Dry) condition in the mix. Once the water is added to the mix, the pores will absorb water to fill these pores whereas the remaining water on the surface will be mixed to the cement paste. Since the aggregate material has an insignificant chloride diffusion coefficient, saturated pores that are opened to the surface are more likely to diffuse chloride. Titi et al. [36] have identified a relationship between the Rapid chloride penetration test and the coarse aggregate water absorption which furthermore justifies this conclusion. Specifications limits on the aggregate water absorption are very rare, although higher water absorption values indicate a more weathered concrete.

Going from the fact that the water absorption is equivalent to a saturated, opened-to-the surface pores in the aggregate, the corresponding effect was subsequently considered as an aggregate surface effect that affects the concrete chloride diffusion.

Clay lumps and friable particles: Clay lumps and Friable Particles are tested in reference to ASTM C142 [84] by soaking the aggregate in distilled water and then trying to break the particle into smaller sizes. The particles that are broken are considered as clay lumps and friable particles. This type of materials is not thus a coating to the aggregate itself; it is a separate standalone type of particle. The testing campaign conducted in this chapter concludes that the presence of this materials affects the chloride diffusion which converge with the hypothesis that lower quality aggregate has lower resistance to chloride diffusion. Going from the fact that the clay lumps and friable particles are considered as a percentage of low-quality materials in the aggregate, this material was attributed a separate category of influence on the chloride diffusion coefficient.

As a conclusion to this section, the coarse aggregate properties reflect two category of effects on the chloride diffusion coefficient as follows:

- Surface condition effects: Materials finer than 75 microns and aggregate water absorption.
- Low quality materials effects: Clay lumps and friable particles

8.1.3. Diffusion volume 4: chloride diffusion in the Interfacial Transition Zone (ITZ)

The interfacial transition zone may be one of the most influencing parameters for the chloride transportation. The chloride diffusion coefficient increases in the ITZ. As estimated by Breton et al. [85] the chloride diffusion in the ITZ can be 12 times higher for an ITZ with a thickness of 100µm. In fresh concrete a water-cement ratio gradient develops around the aggregate particles during casting, resulting in a different microstructure of the surrounding hydrated cement paste [77]. This phenomenon is explained by a microbleeding that leads to an accumulation of water under the aggregate particles before the concrete setting [77]. The microstructure of the interfacial transition zone maybe described in terms of the porous microstructure and the hydration process [77]. Based on this, and in order to characterize the Interfacial Transition Zone, the following should be defined:

- Thickness of the Interfacial Transition Zone
- Porosity of the Interfacial Transition Zone
- Hydration Process in the Interfacial Transition Zone
- Influence of the chemical reactivity of the aggregate on the Interfacial Transition Zone

The porosity of the Interfacial Transition Zone is performed using two methods: The image analysis of flat polished surfaces observed by SEM and mercury intrusion porosimetry [77] (MIP). Figure 2.24 [86] illustrates the porosity as a function of the distance from aggregate. In addition to

the fact that the porosity is identified from the SEM and MIP, the thickness of the interfacial Transition Zone can also be measured. The ITZ thickness will be equal to the distance from the aggregate surface to the point where the porosity starts to be a constant. The graph below notes one important point related to the thickness and porosity of the ITZ when Silica Fume is used as a partial replacement of the cement. The ITZ thickness seems to be insignificant and the porosity remains constant as a function of the distance from the aggregate. This finding was also reported by Bajja et al.[69] in Figure 2.25 where the thickness of the ITZ was found insignificant when using silica fume.

For OPC paste, the ITZ thickness is typically 50µm [77]. In the works reported by Crumbie [87], the ITZ width was varying between 20µm and 30µm with the porosity tending towards 100% at the aggregate interface. The ITZ width was as well dependent from the cement particle size rather than the water-cement ratio or the aggregate size. The reduction of the ITZ thickness when silica fume was used is mainly due to the micro silica's small grain size that can be considered as a microfiller. The consequence will be a reduction in ITZ porosity and thickness.

For the remaining part of the analysis, the width of the ITZ is considered to be equal to 5µm. Based on this literature, it is fair to consider that the ITZ width for mixes including microsilica (above 5% as common silica fume content) is 5µm, and for OPC concrete, equal to 50µm.

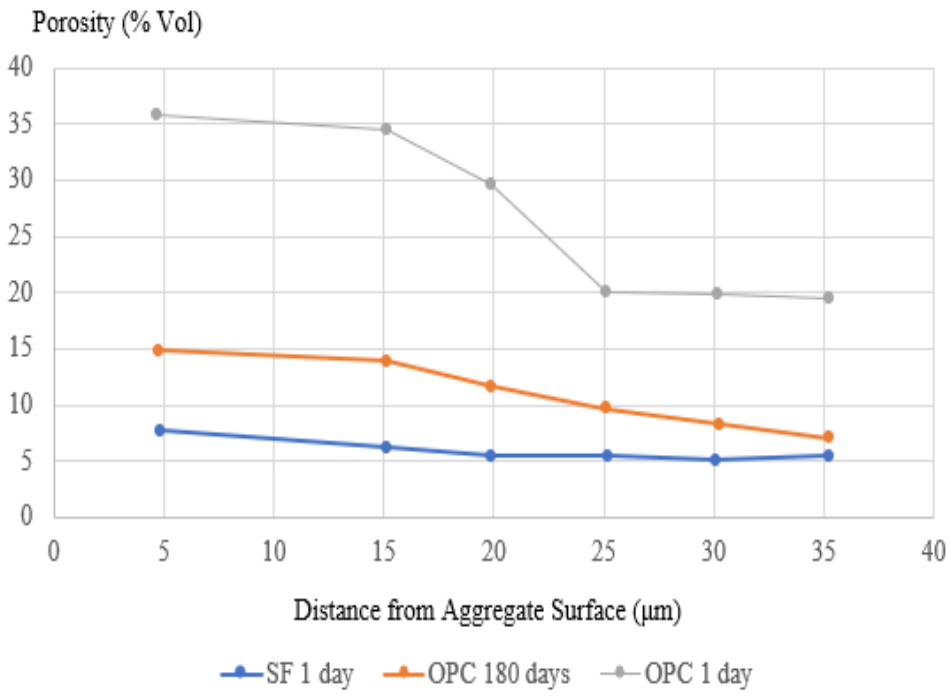

Figure 2.24 - Porosity as a function of the Distance from the Aggregate Surface (Graph Replicated from: Scrivener, K.L.: Bentur, A.: Pratt, P.L. Advances in Cement Research 1988, 1, 230-237)

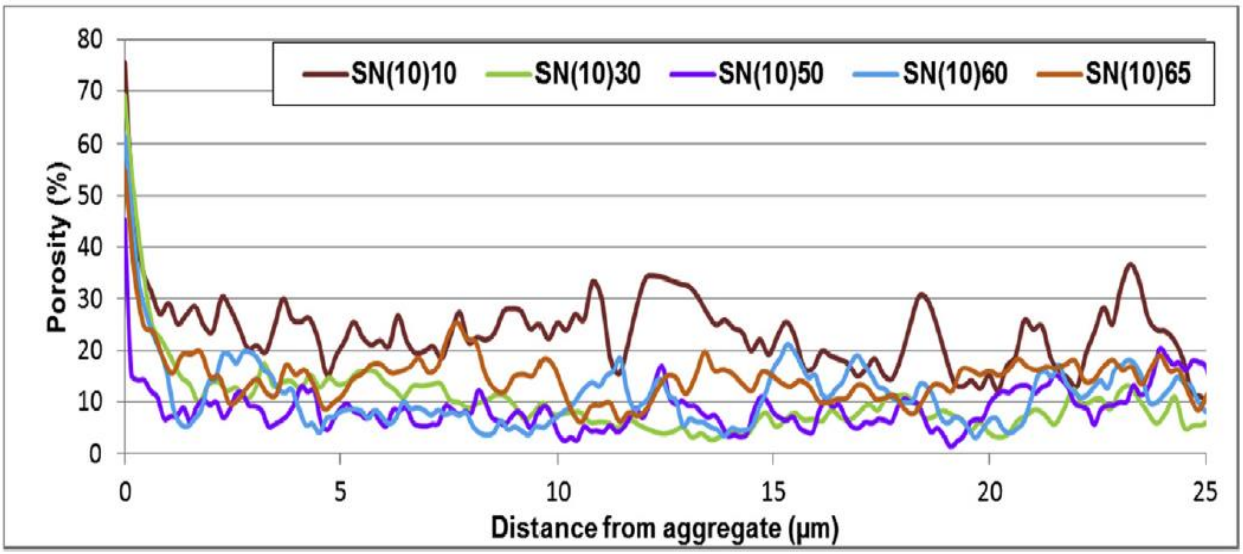

Figure 2.25 - Porosity as a function of the Distance from the Aggregate Surface

8.1.4. Diffusion volume 5: chloride diffusion in the cement paste

The diffusion of the chloride in the bulk cement paste is discussed in other chapters of this thesis as this chapter is limited to the effect of coarse aggregate properties on the chloride diffusion coefficient and chloride surface conditions. This chapter reaches a conclusion regarding the effect of changing the aggregate properties rather than the complete model that will be discussed in chapter 6.

8.2. Chloride surface concentration

The testing campaign concludes that the chloride surface concentration was related to the aggregate density and soundness which are properties related to the aggregate quality in terms of constituent materials. These two properties did not influence or contribute to the diffusion. As a consequence, another chloride transportation mechanism may have increased the chloride at the surface. Noting that the three mechanisms of chloride transportation include diffusion, capillary absorption, and hydraulic pressure, and while excluding the diffusion and hydraulic pressure (the different cores were subjected to same hydraulic pressure), the capillary absorption seems to be the only mechanism responsible for this relationship. This finding is in line with the capillary absorption property that was demonstrated to transport the chloride to a very shallow level [36], thus the increase in chloride concentration. This finding is as well in line with the fact that less dense aggregate and less sound aggregate indicate a more weathered aggregate which will offer less resistance to degradation or chloride ingress. The increase in chloride surface concentration is thus related to the absorption of the chloride at the surface that sums up to the chloride diffusion in the concrete.

9. Numerical method of solving the chloride diffusion coefficient taking into consideration five volume of diffusion

The aggregate properties do not affect directly the concrete chloride diffusion coefficient. These properties are rather dependent, and work in combination with, the concrete properties to affect the overall concrete chloride diffusion. It is thus necessary to consider these entities in combination when developing a function illustrating the effect of the aggregate chloride diffusion coefficient and aggregate properties on the total chloride diffusion coefficient. The base model followed in the analysis is the one represented in figure 2.3. Developing a numerical method to solve the diffusion mechanism in the proposed five-volume diffusion requires the following:

- Step 1: Identification of the total aggregate volume and weight as defined in the concrete mix design.
- Step 2: Identification of the aggregate particle distribution from the aggregate sieve analysis test as per ASTM C136 for an accurate representation.
- Step 3: Identification of the aggregate diffusion coefficient which is demonstrated to be equal to zero in the range of properties tested.
- Step 4: Defining the ITZ thickness (or measuring it through SEM).
- Step 5: Calculating the overall volume of ITZ and Bulk cement paste from the ITZ width and aggregate content and size distribution.
- Step 6: Calculating the cement distribution in the ITZ and the bulk cement paste, in addition to the water-cement ratio as a function of the distance from the aggregate surface.
- Step 7: Simulating a hydration model in order to identify the degree of hydration as a function of the distance from the aggregate surface.
- Step 8: Calculating the volume fraction of capillary pores, gel pores, and total pores as a function of the distance from the aggregate.
- Step 9: Calculating the relative diffusion value as a function of the porosity and the diffusivity of the chloride ions in the pore solution, in the bulk cement paste, and the ITZ.
- Step 10: Updating the concrete diffusion model to yield a concrete diffusion as function of the aggregate diffusion, clay lumps/friable particles effects, surface effects, diffusion of the ITZ and the diffusion in the bulk cement paste.

9.1. Volume fraction calculations

The total aggregate volume and weights were defined in the concrete mix design and tabulated in appendix 2.1. This volume was divided according to the aggregate size distribution concluded from the sieve analysis test. The width of the ITZ for microsilica concrete is taken equal to 5μm and for OPC concrete equal to 50μm based on the available literature. For the remaining part of the analysis, the width of the ITZ is equal to 5μm. The volume of the ITZ and the bulk cement can

be calculated by dividing the aggregate into categories of different sphere sizes based on the corresponding sieve analysis results then adding the thickness of the ITZ to each category of sizes. The total volume of the ITZ is then calculated as the sum of the volumes on the different categories. The width of the bulk cement paste enveloping the aggregate and ITZ is then solved to have a total volume equal to $1m^3$ based on the size categories. The related calculations are tabulated in appendix 2.1.

9.2. Cement distribution and water-cement ratio as a function of the distance from the aggregate surface

The next step includes the calculation of the cement distribution in the ITZ and the bulk cement paste, in addition to the water-cement ratio as a function of the distance from the aggregate surface. In order to execute this calculation, it is worth highlighting the following initial conditions:

- The porosity is 100% at the cement-aggregate interface.
- The width of the ITZ in microsilica concrete is 5μm.
- The cement distribution in the ITZ is different than the bulk cement paste.
- The total volume of cement is equal to the volume of cement in the ITZ and the volume of cement in the bulk cement paste.

Based on the work conducted by Crumbie [87], Zheng et al. [76] have fitted the cement particle distribution in a numerical equation as defined in the following formula. This formula has recorded an R^2 value exceeding 0.99 for the different data reported by Crumbie [87].

$$f_c(r) = \begin{cases} f_{c,bulk} \sum_{j=1}^{4} \left(\frac{b_j}{b_0}\right) \left[\frac{r - r_a}{r_b - r_a}\right]^j, & r_a \le r < r_b \\ f_{c,bulk}, & r_b \le r \le r_c \end{cases} \tag{2.4}$$

where $f_{c,bulk}$ is the cement volume fraction in the bulk paste, r is the distance from the center of the aggregate, r_a is the distance from the center of the aggregate to the edge of the aggregate sphere, r_b is the distance from the center of the aggregate to the outer edge of the ITZ, r_c is the distance from the center of the aggregate to the edge of the encapsulating cement paste sphere, and b_j is a series of empirical functions expressed as a function of the concrete water-cement ratio as follows:

$$b_1 = 4.670 - 5.228(w_{0,c}) \tag{2.5}$$

$$b_2 = -10.569 + 12.700(w_{0,c}) \tag{2.6}$$

$$b_3 = 9.950 - 12.195(w_{0,c}) \tag{2.7}$$

$$b_4 = -3.397 + 4.195(w_{0,c}) \tag{2.8}$$

$$b_0 = \sum b_j$$

(2.9)

where $(w_{0,c})$ is the corrected water-cement ratio excluding the water in the aggregate.
The cement volume fraction in the bulk cement paste is calculated in reference to the same publication as a function of the water-cement ratio, cement density, and the volume fractions of the bulk cement paste and ITZ, noting that the total volume of the cement is equal to the volume of cement in the ITZ and the volume of cement in the bulk cement paste. The cement volume fraction in the bulk cement paste is thus equal to the following:

$$V_c = \frac{4\pi(r_c^3 - r_a^3)}{3[1 + \rho_c(w_{0,c})]} = V_{c,ITZ} + V_{c,bulk}$$

(2.10)

where $r_a$is the distance fromt eh center of the aggregate to the edge of the aggregate sphere, ρ_c is the cement density, r_c is the distance from the center of the aggregate to the edge of the encapsulating cement, and $(w_{0,c})$ is the corrected water-cement ratio, excluding the water in the aggregate.

The volume of cement at any point r varying between r_a and r_b is as follows:

$$V_{c,r} = \frac{4\pi(r^3 - r_a^3)}{3} f_c(r)$$

(2.11)

The volume of cement in the ITZ is calculated by integrating, from $r = r_a$ to $r = r_b$ the following formula:

$$V_{c,ITZ} = \int_{r_a}^{r_b} 4\pi r^2 f_c(r) dr$$

(2.12)

On the other hand, the volume of cement in the bulk cement paste is calculated as follows:

$$V_{c,bulk} = \frac{4\pi(r_c^3 - r_b^3)}{3} f_{c,bulk}$$

(2.13)

Defining the three formulas above as a function of $f_{c,bulk}$, , r_a, , r_b, and r_c while noting that the total volume of cement is equal to sum of the volume of cement in the ITZ and the volume of cement in the bulk cement paste:

$$\frac{4\pi(r_c^3 - r_a^3)}{3[1 + \rho_c(w_{0,c})]} = \frac{4\pi(r_c^3 - r_b^3)}{3} f_{c,bulk} + \int_{r_a}^{r_b} 4\pi r^2 f_c(r) dr$$

$$= \frac{4\pi(r_c^3 - r_b^3)}{3} f_{c,bulk} + \int_{r_a}^{r_b} \left(4\pi r^2 (f_{c,bulk} \sum_{j=1}^{4} \left(\frac{b_j}{b_0}\right) [\frac{r - r_a}{r_b - r_a}]^j)\right) dr$$

Thus:

$$\frac{4\pi(r_c^3 - r_a^3)}{12\pi f_{c,bulk}[1+\rho_c(w_{0,c})]} = \frac{(r_c^3 - r_b^3)}{3} + \int_{r_a}^{r_b}\left(r^2(\sum_{j=1}^{4}\left(\frac{b_j}{b_0}\right)[\frac{r-r_a}{r_b-r_a}]^j)\right)dr$$

$$= \frac{(r_c^3 - r_b^3)}{3} + \frac{\int_{r_a}^{r_b} A(r)dr}{b_0 \times (r_b - r_a)^4}$$

Finally:

$$f_{c,bulk} = \frac{b_0(r_c^3 - r_a^3)(r_b - r_a)^4}{\left[1+\rho_c(w_{0,c})\right]\left[(r_c^3 - r_b^3)b_0(r_b - r_a)^4 + 3\int_{r_a}^{r_b} A(r)dr\right]}$$

where:

$$A(r) = r^2 b_1(r-r_a)(r_b-r_a)^3 + r^2 b_2(r-r_a)^2(r_b-r_a)^2 + r^2 b_3(r-r_a)^3(r_b-r_a)^1 + r^2 b_4(r-r_a)^4$$

Equivalent to:

$$A(r) = Br^2 + Cr^3 + Dr^4 + Er^5 + Fr^6$$

$$\int_{r_a}^{r_b} A(r)dr = B\left(\frac{r_b^3}{3} - \frac{r_a^3}{3}\right) + C\left(\frac{r_b^4}{4} - \frac{r_a^4}{4}\right) + D\left(\frac{r_5^2}{5} - \frac{r_5^2}{5}\right) + E\left(\frac{r_b^6}{6} - \frac{r_a^6}{6}\right) + F\left(\frac{r_b^7}{7} - \frac{r_a^7}{7}\right)$$

where B, C, D, E, and F are constant numbers defined below:

$B = (b_1 + b_2 + b_3 + b_4)r_a^4 + (-3b_1 - 2b_2 - b_3)r_b r_a^3 + (+3b_1 + b_2)r_b^2 r_a^2 - r_b^3 b_1 r_a$
$C = (-b_1 - 2b_2 - 3b_3 - 4b_4)r_a^3 + (+3b_1 + 4b_2 + 3b_3)r_b r_a^2 + (-3b_1 - 2b_2)r_b^2 r_a + r_b^3 b_1$
$D = (b_2 + 3b_3 + 6b_4)r_a^2 + (-b_2 2 - 3b_3)r_b r_a + b_2 r_b^2$
$E = r_b b_3 - r_a(b_3 + 4b_4)$
$F = b_4$

Once $f_{c,bulk}$ and $f_c(r)$ is calculated, the water cement ratio at any point from the aggregate surface is calculated as follows [87]:

$$w_c = \frac{1 - f_c(r)}{\rho_c f_c(r)} \tag{2.14}$$

The work conducted above should be calculated for every size of aggregate separately yielding volume percentages with different water-cement values. The corresponding results are attached in appendix 2.2. The number of zones in the ITZ was taken equal to 5 (N=5), this number could be refined furthermore by taking higher values for N.

For every zone of the ITZ, $f_c(r)$ is calculated as follows:

$$f_c(r) = f_{c,bulk}\left(\left(\frac{b_1}{b_0}\right)\left[\frac{r-r_a}{r_b-r_a}\right]^1 + \left(\frac{b_2}{b_0}\right)\left[\frac{r-r_a}{r_b-r_a}\right]^2 + \left(\frac{b_3}{b_0}\right)\left[\frac{r-r_a}{r_b-r_a}\right]^3 + \left(\frac{b_4}{b_0}\right)\left[\frac{r-r_a}{r_b-r_a}\right]^4\right) \tag{2.15}$$

9.3. Identification of the degree of hydration

The next step includes simulating a hydration model in order to identify the degree of hydration as a function of the distance from the aggregate surface. Developing a mathematical method to simulate the cement hydration has been the quest of many researchers for at least the last 40 years [88]. Probably the two most used empirical methods to simulate the cement hydration were those developed by Parrot and Killoh [89] and by Schindler et al. [90]. The model proposed by schindler which was also adopted by Hansen et al.[91] is found in equation (2.16).

$$\alpha(t_e) = \alpha_u e^{-\left[\frac{\tau}{t_e}\right]^{\beta}} \tag{2.16}$$

where $\alpha(t_e)$ is the degree of hydration at an equivalent age t_e, $\alpha(t_e)$ is the degree of hydration at an equivalent age t_e, α_u is the ultimate degree of hydration, τ is the hydration time parameters in hours, β is the hydration shape parameter, and t_e is the equivalent age as defined by Frieseleben Hansen and Pederson [92]. This method was found the preferred method when actual calibration of α_u, β, and τ was made with the test results [93].

While this method takes the equivalent age and temperature into consideration, the model proposed by Parrot and Killoh included additional correction parameters for the cement's blaine and relative heat hydration which makes the calculation more tailored. This model was consequently used for the remaining calculation and discussed hereafter. This model was used in several publications and was furthermore generalized to include the effect of fly ash by Yogarajah et al. [94]. The hydration model developed by Parrot and Killoh [89] states that the hydration of the cement particles occurs through a dissolution and precipitation process. The reaction rate in this process is the lowest of the three following equations pertaining to the rate of hydration of each material of the clinker phase:

Nucleation and Growth: $$R_{1,i,t} = \frac{k_1}{N_1}\left(1-\alpha_{i,t}\right)[-\ln\left(1-\alpha_{i,t}\right)]^{1-N_1} \tag{2.17}$$

Diffusion: $$R_{2,i,t} = \frac{k_2\left(1-\alpha_{i,t}\right)^{2/3}}{1-\left(1-\alpha_{i,t}\right)^{1/3}} \tag{2.18}$$

Formation and Hydration Shell: $$R_{3,i,t} = k_3\left(1-\alpha_{i,t}\right)^{N_3} \tag{2.19}$$

Degree of Hydration at time t + Δt: $$\alpha_{i,t+\Delta t} = \alpha_{i,t} + \Delta t R_{i,t} \tag{2.20}$$

where t is the time in days, and $\alpha_{i,t}$ is the degree of hydration at the time t for each clinker phase i. The values of k_1, N_1, k_2, k_3, and N_3 are empirical constants developed for this model as per the below table:

Table 2.14 - Hydration Parameters – Parrot and Killoh [89]

Parameter	Clinker Phase			
	Alite C_3S	Belite C_2S	Aluminate C_3A	Ferrite C_4AF
k1	1.5	0.5	1.0	0.37
n1	0.7	1.0	0.85	0.7
k2	0.05	0.006	0.04	0.015
k3	1.1	0.2	1.0	0.4
n3	3.3	5.0	3.2	3.7

The three process rates defined above should be calculated for each of the four clinker phases. The function that takes into consideration the water-cement ratio is $f(\frac{w}{c})$ as defined below:

$$f(w_c) = \begin{cases} (1 + 4.444(w_c) - 3.333\alpha_{i,t})^4, & for\ \alpha_{i,t} > 1.333(w_c) \\ 1, & for\ \alpha_{i,t} \leq 1.333(w_c) \end{cases} \quad (2.21)$$

where w_c is the water-cement ratio, and $\alpha_{i,t}$ is the degree of hydration at the time t for each clinker phase i.

The function that takes into consideration the relative humidity in the degree of hydration is defined below:

$$\beta_{RH} = (\frac{RH - 0.55}{0.45})^4 \quad (2.22)$$

where $RH$is the relative humidity.

The function that takes into consideration the cement's surface area and hydration temperature is as follows:

$$f(A,T) = \frac{A}{A_0}\exp\left(\frac{E_a}{R}\left(\frac{1}{T_0} - \frac{1}{T}\right)\right) \quad (2.23)$$

where A is the actual surface area of the cement (m^2/kg), $A_0$is the reference surface area of the cement, equal to 385 m^2/kg, E_a is the activation energy, equal to 34500 J/mol as defined by Poole et al. [93], R is the natural gas constant, equal to 8.314 J/mol/K, T is the absolute temperature (K), and T_0 is the reference temperature, equal to 293.15 K.

The final hydration degree model will be as follows:

$$R_{i,t} = \min\left(R_{1,i,t}, R_{2,i,t}, R_{3,i,t}\right).f(w_c).\beta_{RH}.\frac{A}{A_0}\exp\left(\frac{E_a}{R}\left(\frac{1}{T_0} - \frac{1}{T}\right)\right) \quad (2.24)$$

Degree of Hydration at time $t + \Delta t$ of a species i is given by equation (2.25):

$$\alpha_{i,t+\Delta t} = \alpha_{i,t} + \Delta t R_{i,t}$$

$$\alpha = f_{C3S}\alpha_{C3S} + f_{C2S}\alpha_{C2S} + f_{C3A}\alpha_{C3A} + f_{C4AF}\alpha_{C4AF} \quad (2.25)$$

Where α is the degree if hydration, f_{C3S}, f_{C2S}, f_{C3A}, and f_{C4AF} are the proportions of C3S, C2S, C3A, and C4AF respectively.

The calculation of the hydration degree was calculated for the mix design used at 150 days and found equal to 0.83. The detailed calculation is attached in appendix 2.3.

9.4. Capillary pores, gel pores, and total pores as a function of the distance from the aggregate surface

The next step aims at calculating the volume fraction of capillary pores, gel pores, and total pores as a function of the distance from the aggregate. In reference to the work conducted by Powers and Brownyard [95] and summarized afterwards by Hansen [96]. The total porosity is related to the water cement ratio and the degree of hydration. It is equal to the volume fractions of the capillary porosity and gel porosity as follows:

$$f_p = f_{cap} + f_{gel} = \frac{(w_c) - 0.36\alpha}{(w_c) + 0.32} + \frac{0.19\alpha}{w_c + 0.32} \quad (2.26)$$

where $f_{cap}$is the capillary porosity, f_{gel} is the gel porosity, f_p is the total porosity, w_c is the water-cement ratio, and α is the degree of hydration.

The tables in appendix 2.3 were updated with the hydration coefficient as a function of the distance from the aggregate surface. The coefficient of hydration changes with the water-cement ratio that changes as a function of the distance from the aggregate surface. This calculation has yielded the porosity as a function of the distance from the aggregate surface. These tables as included in appendix 2.4. The hydration duration is taken as 150 days which is the time of testing.

9.5. Calculating the relative chloride diffusion values

The next step aims at calculating the relative diffusion value as a function of the porosity and the diffusivity of the chloride ions in the pore solution, in the bulk cement paste, and in the ITZ. Based on the works conducted by Zheng and Zhou [97] from one side and Koelman and De Kuijper [98] from the other side, the chloride diffusion of the cement paste was demonstrated to be a function of the porosity and the diffusivity of chloride ions in the pore solution as follows:

$$D_{cp} = \frac{2f_p^{2.5}D_p}{f_p^{1.75}(3-f_p)+14.4(1-f_p)^{2.75}} \quad (2.27)$$

where D_{cp} is the chloride diffusivity of the cement paste, $D_p$is the chloride diffusivity of the pore solution, and f_p is the total porosity.

The chloride diffusivity is not an identified general number and should be calibrated for a specific paste composition. However, for the specific same cement paste where the porosity changes from one location to another, the ratio of the chloride diffusion coefficient for the cement paste is as follows:

$$\frac{D_{cp,area\ 1}}{D_{cp,area\ 2}} = \frac{\frac{2f_{p,1}^{2.5}D_p}{f_{p,1}^{1.75}(3-f_{p,1}) + 14.4(1-f_{p,1})^{2.75}}}{\frac{2f_{p,2}^{2.5}D_p}{f_{p,2}^{1.75}(3-f_{p,2}) + 14.4(1-f_{p,2})^{2.75}}}$$

$$\frac{D_{cp,area\ 1}}{D_{cp,area\ 2}} = \frac{2f_{p,1}^{2.5}[f_{p,2}^{1.75}(3-f_{p,2}) + 14.4(1-f_{p,2})^{2.75}]}{2f_{p,2}^{2.5}[f_{p,1}^{1.75}(3-f_{p,1}) + 14.4(1-f_{p,1})^{2.75}]}$$

where $D_{cp,area\ 1}$is the chloride diffusivity of the cement paste in area 1, $D_{cp,area\ 2}$ is the chloride diffusivity of the cement paste in area 2, $f_{p,1}$ is the total porosity in area 1, and $f_{p,2}$is the total porosity in area 2.

By considering that the chloride diffusivity of the bulk cement paste is equal to " D " associated with a porosity of 0.334, the diffusivity in the ITZ will be proportionally calculated as a function of "D". This calculation will enable modeling the concrete following areas of different chloride diffusivity, while noting that the chloride diffusivity of the aggregate is zero. Therefore, for a random increment in porosity equal to "k_i" going from the reference porosity of 0.334 (i.e. $f_{p,i} = 0.334k_i$), the corresponding chloride diffusivity will be equal to "A_iD" the proportionality formula can thus be rewritten as follows:

$$\frac{D_{cp,area\ 1}}{D_{cp,area\ 2}} = \frac{2f_{p,1}^{2.5}[f_{p,2}^{1.75}(3-f_{p,2}) + 14.4(1-f_{p,2})^{2.75}]}{2f_{p,2}^{2.5}[f_{p,1}^{1.75}(3-f_{p,1}) + 14.4(1-f_{p,1})^{2.75}]}$$

$$\frac{D}{A_iD} = \frac{2(0.334)^{2.5}[(k_i \times 0.334)^{1.75}(3-(k_i \times 0.334)) + 14.4(1-(k_i \times 0.334))^{2.75}]}{2(k_i \times 0.334)^{2.5}[(0.334)^{1.75}(3-0.334) + 14.4(1-0.334)^{2.75}]}$$

$$A_i = \frac{2(k_i \times 0.334)^{2.5}[(0.334)^{1.75}(3-0.334) + 14.4(1-0.334)^{2.75}]}{2(0.334)^{2.5}[(k_i \times 0.334)^{1.75}(3-(k_i \times 0.334)) + 14.4(1-(k_i \times 0.334))^{2.75}]}$$

$$A_i = \frac{0.6576{k_i}^{2.5}}{0.12894[0.146742{k_i}^{1.75}(3-0.334k_i) + 14.4(1-0.334k_i)^{2.75}]}$$

Based on the above formula, the tables in appendix 2.4 were updated to include the coefficient k_i as the ratio of the actual porosity and the reference porosity, these tables are included in appendix 2.5. These tables were as well updated to include the factor A_i as the scaling factor of the diffusivity D associated with the factor k_i. A_i was calculated using the formula above. These tables also include the volumes associated with each value of diffusivity. The value of diffusivity being as a

function of the reference diffusion value " D ". The final output is a diffusivity mapping as function of " D ". The diffusivity of the aggregate int his mapping is equal to " $0 \times D$ ", the highest diffusivity is at the aggregate/paste interface and decrease gradually to reach a constant equal to the diffusivity of the bulk cement paste.

9.6. Updating the concrete diffusion coefficient model

The final step aims at updating the concrete diffusion model to yield a concrete diffusion as function of the aggregate diffusion, clay lumps/friable particles effects, surface effects, diffusion of the ITZ and the diffusion in the bulk cement paste. The model developed by Hobbs [63] was discussed in section 2 of this chapter. In this model, the concrete chloride diffusion is calculated as a function of the chloride diffusion of the aggregate and paste as summarized in equation (2.2). This model is formulated similarly to the modulus of elasticity formula and based on the works done by Hashin-shtrikman [65], going from two boundaries: upper and lower boundaries.

The upper boundary is defined by Voigt model and the lower boundary by Reuss model. Models other than the one developed by Hashin-Shtrikman also exist [99] and illustrated in Figure 2.26 [100]. The different models' equations are defined below for the modulus of elasticity noting that Counto model and Hashin model were developed for a two-phase concrete material (paste and aggregate). Figure 2.27 [99] is a graphical comparison between various models. Hashin-strikman model was selected by Hobbs for the two-phase concrete materials as it was the best fit for the concrete modulus of elasticity values. It is to note that the model developed by Hirsh-Dougill can form a good approximation, as well for two-phase concrete, provided the proportionality value of "θ" is calibrated for the specific concrete.

Table 2.14 - Models for two-phase material

Model	Equation	Reference
Voight's model (Upper Boundary)	$D = \sum_{i=1}^{n} \rho_i D_i$	(2.28)
Reuss's Model (Lower Boundary)	$\frac{1}{D} = \sum_{i=1}^{n} \frac{\rho_i}{D_i}$	(2.29)
Hirsch-Dougill's Model	$\frac{1}{D} = \theta \left[\frac{1}{\sum_{i=1}^{i=n} \rho_i D_i} \right] + (1-\theta) \left[\sum_{i=1}^{i=n} \frac{\rho_i}{D_i} \right]$	(2.30)

Popovics model for two phases materials (paste and aggregate)	$D_c = \frac{1}{2}\left(\frac{1}{\frac{\rho_p}{D_p}+\frac{\rho_a}{D_a}} + \rho_p D_p + \rho_a D_a\right)$	(2.31)
Counto's model for two phases materials (paste and Aggregate)	$\frac{1}{D_c} = \frac{1-\sqrt{\rho_a}}{D_p} + \frac{1}{\left(\frac{1-\sqrt{\rho_a}}{\sqrt{\rho_a}}\right)D_p + D_a}$	(2.32)
Hashin-Shtrikman's model for two phases materials (paste and aggregate)	$D_C = \frac{[(D_a - D_p)\rho_a + (D_p + D_A)]D_p}{(D_p + D_a) - (D_a - D_p)\rho_a}$	(2.33)

Where D_i is the chloride diffusion of the phase i, ρ_i is the volume fraction of the paste i, D is the total chloride diffusion coefficietn, D_c is the concrete chloride diffusion coefficient, D_p is the chloride diffusion coefficient of the paste fraction, D_a is the chloride diffusion coefficient of the aggregate, ρ_p is the volume fraction of the paste, and $\rho_a$is the volume fraction of the aggregate.

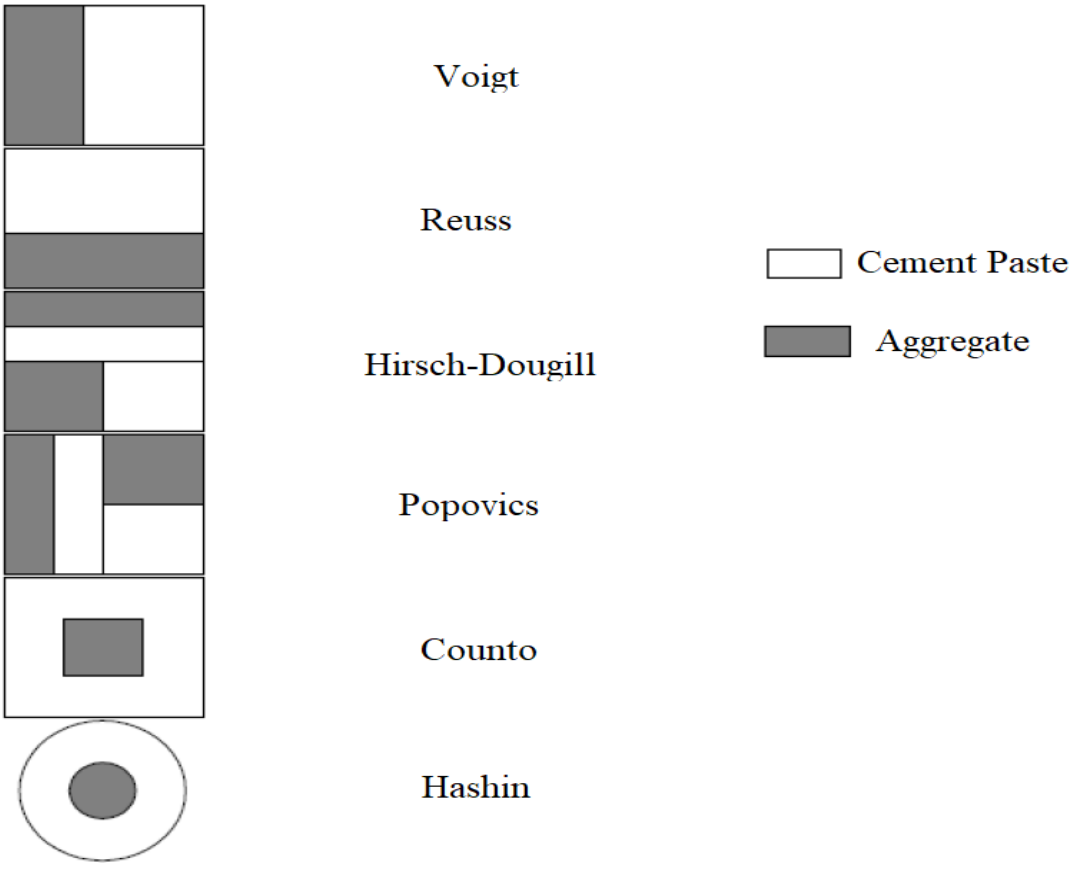

Figure 2.26 - Modulus of Elasticity Illustration Models

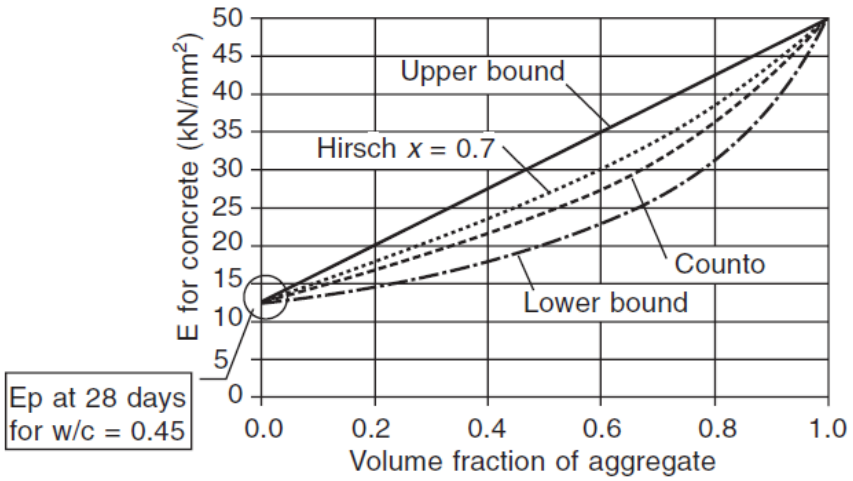

Figure 2.27 - Relationships Between Elastic Modulus of concrete and volume fraction of aggregate for various models assuming Ep =12.5 and Ea=50kn/mm2

While simulating Hashin-Shtrikman model with an aggregate chloride diffusion equal to zero, the relevant equation is simplified to the following:

$$D_{concrete} = \frac{(D_{Paste})\rho_{Aggregate} + (D_{Paste})D_{Paste}}{(D_{Paste}) + (D_{Paste})\rho_{Aggregate}} = \frac{\rho_{Aggregate} + D_{Paste}}{1 + \rho_{Aggregate}}$$

This equation leads to a concrete chloride diffusion that is in greater orders of that of the cement paste. This shows the inapplicability of this model to the chloride diffusion coefficient of concrete. Reuss and Hrish-Dougill models will as well lead to zero when the aggregate chloride diffusion is equal to zero (which is the lower bound representing a total volume of aggregate equal to 1). Popovic model will lead back to Voight model in insignificant aggregate chloride diffusion coefficient.

Based on the above available models, the best estimation of the chloride diffusion coefficient in the concrete will be calculated, going from the fact that it can be simulated to the concrete multiphase modulus of elasticity as follows:

- Hirsh-Dougill model will be used to estimate the chloride diffusion of multi-phase paste fraction
- The value of the chloride diffusion coefficient of the paste will be substituted in Voight equation in order to calculate the total chloride diffusion coefficient. The value of "θ" will be identified based the chloride diffusion test results available in this chapter.

The total concrete chloride diffusion is thus given in the below equations. The function $f(Mf, Ab, Clf)$ is the function that takes into account the aggregate surface effects and impurities as qualitatively discussed in the earlier paragraphs. This function will be solved in the next paragraphs. The tables provided in appendix 2.4 were updated to include the values of $\frac{1}{\sum_{i=1}^{i=n} V_i A_i}$,

and $\sum_{i=1}^{i=n} \frac{V_i}{A_i}$. The total concrete chloride diffusion coefficient related to the five mixes is illustrated in Table 2.15 as a function of D, θ, and $f(Mf, Ab, Clf)$.

$$\frac{1}{Cement\ Paste\ Chloride\ Diffusion\ D_p} = \left[\theta\left[\frac{1}{\sum_{i=1}^{i=n} V_i D_i}\right] + (1-\theta)\left[\sum_{i=1}^{i=n} \frac{V_i}{D_i}\right]\right] \tag{2.34}$$

or

$$\frac{1}{Cement\ Paste\ Chloride\ Diffusion\ D_p} = \left[\frac{1}{D}\left[\theta\left[\frac{1}{\sum_{i=1}^{i=n} V_i A_i}\right] + \left[\sum_{i=1}^{i=n} \frac{V_i}{A_i}\right] - \theta\left[\sum_{i=1}^{i=n} \frac{V_i}{A_i}\right]\right]\right]$$

and

$$Concrete\ Chloride\ Diffusion\ Coef. = f(Mf, Ab, Clf) \sum_{i=1}^{n} V_i D_i \tag{2.35}$$

As demonstrated in section 7.8, the chloride diffusion coefficient varies linearly as a function of the materials finer than 75 microns, the aggregate absorption, and the percentage of clay lumps and friable particles. Based on this, the function $f(Mf, Ab, Clf)$ will have the following form:

$$f(Mf, Ab, Clf) = K.Mf + L.Ab + N.Clf + P \tag{2.36}$$

where K, L, N, and P are constants, Mf is the percentage of materials finer than 75 microns, Ab is the aggregate absorption (%), and Clf is the percentage of clay lumps and friable particles.

When the percentage of the materials finer than 75 microns, the aggregate absorption, and the percentage of clay lumps and friable particles, are zero, these properties will not affect the chloride diffusion coefficient. The constant "P" is thus equal to 1. In Table 2.15, the values of the materials finer than 75 microns, the aggregate absorption, and the percentage of clay lumps and friable particles were replaced by the actual test results values for each aggregate source.

Table 2.15 - Concrete Chloride Diffusion Coefficient as a function of D, θ, and f(MF,Ab,CLF)

Aggregate Source	Chloride Diffusion Coefficient Value as a function of K, L, N, D, and θ	Tested Chloride Diffusion Value
Bin Laheej	$(0.5K + 0.5L + 0.1N + 1) \times \frac{0.32913D}{2.5320\theta + 0.317}$	2.841×10^{-12}
Madinah	$(0.4K + 1.1L + 0.3N + 1) \times \frac{0.32913D}{2.5391\theta + 0.318}$	3.4822×10^{-12}
Stevin Rock	$(0.2K + 0.6L + 0.1N + 1) \times \frac{0.32913D}{2.5391\theta + 0.318}$	1.9493×10^{-12}

Gabro	$(1.1K + 0.8L + 0.2N + 1) \times \frac{0.32913D}{2.5483\theta + 0.317}$	4.2619×10^{-12}
Makah	$(0.2K + 0.4L + 0.2N + 1) \times \frac{0.32913D}{2.5209\theta + 0.320}$	2.4849×10^{-12}

Using the least square non-linear multiple regression analysis to determine the values of the unknowns satisfying these equations yielded the following:

$$K = 1.7258$$
$$L = 0.0963$$
$$N = 3.9165$$
$$\theta = 0.6265$$
$$D = 6.6996 \times 10^{-12}$$

It is to note that in average, for the five mixes used (same cement paste), the value of $D_{bulk\ cement\ paste}$ was equal to 1.0038 D with an acceptable fluctuation of 1.5%. Based on this D can be replaced by $D_{bulk\ cement\ paste}$ as follows:

$$D_{bulk\ cement\ paste} = 6.6742 \times 10^{-12}\ m^2/s$$

The general equation for of the concrete chloride diffusion coefficient while taking into consideration the effect of the aggregate is therefore:

$$D_c = (1.7258Mf + 0.0963Ab + 3.9165Clf + 1) \times \frac{\left(1 - V_{aggregate}\right)D_{bulk\ cement\ paste}}{\left[0.6265\left[\frac{1}{\sum_{i=1}^{i=n} V_i A_i}\right] + \left(0.3735\left[\sum_{i=1}^{i=n} \frac{V_i}{A_i}\right]\right)\right]} \quad (2.37)$$

where Mf is the percentage of materials finer than 75 microns, Ab is the aggregate absorption (%), Clf is the percentage of clay lumps and friable particles, $V_{aggregate}$ is the volume of aggregate fraction in the mix, $D_{bulk\ cement\ paste}$ is the chloride diffusion in the cement paste, and the functions $\sum_{i=1}^{i=n} V_i A_i$ and $\left[\sum_{i=1}^{i=n} \frac{V_i}{A_i}\right]$ are calculated as per the procedures described in this chapter.

Considering that the chloride diffusion coefficient of reference is the chloride diffusion coefficient of the bulk cement paste, the function that takes into consideration the effect of the aggregate on the chloride diffusion coefficient is the following:

$$f(aggregate) =$$
$$(1.7258.Mf + 0.0963.Ab + 3.9165.Clf + 1) \times \frac{(1 - V_{aggregate})}{\left[0.6265\left[\frac{1}{\sum_{i=1}^{i=n} V_i A_i}\right] + \left(0.3735\left[\sum_{i=1}^{i=n} \frac{V_i}{A_i}\right]\right)\right]} \quad (2.38)$$

10. Conclusions

The chloride diffusion in concrete can be theoretically divided into three phases of diffusion, a diffusion that takes place in the aggregate, a diffusion that takes place in the interfacial transition zone between the aggregate and the cement paste, and the diffusion that takes place in the cement paste. Other factors were demonstrated to be added to the equation and include the aggregate surface conditions and friable particles content. The two parameters were empirically quantified based on common aggregate testing: "Materials finer than 75 microns content", the "Water absorption test", and the "Clay lumps and friable particles content". The surface chloride concentration on the other side was found to be affected by the type of the aggregate material, the density and the soundness.

This experimental testing on five mixes has concluded that the aggregate used in the construction industry today have an insignificant diffusion coefficient and that the chloride diffusion takes place only in the interfacial transition zone and the cement paste. This may not be the case for aggregate that are outside the range of properties studied in this chapter.

The remaining diffusion that is taking place in the interfacial transition zone and the cement paste greatly differ with the aggregate properties when the same cement paste is used. This difference can be practically calculated using an empirical formula as demonstrated in section 9.

The aggregate properties do not affect directly the chloride diffusion coefficient. These properties are rather dependent, and work in combination with, the concrete properties to affect the overall concrete chloride diffusion. It is thus necessary to consider these entities in combination when developing a function illustrating the effect of the aggregate properties on the total concrete chloride diffusion coefficient. The concrete properties that are part of the function illustrating the aggregate effect on the concrete chloride diffusion coefficient thus includes the following: Aggregate volume, Aggregate particle distribution and sizes, Aggregate materials finer than 75 microns, Aggregate absorption, Aggregate clay lumps and friable particles, Interfacial transition zone (ITZ) thickness, Cement content, Water-cement ratio, Cement composition (C3S, C2S, C3A, and C4AF), Cement fineness, Cement Density, Cement degree of hydration, Time after placing, Relative humidity, Temperature and Cement Activation Energy.

Based on the above, the function defining the effect of the aggregate on chloride diffusion coefficient includes a total of 16 parameters that defines the extent of effect.

The particular calculations show that the chloride diffusion coefficient for the bulk cement paste was equal to 6.6742×10^{-12} m/s^2 versus an insignificant aggregate chloride diffusion. This finding proves the advantages of increasing the aggregate volume to enhance the concrete durability in chloride environments.

Less dense aggregate and less sound aggregate tends to absorb more chloride at the surface by capillary action. This can be practically and numerically calculated using as input parameters the aggregate density and soundness; the obtained relationship indicates a high correlation.

Chapter 3: Effect of C3A Content

1. Introduction

This chapter aims to assess the effect of the cement's tricalcium aluminate content, noted as C3A, on the chloride diffusion coefficient. It starts by a background discussion identifying the need for this study. It then proceeds by presenting the raw materials testing and mix design. Details of the core specimen preparations and chloride diffusion rate test plan are discussed as well. Finally, the results are presented, and related calculations are performed, in order to reach comprehensive conclusions regarding the effect of the C3A content on the chloride diffusion coefficient.

2. Role of Tricalcium Aluminate in cement and concrete

The present section includes a discussion related to the effect of tricalcium aluminate on the reinforcing steel corrosion in the available literature.

2.1. Tricalcium Aluminate prescriptive based specifications

Many prescriptive-based specifications have indicated the direct effect of the low tricalcium aluminate content on the reinforcing steel corrosion. Some of these references are listed below:

- CIRIA C577 [47] stated the following: *the possibility that C_3A could have a significant and predictable influence on corrosion rates makes this a very important area to investigate further in the future, with the objective being to specify limits in relation to the contamination and the exposure conditions.*

- In several instances, ACI 222 [57], indicates the major effect of the tricalcium aluminate on the reinforcing steel corrosion:

    - Chapter 2 paragraph 2.2.4.1.c states the following: *"Not all the chlorides present in the concrete can contribute to the corrosion of the steel. Some of the chlorides react chemically with the cement components, such as calcium aluminates to form calcium chloroaluminate, and are effectively removed from the pore solution. As the concrete carbonates, the chloride are released and become involved in the corrosion process."*

    - In the same context, chapter 3 paragraph 3.3 states the following: "*When chloride are added to the mixture, some will chemically combine with the hydrating cement phase, predominantly the aluminate phase. The amount of chloride that forms calcium chloroaluminate is a function of the C3A content of the cement".*

- ACI 201.2 [58] concludes that the presence of C3A in the cement appears to be beneficial to the reduction of chloride ingress.

- ACI 318-14 [101] states the following: *Portland cement with higher C3A content improves binding of chlorides present in seawater.*

2.2. Tricalcium Aluminate interference with the chloride diffusion and binding

The tricalcium aluminate in cement reacts with the chloride to produce chloroaluminate. The role of tricalcium aluminate in the chloride diffusion mechanism and its binding with the chloride has been widely discussed in literature. Rasheeduzzafar et al. [37] have demonstrated that the time to corrosion, as well as the amount of binded chloride, are directly proportional to the tricalcium aluminate content as well as Figure 3.1 was extracted from this works. The test experiment confirms a linear relationship between the binded and total chloride. This publication furthermore proves that in the absence of tricalcium aluminate, the formation of calcium chloroaluminate is absent.

Table 3.1 - C3A Effect on corrosion and chloride binding

C3A content (%)	Time to initiation of corrosion (years)	Concentration of water soluble chloride in concrete as a percent of total chloride in concrete (free chloride)	Binded chloride = 1 - free chloride
2	93	86%	14%
9	163	58%	42%
11	180	51%	49%
14	228	33%	67%
Time to Corrosion = 1088.5 x (C3A Content) + 68.038			R^2 = 0.9854
Free Chloride Percentage = -4.2949 x (C3A Content) + 0.9565			R^2 = 0.9895
Binded Chloride Percentage = 4.2949 x (C3A Content) + 0.9565			R^2 = 0.9895

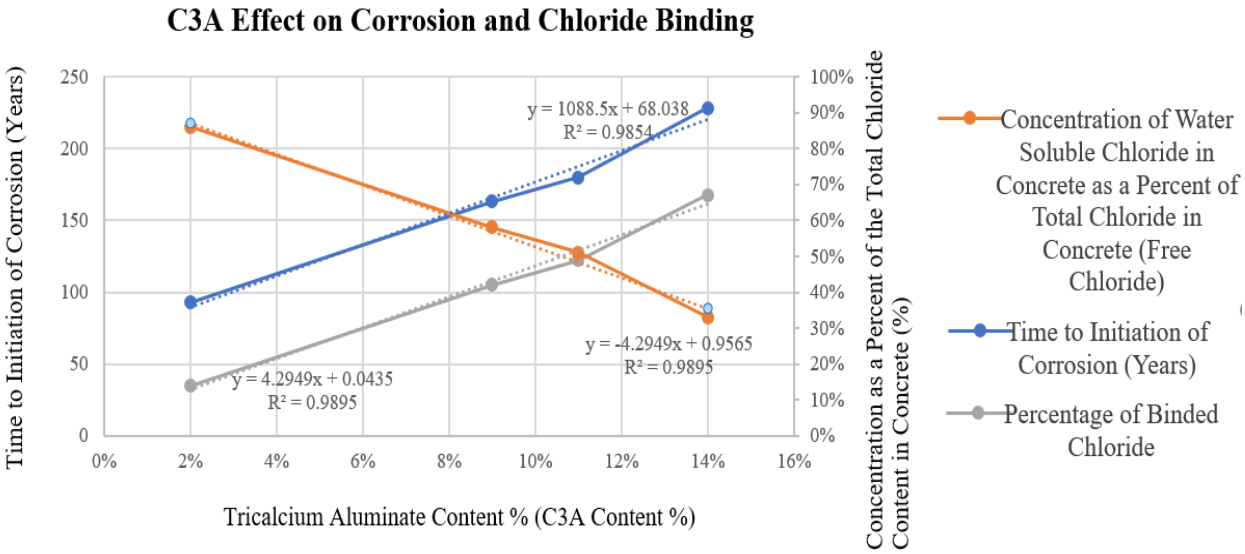

Figure 3.1 - C3A Effect on Corrosion and Chloride Binding

In the same context, Glass and Buenfled [38] have concluded that the chloride binding with the tricaclcium aluminate reduces the free chloride concentration and therefore the quantity of mobile

chloride at all locations within the concrete. However, it also maintains higher concentration gradients for longer periods in the surface zone, thereby increasing the average velocity and quantity of chloride ions entering the concrete through diffusion. The net effect is an increase in the total chloride content (bound plus free) near the surface and a reduction in the total chloride content at depth, as can be seen in Figure 3.2 and Figure 3.3.

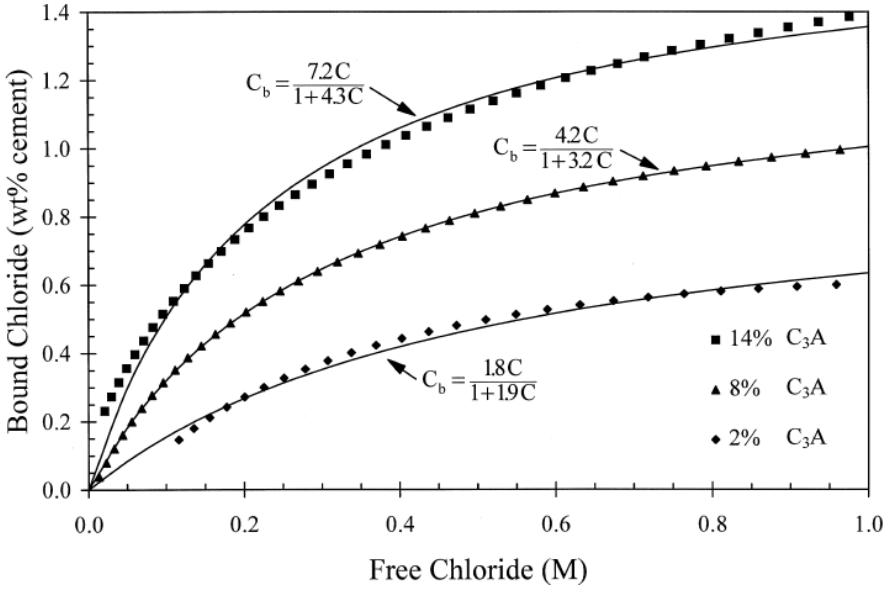

Figure 3.2 - Effect of C3A Content on Chloride Binding [38]

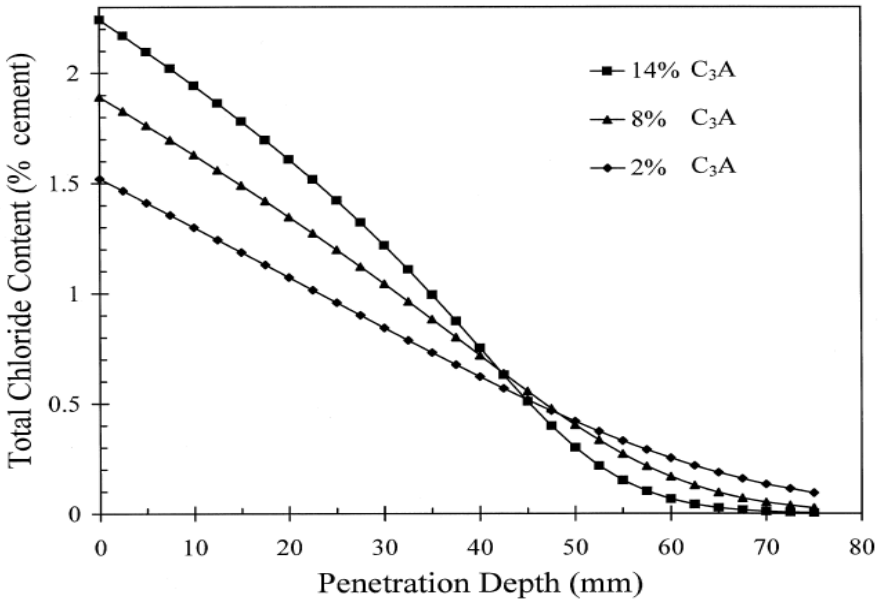

Figure 3.3 - Effect of C3A Content on Chloride Profiles [38]

The work of Sang-Hun Han [39] reached similar conclusions: the more the C3A content, the higher the total chloride ion concentration is obtained on the surface. The difference of total chloride ion

concentration with C3A content decreases with depth and the sequence of total chloride ion concentration with C3A content reverses over a transitional point. Several other references [102][103] have concluded that the chloride binding removes chloride ions from the pore solution and slows down the rate of penetration. The study conducted by Paul Sandberg [40] has equally demonstrated that the binding of chloride affects both the transport rate of chlorides into concrete and the amount of chlorides necessary to initiate active corrosion. Jingpei Li et al. [104] have described the criticality of the chloride binding in view of chloride diffusion by the following mathematical model:

$$\frac{\partial C_f}{\partial t} = D_c^* \frac{1}{r}\frac{\partial C_f}{\partial r} + \frac{\partial}{\partial r}\left(D_c^* \frac{\partial C_f}{\partial r}\right) \quad (3.1)$$

with:

$$D_c^* = \frac{D_c}{1+\left(\frac{1}{w_e}\right)\left(\frac{\partial C_b}{\partial C_f}\right)} \quad (3.2)$$

where D_c^* is the effective chloride diffusion coefficient (m^2/s), w_e is the evaporable water content, r is the depth (m), C_f is the free chloride concentration (kg/m^3), and C_b is the binded chloride concentration.

2.3. Conclusions from the literature review

Based on the literature review, the following conclusions can be made:

- The amount of chloride binded is directly proportional to the tricalcium aluminate (C3A) content.
- The corrosion resistance increases with an increase in the tricalcium aluminate (C3A) content.
- The chloride profiles vary with the C3A content, the literature has reported an increased in the surface concentration and decrease in chloride content at deeper levels.

It is clear thus that the tricalcium aluminate content is one of the parameters that influences the chloride diffusion coefficient. This effect will be quantified in this chapter through the testing program.

3. Summary of the testing Protocol

The reference concrete mix was replicated using five types of cements with different tricalcium aluminate content while maintaining the same mix proportions. These mixes are presented in tables 3.2 to 3.6. A suitable number of concrete cylinders were taken from each mix and cured for 28 days. Further to the curing period, concrete cores were taken from the cylinders with a diameter of 94 mm and a height of 80 mm. Two sets of samples were crushed from each concrete mix design and the initial acid soluble chloride content is determined. All of the remaining sides were then sealed, except the finished surface, with a suitable barrier coating. The sealed specimens are then

saturated in a calcium hydroxide solution, rinsed with tap water, and then placed in a sodium chloride solution. After a duration of respectively 37, 85, 123, 150, 197, and 235 days, sets of test specimens were removed from the sodium chloride solution and thin layers were ground off parallel to the exposed face of the specimen. The thicknesses of the layers are detailed in the corresponding sections. The acid-soluble chloride content of each layer is determined. The apparent chloride diffusion coefficient and the projected surface chloride-ion concentration are then calculated using the initial chloride-ion content, and at least six related values for chloride-ion content and depth below the exposed surface. The apparent chloride diffusion coefficients of the different mixes, at different ages, were compared and analyzed.

Table 3.2 - NORTH REGION CEMENT PLUS Ordinary Portland Cement

Reference Concrete Mix Design - Mix 3 - NORTH REGION CEMENT PLUS Ordinary Portland Cement								
Mix Ingredients		SSD Weight (kg)	Density (kg/m^3)	Moisture (%)	Absorption (%)	Final Weight (kg)	Volume (m^3)	Trial Weights (0.1m^3) (kg)
Cement (NORTH REGION CEMENT Ordinary Portland Cement)		400.00	3150.00			400.00	0.1270	40.00
Micro Silica (ELKEM)		25.00	2200.00			25.00	0.0114	2.50
Water		161.50	1000.00			171.80	0.1718	17.18
CA 3/8 (MAD Source)	15% of particles between 12.500mm and 9.500mm	150.00	2830.00	0.50	1.10	149.10	0.0527	14.91
	85% of particles between 9.500mm and 4.750mm	850.00	2830.00	0.50	1.10	844.90	0.2986	84.49
Washed Sand (MAD Source)	10% of particles between 4.750mm and 2.360mm	86.50	2660.00	0.40	0.90	86.07	0.0324	8.61
	15% of particles between 2.360mm and 1.180mm	129.75	2660.00	0.40	0.90	129.10	0.0485	12.91
	25% of particles between 1.180mm and 0.600mm	216.25	2660.00	0.40	0.90	215.17	0.0809	21.52
	30% of particles between 0.600mm and 0.300mm	259.50	2660.00	0.40	0.90	258.20	0.0971	25.82
	20% of particles between 0.300mm and 0.150mm	173.00	2660.00	0.40	0.90	172.14	0.0647	17.21
Admixture BASF Glenium Sky 504		4.00	1120.00			4.00	0.0036	0.40
Air Content							0.0200	0.00
						Total Volume	1.0085	0.1009

Table 3.3 - SAFWA Sulfate Resistant Cement

Mix 1 - SAFWA Sulfate Resistant Cement								
Mix Ingredients		SSD Weight (kg)	Density (kg/m3)	Moisture (%)	Absorption (%)	Final Weight (kg)	Volume (m3)	Trial Weights (0.1m3) (kg)
Cement (SAFWA Sulfate Resistant Cement)		400.00	3150.00			400.00	0.1270	40.00
Micro Silica (ELKEM)		25.00	2200.00			25.00	0.0114	2.50
Water		161.50	1000.00			171.80	0.1718	17.18
CA 3/8 (MAD Source)	15% of particles between 12.500mm and 9.500mm	150.00	2830.00	0.50	1.10	149.10	0.0527	14.91
	85% of particles between 9.500mm and 4.750mm	850.00	2830.00	0.50	1.10	844.90	0.2986	84.49
Washed Sand (MAD Source)	10% of particles between 4.750mm and 2.360mm	86.50	2660.00	0.40	0.90	86.07	0.0324	8.61
	15% of particles between 2.360mm and 1.180mm	129.75	2660.00	0.40	0.90	129.10	0.0485	12.91
	25% of particles between 1.180mm and 0.600mm	216.25	2660.00	0.40	0.90	215.17	0.0809	21.52
	30% of particles between 0.600mm and 0.300mm	259.50	2660.00	0.40	0.90	258.20	0.0971	25.82
	20% of particles between 0.300mm and 0.150mm	173.00	2660.00	0.40	0.90	172.14	0.0647	17.21
Admixture BASF Glenium Sky 504		4.00	1120.00			4.00	0.0036	0.40
Air Content							0.0200	0.00
						Total Volume	1.0085	0.1009

Table 3.4 - YANBU Moderate Sulfate Resistant Cement

Mix 2 - YANBU Moderate Sulfate Resistant Cement								
Mix Ingredients		SSD Weight (kg)	Density (kg/m3)	Moisture (%)	Absorption (%)	Final Weight (kg)	Volume (m3)	Trial Weights (0.1m3) (kg)
Cement (YANBU Moderate Sulfate Resistant Cement)		400.00	3150.00			400.00	0.1270	40.00
Micro Silica (ELKEM)		25.00	2200.00			25.00	0.0114	2.50
Water		161.50	1000.00			171.80	0.1718	17.18
CA 3/8 (MAD Source)	15% of particles between 12.500mm and 9.500mm	150.00	2830.00	0.50	1.10	149.10	0.0527	14.91
	85% of particles between 9.500mm and 4.750mm	850.00	2830.00	0.50	1.10	844.90	0.2986	84.49
Washed Sand (MAD Source)	10% of particles between 4.750mm and 2.360mm	86.50	2660.00	0.40	0.90	86.07	0.0324	8.61
	15% of particles between 2.360mm and 1.180mm	129.75	2660.00	0.40	0.90	129.10	0.0485	12.91
	25% of particles between 1.180mm and 0.600mm	216.25	2660.00	0.40	0.90	215.17	0.0809	21.52
	30% of particles between 0.600mm and 0.300mm	259.50	2660.00	0.40	0.90	258.20	0.0971	25.82
	20% of particles between 0.300mm and 0.150mm	173.00	2660.00	0.40	0.90	172.14	0.0647	17.21
Admixture BASF Glenium Sky 504		4.00	1120.00			4.00	0.0036	0.40
Air Content							0.0200	0.00
						Total Volume	1.0085	0.1009

Table 3.5 - RABIG ARABIAN CEMENT PLUS Ordinary Portland Cement

Mix 4 - RABIG ARABIAN CEMENT PLUS Ordinary Portland Cement								
Mix Ingredients		SSD Weight (kg)	Density (kg/m3)	Moisture (%)	Absorption (%)	Final Weight (kg)	Volume (m3)	Trial Weights (0.1m3) (kg)
Cement (Rabig Arabian Cement Plus Ordinary Portland Cement)		400.00	3150.00			400.00	0.1270	40.00
Micro Silica (ELKEM)		25.00	2200.00			25.00	0.0114	2.50
Water		161.50	1000.00			171.80	0.1718	17.18
CA 3/8 (MAD Source)	15% of particles between 12.500mm and 9.500mm	150.00	2830.00	0.50	1.10	149.10	0.0527	14.91
	85% of particles between 9.500mm and 4.750mm	850.00	2830.00	0.50	1.10	844.90	0.2986	84.49
Washed Sand (MAD Source)	10% of particles between 4.750mm and 2.360mm	86.50	2660.00	0.40	0.90	86.07	0.0324	8.61
	15% of particles between 2.360mm and 1.180mm	129.75	2660.00	0.40	0.90	129.10	0.0485	12.91
	25% of particles between 1.180mm and 0.600mm	216.25	2660.00	0.40	0.90	215.17	0.0809	21.52
	30% of particles between 0.600mm and 0.300mm	259.50	2660.00	0.40	0.90	258.20	0.0971	25.82
	20% of particles between 0.300mm and 0.150mm	173.00	2660.00	0.40	0.90	172.14	0.0647	17.21
Admixture BASF Glenium Sky 504		4.00	1120.00			4.00	0.0036	0.40
Air Content							0.0200	0.00
						Total Volume	1.0085	0.1009

Table 3.6 - ALSAFWA CEMENT Ordinary Portland Cement

Mix 5 - ALSAFWA CEMENT Ordinary Portland Cement								
Mix Ingredients		SSD Weight (kg)	Density (kg/m3)	Moisture (%)	Absorption (%)	Final Weight (kg)	Volume (m3)	Trial Weights (0.1m3) (kg)
Cement (ALSAFWA CEMENT Ordinary Portland Cement)		400.00	3150.00			400.00	0.1270	40.00
Micro Silica (ELKEM)		25.00	2200.00			25.00	0.0114	2.50
Water		161.50	1000.00			171.80	0.1718	17.18
CA 3/8 (MAD Source)	15% of particles between 12.500mm and 9.500mm	150.00	2830.00	0.50	1.10	149.10	0.0527	14.91
	85% of particles between 9.500mm and 4.750mm	850.00	2830.00	0.50	1.10	844.90	0.2986	84.49
Washed Sand (MAD Source)	10% of particles between 4.750mm and 2.360mm	86.50	2660.00	0.40	0.90	86.07	0.0324	8.61
	15% of particles between 2.360mm and 1.180mm	129.75	2660.00	0.40	0.90	129.10	0.0485	12.91
	25% of particles between 1.180mm and 0.600mm	216.25	2660.00	0.40	0.90	215.17	0.0809	21.52
	30% of particles between 0.600mm and 0.300mm	259.50	2660.00	0.40	0.90	258.20	0.0971	25.82
	20% of particles between 0.300mm and 0.150mm	173.00	2660.00	0.40	0.90	172.14	0.0647	17.21
Admixture BASF Glenium Sky 504		4.00	1120.00			4.00	0.0036	0.40
Air Content							0.0200	0.00
						Total Volume	1.0085	0.1009

In the following section, the type of materials is presented. Five types of cement are used in this research, which are from Al SAFWA CEMENT CO., ARABIAN CEMENT CO., NORTHERN REGION CEMENT CO. and YANBU CEMENT CO., respectively. The chemical and physical properties of the cements were tested and listed in Table 3.7. The aggregate used is from Madinah Area in Saudi Arabia. The silica fume was supplied from Elkem. The chemical admixtures added in the concrete are BASF Glenium Sky 504S and Rheomatrix 110.

The cement content was set to 400kg with an additional 25kg of Silica Fume. The inclusion of silica fume in the mix decreases the bleeding of the concrete mix. This therefore prevents the accumulation of bleeding water under the aggregate and excludes this source of variability from the testing protocol. A water cement ration of 0.38 was selected as it represents a fairly durable concrete in the construction practice. In order to eliminate the variation of aggregate grading. The coarse aggregate and fine aggregate were sieved using standard sieve and separated into a single size buckets as shown in Figure 3.4 below. The targeted percentage from each single size as specified by ASTM C33 (the commonly used aggregate specifications) was used in the five mixes. The five mixes were made in the same day and by the same qualified technicians in order to minimize the human variability. A polycarboxylate based admixture provided by BASF (Glenium 504Sky) was used as high-range-water-reducer. A polycarboxylate based high-range-water-reduce was intentionally used in these trials due to its potential in dispersing the cement particles and reducing the water demand. All the measures above were taken to make sure that only the cement type is changing from one mix to the other.

Figure 3.4 - Sieved Materials

Table 3.7 - Chemical Compositions and Physical Properties of Cement

	Cement Type	Al SAFWA CEMENT CO.	Al SAFWA CEMENT CO.	ARABIAN CEMENT CO.	NORTHERN REGION CEMENT CO.	YANBU CEMENT CO.
Chemical Compositions	Silicon Dioxide (SiO_2), %	20.6	20.84	22.66	22.92	25.03
	Aluminum Oxide (Al_2O_3), %	4.61	3.71	4.93	4.3	4.47
	Iron Oxide (Fe_2O_3), %	3.29	3.91	4.48	4.1	4.85
	Calcium Oxide (CaO), %	60.02	61.23	59.42	59.2	65.24
	Magnesium Oxide (MgO), %	1.14	2.85	3.84	1.14	2.23
	Sulfur Trioxide (SO_3), %	2.39	2.19	3.18	2.34	2.33
	Equivalent Alkalies ($Na_2O+0.658K_2O$), %	0.68	0.27	0.52	0.27	0.66
	Loss on Ignition, %	1.68	2.13	3.32	3.18	2.31
	Insoluble Residue, %	1.47	1.43	5.79	4.1	11.32
	Tricalcium Silicate (C_3S), %	52.06	60.32	30.1	32	36.28
	Dicalcium Silicate (C_2S), %	19.8	14.26	42.27	41.58	45.17
	C_3S+C_2S, %	71.86	74.58	63.65	73.58	62.79
	Tricalcium Aluminate (C_3A), %	6.65	3.22	5.49	4.46	3.64
	Tetracalcium Aluminoferrite (C_4AF), %	10.01	11.9	13.63	12.48	14.76
	CaO/SiO_2	2.91	2.94	2.24	2.58	1.87

4. Laboratory trials experiment

A total of 8 cylinders were taken from each mix and cured for 28 days, the trial records and fresh concrete properties are listed in Table 3.8 . After 28 days of water-curing, cores were drilled from the concrete cylinders. Cores were taken from the inner part of the concrete cylinder. The diameter and length of the core are 94 mm and 75 mm respectively. For each mix, 12 cores were prepared in total, as detailed in Table 3.9. A total of ten specimen out of the twelve were meant to be immersed in Sodium chloride while two samples were left non-immersed to test the original chloride content. The cores were immersed in the NaCl solution for the duration specified in the following sections. The core specimen preparation, and chloride diffusion coefficient testing followed the testing protocol mentioned in chapter 1. The chloride diffusion test plan of C3A series is described in Table 3.10 and Table 3.11. At least two samples were tested at each mentioned date for the chloride diffusion coefficient

In order to test the chloride content profile, the specimens were initially sliced into at least six disks using a water-cooled diamond saw. The relevant increments thicknesses are available in the following sections. The slices are then dried for 24 hours in the laboratory, tagged, placed in watertight plastic bags, and then placed in a freezer until the time of grinding and testing. The

different bags were as well tagged. The portions were placed in a freezer as the samples were not tested at the same time due to their excessive number (more than 60 tests at each age).

At the age of 235 days and since the chloride penetration was still relatively low, the specimen saw cutting was changed. A profile grinder was used to retain samples at an increment of 3 mm. The thickness eventually increased to 4 mm and 5 mm but noted accordingly. Each slice of the core was tested for Acid-Soluble Chloride at the specific age according to BS EN 1881 -124: 2015. The test is thoroughly explained in appendix 1.4.

Table 3.8 - Trial Experiment of C3A Series

Summary of C3A Series Trial Experiment (Madinah Aggregate)								
TRIAL NO.	**MIX NO.**	**CEMENT SOURCE**	**SLUMP (mm)**			**AIR CONTENT**	**TRIAL VOLUME (m3)**	**CYLINDER NOS.**
			Initial	**30 min**	**60 min**			
Trial-1	Mix-1 Trial-1	Alsafwa Sulfate Resistant Cement	240	200	155	2.5%	0.1	10
Trial-2	Mix-1 Trial-2	Alsafwa Sulfate Resistant Cement	245	200	160	2.5%	0.1	10
Trial-3	Mix 2	Yanbu Moderate Sulfate Resistant Cement	250	210	175	2.0%	0.1	10
Trial-4	Mix 3	North Region Cement Plus Ordinary Portland Cement	245	205	165	1.5%	0.1	10
Trial-5	Mix 4	Rabig Arabian Cement Plus Ordinary Portland Cement	240	195	155	2.0%	0.1	10
Trial-6	Mix 5	Alsafwa Cement Ordinary Portland Cement	250	220	180	2.0%	0.1	10

Table 3.9 - Details of Cores Drilled from Each Mix

Mix No.	**Cement Source**	**Core No.**	**Core Size**	
			Diameter (mm)	Length (mm)
Mix-1	Safwa Sulfate Resistant Cement	12	94	75
Mix 2	Yanbu Moderate Sulfate Resistant Cement	12	94	75
Mix 3	North Region Cement Plus Ordinary Portland Cement	12	94	75
Mix 4	Rabig Arabian Cement Plus Ordinary Portland Cement	12	94	75
Mix 5	Alsafwa Cement Ordinary Portland Cement	12	94	75

Table 3.10 - Chloride Diffusion Test Plan of C3A Series

Mix No.	Core Nos.	Immersing Date	Core Id	
			Immersed Core	Non - Immersed Core
Mix 1	12	27-Aug-2017	Sample 1, Sample 2, Sample 4, Sample 5, Sample 7 to Sample 12	Sample 3; Sample 6
Mix 2	12	27-Aug-2017	Sample 1, Sample 2, Sample 4, Sample 5, Sample 7 to Sample 12	Sample 3; Sample 6
Mix 3	12	27-Aug-2017	Sample 1, Sample 2, Sample 4, Sample 5, Sample 7 to Sample 12	Sample 3; Sample 6
Mix 4	12	27-Aug-2017	Sample 1, Sample 2, Sample 4, Sample 5, Sample 7 to Sample 12	Sample 3; Sample 6
Mix 5	12	27-Aug-2017	Sample 1, Sample 2, Sample 4, Sample 5, Sample 7 to Sample 12	Sample 3; Sample 6

Table 3.11 - Chloride Diffusion Test Plan of C3A Series

Sample Number from Each Mix	Date of Immersion	Date of Removal from Solution	Immersion Duration
Sample 1 (2 Specimens)	27-Aug-2017	3-Oct-2017	37 days
Sample 2 (2 Specimens)	27-Aug-2017	20-Nov-2017	85 Days
Sample 3 (2 Specimens)	27-Aug-2017	Not Immersed	
Sample 4 (2 Specimens)	27-Aug-2017	20-Nov-2017	85 Days
Sample 5 (2 Specimens)	27-Aug-2017	28-Dec-2017	123 Days
Sample 6 (2 Specimens)	27-Aug-2017	Not Immersed	
Sample 7 (2 Specimens)	27-Aug-2017	28-Dec-2017	123 Days
Sample 8 (2 Specimens)	27-Aug-2017	28-Dec-2017	123 Days
Sample 9 (2 Specimens)	27-Aug-2017	24-Jan-2018	150 Days
Sample 10 (2 Specimens)	27-Aug-2017	24-Jan-2018	150 Days
Sample 11 (2 Specimens)	27-Aug-2017	12-Mar-2018	197 Days
Sample 12 (2 Specimens)	27-Aug-2017	19-Apr-2018	235 Days

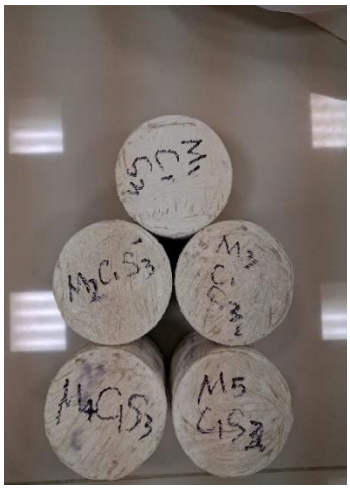

Figure 3.5 - Specimens Before Immersion in NaCl Solution

5. Chloride diffusion test results at different immersion ages

5.1. Initial acid soluble chloride and water-soluble chloride content

The initial acid soluble chloride and water-soluble chloride was tested initially in samples 3 and 6. Sample 3 was completely grinded and tested for acid soluble chloride and water soluble chloride whereas the acid soluble chloride in sample 6 was tested at several depths, namely 5 mm, 35 mm, and 65 mm below the surface. The purpose of taking 4 readings was mainly to check the variability of the results when the same operator is testing the same mix in several times. The results are summarized in Table 3.12 and Table 3.13 .

Table 3.12 - Initial test results for acid-soluble and water-soluble chloride – Sample 3

Initial test results				
Mix	**Sample**	**Test required**	**Water soluble test results (% of concrete weight)**	**Acid soluble test results (% of concrete weight)**
Mix 1 C3A=3.22%	Sample 3	Acid Soluble Chloride and Water Soluble Chloride (grinded and mixed together)	0.002	0.008
Mix 2 C3A=3.64%	Sample 3		0.002	0.010
Mix 3 C3A=4.46%	Sample 3		0.002	0.008
Mix 4 C3A=5.49%	Sample 3		0.002	0.007
Mix 5 C3A=6.65%	Sample 3		0.002	0.005

Table 3.13 - Initial Test Results for Acid-Soluble and Water-Soluble Chloride – Sample 6

Initial test results			
Mix	**Sample**	**Portion depth in mm**	**Acid soluble test results (% of concrete weight)**
Mix 1 C3A=3.22%	Sample 6	5.0	0.01
		20.0	
		35.0	0.008
		50.0	
		65.0	0.008
Mix 2 C3A=3.64%	Sample 6	5.0	0.02
		20.0	
		35.0	0.008
		50.0	
		65.0	0.005
Mix 3 C3A=4.46%	Sample 6	5.0	0.01
		20.0	
		35.0	0.008
		50.0	
		65.0	0.008
Mix 4 C3A=5.49%	Sample 6	5.0	0.01
		20.0	
		35.0	0.008
		50.0	
		65.0	0.008
Mix 5 C3A=6.65%	Sample 6	5.0	0.017
		20.0	
		35.0	0.005
		50.0	
		65.0	0.005

5.2. Acid soluble chloride profile at different ages of immersion

The different chloride diffusion coefficient and surface chloride concentration is included in appendix 3.1; a summary of the results is included in Table 3.14. Appendix 3.1 includes also the chloride content at each depth. The corresponding profiles at different ages of testing are included in Figure 3.6 to Figure 3.13. The graphs representing these parameters as a function of the tricalcium aluminate at different ages are included in Figure 3.14 and Figure 3.15.

Table 3.14 - Chloride diffusion coefficient and surface concentration - summary

Chloride diffusion coefficient and surface concentration				
Immersion duration	**Reference**	**C3A content (%)**	**Calculated chloride diffusion coefficient [m2/sec]**	**Calculated surface concentration [mass %]**
37 Days	Mix 1	3.22	3.40E-12	0.79%
	Mix 2	3.64	3.40E-12	1.03%
	Mix 3	4.46	3.40E-12	0.89%
	Mix 4	5.49	3.40E-12	0.82%
	Mix 5	6.65	3.20E-12	1.04%
85 Days	Mix 1	3.22	4.70E-12	0.65%
	Mix 2	3.64	5.80E-12	1.01%
	Mix 3	4.46	9.00E-12	0.51%
	Mix 4	5.49	3.20E-12	0.66%
	Mix 5	6.65	5.60E-12	0.57%
123 Days	Mix 1	3.22	4.55E-12	0.51%
	Mix 2	3.64	4.80E-12	0.67%
	Mix 3	4.46	4.15E-12	0.52%
	Mix 4	5.49	4.25E-12	0.50%
	Mix 5	6.65	4.90E-12	0.61%
150 Days	Mix 1	3.22	5.20E-12	0.63%
	Mix 2	3.64	9.90E-12	0.60%
	Mix 3	4.46	7.90E-12	0.48%
	Mix 4	5.49	4.20E-12	0.55%
	Mix 5	6.65	7.80E-12	0.47%
197 Days	Mix 1	3.22	5.80E-12	0.65%
	Mix 2	3.64	4.30E-12	0.67%
	Mix 3	4.46	4.12E-12	0.52%
	Mix 4	5.49	2.60E-12	0.61%
	Mix 5	6.65	2.50E-12	0.62%
235 Days	Mix 1	3.22	8.80E-12	0.70%
	Mix 2	3.64	7.20E-12	0.51%
	Mix 3	4.46	3.00E-12	0.98%
	Mix 4	5.49	2.40E-12	0.94%
	Mix 5	6.65	1.20E-12	1.50%

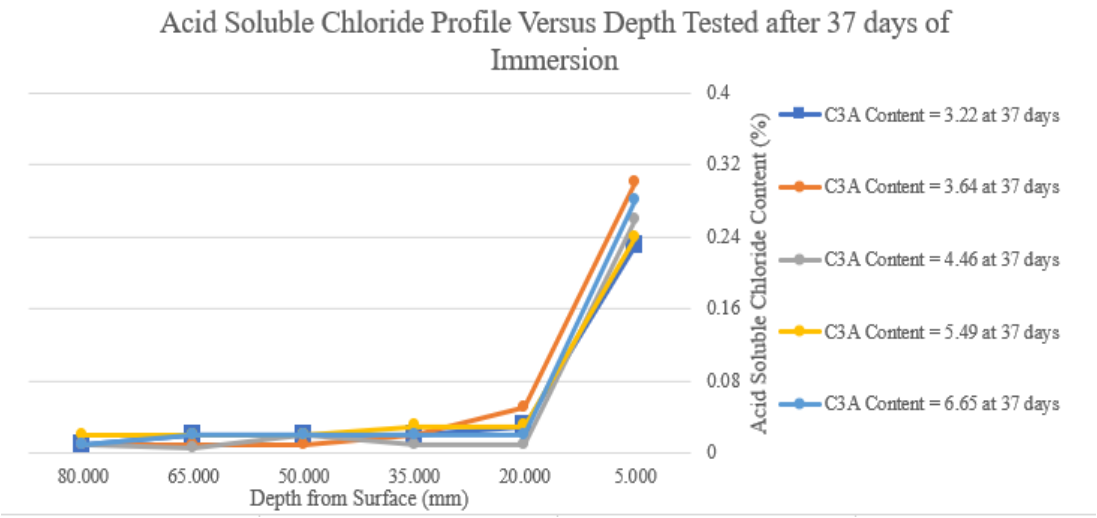

Figure 3.6 - Acid Soluble Chloride Profile at 37 Days

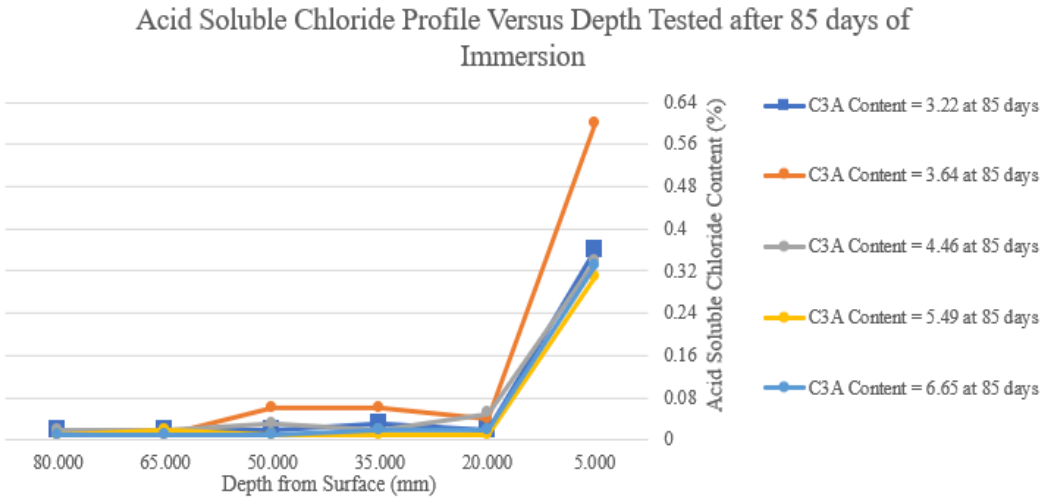

Figure 3.7 - Acid Soluble Chloride Profile at 85 Days

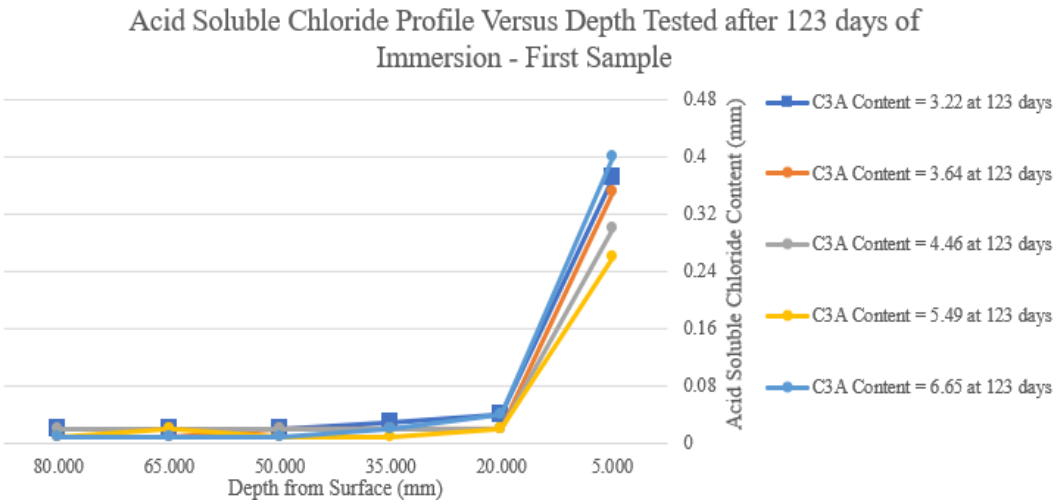

Figure 3.8 - Acid Soluble Chloride Profile at 123 Days – Sample 1

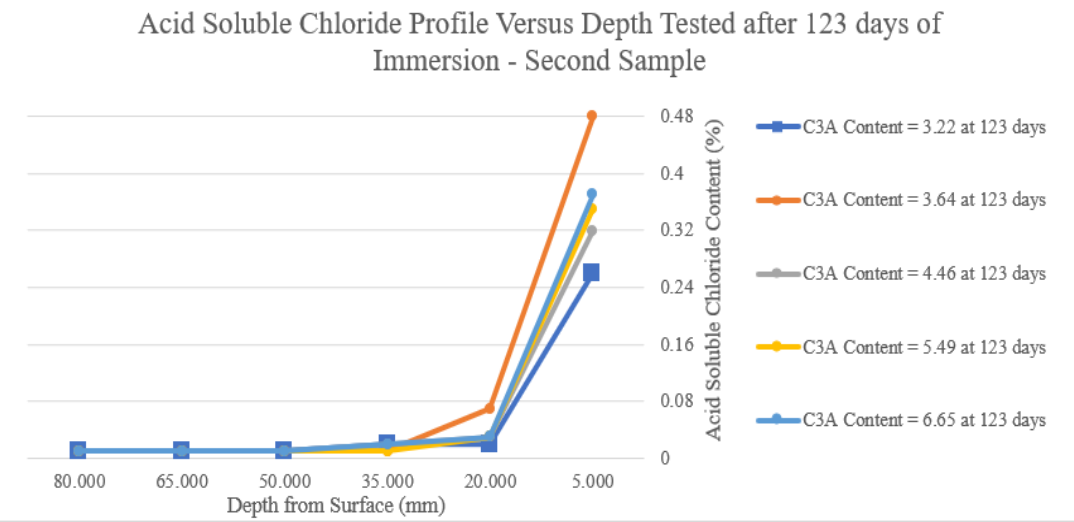

Figure 3.9 - Acid Soluble Chloride Profile at 123 Days – Sample 2

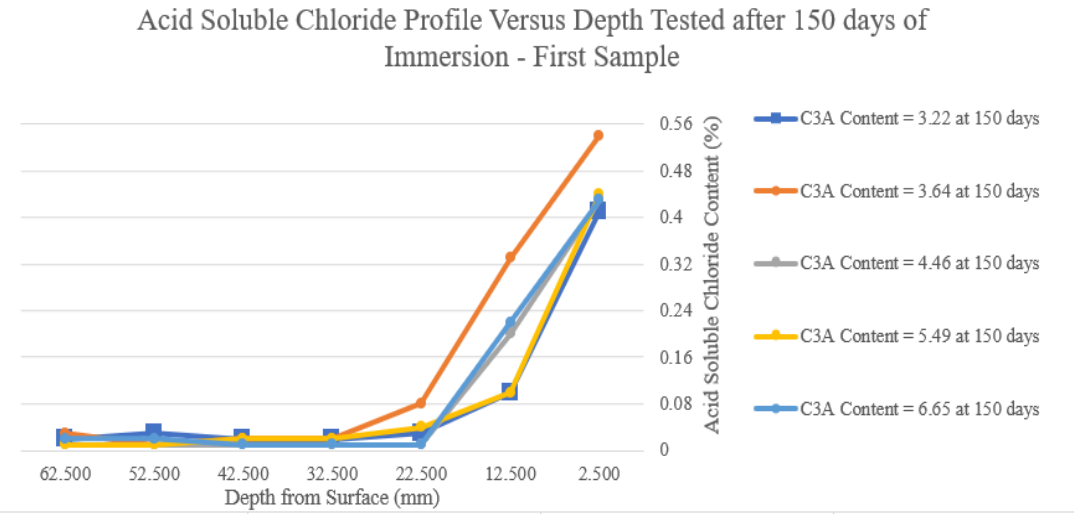

Figure 3.10 - Acid Soluble Chloride Profile at 150 Days - Sample 1

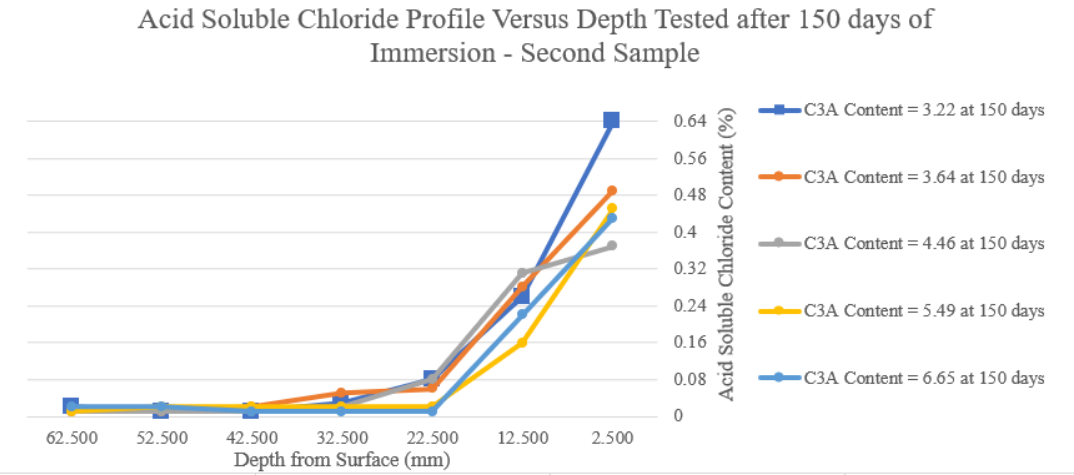

Figure 3.11 - Acid Soluble Chloride Profile at 150 Days - Sample 2

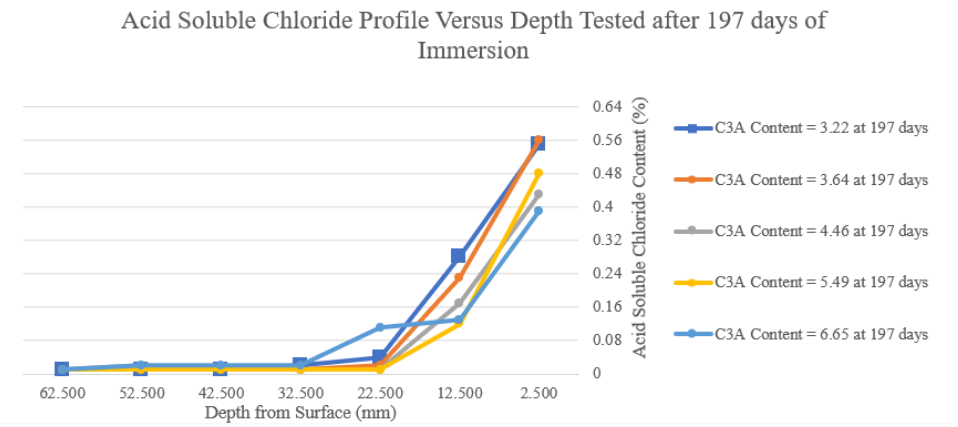

Figure 3.12 - Acid Soluble Chloride Profile at 197 Days

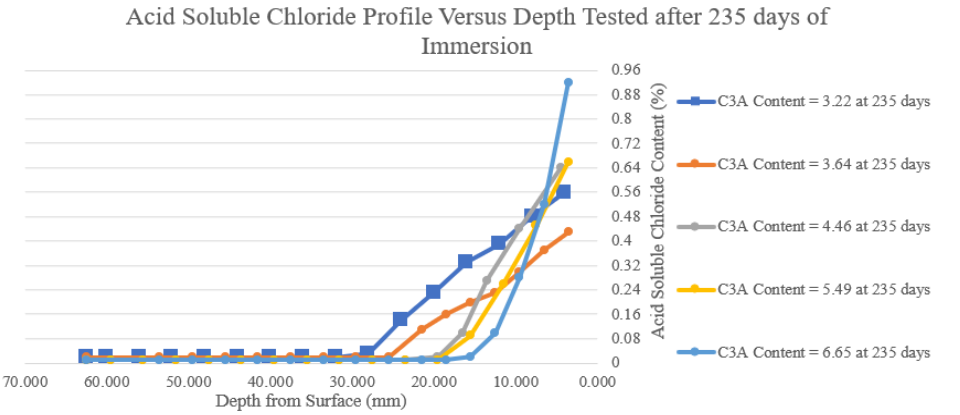

Figure 3.13 - Acid Soluble Chloride Profile at 235 Days

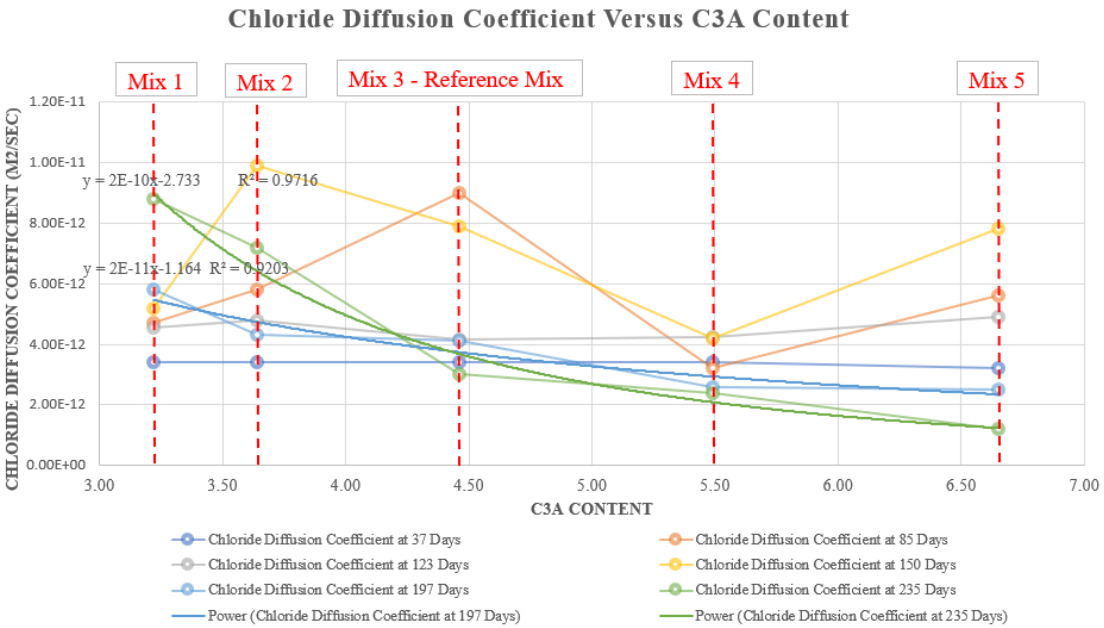

Figure 3.14 - Chloride Diffusion Coefficient as a Function of the C3A Content

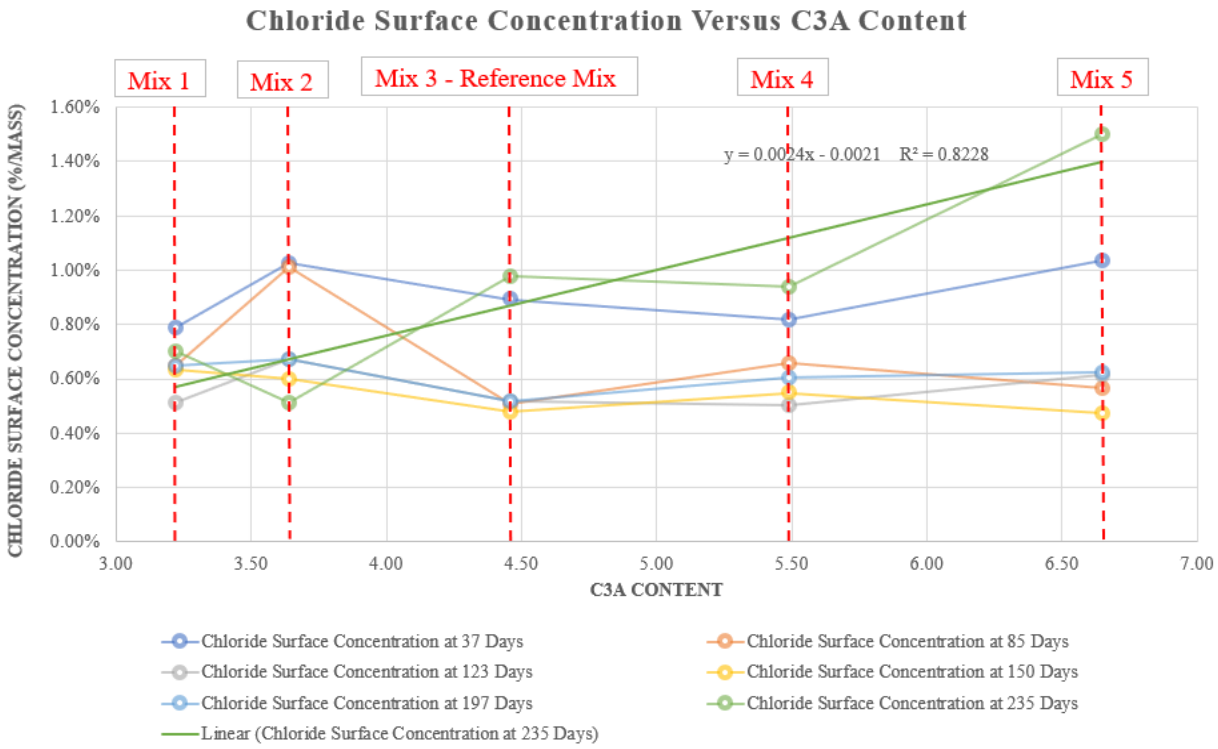

Figure 3.15 - Chloride Surface Concentration as a Function of the C3A Content

6. Results interpretation and C3A influence function

The graphs resulting from the testing campaign have indicated the following descriptions:

- After immersing the concrete samples for 37, 85, 123, and 150 days, the chloride diffusion coefficient for the concrete mixes made with different cement (and different C3A content) was almost equivalent.
- At 197 days of immersion, the concrete having less C3A content started to show a higher chloride diffusion coefficient and relatively lower surface concentration. The same description was made at an age of 235 days, although more pronounced.

The relating equations indicate high degree of correlation as follows:

For the same mix where the only changing parameter is the C3A content, the chloride diffusion coefficient can be calculated as follows:

$$D_c = (2 \times 10^{-10}) \times (C3A\ Content)^{-2.733} \quad R^2 = 0.9716 \tag{3.3}$$

$$c_s = -0.0021 + 0.0024 \times (C3A\ Content) \quad R^2 = 0.8228 \tag{3.4}$$

where D_c is the chloride diffusion coefficient and c_s the chloride surface concentration.

Referring to the literature review in chapter 1, the tricalcium aluminate forms one of the parameters affecting the chloride diffusion coefficient. The literature discussed in section 2 concluded that the increase in the amount of C3A available in the cement will increase the time to corrosion, increase the binded chloride portion, increase the chloride content near the surface and decrease the chloride content with depth. This can be physically explained by a decrease in the chloride ingress rate due to the binding mechanism. This will consequently increase the chloride percentage in the top portion of the concrete and the chloride content will decrease with depth. The graphs presented in section 5 generally confirm the literature review and quantify them in terms of chloride diffusion coefficient. These results should nevertheless be corrected first to take into account of the parameters discussed in chapter 2. Equation 2.37 should be applied to the resulting chloride diffusion coefficient in order to yield the bulk cement paste diffusion coefficient. As different percentages of C3S, C2S, and C4AF are also present, the corresponding hydration coefficient should be corrected which will influence as well the total porosity. The corrections are made in Table 3.15.

Table 3.15 - Corrected Bulk Cement Paste Diffusion Coefficient

Mix	Tested Chloride Diffusion Coefficient ($\times 10^{-12}$ m^2/s)	Materials Finer than 75 Microns (%)	Aggregate Absorption	Clay Lumps and Friable Particles	Aggregate Volume	Coefficient of Hydration	$\sum_{i=1}^{i=n} V_i A_i$	$\left[\sum_{i=1}^{i=n} \frac{V_i}{A_i}\right]$	$f(aggregate)$	Corrected Bulk Cement Paste Diffusion Coefficient ($\times 10^{-12}$ m^2/s)
1	8.80	0.4	1.0	0.3	0.671	0.8253	0.354	0.315	0.342	25.7
2	7.20	0.4	1.0	0.3	0.671	0.8351	0.345	0.323	0.334	21.6
3	3.00	0.4	1.0	0.3	0.671	0.8503	0.332	0.336	0.321	9.34
4	2.40	0.4	1.0	0.3	0.671	0.8419	0.339	0.328	0.328	7.32
5	1.20	0.4	1.0	0.3	0.671	0.9282	0.271	0.412	0.262	4.58

After isolating the effect of the C3A on the chloride diffusion, the function $f(C3A)$ influencing the chloride diffusion coefficient should be calculated. The equations related to the effect of C3A content on the chloride diffusion coefficient, is as follows:

$$D_c = f_D(C3A) \times D_{ref.\ bp} \tag{3.5}$$

and

$$f(C3A) = A \times (C3A)^B \tag{3.6}$$

where $f(C3A)$ is the function related to the C3A effect on the chloride diffusion coefficient, $D_{ref.\ bp}$ is a reference bulk cement paste, A, and B are constants.

The variable $D_{ref.\ bp}$ was used as a reference bulk cement diffusion to calculate the relative variation of the chloride diffusion coefficient as a function of the C3A content. Using the least square non-linear multiple regression analysis to determine the values of the unknowns satisfying these equations yielded the following:

Table 3.16 – Concrete Chloride Diffusion Coefficient as a function of *A* and *B*

Mix	Chloride diffusion coefficient value as a function of A and B	Corrected bulk cement paste diffusion coefficient (m2/s)
Mix 1 C3A=3.22%	$A \times (3.22)^B \times D_{ref.\ bp}$	2.57E-11
Mix 2 C3A=3.64%	$A \times (3.64)^B \times D_{ref.\ bp}$	2.16E-11
Mix 3 C3A=4.46%	$A \times (4.46)^B \times D_{ref.\ bp}$	9.34E-12
Mix 4 C3A=5.49%	$A \times (5.49)^B \times D_{ref.\ bp}$	7.32E-12
Mix 5 C3A=6.65%	$A \times (6.65)^B \times D_{ref.\ bp}$	4.58E-12

Consequently:

$A = 26.644$

$B = -2.552$

$D_{ref.\ bp} = 1.97 \times 10^{-11}$

Based on the above, the function related to the effect of C3A content on the chloride diffusion coefficient is as follows:

$$f(C3A) = 26.644 \times (C3A)^{-2.552} \quad (3.7)$$

7. Conclusion

The following conclusions can be made, based on the research conducted in this chapter:

The literature discussed in section 2 concluded that the increase in the amount of C3A available in the cement will increase the time to corrosion, increase the binded chloride portion, increase the chloride content near the surface and decrease the chloride content with depth. This can be physically explained by a decrease in the chloride ingress rate due to the binding mechanism. This will consequently increase the chloride percentage in the top portion of the concrete and the chloride content will decrease with depth.

Based on the testing campaign conducted the chloride diffusion coefficient increases with a decrease in the tricalcium aluminate content. On the other hand, the chloride surface concentration increases with an increase in the tricalcium aluminate content.

The effect of C3A content on the chloride diffusion coefficient and surface concentration was only pronounced at a duration exceeding 150 days.

The final C3A function affecting the chloride diffusion coefficient and the chloride surface concentration is concluded in section 6.

The results are valid for binary concrete mixes made with cement and including 6% Micro Silica as a percentage of the cementitious materials.

More study is needed to generalize this theory on mixes that includes other types of cementitious materials.

Chapter 4 - Effect of mixing time, consolidation, and curing time

1. Introduction

The main objective of this chapter is to assess the effect of the field practices, namely the concrete mixing time, consolidation degree, and curing time, on the chloride diffusion coefficient. The effect of the curing time and hydration were presented in chapter 2 due to its combination with the aggregate interfacial zone thickness. The remaining parameters (i.e. the mixing time and concrete consolidation degree) are detailed in this chapter. After presenting the testing protocol, followed by the raw materials test and mix design, details of the core specimen preparations and chloride diffusion rate test plan are provided. Further to the test procedures, the results are presented, and related calculations are performed. This chapter finally reaches comprehensive conclusions regarding the effect of these parameters on the chloride diffusion coefficient.

2. Effect of mixing time and concrete consolidation

Concrete is considered as a porous material, the distribution and size of pores significantly affect its performance, especially when it comes to durability parameters including the chloride diffusion coefficient. The past chapters have concluded that several factors affect the chloride diffusion coefficient. These factors initially change the pores distribution and size in concrete. Several construction codes and standards emphasized the importance of a uniform and well consolidated concrete end-product to secure the intended concrete durability. Construction standards similarly to AASHTO M157 [105], ACI 304 [106], and ASTM C94 [107] place limits on the concrete mixing time, placement time, and number of truck revolutions. The list of the prescriptive-based concrete durability codes described in chapter 1 include a list of construction recommendation to yield high concrete quality. These recommendations stress more often on good consolidation and uniform concrete.

Pores in concrete originates from several factors and can be divided into four main categories [108], capillary pores, entrained air voids, entrapped air voids, and water voids, as follows:

- Capillary voids are usually less than 5-10 μm and controlled by the water-cementitious materials ratio, degree of hydration and cementitious material type.

- Entrained Air voids are caused by the addition of air entraining agent, they are larger than the capillary voids but usually less than 1 mm.

- Entrapped Air voids and Water voids are all the voids in concrete that have a diameter of more than 1 mm and are formed by entrapping air or water in concrete. Water voids are usually found in concrete mixes with high water-cementitious materials ratio.

The below chart illustrates the size distribution of the pores in concrete.

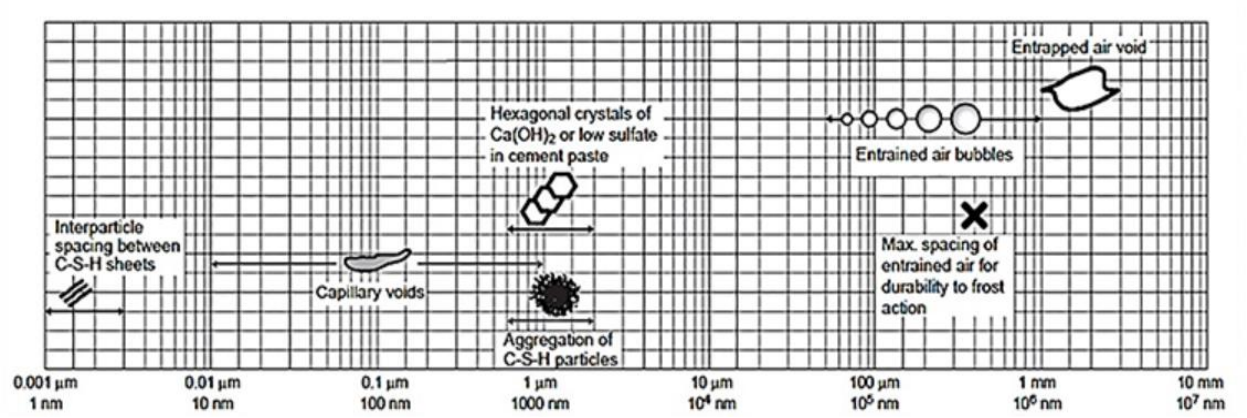

Figure 4.1 - Pore Size Distribution in Concrete [109]

As a conclusion, the pore types in concrete can be divided into two broader general categories. A pores structure that have a dimeter of less than 10 µm and defined by the concrete mix parameters, and a larger diameter pore structure of entrapped air that originate from the additional concrete practices. Apart from the entrained air that originates from specific admixtures, the entrapped air structure originates from mixing and consolidation practices. Zhang et al. [110] investigated the effect of the concrete pores structure on the chloride diffusion coefficient which was found well dependent on the pore sizes exceeding 100 nm, the pores structure that changed with the water-cementitious materials ratio, up to a size of 1000 nm. This research also found that the pores portion below 10 nm did not change with the concrete composition. In this experiment, the samples were well compacted and the change of pore structure originated from the change in concrete mix design parameters. Several other researches [111][112] have linked the capillary pore structure to the chloride diffusion and permeation properties of concrete. Nevertheless the samples under consideration in these researches were standardly compacted and the pores considered were mainly the capillary pores.

The present chapter focuses on the effect of the pore sizes range larger than 10µm on the chloride diffusion coefficient in non-air-entrained concrete, more specifically, the entrapped air originating from the concrete initial mixing time and consolidation degree. The effect of the initial mixing time and consolidation degree on the concrete durability and change in concrete properties is well documented as discussed in the following paragraphs. The missing link remains a quantification of the effect of the initial mixing time and consolidation degree on the chloride diffusion coefficient.

ACI 201.2 [58] states that the air-void structure of concrete is created during mixing of the fresh concrete, which suggests the effect of concrete mixing on the pore structure. The same document also states that:" *Both Mixing and placement methods of fresh concrete contribute to determining the final arrangement of the concrete pore structures which significantly influence the durability*

and degree of satisfactory performance of the structure relative to interaction with environmental conditions and internal reactions."

Lapyote and Trejo [113] demonstrated that the concrete porosity increases as a function of the mixing time and the number of concrete drum revolutions. Figure 4.2 and 4.3 below are extracted from this work. Knowing that the pore structure affects the chloride diffusion coefficient, no clear trend was found between the chloride diffusion coefficient and the concrete mixing time. The corresponding graphs extracted from the same research are included in figure 4.4 and 4.5. This research finally concluded that the microstructure of the hydrated products also changes as a function of the concrete mixing time. The range of mixing time used in this research vary from two minutes to 90 minutes. This range is not realistically applied in the construction industry today where the mixing time followed comply with the requirements of ASTM C94 and frequently below 2 minutes.

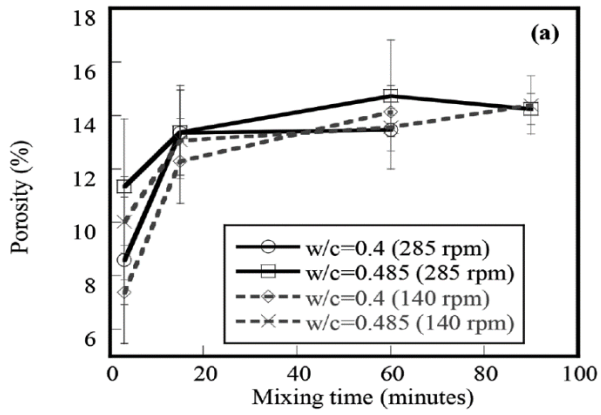

Figure 4.2 - Effect of Mixing Time on the Porosity

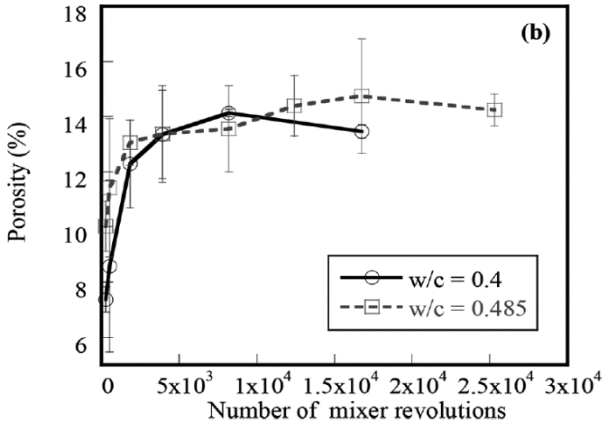

Figure 4.3 - Effect of the mixer Revolution on the Porosity

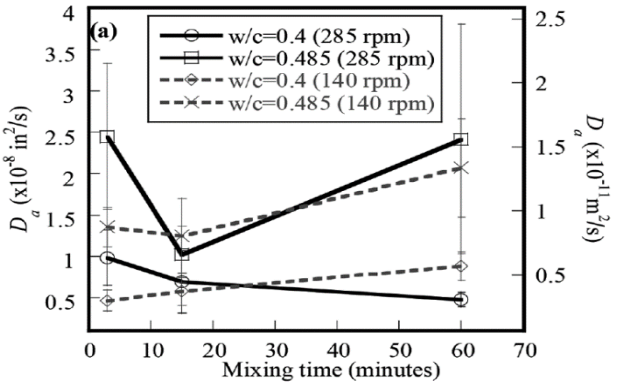

Figure 4.4 – Effect of Mixing Time on the Diffusion Coefficient

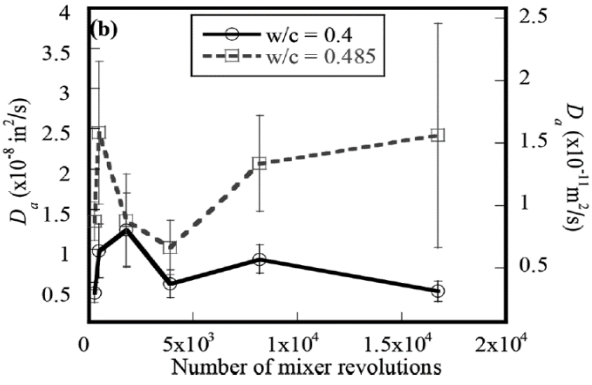

Figure 4.5 - Effect of Mixing Revolutions on the Diffusion Coefficient

Jiaming Chen [114] also investigated the effect of the mixing time and mixing speed on the concrete fresh and hardened properties. The mixing time significantly affected the fresh concrete properties in addition to the significant effect on the concrete compressive strength. The findings

of this research also concluded that the mixing time did not significantly affect the modulus of Rupture and the chloride diffusion coefficient. The research conducted by Urban and Sicakova [115] and Ravina [116] have equally concluded a significant effect of mixing time on the hardened concrete properties.

The American Petroleum Institute (API2002) [117] concluded that the specific mixing energy which is dependent from the mixing time and speed will affect the hardened concrete compressive strength [118]. The effect of mixing energy on the concrete end product properties was also reported by Williams et al. [119] and Rupnow et al. [120]. These researches reach the conclusion that, with greater energy, a greater structure breakdown is reached. Furthermore, and in the same context, Beitzel [121] concluded that an upper and lower boundary for the mixing time should be set as different concrete properties will require different optimum mixing time.

On the other hand, the degree of consolidation or in other terms, achieving an adequately consolidated concrete for a durable concrete, with lower chloride diffusion, was mentioned in several references. ACI 201.2 [58], the American Society Guide for Durability includes several statements that indicates this fact, and emphasize the necessity of good consolidation for a durable concrete: *"Good consolidation is a prerequisite for obtaining low permeability, which is critical for m*aking concrete resistant to weathering and most agents of deterioration". This standard stresses that the use of good materials and proper mixture proportioning will not by itself ensure durable concrete. The placement and workmanship are equally essential to the production of durable concrete. ACI 222 [57] equally stresses this fact. Figure 4.6 was extracted from this standard and shows the effect of inadequate consolidation on the chloride penetration in concrete.

Alkhaja [122] investigated the chloride ingress in two samples of concrete where the first was subjected to a full consolidation and the second consolidated to 50% of the vibration energy used in the first one. The half-consolidated concrete showed a higher chloride ingress when compared to the adequately consolidated one. Akili [123] investigated the effect of consolidation level on the chloride ingress using the Rapid Chloride Penetration Test in structural concrete and piling concrete. In the different instances, the adequately consolidated concrete was more resistance to chloride ingress than the inadequately consolidated one. Figure 4.7 was extracted from his research. The investigation conducted by the Land Transport New Zealand Research [124] also concluded that the corrosion damage is more likely when the concrete permeability is increased by inadequate compaction.

Going from different literature review made in this paragraph, it is obvious that the concrete pore structure, the concrete mixing time and the concrete degree of consolidation are dependent parameters that jointly affect the concrete final durability level and consequently the chloride diffusion coefficient. Although the chloride diffusion coefficient was mainly linked to the concrete constituent materials yielding the pores structures that are below 10 µm in diameter, the construction practices may embed in concrete, pores having a diameter that exceeds 1 mm in diameter. The effect of this range of pores diameters, originating from the concrete initial mixing

time and degree of consolidation, on the chloride diffusion coefficient will be investigated in this chapter.

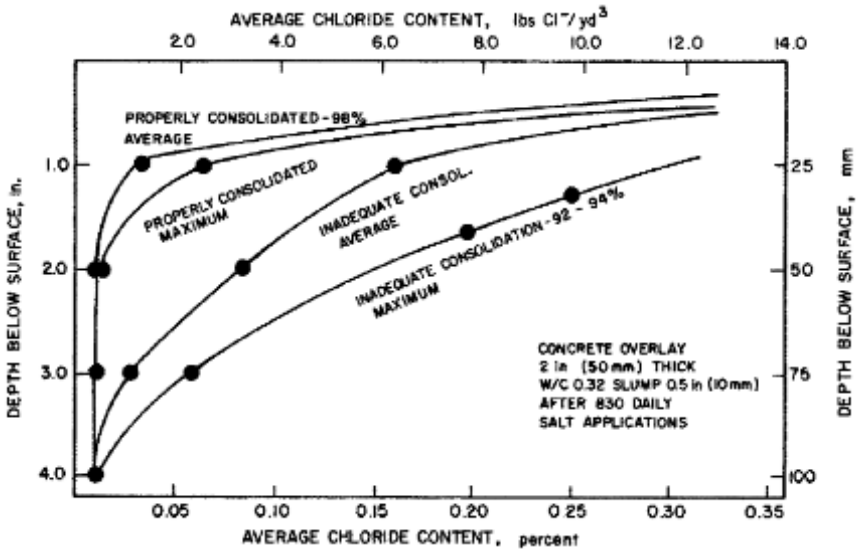

Figure 4.6 - Effect of Inadequate Consolidation on Salt Penetration (as extracted from ACI 222) [57]

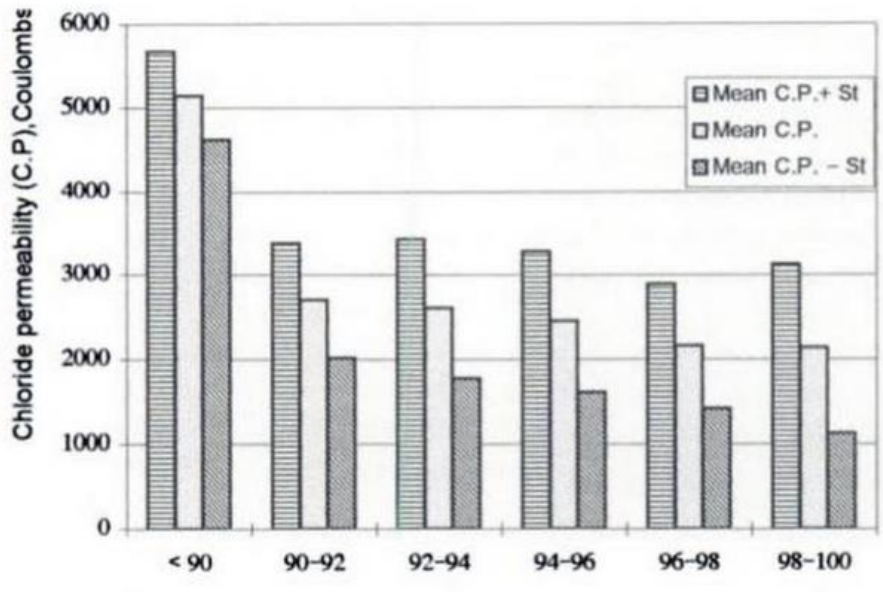

Figure 4.7 - Chloride Permeability Versus Percent Consolidation in Piling Concrete [122]

3. Testing protocol

The referenced concrete mix design used in the previous chapters was replicated in a twin-shaft mixer at PREMCO batching plant located in Obhur – Saudi Arabia following five batches. The five batches were identically proportioned and mixed using five different initial mixing times. The initial mixing time for batches 1 to 5 were 45, 90, 135, 180, and 225 seconds, respectively. Each

batch included a total quantity of 2.0m^3. The trial records and fresh concrete properties are listed in table 4.1. Pictures of the trial mixes are included in figures 4.8 to 4.11. A suitable number of concrete cylinders were taken from each mix and cured for 28 days. Further to the curing period, concrete cores were taken from the cylinders with a diameter of 94 mm and a height of 75 mm. For each mix, 15 cores were prepared in total, the corresponding details are listed in table 4.3.

One additional batch was furthermore prepared and a total of 24 concrete cylindrical specimens were taken from this batch. ASTM C31 [60] states that the cylinders should be filled following three layers where each layer is consolidated by a rod 25 times. This level of consolidation is taken as the reference level of consolidation. The 24 cylinders were divided into 6 groups of consolidation where the first set was filled with three layers without any consolidation, the second set of cylinders was filled with three layers where each one is consolidated 5 times, the four remaining sets where filled with three layers while consolidating each layer 10, 15, 25 and 35 times for set 3, 4, 5, and 6 respectively. The trial records and fresh concrete properties are listed in table 4.2. The picture of the cylinders after demolding is included in figure 4.12. The top surface of all the cylinders were properly finished to avoid percolation of the chloride solution in the samples after immersion. All cylinders were cured for 28 days, then cores were drilled from the concrete cylinders. For each mix, 12 cores were prepared in total, the corresponding details are listed in table 4.4. The cores identification for MIXT and CONS series, representing the samples related to the mixing time effect quantification and the consolidation effect quantification respectively, are included in appendix 4.1.

Two sets of samples from each category were crushed from each concrete mix design and the initial acid soluble chloride content determined. All of the remaining sides were then sealed, except the finished surface, with a suitable barrier coating. The sealed specimens are then saturated in a calcium hydroxide solution, rinsed with tap water, and then placed in a sodium chloride solution. After a duration of 341 days, the cores were tested for apparent chloride diffusion coefficient as detailed in chapter 1. The samples were taken using a profile grinder with an increment thickness of 3mm. The acid soluble chloride in the different increment was tested using the procedure detailed in chapter 1.

Table 4.1 - Trial experiment of MIXT series

Summary of MIXT series trial experiment (Northern Region Cement)				
Trial No.	**Mixing time (Seconds)**	**Initial slump (mm)**	**Trial volume (m3)**	**Cylinder Nos.**
1	45	245	2.0	5
2	90	245	2.0	5
3	135	240	2.0	5
4	180	245	2.0	5
5	225	230	2.0	5

Table 4.2 - Trial experiment CONS series

Summary of Cons series trial experiment (Northern Region Cement)			
Trial No.	**Consolidation times (rods)**	**Initial slump (mm)**	**Cylinder Nos.**
6	0	200	4
7	5	210	4
8	10	210	4
9	15	230	4
10	25	230	4
11	35	230	4

Table 4.3 - Details of cores drilled from each trial mix – MIXT series

Trial No.	**Mixing (Seconds)**	**Core Nos.**	**Core size**	
			Diameter (mm)	Length (mm)
1	45	15	100	75
2	90	15	100	75
3	135	15	100	75
4	180	15	100	75
5	225	15	100	75

Table 4.4 - Details of Cores Drilled from Each Mix – CONS Series

Trial No.	**Consolidation Times (rods)**	**Core Nos.**	**Core Size**	
			Diameter, mm	Length, mm
6	0	12	100	75
7	5	12	100	75
8	10	12	100	75
9	15	12	100	75
10	25	12	100	75
11	35	12	100	75

Figure 4.8 - Cement Mixer Truck for MIXT Series

Figure 4.9 - Fresh Concrete Properties Measurement

Figure 4.10 - Concrete Cylinders Preparation

Figure 4.11 – Concrete Cylinders Preparation

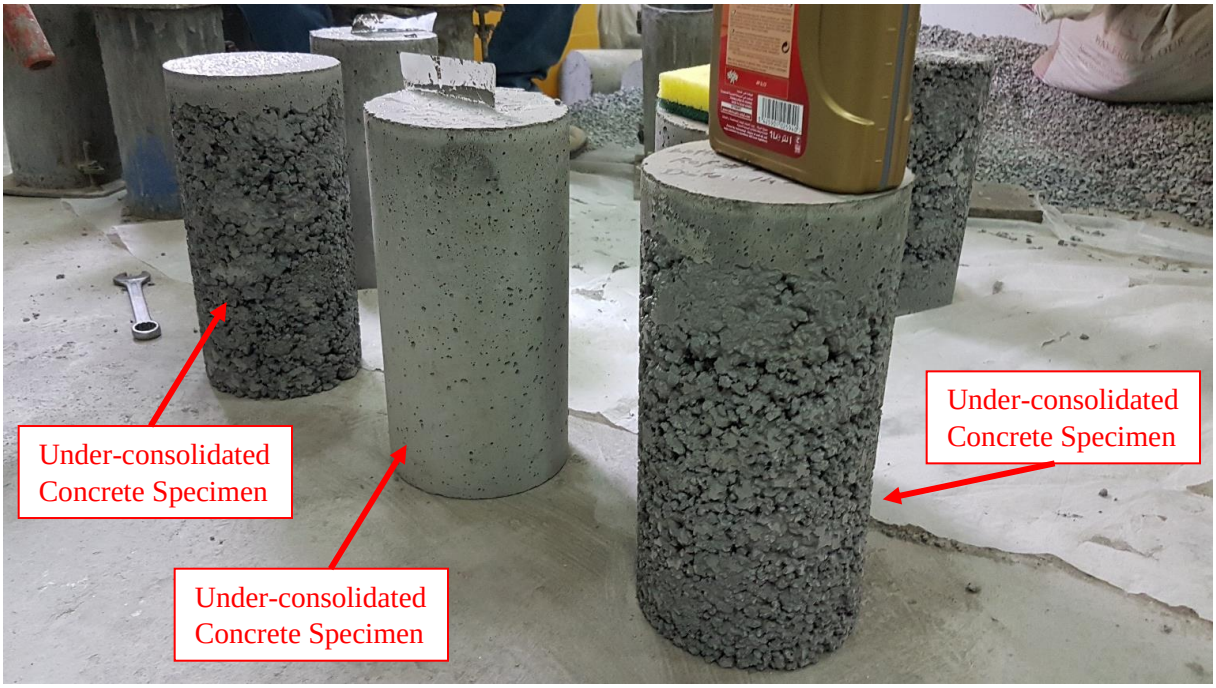

Figure 4.12 - Cylindrical Specimens after Demold for CONS Series

Figure 4.13 - Cores Drilled for Chloride Diffusion Test – MIXT Series

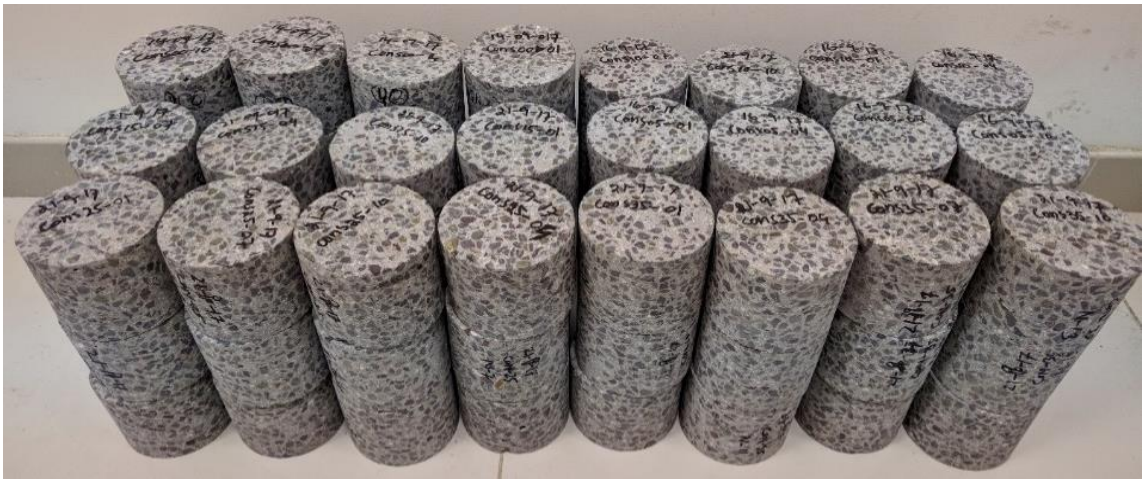

Figure 4.14 - Cores Drilled for Chloride Diffusion Test – CONS Series

4. Chloride diffusion test results

The density test of the different concrete cores made with different mixing times and consolidation degrees was first conducted in order to identify the effect of these parameters on the concrete density. It was obvious that a higher degree of consolidation will result in a higher concrete density. Nevertheless, additional mixing time was found to be slightly beneficial in yielding a denser mix. As additional testing that can affect the chloride diffusion in concrete, the water absorption and the volume of permeable pores were tested. The concrete density, water absorption and volume of permeable pores were tested in reference to the requirements of ASTM C642 [125]. The results of the density as well as the water absorption and volume of permeable voids are tabulated in tables 4.5 to 4.7. The water permeability was furthermore conducted for CONS series. The water permeability versus the concrete consolidation degree is tabulated in table 4.7. The variations of these different parameters are presented in Figures 4.15 to 4.20 hereafter.

Table 4.5 - Concrete Density, Absorption and Volume of Permeable Pores - MIXT Series

Reference	Mixing Time (seconds)	Absorption (%)		Apparent Density (kg/m3)		Volume of Permeable Voids (%)	
		Individual Reading	Average	Individual Reading	Average	Individual Reading	Average
MIXT45-11	45	3.08	3.405	2612	2617	7.5	8.25
MIXT45-12	45	3.73		2622		9	
MIXT90-11	90	4.44	3.865	2645	2628.5	10.7	9.35
MIXT90-12	90	3.29		2612		8	
MIXT135-11	135	3.43	3.34	2617	2622	8.3	8.15

MIXT135-12	135	3.25		2627		8	
MIXT180-11	180	3.49	3.98	2624	2626	8.4	9.95
MIXT180-12	180	4.47		2628		11.5	
MIXT225-11	225	4.46	4.07	2657	2639	10.8	9.85
MIXT225-12	225	3.68		2621		8.9	

Table 4.6 - Concrete Density, Absorption and Volume of Permeable Pores - CONS Series

Reference	Rodding Number	Absorption (%)		Apparent Density (kg/m3)		Volume of Permeable Voids (%)	
		Individual Reading	Average	Individual Reading	Average	Individual Reading	Average
CONS00-11	0	4.15	3.82	2542	2542	11.1	9.7
CONS00-12	0	3.49		2542		8.3	
CONS05-11	5	3.78	3.635	2601	2591	9	8.65
CONS05-12	5	3.49		2581		8.3	
CONS10-11	10	4.79	4.26	2667	2643	12.1	10.55
CONS10-12	10	3.73		2619		9	
CONS15-11	15	5.03	4.445	2656	2622	12.3	10.75
CONS15-12	15	3.86		2588		9.2	
CONS25-11	25	4	4.35	2610	2629	9.5	10.3
CONS25-12	25	4.7		2648		11.1	
CONS35-11	35	5.19	4.425	2666	2641.5	12.9	10.85
CONS35-12	35	3.66		2617		8.8	

Table 4.7 – Concrete Permeability - CONS Series

Reference	Rodding Number	Water Permeability (mm)
		Average of Two Readings
CONS00-11	0	66.5
CONS05-11	5	7.6
CONS10-10	10	11.5
CONS15-12	15	7.3
CONS25-09	25	6.9
CONS35-07	35	11.9

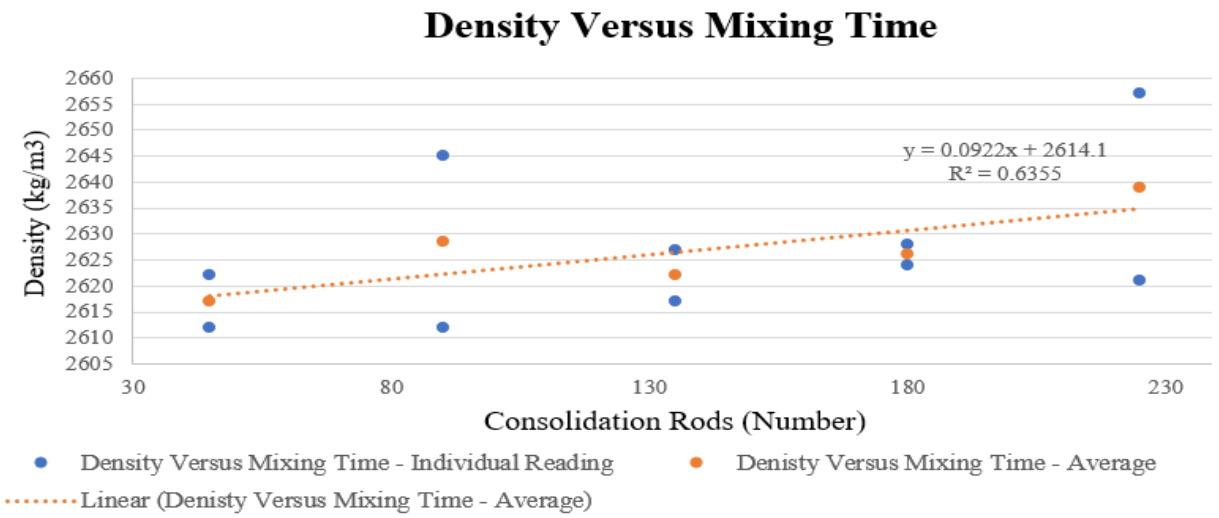

Figure 4.15 - Concrete Density versus Mixing Time

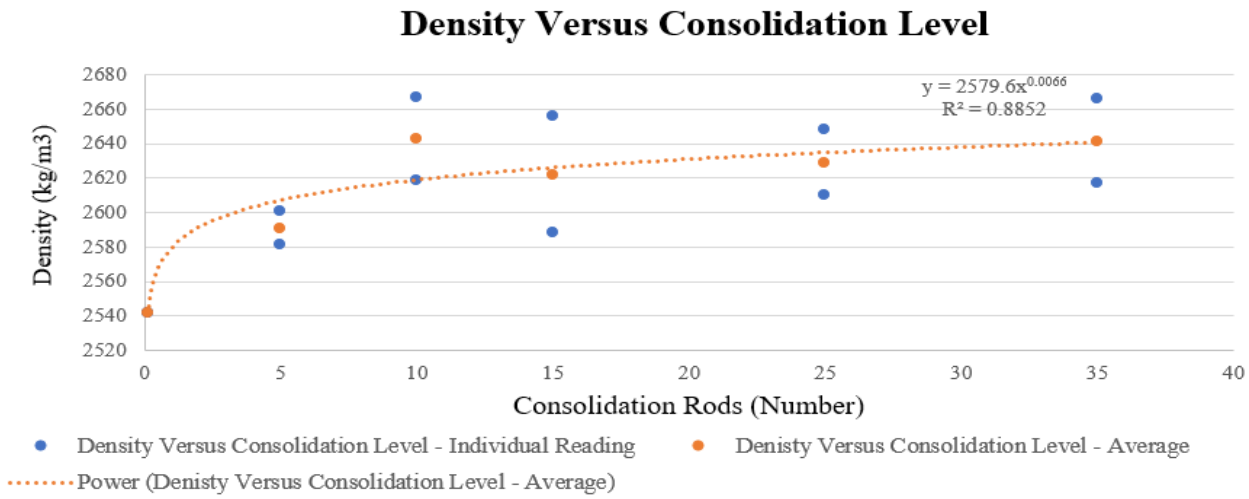

Figure 4.16 - Concrete Density Versus Consolidation Level

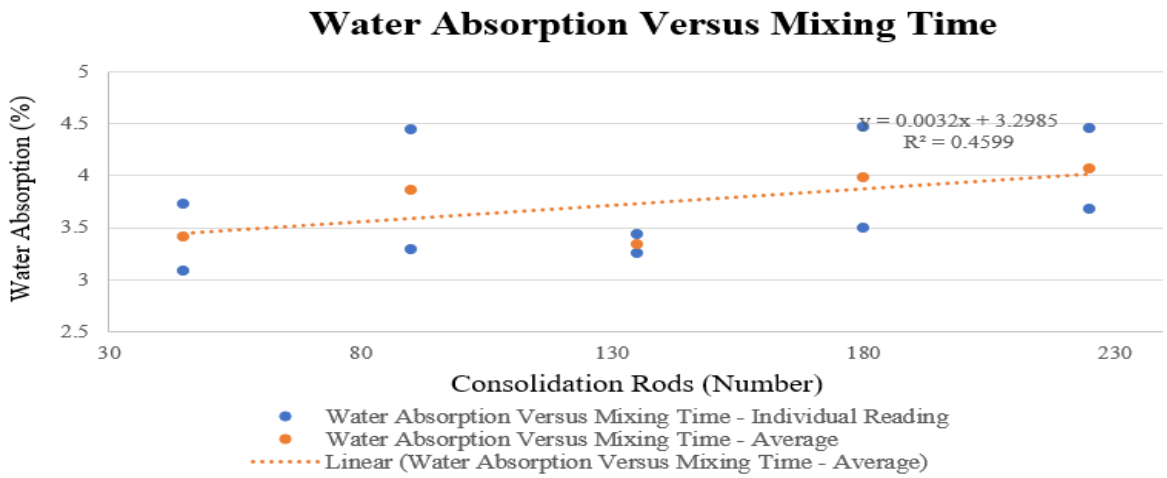

Figure 4.17 - Concrete Water Absorption Versus Mixing Time

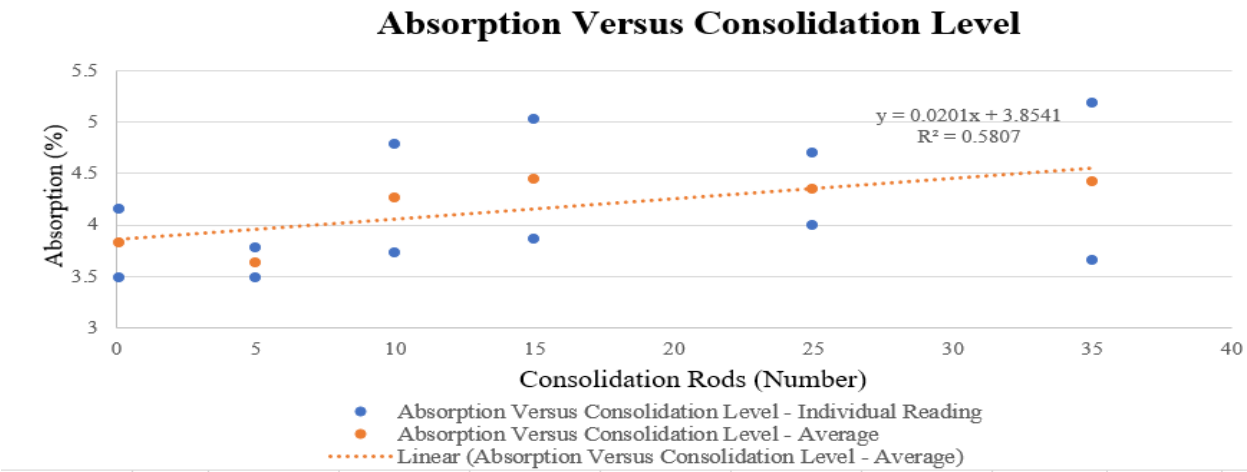

Figure 4.18 - Water Absorption versus Consolidation Level

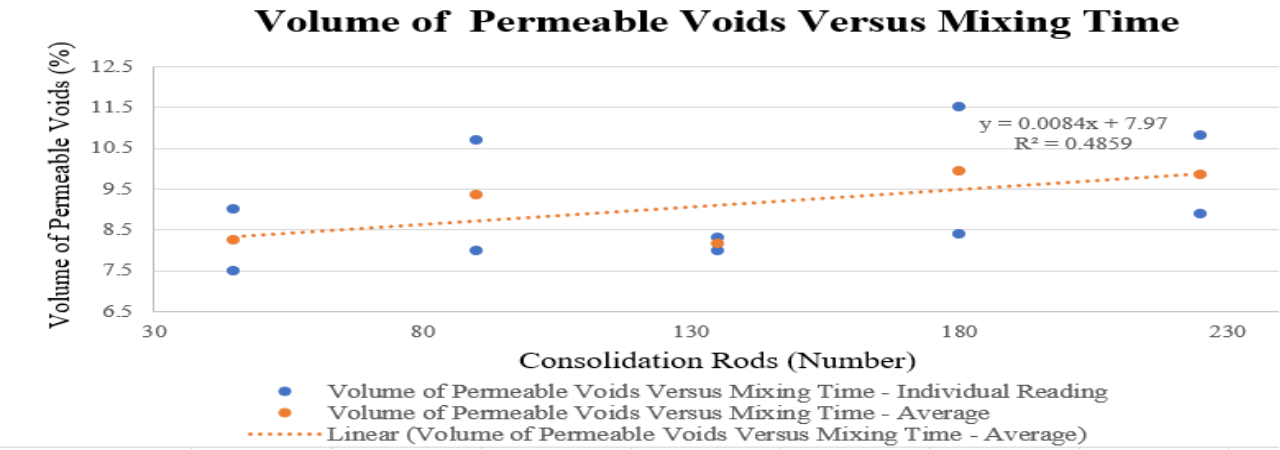

Figure 4.19 - Volume of Permeable Voids versus Mixing Time

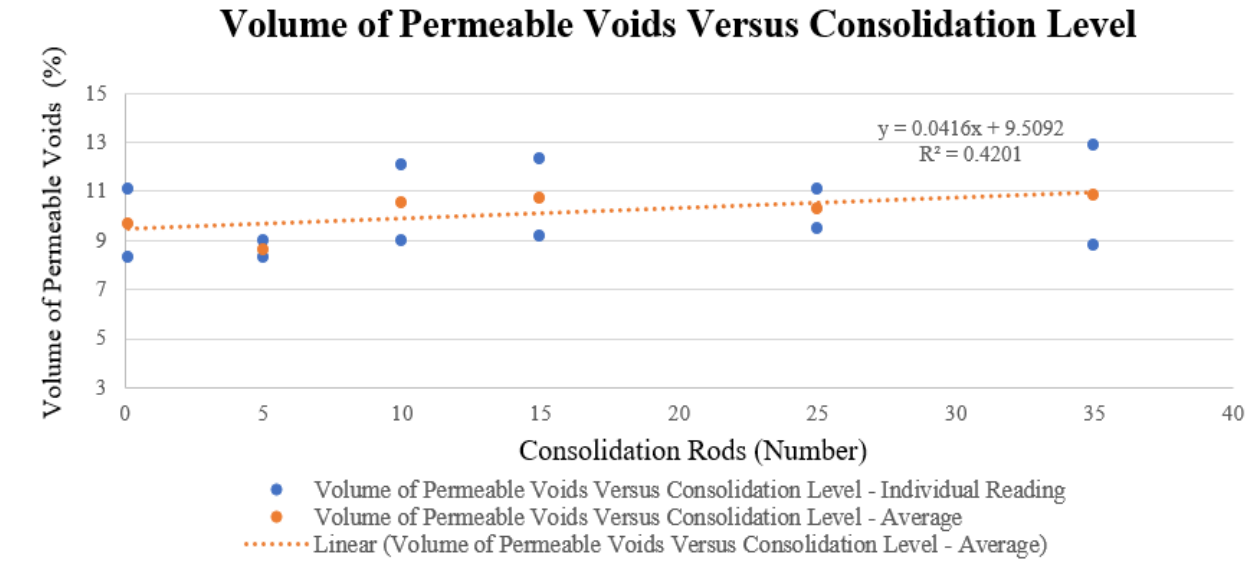

Figure 4.20 - Volume of Permeable Voids versus Consolidation Level

The apparent chloride testing protocol detailed in chapter 1 is used to determine the chloride diffusion coefficient of different mixes. The results are given in tables 4.8 and 4.9. The chloride profile in each core is presented in figures 4.21 and 4.22. The apparent chloride diffusion coefficients of the different cores are included in figures 4.10 and 4.11. The related chloride diffusion coefficient calculations are included in appendix 4.2.

Table 4.8 - MIXT Series Chloride Content Determination

MIXT Series - Acid Soluble Chloride Content					
Reference	Depth (mm)	Acid Soluble Chloride Content (%)	Reference	Depth (mm)	Acid Soluble Chloride Content (%)
MIXT45-07	2.5	1.21	MIXT45-09	2.5	0.98
	5.5	0.74		5.5	0.63
	8.5	0.57		8.5	0.44
	11.5	0.4		11.5	0.28
	14.5	0.26		14.5	0.14
	17.5	0.15		17.5	0.06
	20.5	0.07		20.5	0.02
MIXT90-09	2.5	0.95	MIXT90-10	2.5	1.26
	5.5	0.67		5.5	0.81
	8.5	0.51		8.5	0.62
	11.5	0.39		11.5	0.47
	14.5	0.26		14.5	0.34
	17.5	0.14		17.5	0.2
	20.5	0.07		20.5	0.1
MIXT135-08	2.5	0.87	MIXT135-09	2.5	1.21
	5.5	0.58		5.5	0.77
	8.5	0.52		8.5	0.52
	11.5	0.38		11.5	0.35
	14.5	0.26		14.5	0.2
	17.5	0.16		17.5	0.09
	20.5	0.09		20.5	0.04
MIXT180-04	2.5	1.24	MIXT180-06	2.5	1.07
	5.5	0.78		5.5	0.68
	8.5	0.58		8.5	0.52
	11.5	0.41		11.5	0.37
	14.5	0.28		14.5	0.21
	17.5	0.16		17.5	0.09
	20.5	0.06		20.5	0.04
MIXT225-07	2.5	1.24	MIXT225-09	2.5	1.28
	5.5	0.86		5.5	0.69
	8.5	0.59		8.5	0.5
	11.5	0.43		11.5	0.32

	14.5	0.28		14.5	0.17
	17.5	0.14		17.5	0.05
	20.5	0.07		20.5	0.02

Table 4.9 - CONS Series Chloride Content Determination

CONS Series - Acid Soluble Chloride Content					
Reference	Depth (mm)	Acid Soluble Chloride Content (%)	Reference	Depth (mm)	Acid Soluble Chloride Content (%)
CONS00-04	2.5	1.25	CONS00-10	2.5	1.24
	5.5	0.65		5.5	0.84
	8.5	0.37		8.5	0.64
	11.5	0.16		11.5	0.48
	14.5	0.07		14.5	0.36
	17.5	0.03		17.5	0.24
	20.5	0.02		20.5	0.13
CONS05-10	2.5	1.02	CONS05-07	2.5	1.12
	5.5	0.69		5.5	0.65
	8.5	0.51		8.5	0.4
	11.5	0.31		11.5	0.26
	14.5	0.14		14.5	0.14
	17.5	0.06		17.5	0.06
	20.5	0.02		20.5	0.02
CONS10-07	2.5	1.28			
	5.5	0.78			
	8.5	0.55			
	11.5	0.37			
	14.5	0.22			
	17.5	0.12			
	20.5	0.06			
CONS15-05	2.5	1.14	CONS15-04	2.5	1.07
	5.5	0.76		5.5	0.79
	8.5	0.58		8.5	0.58
	11.5	0.41		11.5	0.48
	14.5	0.29		14.5	0.36
	17.5	0.16		17.5	0.24
	20.5	0.07		20.5	0.16
CONS25-10	2.5	1.58	CONS25-08	2.5	1.26
	5.5	0.88		5.5	0.87
	8.5	0.59		8.5	0.65
	11.5	0.43		11.5	0.48
	14.5	0.29		14.5	0.37
	17.5	0.17		17.5	0.23

	20.5	0.09		20.5	0.13
CONS35-10	2.5	1.26	CONS35-06	2.5	1.21
	5.5	1.01		5.5	0.76
	8.5	0.65		8.5	0.58
	11.5	0.4		11.5	0.43
	14.5	0.23		14.5	0.3
	17.5	0.14		17.5	0.16
	20.5	0.09		20.5	0.09

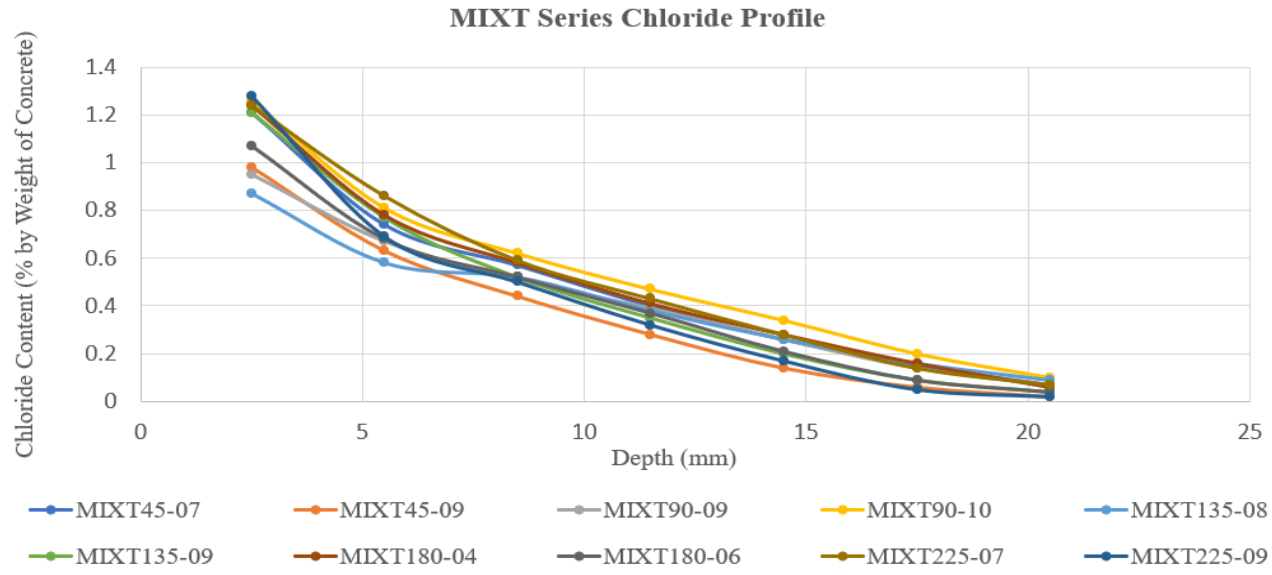

Figure 4.21 - MIXT Series Cores Chloride Profile

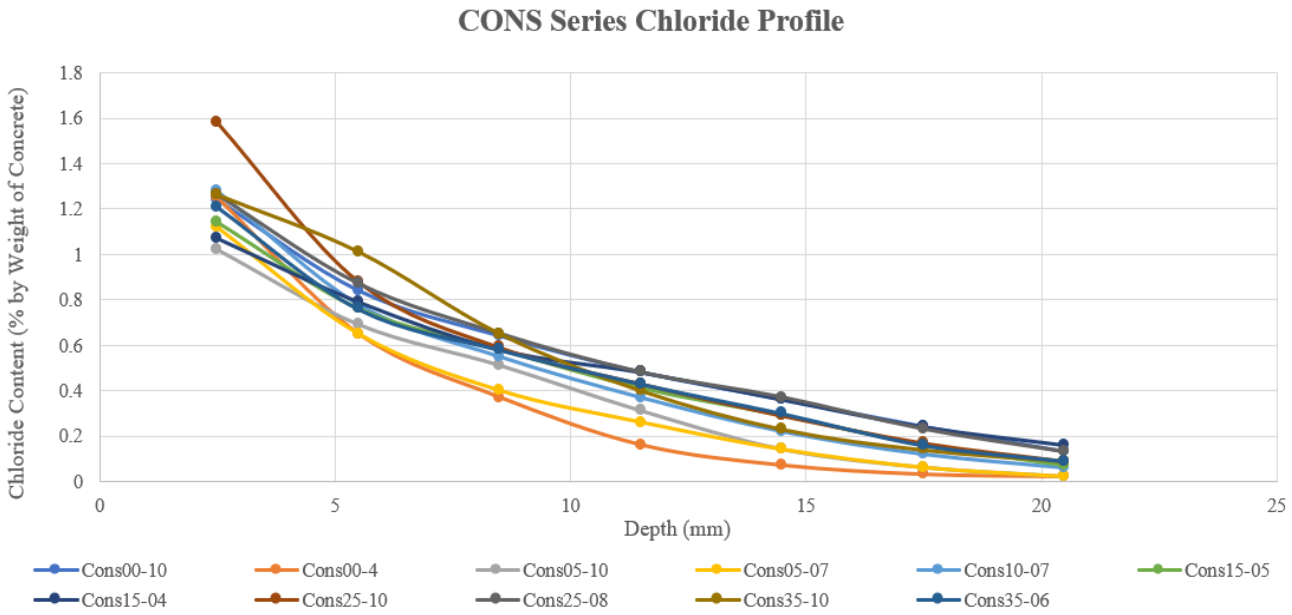

Figure 4.22 - CONS Series Chloride Profile

Chloride Diffusion Coefficient Verus Mixing Time - Tested at 341 Days

Reference	Mixing Time (seconds)	Chloride Diffusion Coefficient (Individual Test) (m2/s)	Average Chloride Diffusion Coefficient (m2/s)
MIXT45-07	45	1.80E-12	1.60E-12
MIXT45-09	45	1.40E-12	
MIXT90-09	90	2.20E-12	2.15E-12
MIXT90-10	90	2.10E-12	
MIXT135-08	135	2.60E-12	2.00E-12
MIXT135-09	135	1.40E-12	
MIXT180-04	180	1.80E-12	1.75E-12
MIXT180-06	180	1.70E-12	
MIXT225-07	225	1.80E-12	1.45E-12
MIXT225-09	225	1.10E-12	

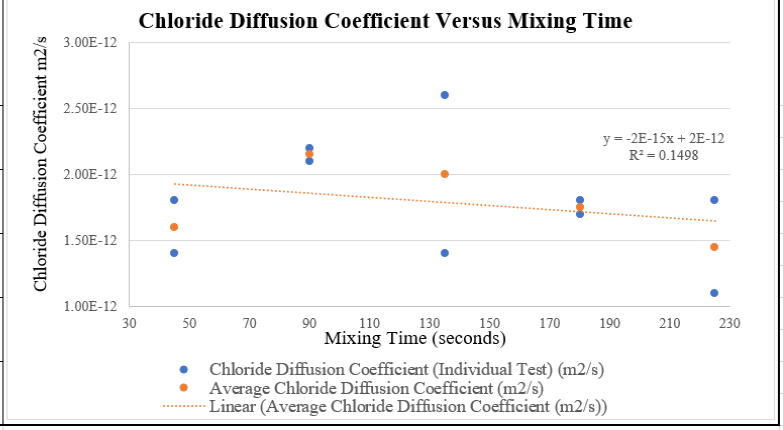

Figure 4.23 - Chloride Diffusion Coefficient - MIXT Series

Chloride Surface Concentration Verus Mixing Time - Tested at 341 Days

Reference	Mixing Time (seconds)	Chloride Surface Concentration (Individual Test) (%)	Average Chloride Surface Concentration (%)
MIXT45-07	45	1.42	1.33
MIXT45-09	45	1.23	
MIXT90-09	90	1.12	1.28
MIXT90-10	90	1.44	
MIXT135-08	135	0.99	1.25
MIXT135-09	135	1.50	
MIXT180-04	180	1.42	1.35
MIXT180-06	180	1.29	
MIXT225-07	225	1.49	1.55
MIXT225-09	225	1.60	

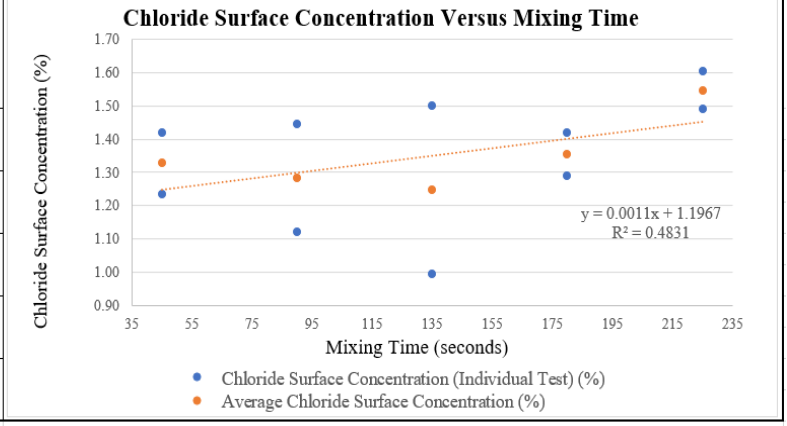

Figure 4.24 - Chloride Surface Concentration - MIXT Series

Chloride Diffusion Coefficient Verus Consolidation - Tested at 341 Days

Reference	Crack Width (mm)	Chloride Diffusion Coefficient (Individual Test) (m2/s)	Average Chloride Diffusion Coefficient (m2/s)
CONS00-04	0	7.20E-13	1.56E-12
CONS00-10	0	2.40E-12	
CONS05-10	5	1.50E-12	1.30E-12
CONS05-07	5	1.10E-12	
CONS10-07	10	1.50E-12	1.50E-12
CONS15-05	15	2.00E-12	2.45E-12
CONS15-04	15	2.90E-12	
CONS25-10	25	1.40E-12	1.90E-12
CONS25-08	25	2.40E-12	
CONS35-10	35	1.70E-12	1.85E-12
CONS35-06	35	2.00E-12	

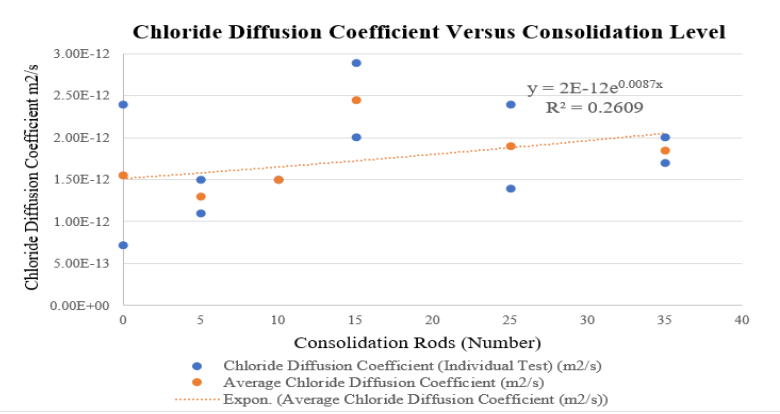

Figure 4.25 - Chloride Diffusion Coefficient - CONS Series

Chloride Surface COncentration Verus Consolidation - Tested at 341 Days

Reference	Crack Width (mm)	Chloride Surface Concentration (Individual Test) (%)	Average Chloride Surface Concentration (%)
CONS00-04	0	1.750	1.520
CONS00-10	0	1.289	
CONS05-10	5	1.289	1.364
CONS05-07	5	1.439	
CONS10-07	10	1.557	1.557
CONS15-05	15	1.340	1.276
CONS15-04	15	1.212	
CONS25-10	25	1.893	1.670
CONS25-08	25	1.447	
CONS35-10	35	1.608	1.505
CONS35-06	35	1.401	

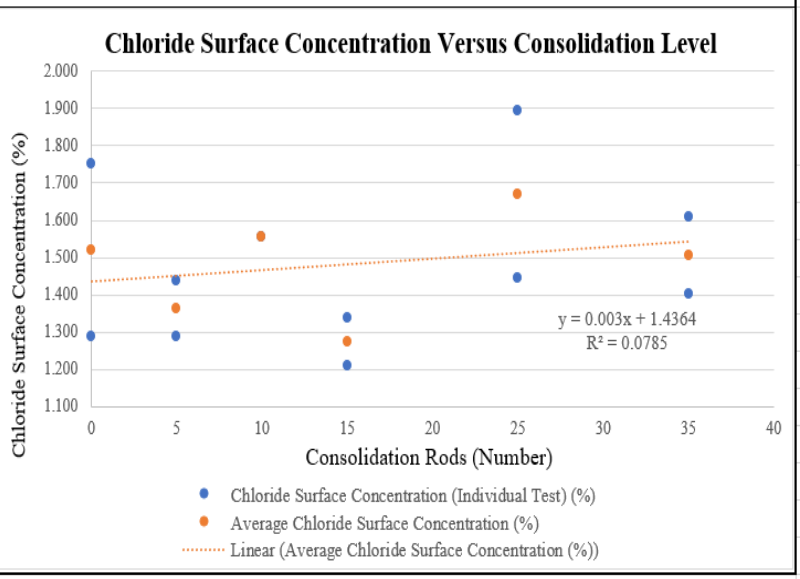

Figure 4.26 - Chloride Surface Concentration - CONS Series

The graphs shown above conclude the independence of the chloride diffusion coefficient from the degree of consolidation and the initial mixing time. Going more into the details of chloride content calculation according to appendix 1.4, the total quantity of chloride is calculated as a percentage of the concrete sample. Since the concrete density increases with the degree of consolidation, the weight of the concrete samples retained in the 3mm grinding increments increases with the degree of consolidation. Therefore, the chloride quantity in an increment volume with a thickness of 3mm increases with the concrete density.

In order to quantify this fact, the chloride mass was calculated in each 3mm increment of the different categories. The following parameters were taken into consideration in the below tables: Concrete density, volume of increment, weight of concrete in increment, entrapped air, mass of chloride in increment, and mass of chloride in each meter cube per increment. This exercise was made for each sample of both categories CONS and MIXT series. The entrapped air content was calculated while taking into consideration that the category of maximum density has no entrapped air. The chloride diffusion calculation was calculated a second time while taking into consideration the weight of chloride by meter cube rather than the percentage by weight of concrete. The following graphs were as well obtained.

Although the chloride diffusion coefficient was still found independent from the consolidation degree or the initial mixing time, the quantity of chloride has obviously increased with the consolidation degree as shown in figure 4.28. The chloride quantity was also found higher with higher density in MIXT series (figure 4.27).

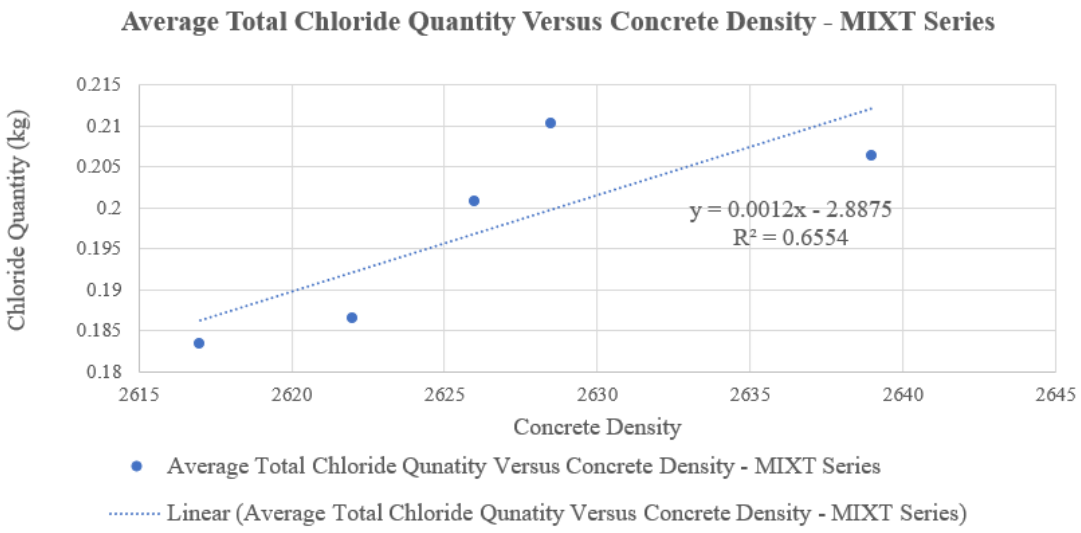

Figure 4.27 - Average Total Chloride Quantity versus Concrete Density in MIXT Series

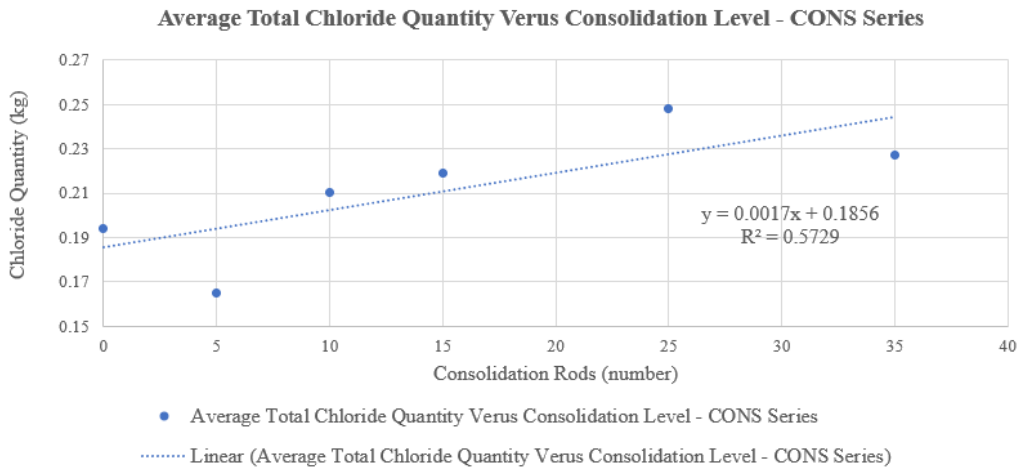

Figure 4.28 - Average Total Chloride Quantity versus Consolidation Level in CONS Series

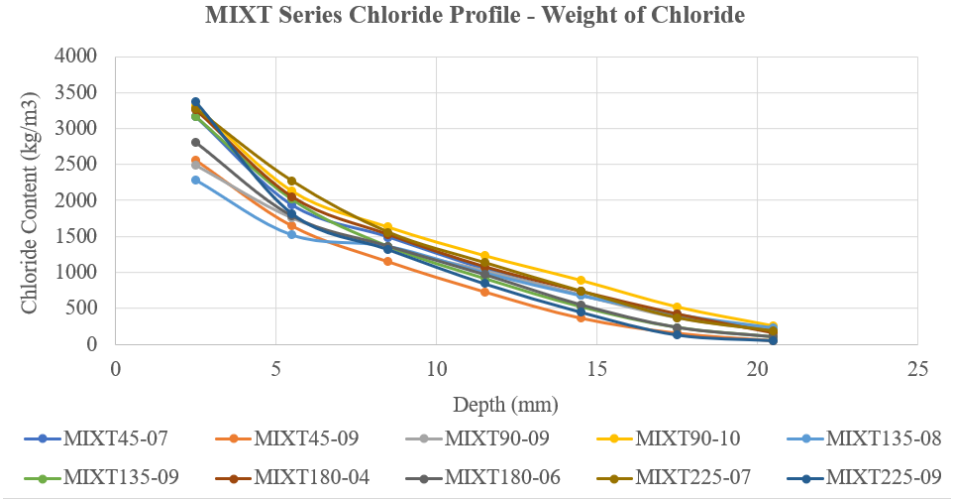

Figure 4.29 - Chloride Profile in MIXT Series Based on the Chloride Quantity

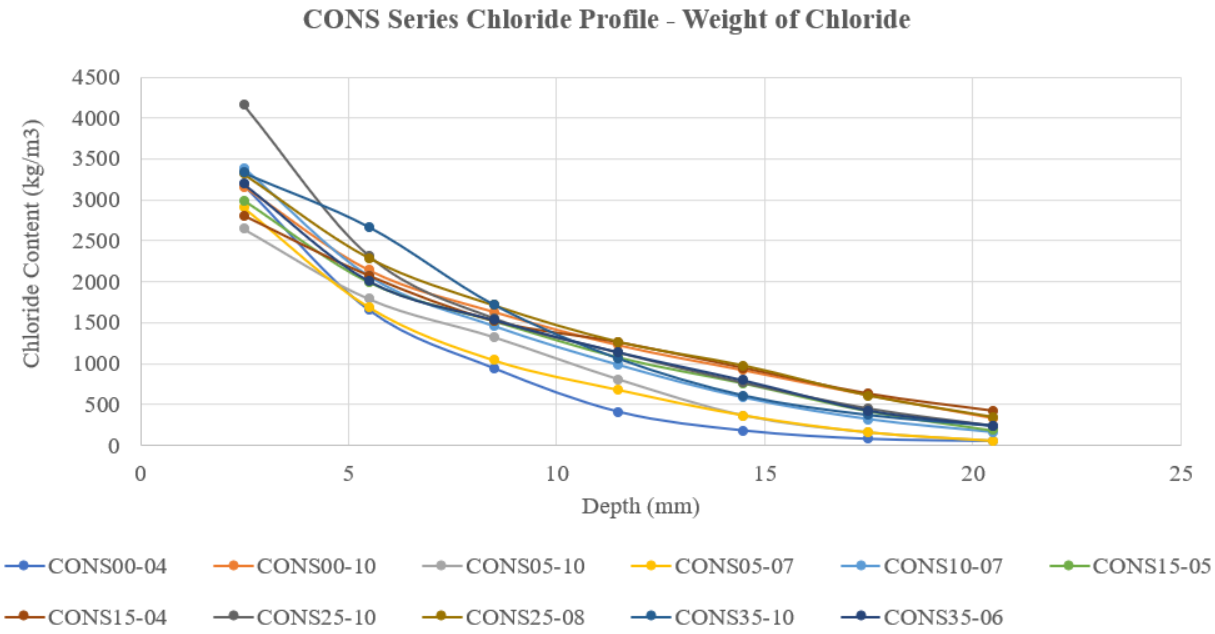

Figure 4.30 - Chloride Profile in CONS Series Based on the Chloride Quantity

Table 4.10 - Acid Soluble Chloride in Concrete Cores - MIXT Series

MIXT Series - Acid Soluble Chloride Content											
Reference	Density (kg/m^3)	Volume of Section ($\times 10^{-5}$m^3)	Percentage of Entrapped Air (%)	Weight of Concrete per increment (g)	Depth (mm)	Acid Soluble Chloride Content (percentage by weight)	Chloride Mass per Increment (g)	Acid Soluble Chloride Content (kg/m^3)	Chloride Diffusion Coefficient ($\times 10^{-12}$m^2/sec)	Total Quantity of Chloride (g)	Total Quantity of Chloride - Average (g)
MIXT45-07	2617	2.36	0.83%	61.66	2.50	1.21	74.61	3166.57	1.76	209.65	183.44
				61.66	5.50	0.74	45.63	1936.58			
				61.66	8.50	0.57	35.15	1491.69			
				61.66	11.50	0.40	24.66	1046.80			
				61.66	14.50	0.26	16.03	680.42			
				61.66	17.50	0.15	9.25	392.55			
				61.66	20.50	0.07	4.32	183.19			
MIXT45-09	2617	2.36	0.83%	61.66	2.50	0.98	60.43	2564.66	1.40	157.24	
				61.66	5.50	0.63	38.85	1648.71			
				61.66	8.50	0.44	27.13	1151.48			

				61.66	11.50	0.28	17.27	732.76			
				61.66	14.50	0.14	8.63	366.38			
				61.66	17.50	0.06	3.70	157.02			
				61.66	20.50	0.02	1.23	52.34			
MIXT90-09	2628.5	2.36	0.40%	61.93	2.50	0.95	58.84	2497.08	2.20	185.18	210.26
				61.93	5.50	0.67	41.49	1761.10			
				61.93	8.50	0.51	31.59	1340.54			
				61.93	11.50	0.39	24.15	1025.12			
				61.93	14.50	0.26	16.10	683.41			
				61.93	17.50	0.14	8.67	367.99			
				61.93	20.50	0.07	4.34	184.00			
MIXT90-10	2628.5	2.36	0.40%	61.93	2.50	1.26	78.04	3311.91	2.10	235.34	
				61.93	5.50	0.81	50.17	2129.09			
				61.93	8.50	0.62	38.40	1629.67			
				61.93	11.50	0.47	29.11	1235.40			
				61.93	14.50	0.34	21.06	893.69			
				61.93	17.50	0.20	12.39	525.70			
				61.93	20.50	0.10	6.19	262.85			
MIXT135-08	2622	2.36	0.64%	61.78	2.50	0.87	53.75	2281.14	2.60	176.67	186.57
				61.78	5.50	0.58	35.83	1520.76			
				61.78	8.50	0.52	32.13	1363.44			
				61.78	11.50	0.38	23.48	996.36			
				61.78	14.50	0.26	16.06	681.72			
				61.78	17.50	0.16	9.88	419.52			
				61.78	20.50	0.09	5.56	235.98			
MIXT135-09	2622	2.36	0.64%	61.78	2.50	1.21	74.75	3172.62	1.40	196.46	
				61.78	5.50	0.77	47.57	2018.94			
				61.78	8.50	0.52	32.13	1363.44			
				61.78	11.50	0.35	21.62	917.70			
				61.78	14.50	0.20	12.36	524.40			

				61.78	17.50	0.09	5.56	235.98			
				61.78	20.50	0.04	2.47	104.88			
MIXT180-04	2626	2.36	0.49%	61.87	2.50	1.24	76.72	3256.24	1.80	217.18	200.78
				61.87	5.50	0.78	48.26	2048.28			
				61.87	8.50	0.58	35.89	1523.08			
				61.87	11.50	0.41	25.37	1076.66			
				61.87	14.50	0.28	17.32	735.28			
				61.87	17.50	0.16	9.90	420.16			
				61.87	20.50	0.06	3.71	157.56			
MIXT180-06	2626	2.36	0.49%	61.87	2.50	1.07	66.20	2809.82	1.70	184.38	
				61.87	5.50	0.68	42.07	1785.68			
				61.87	8.50	0.52	32.17	1365.52			
				61.87	11.50	0.37	22.89	971.62			
				61.87	14.50	0.21	12.99	551.46			
				61.87	17.50	0.09	5.57	236.34			
				61.87	20.50	0.04	2.47	105.04			
MIXT225-07	2639	2.36	0.00%	62.18	2.50	1.24	77.10	3272.36	1.80	224.47	206.44
				62.18	5.50	0.86	53.47	2269.54			
				62.18	8.50	0.59	36.69	1557.01			
				62.18	11.50	0.43	26.74	1134.77			
				62.18	14.50	0.28	17.41	738.92			
				62.18	17.50	0.14	8.71	369.46			
				62.18	20.50	0.07	4.35	184.73			
MIXT225-09	2639	2.36	0.00%	62.18	2.50	1.28	79.59	3377.92	1.10	188.41	
				62.18	5.50	0.69	42.90	1820.91			
				62.18	8.50	0.50	31.09	1319.50			
				62.18	11.50	0.32	19.90	844.48			
				62.18	14.50	0.17	10.57	448.63			
				62.18	17.50	0.05	3.11	131.95			
				62.18	20.50	0.02	1.24	52.78			

Table 11 - Chloride Quantity in Concrete Cores – CONS Series

CONS Series - Acid Soluble Chloride Content											
Reference	Density (kg/m^3)	Volume of Section ($\times 10^{-5}$m^3)	Percentage of Entrapped Air (%)	Weight of Concrete per increment (g)	Depth (mm)	Acid Soluble Chloride Content (percentage by weight)	Chloride Mass per Increment (g)	Acid Soluble Chloride Content (kg/m^3)	Chloride Diffusion Coefficient ($\times 10^{-12}$m^2/sec)	Total Quantity of Chloride (kg)	Total Quantity of Chloride - Average (g)
CONS00-04	2542	2.36	3.82%	59.89	2.50	1.25	74.87	3177.50	0.72	152.73	194.06
				59.89	5.50	0.65	38.93	1652.30			
				59.89	8.50	0.37	22.16	940.54			
				59.89	11.50	0.16	9.58	406.72			
				59.89	14.50	0.07	4.19	177.94			
				59.89	17.50	0.03	1.80	76.26			
				59.89	20.50	0.02	1.20	50.84			
CONS00-10	2542	2.36	3.82%	59.89	2.50	1.24	74.27	3152.08	2.40	235.39	
				59.89	5.50	0.84	50.31	2135.28			
				59.89	8.50	0.64	38.33	1626.88			
				59.89	11.50	0.48	28.75	1220.16			
				59.89	14.50	0.36	21.56	915.12			
				59.89	17.50	0.24	14.38	610.08			
				59.89	20.50	0.13	7.79	330.46			
CONS05-10	2591	2.36	1.97%	61.05	2.50	1.02	62.27	2642.82	1.50	167.88	164.83
				61.05	5.50	0.69	42.12	1787.79			
				61.05	8.50	0.51	31.14	1321.41			
				61.05	11.50	0.31	18.93	803.21			
				61.05	14.50	0.14	8.55	362.74			
				61.05	17.50	0.06	3.66	155.46			
				61.05	20.50	0.02	1.22	51.82			
CONS05-07	2591	2.36	1.97%	61.05	2.50	1.12	68.38	2901.92	1.10	161.78	
				61.05	5.50	0.65	39.68	1684.15			
				61.05	8.50	0.40	24.42	1036.40			

				61.05	11.50	0.26	15.87	673.66			
				61.05	14.50	0.14	8.55	362.74			
				61.05	17.50	0.06	3.66	155.46			
				61.05	20.50	0.02	1.22	51.82			
CONS10-07	2643	2.36	0.00%	62.27	2.50	1.28	79.71	3383.04	1.50	210.49	210.49
				62.27	5.50	0.78	48.57	2061.54			
				62.27	8.50	0.55	34.25	1453.65			
				62.27	11.50	0.37	23.04	977.91			
				62.27	14.50	0.22	13.70	581.46			
				62.27	17.50	0.12	7.47	317.16			
				62.27	20.50	0.06	3.74	158.58			
CONS15-05	2622	2.36	0.79%	61.78	2.50	1.14	70.43	2989.08	2.00	210.67	219.01
				61.78	5.50	0.76	46.95	1992.72			
				61.78	8.50	0.58	35.83	1520.76			
				61.78	11.50	0.41	25.33	1075.02			
				61.78	14.50	0.29	17.92	760.38			
				61.78	17.50	0.16	9.89	419.52			
				61.78	20.50	0.07	4.33	183.54			
CONS15-04	2622	2.36	0.79%	61.78	2.50	1.07	66.10	2805.54	2.90	227.35	
				61.78	5.50	0.79	48.81	2071.38			
				61.78	8.50	0.58	35.83	1520.76			
				61.78	11.50	0.48	29.65	1258.56			
				61.78	14.50	0.36	22.24	943.92			
				61.78	17.50	0.24	14.83	629.28			
				61.78	20.50	0.16	9.89	419.52			
CONS25-10	2629	2.36	0.53%	61.94	2.50	1.58	97.87	4153.82	1.40	249.64	248.40
				61.94	5.50	0.88	54.51	2313.52			
				61.94	8.50	0.59	36.55	1551.11			
				61.94	11.50	0.43	26.64	1130.47			
				61.94	14.50	0.29	17.96	762.41			
				61.94	17.50	0.17	10.53	446.93			
				61.94	20.50	0.09	5.58	236.61			
CONS25-08	2629	2.36	0.53%	61.94	2.50	1.26	78.05	3312.54	2.40	247.16	
				61.94	5.50	0.87	53.89	2287.23			
				61.94	8.50	0.65	40.26	1708.85			
				61.94	11.50	0.48	29.73	1261.92			
				61.94	14.50	0.37	22.92	972.73			
				61.94	17.50	0.23	14.25	604.67			

				61.94	20.50	0.13	8.05	341.77			
CONS35-10	2641.5	2.36	0.06%	62.24	2.50	1.26	78.42	3328.29	1.70	235.26	227.48
				62.24	5.50	1.01	62.86	2667.92			
				62.24	8.50	0.65	40.46	1716.98			
				62.24	11.50	0.40	24.90	1056.60			
				62.24	14.50	0.23	14.32	607.55			
				62.24	17.50	0.14	8.71	369.81			
				62.24	20.50	0.09	5.60	237.74			
CONS35-06	2641.5	2.36	0.06%	62.24	2.50	1.21	75.31	3196.22	2.00	219.70	
				62.24	5.50	0.76	47.30	2007.54			
				62.24	8.50	0.58	36.10	1532.07			
				62.24	11.50	0.43	26.76	1135.85			
				62.24	14.50	0.30	18.67	792.45			
				62.24	17.50	0.16	9.96	422.64			
				62.24	20.50	0.09	5.60	237.74			

5. Chloride diffusion test results analysis

The literature review made in this chapter concluded the qualitative effect of initial mixing time and degree of consolidation on the pores structure and the corresponding durability of concrete. The testing campaign subsequently conducted has reached the following conclusions:

- The concrete initial mixing time and degree of consolidation significantly affected the concrete density and inherent entrapped air content. It is to note that the entrapped air content has by definition a pore diameter exceeding 1mm.
- Properties similar to the water absorption and volume of permeable pores were as well affected by the concrete initial mixing time and degree of consolidation.
- The chloride diffusion coefficient was not affected neither by the initial mixing time nor by the degree of concrete consolidation which suggest that the diffusion happens in pores having a diameter below the relevant diameter of the entrapped air.
- The chloride content was on the other hand affected by the degree of consolidation. The conclusion that the diffusion is taking place in the pores that are below 1mm has made the chloride content proportional to paste fraction excluding the entrapped air. As the amount of entrapped air varied, the chloride content tested in the solid paste remained consistent to the solid sample tested, but varied as a total quantity in a specific volume.
- The permeability on the other hand was drastically affected by the degree of concrete consolidation which suggests that the chloride permeability takes place in the different range of pore sizes.

Figure 4.31 is an updated version of figure 4.1 and indicates in which range of pores size the permeability and the diffusion take place, respectively. The above findings that were concluded from the literature review and the testing campaign will be evaluated in this section.

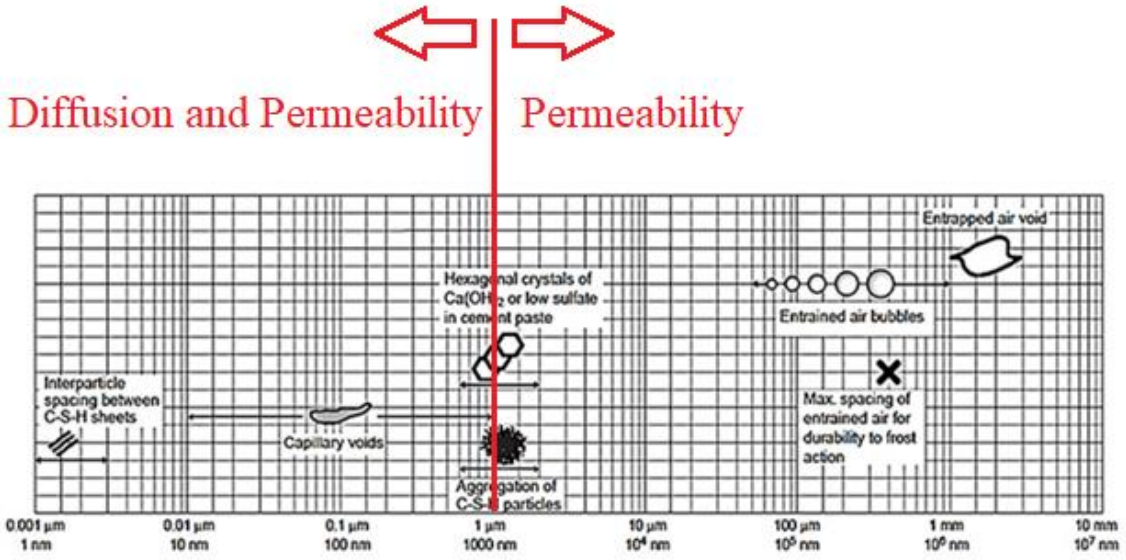

Figure 4.31 - Suggested Pore Size Range for Permeability and Diffusion (Updated form of Figure 4.1)

The diffusion in porous materials restricted by a certain pore size diameter can be explained by the notion of diffused substance's particles mean free path. The concrete is considered physically as an unconsolidated porous media; i.e. formed by a solid phase constituted by isolated particles that rest one on another [126]. This type of porous material is characterized by the porosity, the specific surface, and the pore sizes. The diffusion in porous materials can be carried out by three ways [127]: Ordinary Diffusion, Knudsen Diffusion and Surface Diffusion, as follows:

- Ordinary Diffusion: The ordinary diffusion takes place when the size of the pores is very large when compared to the diffused substance's particle mean free path [126]. Based on this, the effective diffusivity depends from the porous materials porosity and tortuosity, which is defined as the ratio of the length of the path followed by the particles and the minimum length between two points of the medium [128].
- Knudsen Diffusion: The Knudsen diffusion occurs when the mean free path of the diffused particles is greater than the average pore size. In this type of diffusion, the transfer rate of particles is highly influenced by the collisions with the walls of the pores [126].
- Surface Diffusion: The surface diffusion takes place when the particles that are absorbed by a porous material, are transported across the surface of the porous media as a result of surface gradient concentration [126].

The diffusion mechanism is thus a combination of three diffusion mechanisms that also concludes that the diffusion will not occur in pores that are larger than the diffused substance's particle mean free path.

Applying this concept to chloride diffusion, the particle mean free path is given by the below formula yielded from the Kinetic Theory Concept:

$$\lambda = \frac{RT}{\sqrt{2}\pi d^2 N_A P} \quad (4.1)$$

where λ is the chloride solution mean free path and R is the gas constant (equal to 8.3145 $m^3.Pa.mol^{-1}.K^{-1}$) , T is the temperature in Kelvin, d is the particle diameter, N_A is Avogadro's number (equal to $6.0221.10^{23}$ mol^{-1}), and P is the pressure in Pa.

The chloride ion diameter is theoretically equal to 102 pm (Periodic Table) which is equal to 1.10^{-10} meters. This diameter yields a mean free path, using equation 4.1, of 0.917 µm which is approximately 1000 nm. Going back to figure 4.1, the diffusion will not take place outside the capillary pores (pores sizes below 1000 nm), this furthermore confirms the suggested range taken in figure 4.31.

Based on the above conclusion, the functions $f_7(Cs)$ and $f_8(Mi)$ that considers the effect of the consolidation level and the initial mixing time on the chloride diffusion coefficient are equal to:

$$f_7(Cs) = 1$$

$$f_8(Mi) = 1$$

On the other hand, the increase in density and consequently paste content with higher degree of consolidation has increased considerably the chloride content in the relevant concrete cores, while keeping the chloride diffusion coefficient constant. It is also to highlight the fact of additional chloride content with a fixed chloride diffusion coefficient is an item that should be considered while evaluating the chloride threshold causing the reinforcement corrosion. In the present time, the chloride threshold investigated to trigger the reinforcement corrosion is usually calculated as a percentage of concrete mass or cement mass, based on the chloride diffusion in concrete. For the same concrete composition, leading to the same chloride diffusion coefficient, variation in entrapped air may vary the chloride content in the concrete samples and may consequently affect the time as to when the corrosion will be triggered.

The chloride diffusion is not the sole mechanism that ingress chloride in concrete, permeation and absorption play an important role as described in chapter 1. The chloride permeation in concrete seemed to be taken place in the different pores size as concluded from the testing campaign conducted in section 4. While the two parameters, initial mixing time and degree of consolidation, did not affect the chloride diffusion, they influenced the water (and thus chloride) permeation in concrete. The chloride permeation in concrete based in the range of pores sizes, including the entrapped air, needs further investigation.

The adverse effect of lack of consolidation or initial mixing time on the concrete durability discussed in the different prescriptive specifications and literature review do not therefore originate

from additional chloride diffusion. It rather affects other chloride transportation mechanisms like permeation and absorption.

6. Conclusions

This chapter aims at identifying the effect of the concrete initial mixing time and consolidation level on the chloride diffusion coefficient. Additional performance-based durability testing, namely the water permeability, water absorption, and volume of permeable pores, were done to check the additional effect of these two parameters on the chloride transportation.

The initial mixing time and level of concrete consolidation affected the concrete density and entrapped air percentage. However, the chloride diffusion was found independent from the entrapped air percentage and consequently no effect of the two investigated parameters was found on the chloride diffusion coefficient.

The chloride diffusion was demonstrated to take place in the pores less than 1000nm in diameter. This range of diameters is below the size of entrapped air. This demonstration has confirmed the finding of the testing campaign. The two functions that consider the effect of the investigated parameters on the chloride diffusion were consequently equal to 1.

The adverse effect of lack of consolidation or initial mixing time on the concrete durability discussed in the literature was found to originate from transportation mechanisms other than the diffusion, namely the permeation and the absorption.

Chapter 5: Effect of crack width

1. Introduction

The main objective of this chapter is to assess the effect of crack width on the apparent chloride diffusion coefficient. It starts by presenting the available literature review that studied the effect of cracks on concrete durability in chloride environment, followed by the testing protocol. Details of the core specimen preparations and chloride diffusion test plan are discussed as well. Further to the test procedures, the results are presented and analyzed, and related calculations are performed. This chapter finally reaches comprehensive conclusions regarding the effect of the crack widths on the apparent concrete mix chloride diffusion coefficient.

2. The general effects of cracks on concrete durability in chloride environment

Cracking in concrete is a normal occurrence and happens at the plastic phase as well as at the hardened phase of concrete. Two types of cracks mainly occur at the plastic stage: plastic settlement cracks and plastic shrinkage cracks. The former occurs in high water-cement ratio concrete combined with low concrete cover, whereas the later occurs when the environment rate of evaporation exceeds the concrete rate of bleeding. In the hardened stage, cracks occur when the tensile strain magnitude in concrete exceed the ultimate tensile strain. This additional strain is converted into cracks. The tensile strain is a combination of several root causes as follows:

- Structural Tensile strains
- Autogenous Shrinkage
- Drying Shrinkage
- Differential temperature in the concrete element
- Restraint temperature changes
- Restraint volume changes

The six causes above are combined together into a final resulting tensile strain distribution that is converted to cracks, provided it exceeds the allowable concrete tensile strain. The presence of cracks is in some cases significantly detrimental to the concrete serviceability. From durability point view, the presence of cracks decreases the concrete durability. In higher width, the cracks may affect the concrete serviceability. The cracks may be as well aesthetically objectionable even when they will not affect the structural durability, serviceability or integrity.

Cracks in concrete structure may partially or completely seal in the presence is water. This phenomenon is referred to as the “Autogenous healing of cracks”. Autogenous healing is a natural process of crack self-repair that can occur in concrete in the presence of moisture [129]. BS8007

implies that cracks up to 0.2mm wide will autogenously seal within 28 days, whereas cracks up to 0.1mm seal within 14 days [130].

The following two reasons for autogenous healing of cracks were reported by Fagerlund et al. [131]:

- Continued hydration of the cement. The hydration products enter the crack and might eventually fill this completely. This effect ought to be most active when cracks appear early after production when there is still a large amount of un-reacted cement.
- Precipitation of CaCO3 (calcite) by reaction of calcium ions in the pore solution with carbonate ions dissolved in the crack water.

The later reason was reported to be the governing mechanism [131]. On the other hand, Maes et al [132] grouped the autogenous healing process depending on whether the concrete is completely immersed or subjected to a cyclic wetting and drying. When the concrete is subjected to cyclic wetting and drying, the autogenous healing occurs as a result of the continuing hydration and the calcium carbonate hydration. When the concrete is completely immersed, the autogenous healing occurs at much slower rate and mainly due to the ongoing hydration. The autogenous healing of the cracks has also improved the chloride resistance. While it is obvious that the hydration depends on the cement composition, the additional ongoing hydration of a specific type of cement will depend on the initial unhydrated cement quantity and thus the initial water-cement ratio. Other researches have also suggested the main reasons for autogenous healing [133,134,135,136] as follows:

- Swelling and Hydration of the cement
- Precipitation of the calcium carbonate
- Blocking the water path by water impurities
- Blocking the water path by cracked concrete particles

In the absence of impurities (third and fourth main reason defined above), the continuous hydration and the precipitation of the calcium carbonate remains the two main causes. Edvardsen [137] investigated the autogenous healing in a large-scale study reaching a model for the reduction in water flow due to autogenous healing. This research concluded that the autogenous healing is mainly dependent on the precipitation of calcium carbonate crystals. This precipitation is in its turn dependent on the crack width and water pressure, whereas the concrete composition (type of cement and aggregate) and type of water has no influence. In a state-of-the-art review of the autogenous healing done by Sidiq et al. [138], the phenomenon of the autogenous healing was mainly attributed to the hydration of the unhydrated cementitious materials particles at the crack's wall. In another context, Tittelboom et al. [139] investigated the effect of the concrete composition on the autogenous healing of cracks. This research concluded that the increase of water-cement ratio decreases the autogenous crack healing efficiency due to further hydration. This study also concluded that the calcium carbonate precipitation and the further hydration are the main

mechanisms behind the autogenous healing. The presence of supplementary cementitious materials (Fly Ash and Slag) has also enhanced the autogenous healing with the slag having the higher effect.

Several prescriptive durability specifications have discussed the effect of the cracking and crack width on the concrete durability. The American concrete Institute guide to durable concrete [58] emphasized the adverse effect of the cracks on the concrete durability whereby the different transport mechanisms were deemed to be affected by the presence of cracks. This reference also states that the corrosion of reinforcement is generally more sever and begins earlier at cracks. Other guide from the American Concrete Institute, similar to ACI 222 [57] and ACI 362.1 [59], have also discussed the effect of cracks in reducing the concrete durability and chloride resistance. Other prescriptive durability specifications and guidelines [140] tend to limit the cracks width in order to prevent their adverse effect on the concrete durability, the Eurocodes for example limit the crack width to 0.2-0.3mm depending on the corresponding exposures. This furthermore emphasizes the effect of cracks on the concrete durability.

In addition to the prescriptive specifications, the effect of the cracking on the chloride transportation was studied by several researches in order to identify and eventually quantify it. Several field surveys were as well conducted to identify the effect of the crack width on the chloride diffusion. The researches done in this regard were mainly divided into five main categories:

- Qualitative effect of the cracks on the chloride penetration and diffusion.
- Using accelerated chloride penetration tests, steady-state and non-steady state chloride migration tests to generate models simulating the effect of the cracks on the chloride penetration.
- Using long duration ponding test to assess the effect of the crack on chloride transportation in concrete.
- Testing the chloride diffusion coefficient from existing structures at cracked location and uncracked locations
- Using numerical models to simulate this mechanism.

Few other researches have established correlation models between the transport properties of cracked concrete and the loading level, the tensile stress of concrete, or the inelastic concrete strain. [141][142][143][144].

Lindquist et al. [145] investigated the effect of cracks on the chloride penetration in bridge decks. The investigation concluded that chloride threshold at the reinforcement level in bridge decks was exceeded in less than 2 years compared to more than 12 years in uncracked concrete. P.P. Win et al. [146] presented the experimental data of the chloride penetration in cracked samples. The samples were cracked using three points load testing before being subjected to chloride solution. The research concluded that the chloride penetration increased in the presence of cracks and high water-cement ratio.

S. Jacobsen et al. [147] studied the effect of crack density on the chloride migration. The samples used in this research were subjected to cycles of freeze and thaw in order to create a cracking density that was identified by red dye technique. Accelerated chloride migration test was used to compare the effect of cracking on the chloride transportation. Some of the cracked samples were immersed in lime saturated solution in order to take into consideration the cracks self-healing mechanism. The research concluded that the internal cracking has increased the chloride penetration rate by 2.5 to 7.9 times. On the other hand, this research has concluded that the cracks self-healing has reduced the chloride penetration rate by 28 to 35% when compared to newly cracks concrete. This study was furthermore complemented by a subsequent research done by B. Gerard et al. [148] creating models for the influence of continuous (transverse) cracking on the steady state regime, these models were compared to the results obtained from the accelerated migration test in the first research. The models were however limited to the steady state regime considering the flow of the chloride in cracked concrete is equal to the sum of the flow of chloride in concrete and the flow of chloride in cracks. The model simulated cracked concrete to a crack network superimposed to a homogenous reference material. This work concluded the graph illustrated in figure 5.1. The parameters taken into consideration are the diffusion coefficient of a given ionic species in free concentration noted D_1, the diffusion coefficient of the species in the uncracked concrete noted as D_0, the apparent diffusion coefficient of cracked concrete noted as D, and the crack spacing factor which is the ratio of the crack spacing over the crack width, noted as f. The ratio of the apparent diffusion coefficient D over the uncracked concrete diffusion coefficient was noted as 1/n in figure 5.1. This model analytically concluded that the chloride diffusion coefficient of cracked concrete ranges from 2 to 10 times that of uncracked concrete. The model also concludes the role of the diffusion coefficient of the ionic species in free solution: The influence of cracking increases when the ratio of the diffusion coefficient of the ionic species in free solution over the chloride diffusion coefficient in concrete increases. The model was conducted from anisotropic crack network (one direction) and isotropic crack network (two directions).

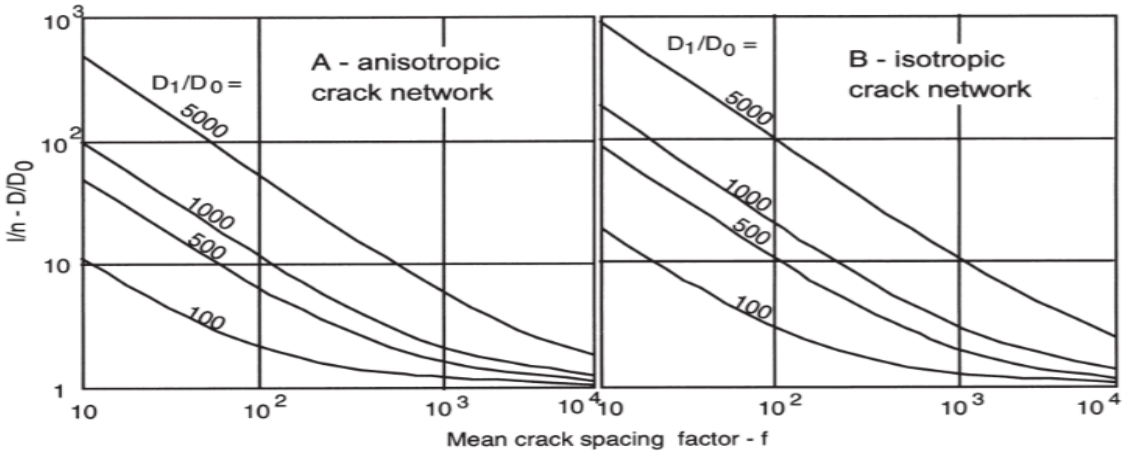

Fig. 2. Variation of the equivalent diffusivity of the material (1/*n*) as a function of D_1/D_0 and *f* (anisotropic and isotropic crack networks).

Figure 5.1 - Influence of Transverse Cracks on the Chloride Diffusion Coefficient in Steady-State Flow [148]

Using the steady state accelerated chloride testing to simulate the effect of the cracks was also used in many other researches. Kato et al. [149] used this approach to generate a model for the effect of cracks on chloride diffusion coefficient whereby two different water cement ratios were used. The model thus created matched well the results of the cracked concrete where accelerated steady-state testing was used along with a steel slit that simulates the cracking. S. Y. Jang et al. [150] also used the steady-state migration test on cracked samples made by controlled splitting tensile test. The research concluded that the chloride diffusion coefficient will increase as a function of the crack width above a certain threshold value equal to 80µm. A linear relationship was established between the equivalent chloride diffusion coefficient and the crack width. Using the steady state accelerated testing, Djerbi et al. [151] identified the effect of the crack width on chloride diffusion. The cracks were initiated by splitting tensile test and three types of concrete were used with different water-cement ratios and silica fume addition. The crack widths varied from 30 to 250 µm. The research concluded that the chloride diffusion increased with the crack width but was constant after a crack width of 80µm where the value obtained was the diffusion coefficient of chloride in free solution. Ismail et al. [152] also investigated the effect of cracks on chloride diffusion using cracked mortar fitted into a chloride penetration cell. The cracks simulation in this research were made using expansive core at the center of ring shape mortar sample. The crack width varies between 6 and 325µm. Based on this work, a crack width lower than 30µm does not affect the chloride diffusion. The chloride diffusion otherwise increased with the crack width.

Park et al. [153] used the non-steady state accelerated chloride testing as per ASTM C1202 [53] to identify the effect of the crack width on the chloride diffusion coefficient which was calculated based on Tang's method [154]. The cracks were simulated by the splitting tensile test described earlier. The crack width considered varied between 0.1 and 0.4mm. The chloride diffusion was measured at the duration of one hour. The research concluded a numerical equation of the chloride diffusion coefficient as a function of the crack width. Based on this equation, the chloride diffusion coefficient for a crack width of 0.4mm increases at a ratio of 135 times at 3 days, 149 times at 7 days, and 156 times at 28 days. Wang et al. [155] have also used this category of accelerated testing (non-steady state as per NT Build 492 [156]) to identify the effect of the cracks on the chloride diffusion coefficient. The cracks in this research were defined as cracking density instead of continuous traverse cracks with known width. The crack density was established as a function of the crack length and the number of cracks in a specific sample. The research yielded a high linear correlation between the ratio of the cracked to sound concrete and the cracking density. Marsavina et al. [157] used as well the NT Build 492 [156] accelerated non-steady state testing to identify the effect of the cracking on the chloride diffusion and compared it to a numerical simulation. Artifical cracks through notches were made in this research to simulate the concrete cracking. While the results predictively concluded that the chloride ingress increases with increase crack depth and width, no clear conclusion for a relationship between the crack width and diffusion was made. Nevertheless, the test results correlated fairly well with the presented numerical simulation.

Apart from the accelerated chloride testing to identify the effect of the crack width, Kanjee [158] used ponding test (ASTM C1556 [159]) on three type of cracks levels, uncracked concrete, concrete cracks ranging from 0.1mm to 0.4mm and concrete cracks ranging from 0.5mm to 0.8mm. The research concluded that the increase in chloride diffusion for the first crack range varied between 131 to 172 times when compared to uncracked concrete. In the higher concrete crack range, the chloride diffusion coefficient was 227 to 958 times higher than that of uncracked concrete. The ponding test in cycle of wetting and drying was used by Shao-feng et al. [160] where five beams of C30 concrete with 429 kg/m^3 of cement were considered. The cracks were simulated by inserting bolts in the beams and applying a tensile strength until tensile cracks develop in concrete. The chloride profile was tested using rapid chloride determination test. A relationship between the chloride diffusion coefficient and the crack width was then generated. Considering a crack width of 0.8mm and following this equation, the cracked concrete diffusion coefficient is almost 25 times higher than that of sound concrete.

Kwon et al. [161] collected concrete cores from actual marine structures, two wharfs that were operational for 8 and 11 years respectively, at cracked locations. Three widths of cracks were selected, 0.1mm, 0.2mm, and 0.3mm. Cores at uncracked locations were also extracted. The cores were tested for the chloride diffusion coefficient by testing the chloride content at successive increments in reference to AASHTO T260 [162]. From regression analysis, a relationship between the chloride diffusion coefficient and crack width was generated. Based on this equation, the chloride diffusion coefficient for the 0.3mm cracked concrete was approximately 5 times higher than companion sound concrete.

Bentz et al. [163] presented two modeling approaches in solving the diffusion of chloride in cracked concrete using modeling software. The first modeling approach include the use of the software ANSYS primarily used in the heat transfer and mechanical stress problems. In this model, an analogy is established between the mass transfer and heat transfer. The chloride concentration is mapped to temperature, the diffusion coefficient is mapped to thermal conductivity, the heat capacity and the density parameters are set to 1. The solid volume is modified by introducing a rectangular crack with a known width and depth. The diffusion coefficient of this crack is taken equal to the diffusion coefficient of the chloride in water (1.8×10^{-9}m^2/s) [164]. The second approach includes using another modeling software, COMSOL. The approach is very similar to the one used in ANSYS except that COMSOL can allow for additional parameters to take into consideration the chloride binding through the implementation of a sorption isotherm. A similar modeling approach was also conducted by Du et al. [165] who created a meso-scale numerical model for chloride diffusivity. Conveniently, this model added the presence of aggregate and Interfacial Transition Zone, as part of the model, in addition to the presence of cracks. The numerical results suggested the presence of a good relationship between the meso-scale simulation method and available experimental observations. Ishida et al. [166] used a similar approach using a DuCOM model which is developed by Concrete Laboratory at the university of Tokyo in Japan [167,168,169]. The model is updated to yield the chloride diffusivity coupled with non-linear

binding capacity in sound and cracked concrete. The chloride binding in this model is defined as Langmur type equation based on the experiments conducted by the same author [170]. The corresponding decrease in chloride diffusion caused by the binded chloride is taken into account by two assumed mathematical parameters that takes into consideration the dimensional changes and connectivity of pores, and as second parameter for electrical interaction. The cracks are modeled as areas of different diffusion coefficient. Šavija et al. [171] proposed a Lattice model to simulate chloride ingress in sound and cracked concrete. This model was validated from the available literature on chloride ingress through cracked concrete that relies on accelerated chloride testing.

Based on the literature review conducted in this section, it is clear that the occurrence of cracks decreases the concrete durability and increases the chloride penetration in concrete. The adverse effect of the cracking increases with the crack width and depth. Another important parameter influencing the concrete durability in the presence of cracks, concerns the autogenous healing. This phenomenon does not occur instantaneously and needs more than 28 days to reach a significant completion percentage. The autogenous healing depends also on the concrete water-cement ratio, for the same type of binder.

The different researches made in this topic have used several approaches including several types of chloride migration test, several ways to induce cracking of concrete samples, different ways of chloride content testing, specific concrete composition, and different testing duration. The results thus varied significantly. The effect of a cracked concrete where the crack width increases from 0.1mm to 0.8mm may have an adverse effect ranging from 0 (in accelerated steady state testing) to 958 time; the later value was reported by Kanjee [158]. The testing regimes of short durations and numerical models do not successfully simulate autogenous healing and its corresponding effects. Different types of crack initiation may as well yield different results especially when the cracking mechanism does not produce a crack with a known consistent width. Some researchers concluded that the use of cracked samples with varying crack width is complicated to evaluate [149]. The use of accelerated testing programs may not eventually simulate the actual real case. Otieno et al. [172] conducted a research program to identify the effect of crack width on the corrosion rate of cracked samples that were divided into two groups: the first was subjected to accelerated testing in the laboratory and the second group was placed in a natural marine environment. While this research identified that the corrosion rate increased with and increased crack width, it also concluded that the corrosion performance of concrete in the field under natural corrosion cannot be inferred from its performance in the laboratory under accelerated corrosion. In addition to the shortcoming discussed in this paragraph, having the crack geometry as the sole changing parameter in the testing program does not identify the coupled effect of the crack with other concrete parameters.

As a result of the above, and in order to reach a better quantification of the crack effect on chloride migration, some benchmarks for the further testing program should set. These benchmarks aim at

overcoming the shortfalls discussed in the previous paragraph. The main items that should be taken into consideration are as follows:

- Crack Geometry and properties: The cracks initiated for further testing should have a fixed width throughout the length of the specimen. While this geometry is not necessarily the real case in concrete, its use is essential to quantify the effect based on known crack width. The modeling in concrete structures may be furthermore done by taking several layers with different crack widths and different properties. The initiated cracks tortuosity and surface condition should also simulate the actual properties of the cracks in reinforced concrete elements.

- Type of laboratory testing used for chloride migration: Whereas gathering actual field data from several cracked structures subjected to chloride environment may seem the most accurate, the number of unknow parameters involved in the operation overcome the benefits of field data. These unknowns may include variation in concrete mixes, absence of precise data, different exposure, and coupling of other degradation mechanisms. Laboratory tests should thus simulate as close as possible the real chloride migration while omitting these shortfalls. Based on appendix 1.2, ponding test in reference to ASTM C1556 seems to be the closest to the actual chloride migration.

- Autogenous healing of cracks: The autogenous healing of cracks can be taken into account by immersing the samples for a considerable long duration in the chloride solution. During this period, the autogenous healing will take place and the subsequent effect on the chloride diffusion can be evaluated.

- Concrete composition: Varying the crack geometry alone will omit the coupling effect of other concrete properties. The concrete properties that need to be taken into consideration are derived from the literature review conducted in this section. Since the chloride and water-cement ratio were also found to affect the chloride transportation in concrete, the coupled effect of these two parameters should be studied along with the crack geometry. Since the effect of the tricalcium aluminate content and chloride binding on chloride transportation was conducted in chapter 3, a reference concrete with varying water-cement ratio and varying crack widths should be considered.

- Sample size: In testing the chloride content of successive increments further to the immersion period and since the chloride is simulated to ingress perpendicularly to the concrete surface between two points of different concentrations, the size to the concrete core extracted from the sample is of vital importance. On the contrast of a uniform concrete and in the presence of cracks, chloride may diffuse in both directions. Therefore, the higher the core diameter, the lower the gradient difference. As a result, the concrete core diameter should have a fixed diameter synchronized with the further modeling approach that will be used. For example, if a further discretization is made for the concrete member to identify

the chloride diffusion, the discretization mesh should be consistent with the size of the core based on which the equations for chloride diffusion coefficient were established.

Therefore, the testing campaign needed to quantify the effect of the crack width in question should consider different water-cement ratios, and crack widths, and shall be tested using long term chloride ponding. The testing campaign used to quantify the coupled effect of the two parameters mentioned above is detailed in the next section.

3. Summary of the testing protocol

The same reference concrete mix design considered in the previous chapters was replicated and cracks from different cracks width (0.12mm, 0.24mm, 0.36mm, 0.48mm, and 0.60mm) were intentionally produced in the samples. The same concrete mix was furthermore replicated with different water-cement ratio while fine-tuning the mix to get the final volume of $1m^3$. As the quantity of water increases or decreases, the final quantity of sand should be adjusted. The combinations of these cases yielded 25 combinations, i.e. five water-cement ratio groups, and five different crack widths for each water cement ratio.

The main challenge of this operation was to accurately crack the concrete samples into the intended crack width. The cracks in the cores should satisfy the following criteria:

- The cracks should be initiated at the center of the core.
- The cracks should be perpendicular to the surface of the concrete sample
- The cracks in the core should satisfy the surface and the tortuosity conditions of the cracks in real cases.
- The crack width should be accurate enough to be considered as reliable for the quantification of the crack width effect on the chloride diffusion.

In the following, three methods were considered is this application. The first two methods did not yield the crack width precision, and the third method explained hereafter was finally considered.

Method 1: The first method used consisted of subjecting the concrete cores to a controlled splitting tensile in reference to ASTM C496 [173] test using the concrete compressive machine defined in ASTM C39 [174]. The concrete cores were instrumented with a Linear Variable Differential Transformer (LVDT) in order to measure the tensile strain at the center of the cores and the corresponding resulting cracks width. Even with the slowest controlled rate of vertical stress application, the minimum crack width obtained by this method was 0.3mm. This range of cracks width was higher than the range intended for this study and the method was thus aborted.

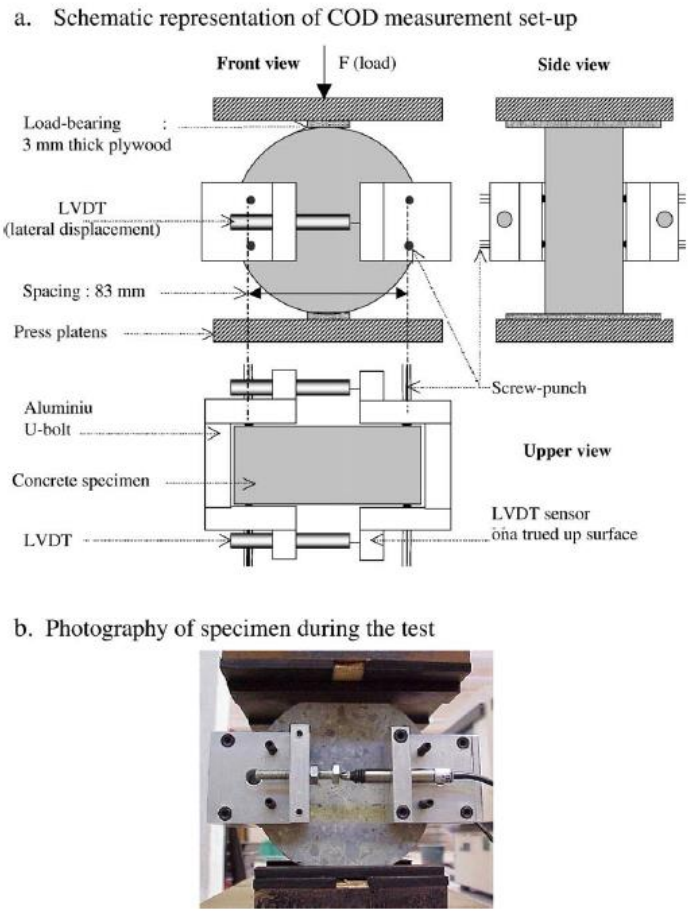

Fig. 1. Controlled splitting test.

Figure 5.2 - Method 1 of Cracks Formation - Controlled Rate of Splitting Tensile [151]

Method 2: The second method included the embedment of a thin plastic film, having a thickness equal to the thickness of the intended crack width in the fresh concrete further to the placing operation of the concrete sample. The technicians will then have to wait until the concrete starts to set, so the plastic sheets will be removed, leaving the required space in the concrete. Plastic sheets with thicknesses of 0.12mm, 0.24mm, 0.36mm, 0.48mm, and 0.60mm were procured for this reason. Pictures of this operation are included in figure 5.3 below. After the demolding of the concrete samples, the final crack width was measured using a crack width microscope. The final crack width was found very high when compared to the initial plastic sheets insert width. The final crack width was thus not meeting the intended crack width. The measurement of the final crack width and the corresponding difference with the initial insert's width are detailed in appendix 5.2. Moreover, the inner surface of the crack was smooth as a result of the plastic insert. This surface condition was different form the actual cracks surface and touristy. The cracks resulting from this method would not thus simulate an actual crack width formation. This second method was thus aborted.

Figure 5.3 - Method 2 of Cracks Formation - Plastic Sheet Inserts

Method 3: The third method included extracting a concrete core from the concrete cylindrical specimen and splitting the concrete into two portions using the splitting tensile test detailed in ASTM C496 [173] using a very low rate of stress application (0.1 MPa/s). The two portions of the concrete core were then jointed evenly using steel ring fasteners while keeping flexible shims on the side to control the space width. The steel fasteners were then tighten until the space between the two portions of the core was equal to the intended crack width consistently along the length of the core. All sides of the concrete core were then sealed, except the finished top surface, and covered a suitable barrier coating, and allowed to dry. The crack width at the top of the core was then measured using a cracks width microscope (OMAX 20X-40X-100X Measuring Microscope). The crack widths were verified to meet the intended crack width. This method yielded an accurate crack width along the length of the concrete core. The surface condition of the cracks was also matching the real crack surface condition and tortuosity. This method was thus adopted. Pictures of this operation are presented in figures 5.4 to 5.6.

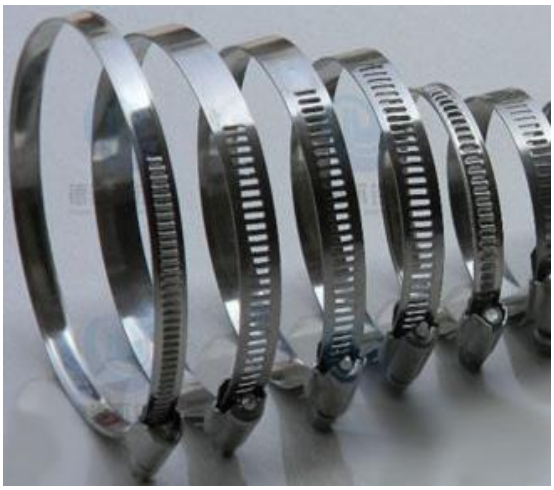

Figure 5.4 - Steel Rings Fasteners

Figure 5.5 - Concrete Core Jointed by Steel Rings

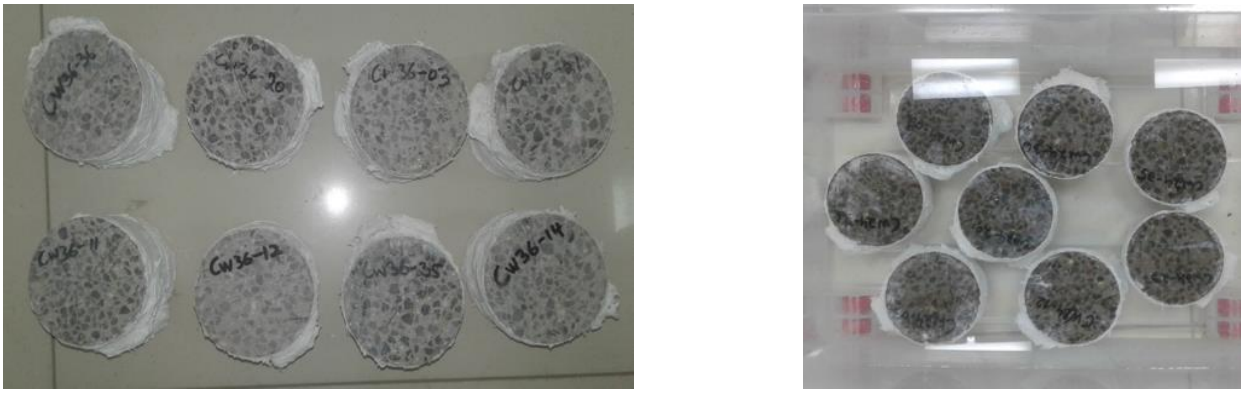

Figure 5.6 - Final Samples

A total of 29 concrete batches were made to reach the required total number of samples. The details of the batch trials conducted are included in appendix 5.1. The concrete cylindrical specimens fabricated during these batches were then cured for 28 days. After 28 days water-curing, cores were drilled from the inner part of the concrete cylinders. The diameter and length of the core are 94 mm and 100 mm respectively. The cores were then cracked using the third method described above. All sides of the cores were then sealed, except the finished surface, with a suitable barrier coating. The sealed specimens were then saturated in a calcium hydroxide solution, rinsed with tap water, and then placed in a sodium chloride solution. The cores identification references are presented in appendix 5.3. After the immersion duration mentioned in section 4 of this chapter, the cores were tested for apparent chloride diffusion coefficient as detailed in chapter 1. The use of the profile grinder was not feasible due to the excessive number of cores. The alternative method of using the saw cut as per ASTM C1556 [159] was therefore used. Each concrete core was divided into 8 portions of 4mm using saw cutting. The portions were cut parallel to the exposed surface. The first seven portions were used in testing the total acid soluble chloride. The acid soluble chloride in the different increment was tested using the procedure detailed in chapter 1. The apparent chloride diffusion coefficient and the projected surface chloride-ion concentration were then calculated using the initial chloride-ion content, and seven related values for chloride-ion content and depth below the exposed surface.

Figure 5.7 - Cores Drilled for Chloride Diffusion Test

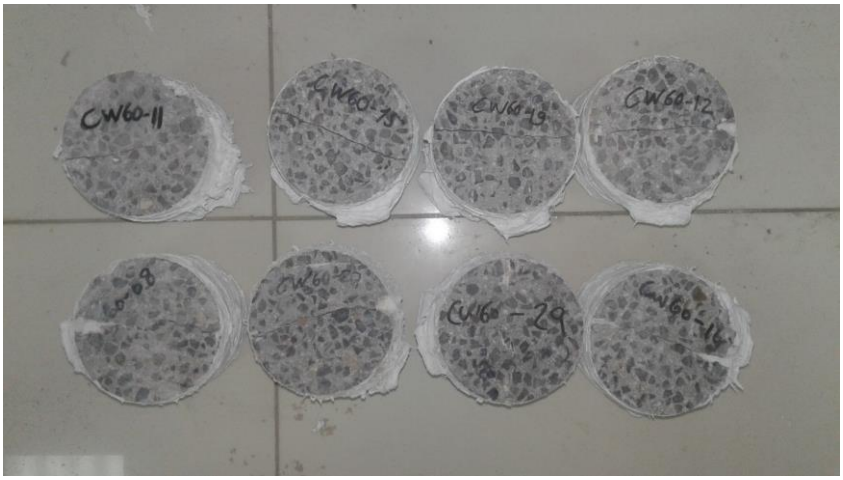

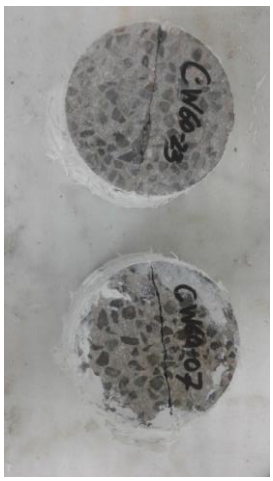

Figure 5.8 - Cores with Artificial Cracks and Coating

4. Chloride diffusion test results description, analysis, and interpretation

The chloride diffusion coefficient in CW Series was tested following five water-cement ratio values and five values from crack width as explained in the testing protocol. The chloride diffusion coefficient as well as the chloride surface concentration are detailed in the figures below. The tables including the total acid soluble chloride at each section are included in appendix 5.4. The calculations of the chloride diffusion coefficient in refence to ASTM C1556 are included in appendix 5.5.

Chloride Diffusion Coefficient Verus Crack Width - Summary - W/C =0.38 - Tested at 186 Days

Reference	Crack Width (mm)	Chloride Diffusion Coefficient (Individual Test) (m2/s)	Average Chloride Diffusion Coefficient (m2/s)
CW12-31	0.12	8.50E-12	8.80E-12
CW12-08	0.12	9.10E-12	
CW24-03	0.24	6.50E-12	1.23E-11
CW24-20A	0.24	1.80E-11	
CW36-11	0.36	1.20E-11	1.15E-11
CW36-14	0.36	1.10E-11	
CW48-23	0.48	1.30E-11	1.50E-11
CW48-24	0.48	1.70E-11	
CW60-11	0.6	4.00E-11	4.50E-11
CW60-15	0.6	5.00E-11	

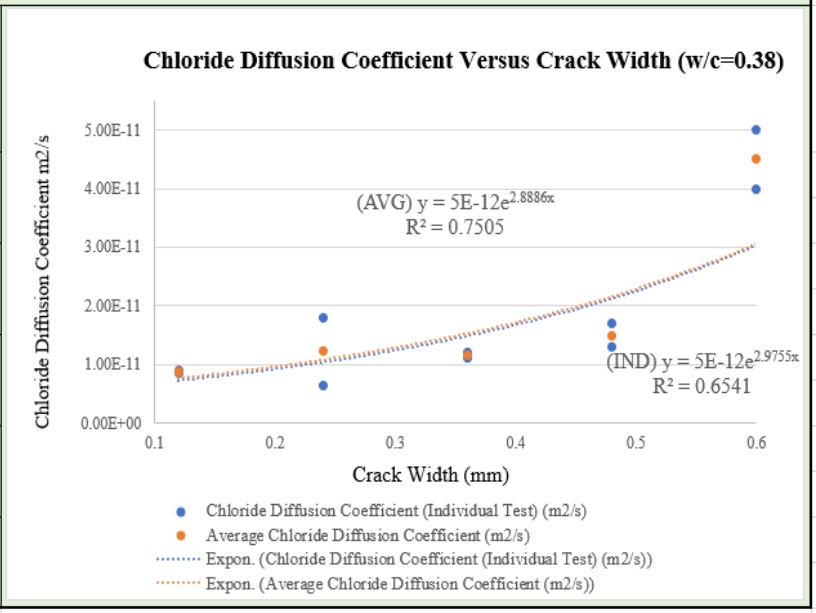

Figure 5.9 – Chloride Diffusion Versus Crack Width – W/C=0.38

Chloride Diffusion Coefficient Verus Crack Width - Summary - W/C =0.36 - Tested at 191 Days

Reference	Crack Width (mm)	Chloride Diffusion Coefficient (Individual Test) (m2/s)	Average Chloride Diffusion Coefficient (m2/s)
CW 12 -31B	0.12	1.80E-12	2.10E-12
CW 12 -25B	0.12	2.40E-12	
CW 24-14A	0.24	2.20E-11	1.90E-11
CW 24-19A	0.24	1.60E-11	
CW 36-14B	0.36	9.90E-12	1.10E-11
CW 36-17A	0.36	1.20E-11	
CW 48-16A	0.48	9.00E-12	1.00E-11
CW 48-20B	0.48	1.10E-11	
CW 60-13A	0.6	1.10E-11	1.04E-11
CW 60-14B	0.6	9.70E-12	

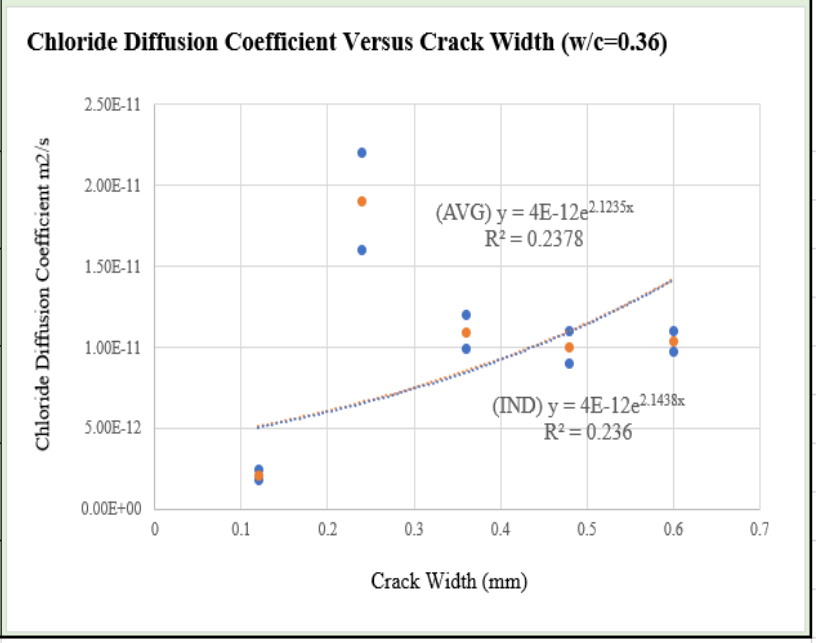

Figure 5.10 – Chloride Diffusion Versus Crack Width – W/C=0.36

Chloride Diffusion Coefficient Verus Crack Width - Summary - W/C =0.34 - Tested at 191 Days

Reference	Crack Width (mm)	Chloride Diffusion Coefficient (Individual Test) (m2/s)	Average Chloride Diffusion Coefficient (m2/s)
CW12-38A	0.12	2.00E-12	2.05E-12
CW12-42C	0.12	2.10E-12	
CW 24-29A	0.24	3.70E-12	3.20E-12
CW 24-33A	0.24	2.70E-12	
CW36-24B	0.36	3.80E-12	3.30E-12
CW 36-25A	0.36	2.80E-12	
CW48-26C	0.48	7.10E-12	6.10E-12
CW48-28A	0.48	5.10E-12	
CW-60-24A	0.6	1.10E-11	9.05E-12
CW 60-27A	0.6	7.10E-12	

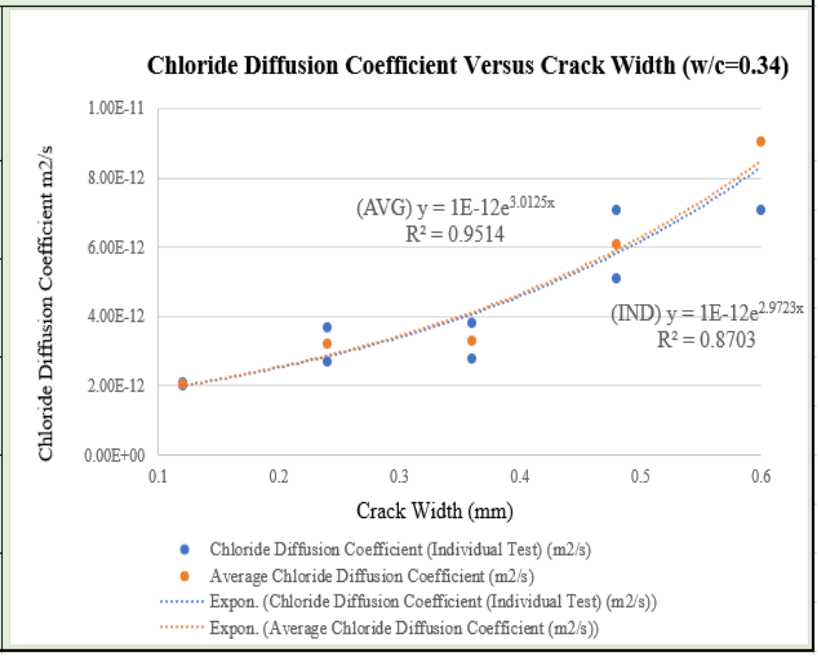

Figure 5.11 – Chloride Diffusion Versus Crack Width – W/C=0.34

Chloride Diffusion Coefficient Verus Crack Width - Summary - W/C =0.32 - Tested at 191 Days

Reference	Crack Width (mm)	Chloride Diffusion Coefficient (Individual Test) (m2/s)	Average Chloride Diffusion Coefficient (m2/s)
CW 12-49A	0.12	7.60E-12	6.75E-12
CW 12-55A	0.12	5.90E-12	
CW 24-36B	0.24	7.30E-12	9.15E-12
CW 24-40A	0.24	1.10E-11	
CW 36-37A	0.36	2.20E-11	2.40E-11
CW 36-42A	0.36	2.60E-11	
CW 48-41A	0.48	6.00E-12	5.45E-12
CW 48-45A	0.48	4.90E-12	
CW 60-37A	0.6	3.40E-12	3.95E-12
CW 60-42A	0.6	4.50E-12	

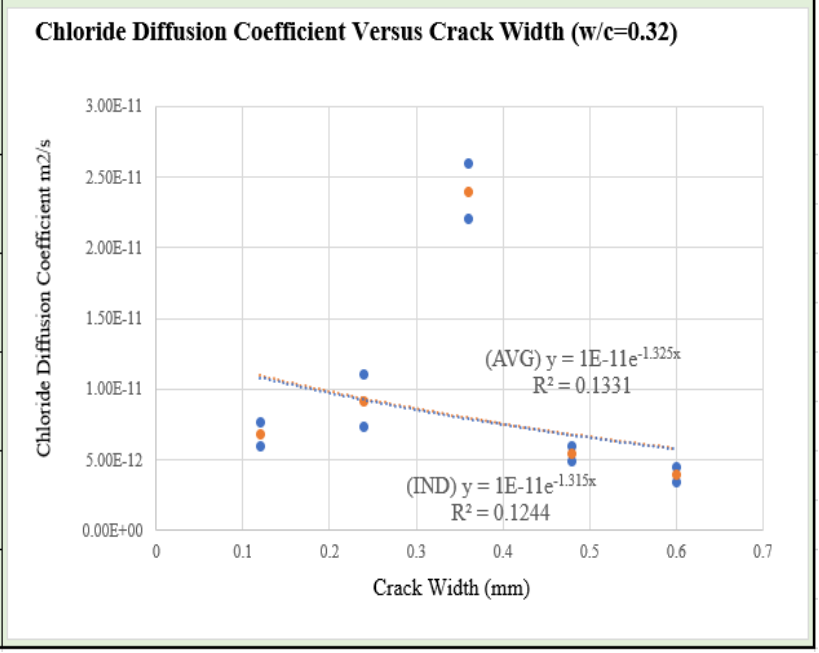

Figure 5.12 – Chloride Diffusion Versus Crack Width – W/C=0.32

Chloride Diffusion Coefficient Verus Crack Width - Summary - W/C =0.30 - Tested at 191 Days

Reference	Crack Width (mm)	Chloride Diffusion Coefficient (Individual Test) (m2/s)	Average Chloride Diffusion Coefficient (m2/s)
CW12-58B	0.12	7.80E-13	2.64E-12
CW12-66B	0.12	4.50E-12	
CW24-47B	0.24	5.00E-12	4.40E-12
CW24-56A	0.24	3.80E-12	
CW36-48A	0.36	3.90E-12	3.50E-12
CW36-50A	0.36	3.10E-12	
CW48-53B	0.48	6.90E-12	6.35E-12
CW48-54A	0.48	5.80E-12	
CW60-53A	0.6	4.90E-12	5.00E-12
CW60-56A	0.6	5.10E-12	

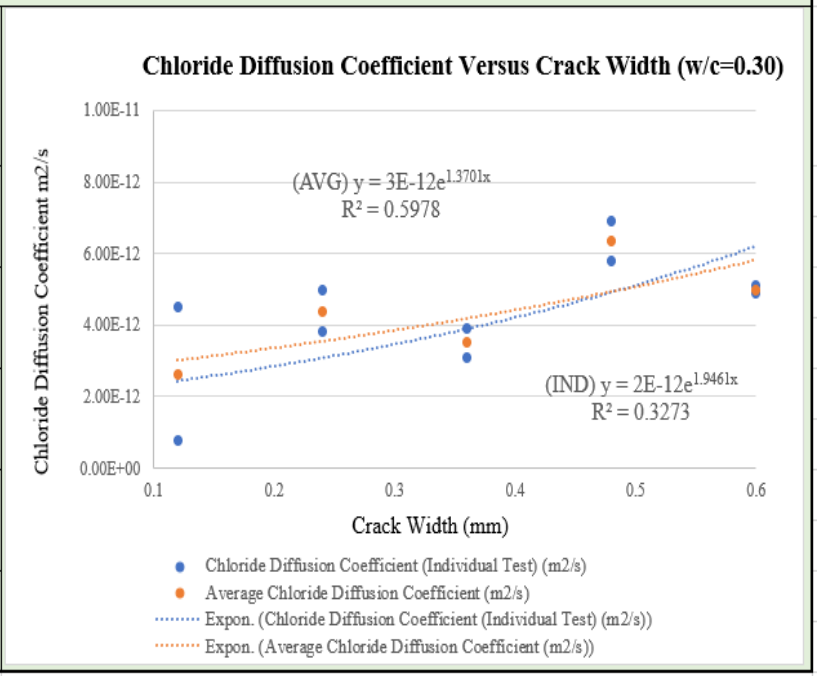

Figure 5.13 – Chloride Diffusion Versus Crack Width – W/C=0.30

Chloride Surface Concentration Verus Crack Width - Summary - W/C =0.38 - Tested at 186 Days

Reference	Crack Width (mm)	Chloride Surface Concentration (Individual Test) (%)	Average Chloride Surface Concentration (%)
CW12-31	0.12	0.726	0.656
CW12-08	0.12	0.586	
CW24-03	0.24	0.702	0.678
CW24-20A	0.24	0.654	
CW36-11	0.36	0.592	0.575
CW36-14	0.36	0.557	
CW48-23	0.48	0.655	0.624
CW48-24	0.48	0.592	
CW60-11	0.6	0.521	0.548
CW60-15	0.6	0.575	

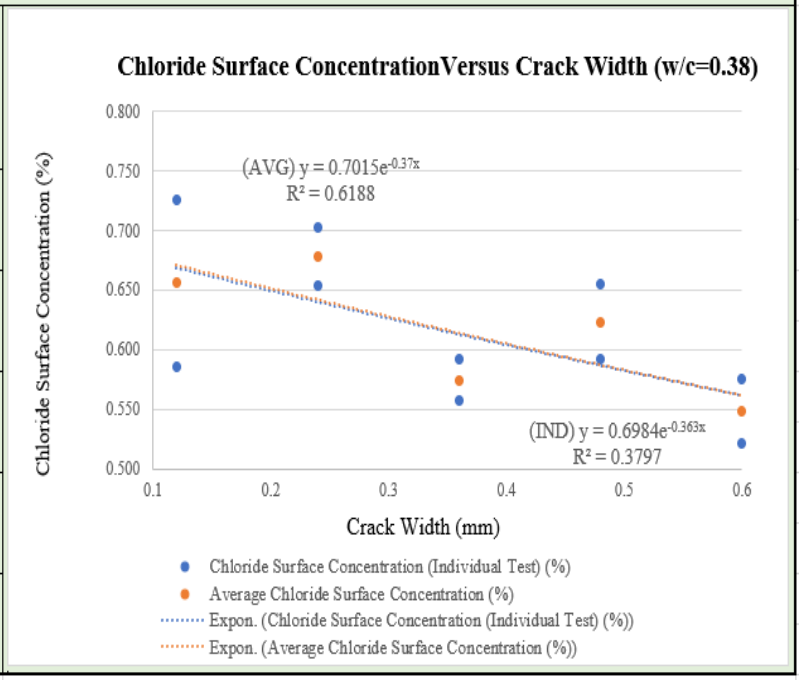

Figure 5.14 – Chloride Surface Concentration Versus Crack Width – W/C=0.38

Chloride Surface Concentration Verus Crack Width - Summary - W/C =0.36 - Tested at 191 Days

Reference	Crack Width (mm)	Chloride Surface Concentration (Individual Test) (%)	Average Chloride Surface Concentration (%)
CW 12 -31B	0.12	0.820	0.794
CW 12 -25B	0.12	0.767	
CW 24-14A	0.24	0.526	0.554
CW 24-19A	0.24	0.581	
CW 36-14B	0.36	0.642	0.639
CW 36-17A	0.36	0.636	
CW 48-16A	0.48	0.614	0.568
CW 48-20B	0.48	0.521	
CW 60-13A	0.6	0.597	0.576
CW 60-14B	0.6	0.554	

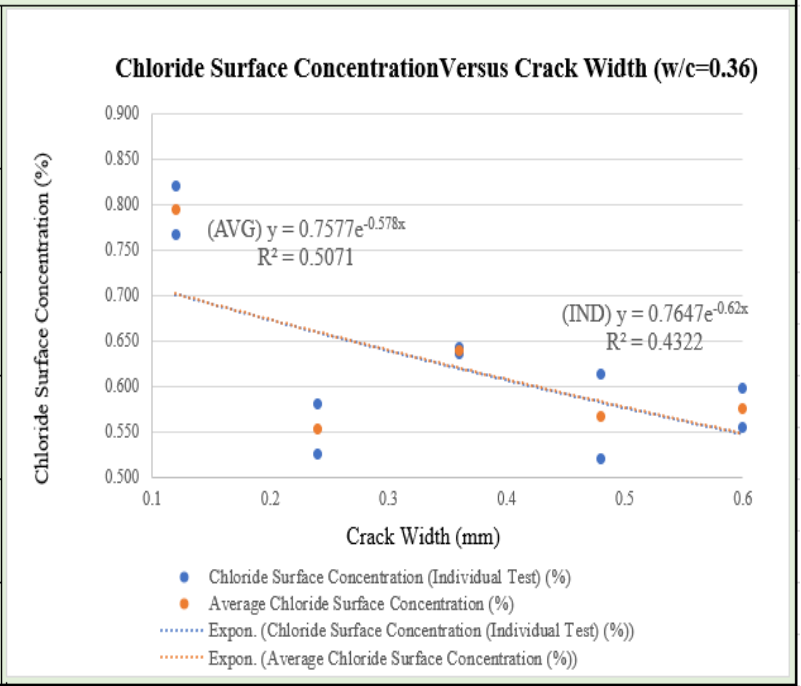

Figure 5.15 – Chloride Surface Concentration Versus Crack Width – W/C=0.36

Chloride Surface Concentration Verus Crack Width - Summary - W/C =0.34 - Tested at 191 Days

Reference	Crack Width (mm)	Chloride Surface Concentration (Individual Test) (%)	Average Chloride Surface Concentration (%)
CW12-38A	0.12	0.741	0.756
CW12-42C	0.12	0.771	
CW 24-29A	0.24	0.716	0.755
CW 24-33A	0.24	0.793	
CW36-24B	0.36	0.662	0.689
CW 36-25A	0.36	0.715	
CW48-26C	0.48	0.625	0.651
CW48-28A	0.48	0.677	
CW-60-24A	0.6	0.594	0.577
CW 60-27A	0.6	0.559	

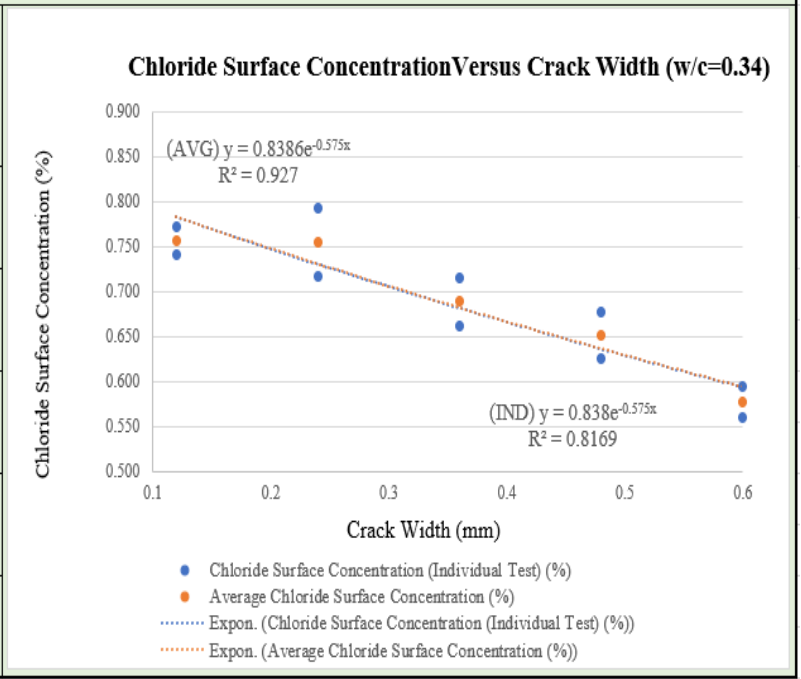

Figure 5.16 – Chloride Surface Concentration Versus Crack Width – W/C=0.34

Chloride Surface Concentration Verus Crack Width - Summary - W/C =0.32 - Tested at 191 Days

Reference	Crack Width (mm)	Chloride Surface Concentration (Individual Test) (%)	Average Chloride Surface Concentration (%)
CW 12-49A	0.12	0.616	0.636
CW 12-55A	0.12	0.655	
CW 24-36B	0.24	0.607	0.555
CW 24-40A	0.24	0.502	
CW 36-37A	0.36	0.510	0.504
CW 36-42A	0.36	0.498	
CW 48-41A	0.48	0.490	0.499
CW 48-45A	0.48	0.508	
CW 60-37A	0.6	0.624	0.617
CW 60-42A	0.6	0.609	

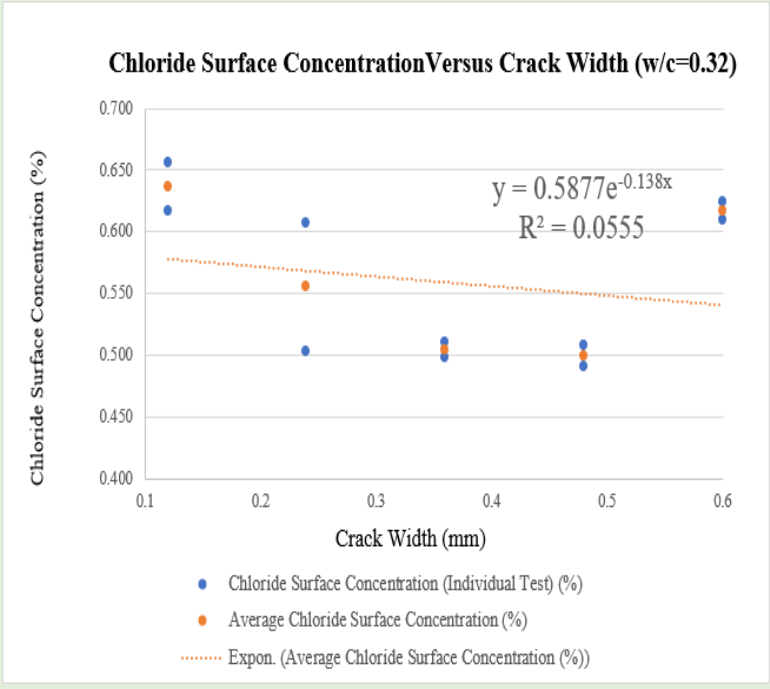

Figure 5.17 – Chloride Surface Concentration Versus Crack Width – W/C=0.32

Chloride Surface Concentration Verus Crack Width - Summary - W/C =0.30 - Tested at 191 Days

Reference	Crack Width (mm)	Chloride Surface Concentration (Individual Test) (%)	Average Chloride Surface Concentration (%)
CW12-58B	0.12	0.788	0.708
CW12-66B	0.12	0.627	
CW24-47B	0.24	0.621	0.638
CW24-56A	0.24	0.654	
CW36-48A	0.36	0.589	0.670
CW36-50A	0.36	0.751	
CW48-53B	0.48	0.559	0.574
CW48-54A	0.48	0.588	
CW60-53A	0.6	0.596	0.585
CW60-56A	0.6	0.574	

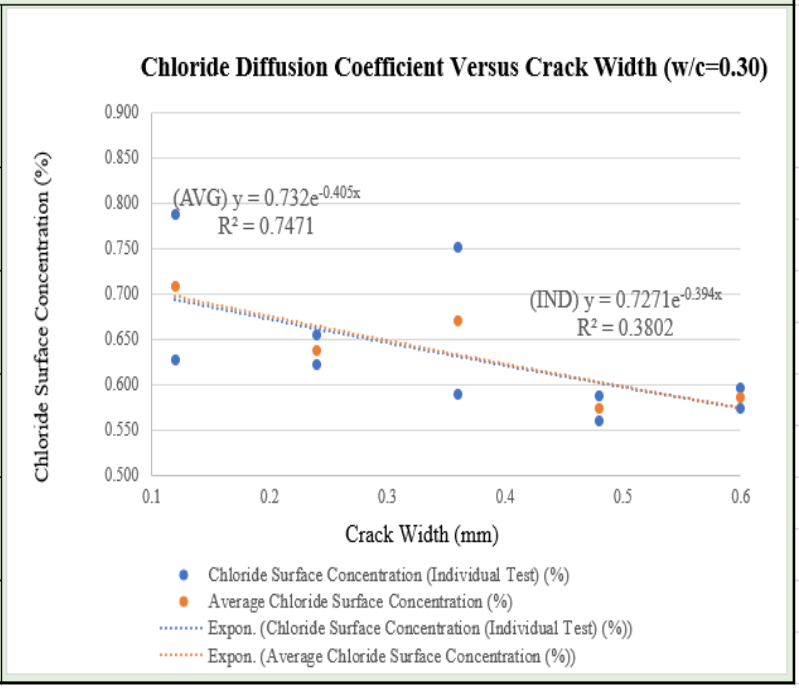

Figure 5.18 – Chloride Surface Concentration Versus Crack Width – W/C=0.30

The following observations were made in figures 5.9 to 5.18:

The chloride diffusion coefficient grew exponentially as a function of the crack width with a relatively high correlation factor for the water-cement ratios of 0.38, 0.34 and 0.30. The surface concentration on the other hand decreased in the same pattern. These test results confirm the fact that the chloride diffusion coefficient will increase as a function of the crack width. The regression analysis concluded the mathematical model of this increase which is an exponential form.

In the groups pertaining to the water-cement ratios of 0.36 and 0.32, the relationship concluded in the other three groups was not evident. It is clear from the data that three results out of 25 test results do not follow the general trends obtained. These results are namely the following:

- Crack width of 0.24 mm and a water-cement ratio of 0.36.
- Crack Width of 0.48 mm and a water-cement ratio of 0.32.
- Crack Width of 0.60 mm and a water-cement ratio of 0.32.

The three set of data were thus removed from further statistical analysis to identify the function f_{10}.

The below tables summarize the most suitable correlation obtained from the graphs above. Figures 5.19 and 5.20 form a graphic illustration for these tables.

Table 5.1 - Chloride Diffusion Coefficient Versus Cracks Width Correlation for Different Water-Cement Ratios

Water-Cement Ratio	Correlation	R-Squared Factor
0.38	$5 \times 10^{-12} \times e^{2.89\times(\xi)}$	0.75
0.36	$4 \times 10^{-12} \times e^{2.12\times(\xi)}$	0.24
0.34	$1 \times 10^{-12} \times e^{3.01\times(\xi)}$	0.95
0.32	$1 \times 10^{-11} \times e^{-1.36\times(\xi)}$	0.13
0.30	$3 \times 10^{-12} \times e^{1.37\times(\xi)}$	0.60

where ξ is the crack width.

Table 5.2 - Chloride Surface Concentration Versus Cracks Width Correlation for Different Water-Cement Ratios

Water-Cement Ratio	Correlation	R-Squared Factor
0.38	$0.715 \times e^{-0.37\times(\xi)}$	0.62
0.36	$0.758 \times e^{-0.58\times(\xi)}$	0.51
0.34	$0.839 \times e^{-0.58\times(\xi)}$	0.93
0.32	$0.588 \times e^{-0.14\times(\xi)}$	0.06
0.30	$0.732 \times e^{-0.405\times(\xi)}$	0.75

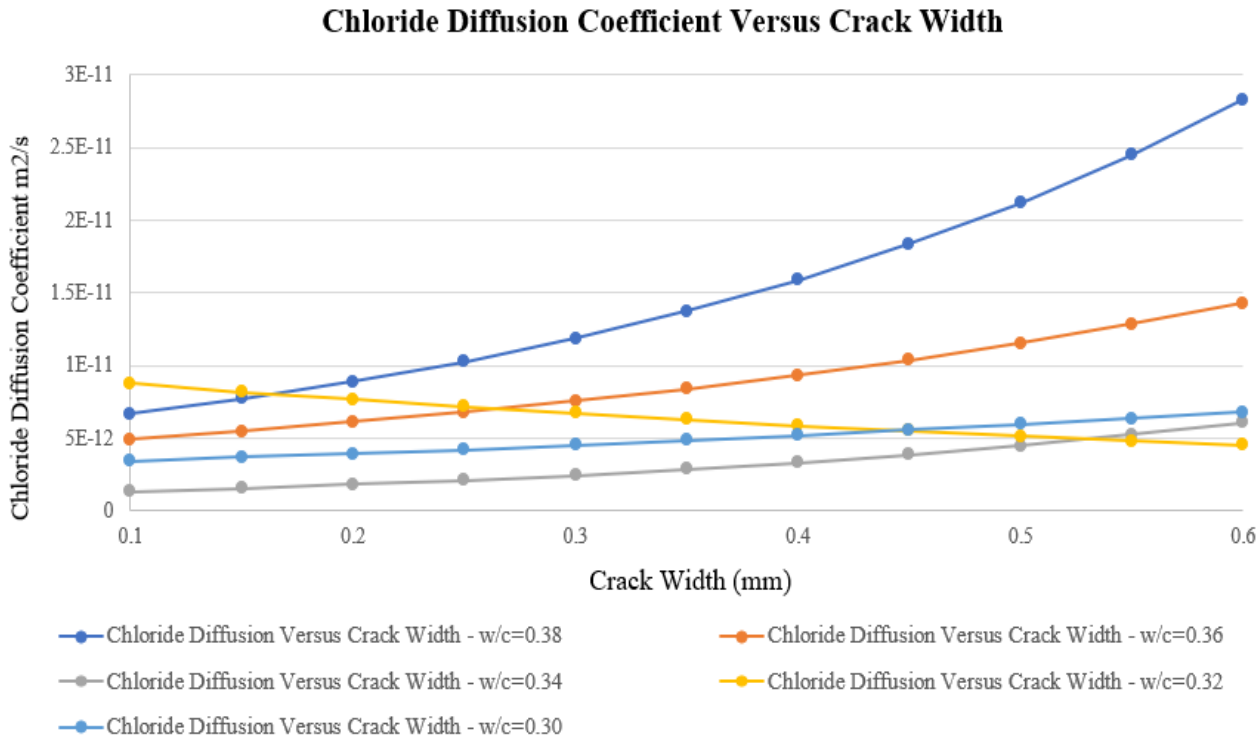

Figure 5.19 - Chloride Diffusion Coefficient versus Cracks Width for the Different Water-Cement Ratios

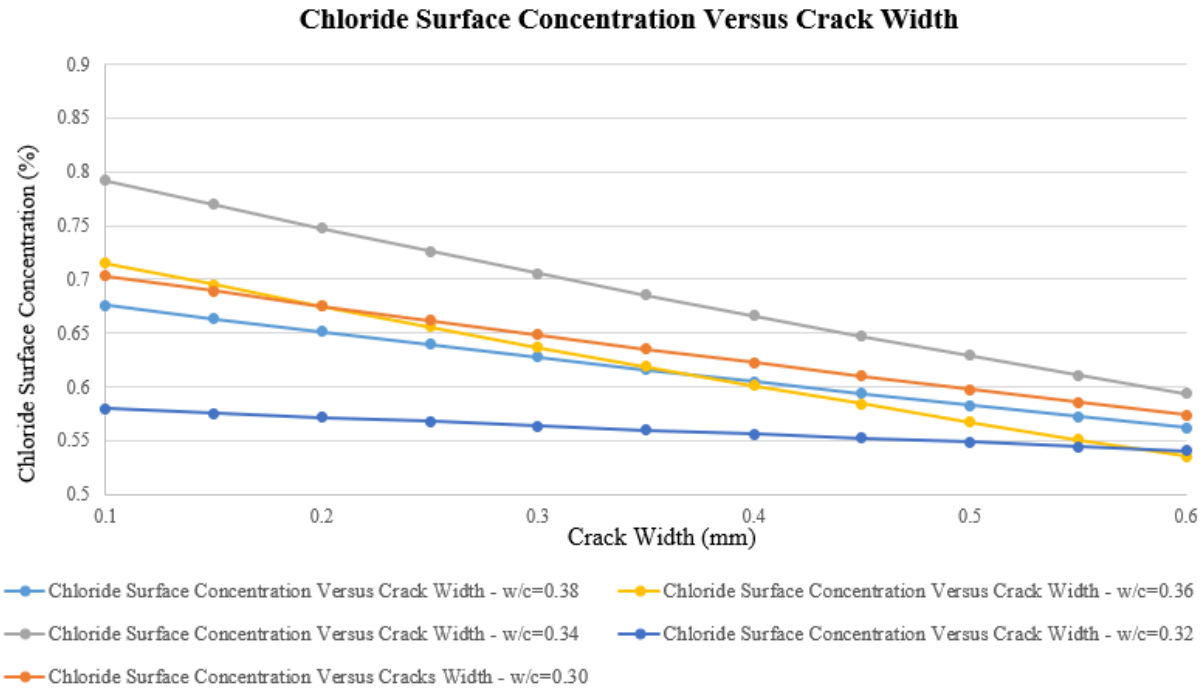

Figure 5.20 -Chloride Surface Concentration versus Cracks Width for the Different Water-Cement Ratios

The above graphs confirm that the chloride diffusion coefficient increases in an exponential form with the crack width. This exponential form is limited in the upper side by the chloride diffusion in water, taking into consideration that, at a certain crack width, the diffusion is made independently from the concrete substance.

On the other hand, the literature review conducted in chapter 1, demonstrated that, in average, the chloride diffusion coefficient increases in an exponential form with the water-cement ratio through equation (1.78):

$$D_c = 7 \times 10^{-13} e^{6.1705(w_c)} \qquad R^2 = 0.984$$

As a consequence, the following general formula is the most suitable to define the combined effect of the crack width and water-cement ratio on the chloride diffusion coefficient when all the other constituent materials are constant (taking into consideration that when the crack width is zero, the function that considers the effect of the crack width is equal to 1):

$$D(w_c;\xi) = (e^{[A\times(w_c)\times\xi]}) \times Be^{D(w_c)} \tag{5.1}$$

where $D(w_c;\xi)$ is the chloride diffusion coefficient, w_c is the water-cement ratio, ξ is the crack width, A, B, and D, are constants.

The tested values for the different water-cement ratio, and crack widths were tabulated in table 5.3. A multiple regression analysis was made to identify the values of A, B, and D. The MS Excel solver was used in order to yield the final formula defined above, identifying the parameters A, B, and D. The final values of these constants were as follows:

$A = 9.31$, $B = 0.15 \times 10^{-14}$, and $D = 20.81$.

Equation (5.1) is thus:

$$D(w_c;\xi) = (e^{[9.31\times(w_c)\times\xi]}) \times (0.15 \times 10^{-14})e^{20.81(w_c)}$$

The final form of the function f_{10} that considers the effect of the crack width on the chloride diffusion coefficient is thus concluded by dividing equation (5.1) by (1.78):

$$f_{10}(w_c,\xi) = e^{[9.31\times(w_c)\times\xi]} \times (2.1 \times 10^{-3})e^{14.64(w_c)} \quad (5.2)$$

A graphical representation of the tested versus predicted model is available in figure 5.21. The average error between the predicted and tested values on the range of values tested is presented in table 5.3. The error was in average equal to 47.46% when compared to the average within test error of 30.71%. The error associated with the model originate thus from the initial error inherent in the test itself which is equal to 39.8% in reference to ASTM C1556 paragraph 12. This paragraph states the following:" *the apparent diffusion coefficient results of two properly conducted tests should not differ by more than 39.8 % of the mean value".*

The model thus predicted confirms also the major effect of the water cement ratio on the chloride diffusion in cracked concrete. The role of autogenous healing is evident in reducing the chloride diffusion in lower water cement ratio mixes of cracked concrete.

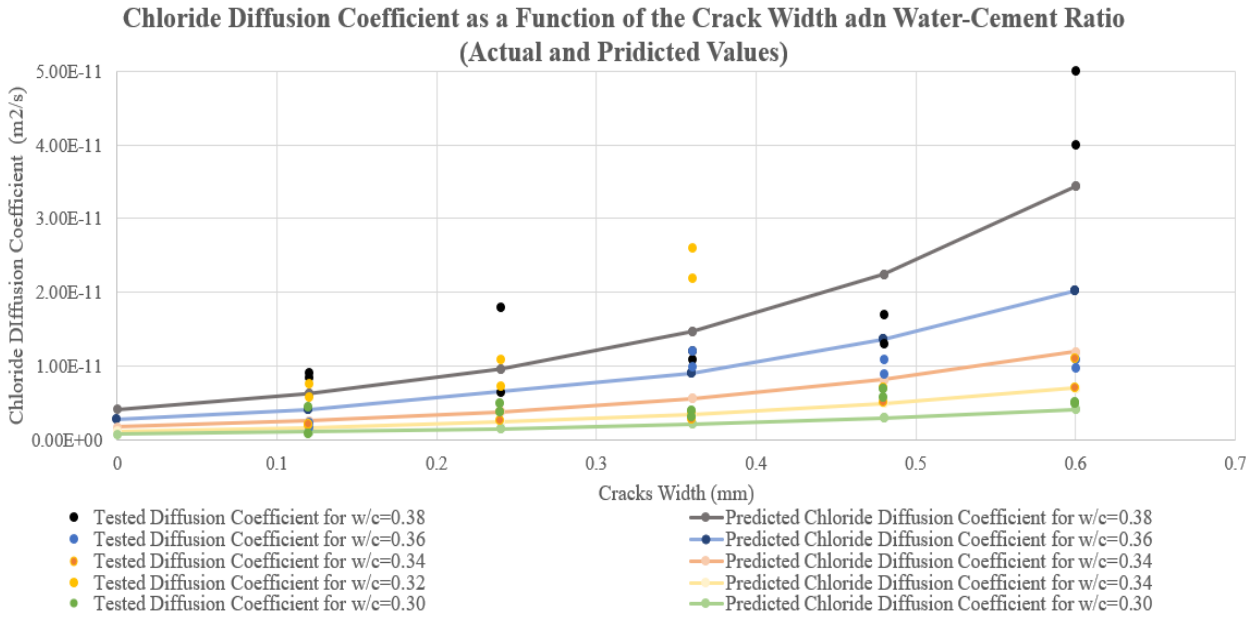

Figure 5.21 - Tested Values versus Predicted Model

Table 5.3 - Individual Test Data for the Chloride Diffusion Coefficient in Cracked Concrete

Water Cement Ratio	Crack Width	Tested Values for Cracked Concrete (10^{-12} m^2/sec)	Average Tested Values for Cracked Concrete (10^{-12} m^2/sec)	Within-test Error (%)	Predicted Values based on the equation (10^{-12} m^2/sec)	Prediction Error (%)
0.38	0.12	8.5	8.8	6.82%	6.3	28.41%
0.38	0.12	9.1				
0.38	0.24	6.5	12.25	93.88%	9.62	21.47%
0.38	0.24	18				
0.38	0.36	12	11.5	8.70%	14.71	27.91%
0.38	0.36	11				
0.38	0.48	13	15	26.67%	22.49	49.93%
0.38	0.48	17				
0.38	0.6	40	45	22.22%	34.37	23.62%
0.38	0.6	50				
0.36	0.12	1.8	2.1	28.57%	4.06	93.33%
0.36	0.12	2.4				
0.36	0.36	9.9	10.95	19.18%	9.07	17.17%
0.36	0.36	12				
0.36	0.48	9	10	20.00%	13.56	35.60%
0.36	0.48	11				
0.36	0.6	11	10.35	12.56%	20.28	95.94%
0.36	0.6	9.7				
0.34	0.12	2	2.05	4.88%	2.62	27.80%
0.34	0.12	2.1				
0.34	0.24	3.7	3.2	31.25%	3.83	19.69%
0.34	0.24	2.7				
0.34	0.36	3.8	3.3	30.30%	5.6	69.70%
0.34	0.36	2.8				
0.34	0.48	7.1	6.1	32.79%	8.18	34.10%
0.34	0.48	5.1				
0.34	0.6	11	9.05	43.09%	11.96	32.15%
0.34	0.6	7.1				
0.32	0.12	7.6	6.75	25.19%	1.69	74.96%
0.32	0.12	5.9				
0.32	0.24	7.3	9.15	40.44%	2.42	73.55%
0.32	0.24	11				
0.32	0.36	22	24	16.67%	3.45	85.63%
0.32	0.36	26				

0.3	0.12	0.78	2.64	140.91%	1.09	58.71%
0.3	0.12	4.5				
0.3	0.24	5	4.4	27.27%	1.52	65.45%
0.3	0.24	3.8				
0.3	0.36	3.9	3.5	22.86%	2.13	39.14%
0.3	0.36	3.1				
0.3	0.48	6.9	6.35	17.32%	2.98	53.07%
0.3	0.48	5.8				
0.3	0.6	4.9	5	4.00%	4.16	16.80%
0.3	0.6	5.1				
Average Within Test Error (%)			30.71%			
Average Prediction Error (%)			47.46%			

5. Conclusions

The effects of cracks on the overall durability of concrete was discussed and analyzed in many researches and literatures. The cracks were found to decrease the concrete durability and to increase the chloride diffusion.

This effect was as well found coupled with the concrete water-cement ratio whereby mixes with lower water-cement ratio exhibit a higher autogenous healing that effectively reduces the crack width, forming more hydration products.

A testing campaign is carried out to quantify the coupled effect of the crack width and water-cement ratio on the chloride diffusion in concrete. This testing campaign used the long-term chloride ponding in reference to ASTM C1556 while simulating the real case cracks tortuosity and surface condition. This type of testing was essential to simulate as close as possible the real cases and to take into account the effect of the autogenous healing. The crack width was accurately initiated throughout the length of the concrete sample. A set of 25 combinations including mixes with five different water-cement ratios and five different crack widths were prepared and immersed in the chloride solution. The different water-cement ratio levels were considered to take into consideration the crack autogenous healing.

Two samples from every combination was made. Further to the immersion period, the chloride diffusion coefficient was tested in the 50 prepared samples.

The results show that the chloride diffusion coefficient increases exponentially with the crack width in the five water-cement ratio groups. The effect was less pronounced in mixes with lower water-cement ratio.

An exponential model for the function considering the effect of the crack width on the chloride diffusion coefficient was predicted with accuracy based on the test results provided. This function is also affected by the water-cement ratio.

The exponential effect of the crack width on the chloride diffusion coefficient was thus quantified as a function of the crack width and the water-cement ratio. This result furthermore confirms the role of the autogenous healing in reducing the chloride diffusion in cracked concrete following the value of the water-cement ratio.

Specifying an absolute crack width value in durability specifications may be revisited to take into account the coupled effect of the crack width and the water-cement ratio. The same value of the crack width limit may be less or more stringent based on the concrete water-cement ratio.

Chapter 6: Updated Model and Numerical Application

1. Introduction

The main intent of our work is to reach a comprehensive model for chloride diffusion in concrete. Based on the literature review made in chapter 1, several parameters were identified to affect the chloride diffusion coefficient. These parameters were studied in chapters 2 to 5. The final model can thus be obtained by combining the above results to the reference chloride diffusion coefficient that is presented in this chapter. The finite difference method is then used for chloride ingress calculations and an Excel sheet is presented for further application.

2. Final updated model for chloride diffusion coefficient

By combining the results in the previous chapters, the final diffusion coefficient can be expressed by the following equation, and depends on the following parameters:

$$D_c = D_{c,ref}.f_1(T).f_2(h).f_3(x).f_4(CA,Hy).f_5(C3A).f_6(Cs).f_7(Mi).f_8(CW,w/c) \qquad (6.1)$$

- Environmental input parameters
    - Temperature
    - Age
    - Relative humidity
- Concrete properties input parameters
    - Water-cement ratio
    - Cementitious materials content
    - Cementitious materials replacement percentage (Fly ash, silica fume, slag)
    - Cement Density
    - Cement Surface Area
    - Alite Percentage in Cement
    - Belite Percentage in Cement
    - Aluminate Percentage in Cement (C3A content)
    - Ferrite Percentage in Cement
    - Aggregate content and properties
    - Hydration Coefficient
- Workmanship input parameters
    - Curing time
    - Initial Mixing Time
    - Consolidation Degree
- Post-placing input parameters
    - Crack Width

Chapter 2 has demonstrated that the degree of hydration, age, and initial curing time are combined together into the degree of hydration. This factor is associated with the aggregate content as this later will change the pores distribution as discussed in the same chapter. The same relationship is applied to the cement's density and surface area, in addition to the alite, belite, and Ferrite percentages. These parameters change the pores distribution as explained in chapter.

The functions mentioned in equation 6.1 are defined in table 6.1 below. The subsequent paragraphs include the final model of each function. The calculation of the reference chloride diffusion coefficient is included in section 3

Table 6.1 - Influencing Functions

Function	Terminology
D_c	concrete diffusion coefficient
$D_{c,ref}$	Reference diffusion coefficient at an age of 28 days, a temperature of 23℃, and a relative humidity of 100%. This parameter is a function of the water-cement ratio, cement content, and cementitious materials percentage replacement.
$f_1(T)$	dependence on the temperature
$f_2(h)$	dependence on the concrete pores relative humidity
$f_3(x)$	dependence on the distance from the surface
$f_4(CA, Hy)$	dependence on the coarse aggregate coarse aggregate content, aggregate properties, and degree of hydration
$f_5(C3A)$	dependence on the tricalcium aluminate content
$f_6(Cs)$	dependence on the consolidation level
$f_7(Mi)$	dependence on the initial mixing time
$f_8(CW, w_c)$	dependence on the cracks width

The below paragraphs include the final form of each of the above functions:

- **Temperature dependent function $f_1(T)$**

The literature review conducted in chapter 1 concluded that the form of this function is as follows:

$$\boldsymbol{f_1(T) = \frac{T}{296.15} \exp\left[\frac{U}{R}.\left(\frac{1}{296.15} - \frac{1}{T}\right)\right]} \quad (6.2)$$

where U is the activation energy of the chloride diffusion process, equal to 34500 J/mol, R is the gas constant, equal to 8.314 (J/K·mol), and T is the actual absolute temperature of the concrete (K).

- **Relative humidity dependence function $f_2(h)$**

The literature review conducted in chapter 1 concluded that the form of this function is as follows:

$$f_2(h) = \left[1 + \frac{(1-h)^4}{(1-0.75)^4}\right]^{-1} \quad (6.3)$$

where h is the relative humidity of the pores.

- **Distance from the surface dependence function $f_3(x)$**

The literature review conducted in chapter 1 concluded that this function is as follows:

$$f_3(x) = \begin{bmatrix} 0.53 + (1-0.53)\left(\frac{x}{20}\right)^{\beta} & for\ x < 20mm \\ 1 & for\ x \geq 20mm \end{bmatrix} \quad (6.4)$$

Where x is the depth in mm, and β is a constant equal to 0.68 [56].

- **Aggregate and hydration dependence function $f_4(CA, Hy)$**

The works conducted in chapter 2 has concluded that the function defining the dependence of the chloride diffusion coefficient on the aggregate volume and properties is as follows.

$$f_4(CA, Hy) = (1.7258.Mf + 0.0963.Ab + 3.9165.Clf + 1) \times \frac{(1-V_{aggregate})}{\left[0.6265\left[\frac{1}{\sum_{i=1}^{i=n} V_i A_i}\right] + \left(0.3735\left[\sum_{i=1}^{i=n} \frac{V_i}{A_i}\right]\right)\right]} \quad (6.5)$$

where Mf is the percentage of materials finer than 75 microns in (%), Ab is the aggregate absorption in (%), Clf is the percentage of clay lumps and friable particles in (%), $V_{aggregate}$ is the volume of aggregate in the concrete mix, $\sum_{i=1}^{i=n} V_i A_i$ and $\left[\sum_{i=1}^{i=n} \frac{V_i}{A_i}\right]$ are calculated as per the procedure described in chapter 2.

- **Tricalcium aluminate dependence function $f_5(C3A)$**

Based on the works conducted in chapter 3, the function related to the effect of C3A content on the chloride diffusion coefficient is as follows:

$$f_5(C3A) = 26.644 \times (C3A)^{-2.552} \quad (6.6)$$

- **Degree of consolidation and initial mixing time dependence functions $f_6(Cs)$ and $f_7(Mi)$**

Chapter 4 has concluded that the degree of consolidation and the initial mixing time do not affect the chloride diffusion coefficient, the functions $f_6(Cs)$ and $f_7(Mi)$ are thus equal to 1.

- **Crack width dependence function $f_8(cw, w_c)$**

Based on the works conducted in chapter 5, the function that takes into consideration the dependence of the chloride diffusion coefficient on the crack width is as follows:

$$f_8(cw, w_c) = e^{[8.29\times(w_c)\times cw]} \quad (6.7)$$

where cw is the crack width in mm, and w_c is the water-cement ratio.

3. Reference chloride diffusion coefficient

The eight functions concluded from chapters 2 to 5 and defined earlier in this chapter described the influence of the corresponding parameters on the reference chloride diffusion coefficient. The reference chloride diffusion coefficient as a function of the cementitious materials quantity, water-cement ratio, and cementitious materials type can be concluded by taking into consideration the different involved parameters. In addition to the water-cement ratio, cementitious materials type and quantity, the parameters that may influence this reference coefficient are tabulated in table 6.2. Refining this coefficient will thus require another large-scale testing campaign including a minimum 200 combinations for an acceptable adjusted R-squared factor. Going for this demanding application, the calculation of the reference chloride diffusion is based on the available literature review.

Table 6.2 – Parameter affecting the refence chloride diffusion coefficient

Cement	Microsilica	Fly Ash	Slag
Aluminium Oxide Content	Silicon dioxide (SiO2) content	Silicon dioxide (SiO2) content	Sulfide Sulfur Content
Ferric oxide (Fe2O3) Content	Moisture Content	aluminum oxide (Al2O3) content	Fineness
Magnesium oxide (MgO) Content	Loss on Ignition		Air Content
Sulfur trioxide (SO3) Content	Accelerated pozzolanic strength activity index	iron oxide (Fe2O3) content	Slag Activity Index
Loss on ignition		Sulfur trioxide (SO3) content	Compressive strength
Insoluble residue		Moisture content	
Tricalcium silicate (C3S) Content		Loss on ignition	
Dicalcium silicate (C2S) Content	Percent retained on 45-µm	Fineness	
Tetracalcium aluminoferrite (C3A)		Strength activity index	
Air content of mortar	Specific surface	Water requirement	
Fineness, specific surface		Soundness	
Compressive strength		Density	
Time of setting		Percent retained on 45-µm	
Cement Density			

The reference chloride diffusion coefficient is considered at an age of 28 days, a temperature of 23°C, and a relative humidity of 100%. This parameter is a function of the water-cement ratio, cement content, and cementitious materials percentage replacement. The literature review was conducted in chapter 1 where several researchers have identified the effect of these three parameters on the reference chloride diffusion coefficient. Figure 6.1 below presents the chloride diffusion coefficient resulted from the application of various models for a concrete having a fixed cement content of 425 kg/m^3 as a function of the water-cement ratio. The models used are discussed in detail in chapter 1.

To construct this graph, the chloride diffusion coefficient resulting from the application of each model, considering a cement content of 425 kg/m^3 is plotted as a function of the water cement ratio. At each water-cement level, the average value given by various models was calculated. A regression analysis was made for the average values resulting in equation (6.8) below. The average values fit well an exponential function with a high correlation factor.

$$D_c = 7 \times 10^{-13} e^{6.1705(w_c)} \qquad R^2 = 0.984 \qquad (6.8)$$

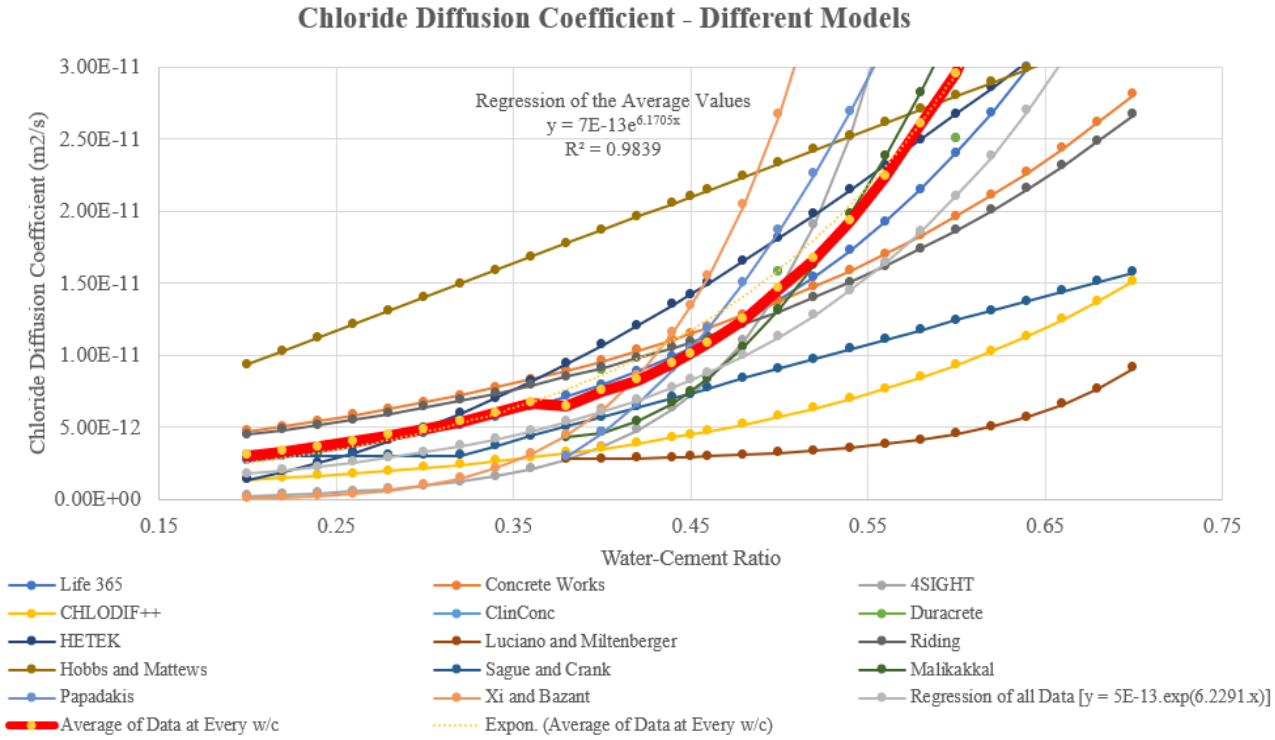

Figure 6.1 - Chloride Diffusion Coefficient (Different Models; Cement Content = 425kg/m3)

Similar graphs were drawn for a cement content of 300 kg/m^3, 325 kg/m3, 350 kg/m3, 375 kg/m3, 400 kg/m3, 450 kg/m3, 475 kg/m3, 500 kg/m^3, are presented in figure 6.2, 6.3, 6.4, 6.5, 6.6, 6.7, 6.8, and 6.9 respectively. The relationship remains necessarily exponential as a function of the water cement ratio when the other parameters are fix, with the following form:

$$D_c = Ae^{K(w_c)} \qquad (6.9)$$

where w_c is the cement content, A and K are constant values, given in the corresponding figures.

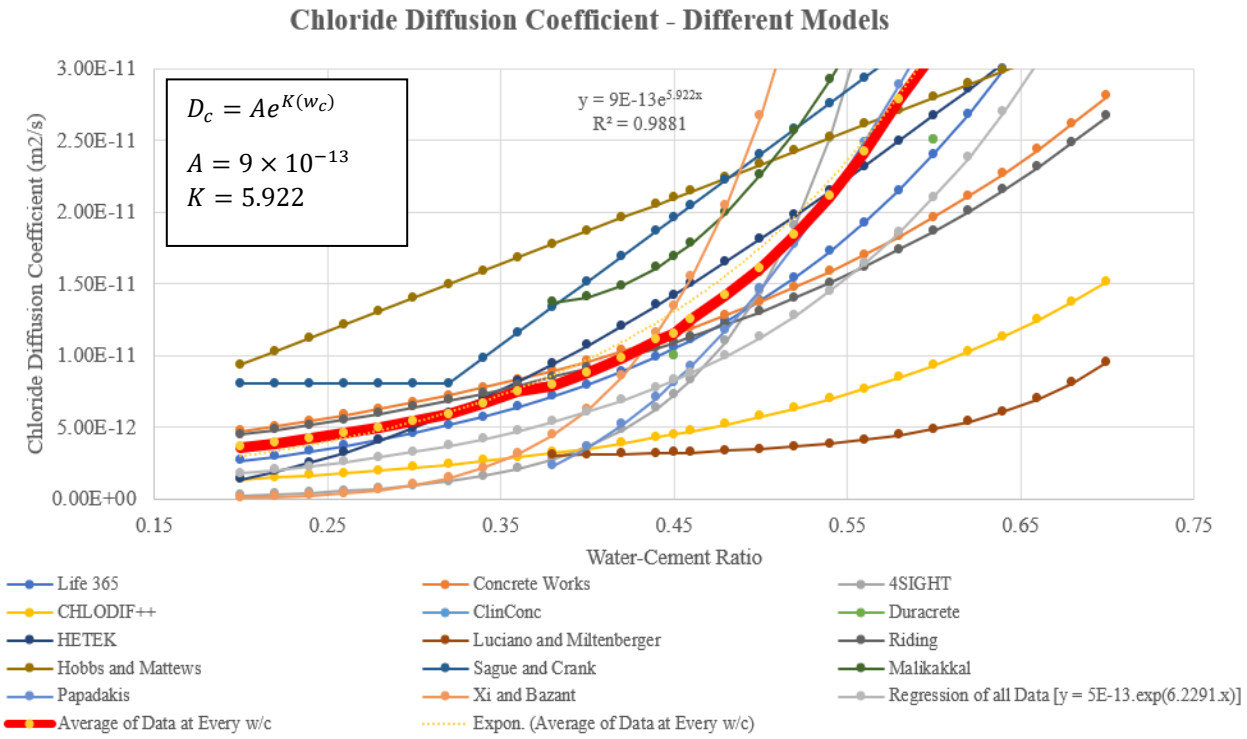

Figure 6.2 - Chloride Diffusion Coefficient (Different Models; Cement Content = 300kg/m3)

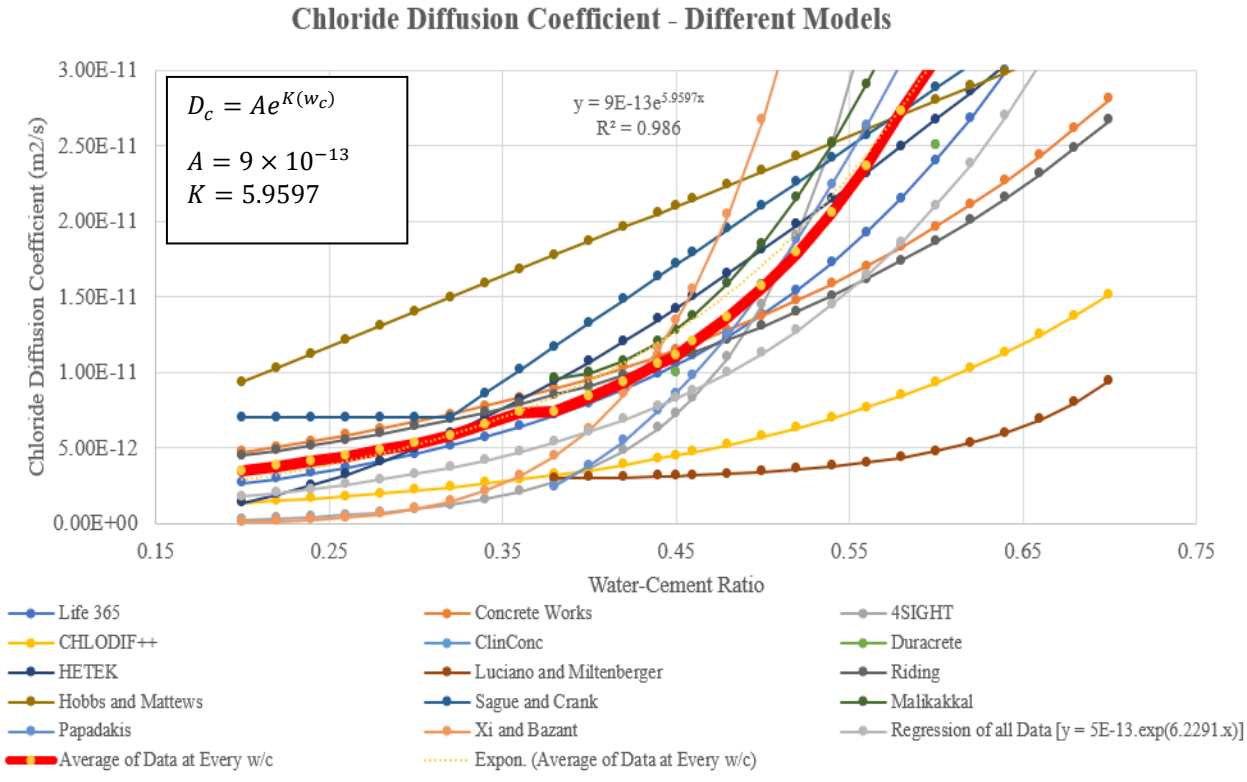

Figure 6.3 - Chloride Diffusion Coefficient (Different Models; Cement Content = 325kg/m3)

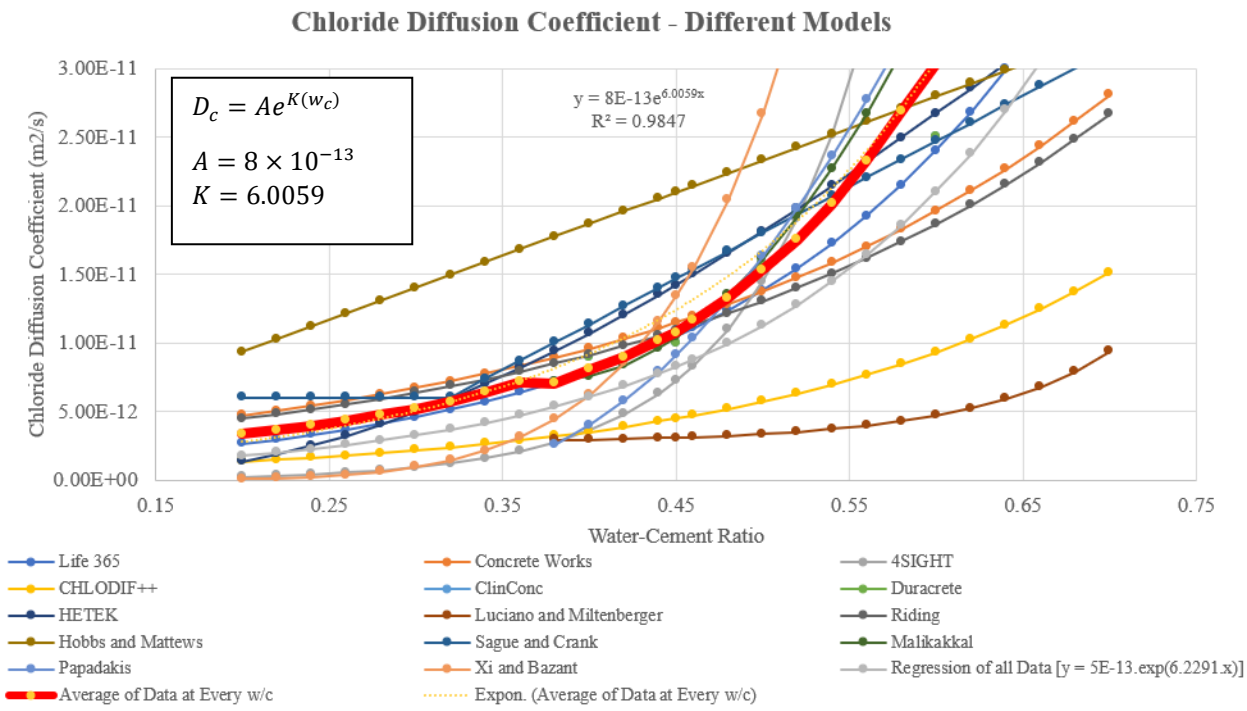

Figure 6.4 - Chloride Diffusion Coefficient (Different Models; Cement Content = 350kg/m3)

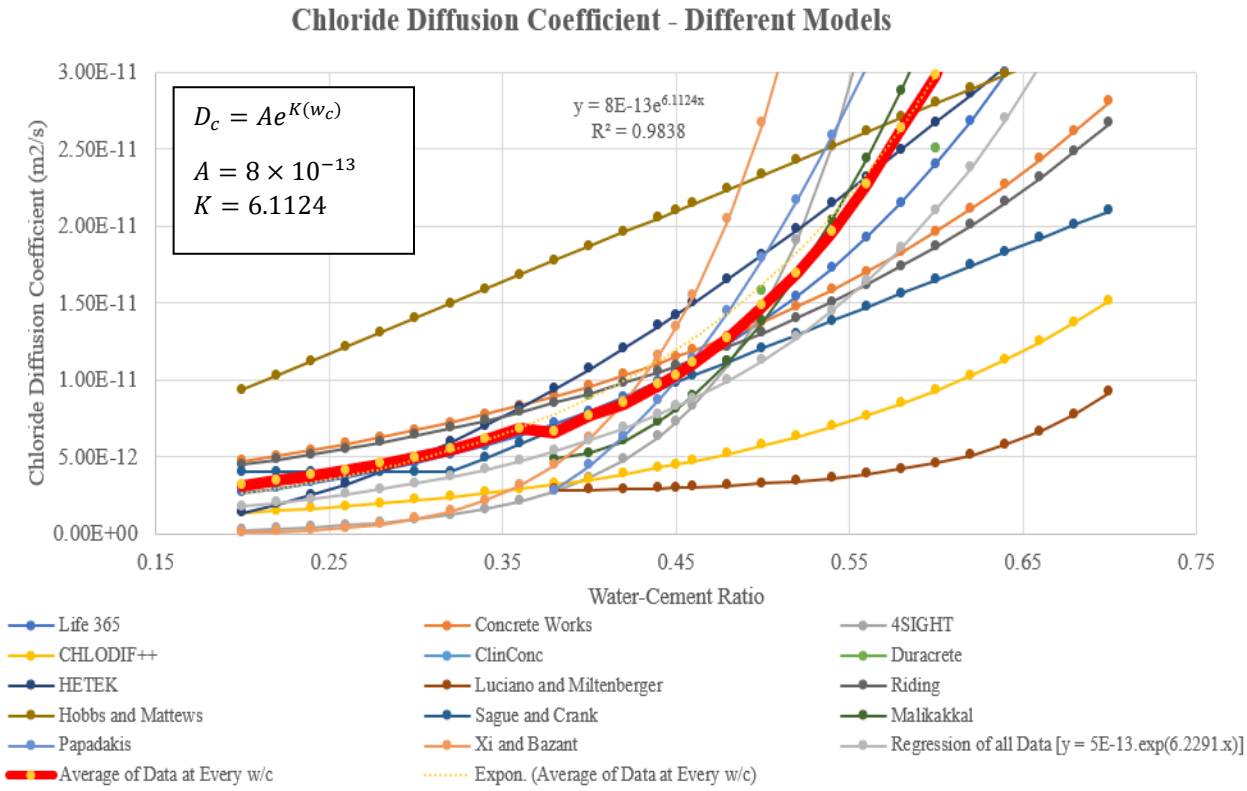

Figure 6.5 - Chloride Diffusion Coefficient (Different Models; Cement Content = 375kg/m3)

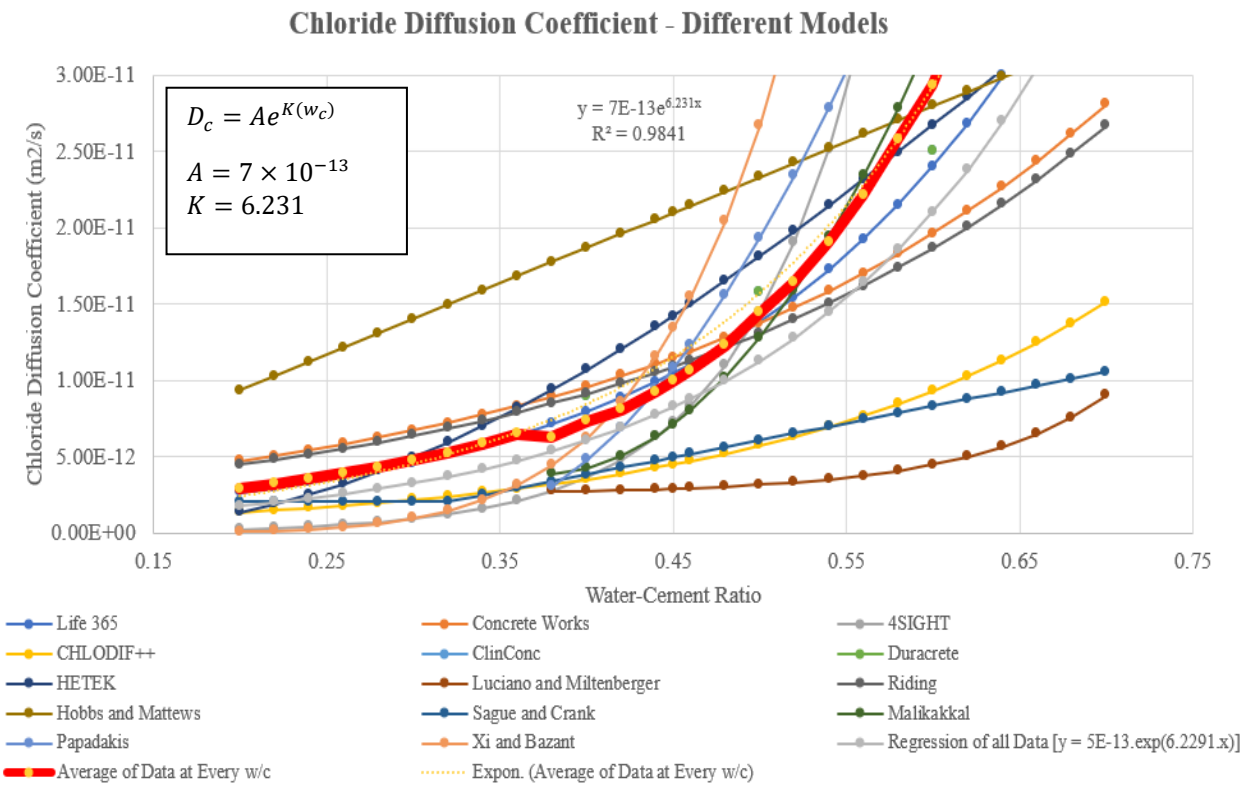

Figure 6.6 - Chloride Diffusion Coefficient (Different Models; Cement Content = 400kg/m3)

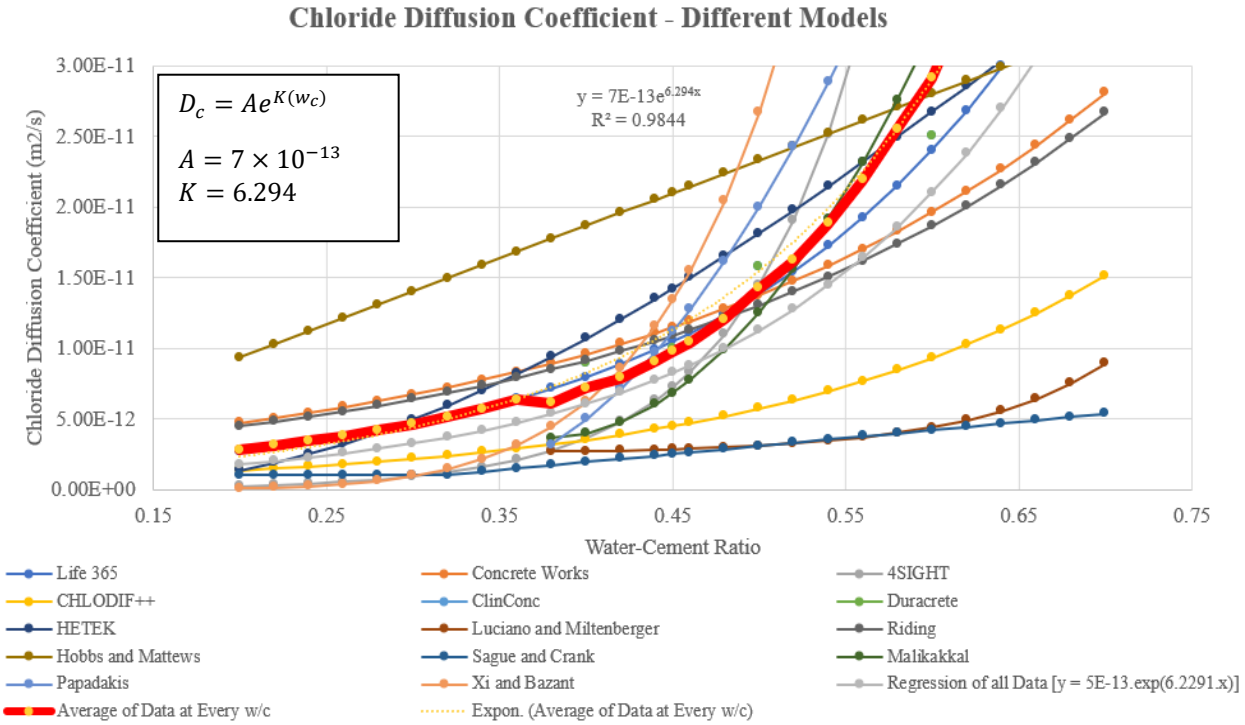

Figure 6.7 - Chloride Diffusion Coefficient (Different Models; Cement Content = 450kg/m3)

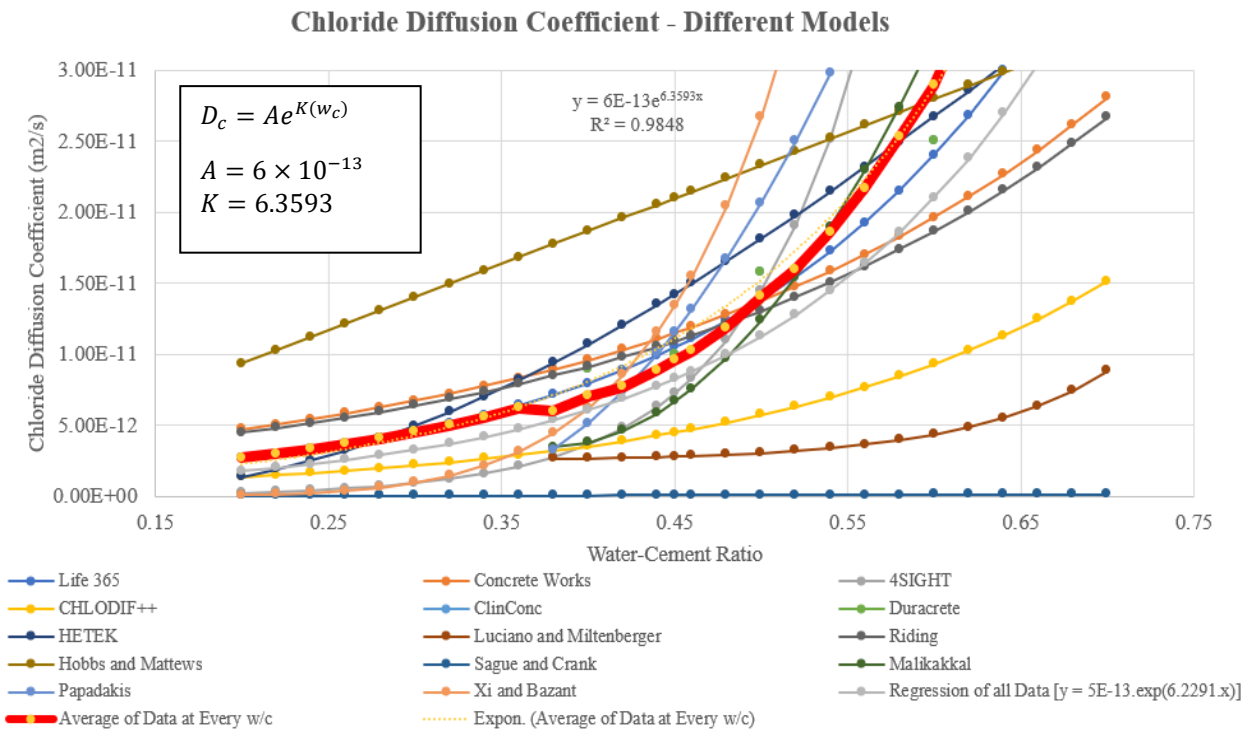

Figure 6.8 - Chloride Diffusion Coefficient (Different Models; Cement Content = 475kg/m3)

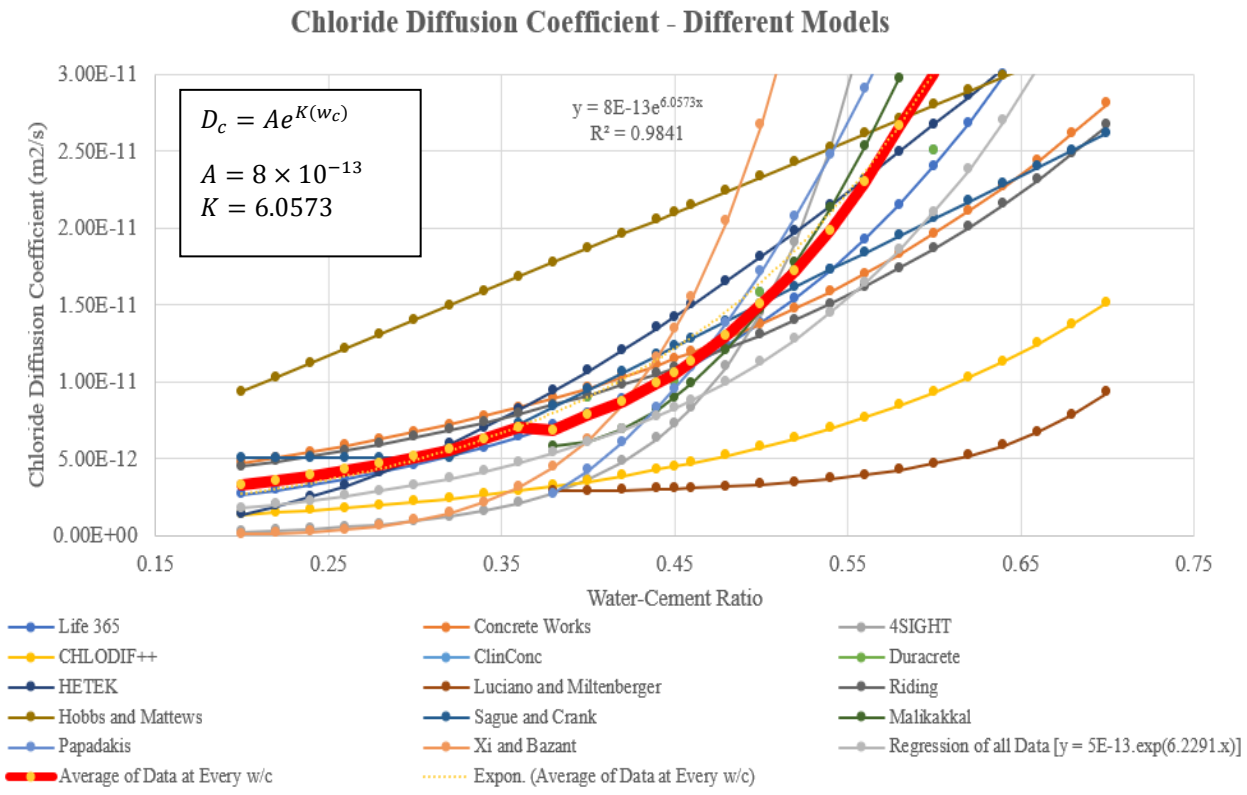

Figure 6.9 - Chloride Diffusion Coefficient (Different Models; Cement Content = 500kg/m3)

The same exercise was made at a fixed water-cement ratio; the various models identified in chapter 1 were used to calculated the chloride diffusion coefficient as a function of the cement content for a fixed water-cement ratio. A summary of the results is presented in figure 6.10. For a fixed water-cement ratio, the increase in cement content is likely to slightly decrease the chloride diffusion coefficient in a linear fit verifying the below form:

$$D_c = -B \times Cem + F \tag{6.9}$$

where Cem is the cement content, B and F are constant values.

Figure 6.10 also show that the constants B and F decrease at lower water-cement ratios.

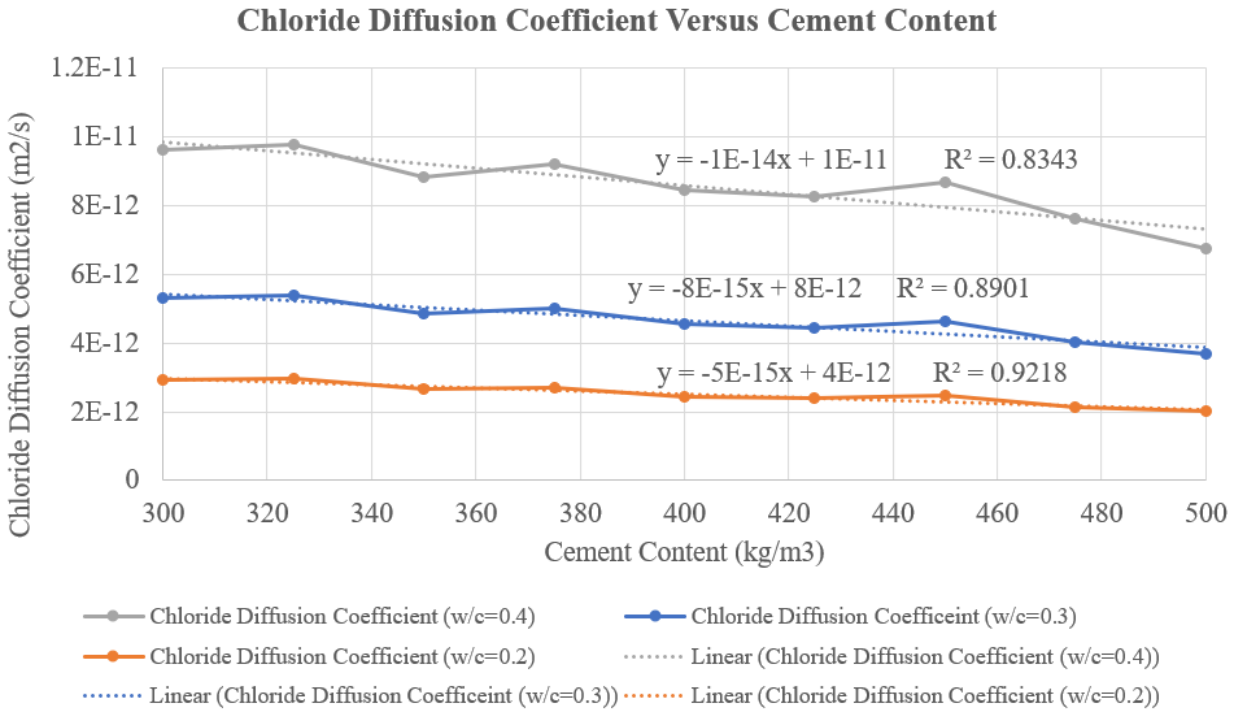

Figure 6.10 - Chloride Diffusion Coefficient as a Function of the Cement Content for a fixed Water-Cement Ratio

Combining the findings of equations (6.8) and (6.9) in order to yield one final equation that takes into consideration the combined effect of the water-cement ratio and the cement content, the following suggested form is obtained.

$$D_{c,ref} = -Ge^{H(w_c)} \times w_c \times Cem + Ie^{J(w_c)} \tag{6.10}$$

where w_c is the water-cement ratio, Cem is the cement content, G, H, I, and J are constants.

The application of this form will be furthermore verified though a non-linear multiple regression taking as input all the average values obtained from figures 6.1 to 6.9 which are tabulated in table 6.3 below for a total of 99 combinations of cement contents and water-cement ratio. The non-linear multiple regression analysis was carried out using the software IBM® SPSS® Statistics Software.

The solution given by this software has concluded the following values for the constants defined in equation (6.10), with a high R-squared value:

$G = 1.55 \times 10^{-14}$ $H = 1.834$ $I = 1.50 \times 10^{-12}$ $J = 5.52$ ($R^2 = 0.991$)

The reference chloride diffusion coefficient when only Portland cement is used as cementitious materials is thus as follows:

$$D_{c,ref} = -1.55 \times 10^{-14}\, e^{1.834 w_c} \times w_c \times Cem + 1.50 \times 10^{-12}\, e^{5.52 w_c} \quad (6.11)$$

where w_c is the water-cement ratio, Cem is the cement content,

Table 6.3 - Average chloride Diffusion coefficient based on literature review

Cement Content	Water Cement Ratio	Average Chloride Diffusion Coefficient Based on Literature Review	Cement Content	Water Cement Ratio	Average Chloride Diffusion Coefficient Based on Literature Review
300	0.5	1.74E-11	425	0.35	6.07E-12
325	0.5	1.77E-11	450	0.35	6.34E-12
350	0.5	1.61E-11	475	0.35	5.56E-12
375	0.5	1.70E-11	500	0.35	5.00E-12
400	0.5	1.58E-11	300	0.32	5.99E-12
425	0.5	1.53E-11	325	0.32	6.06E-12
450	0.5	1.63E-11	350	0.32	5.47E-12
475	0.5	1.44E-11	375	0.32	5.66E-12
500	0.5	1.24E-11	400	0.32	5.14E-12
300	0.47	1.46E-11	425	0.32	5.04E-12
325	0.47	1.48E-11	450	0.32	5.25E-12
350	0.47	1.35E-11	475	0.32	4.59E-12
375	0.47	1.41E-11	500	0.32	4.17E-12
400	0.47	1.31E-11	300	0.29	5.01E-12
425	0.47	1.27E-11	325	0.29	5.07E-12
450	0.47	1.35E-11	350	0.29	4.57E-12
475	0.47	1.19E-11	375	0.29	4.71E-12
500	0.47	1.03E-11	400	0.29	4.26E-12
300	0.44	1.22E-11	425	0.29	4.19E-12
325	0.44	1.24E-11	450	0.29	4.34E-12

350	0.44	1.12E-11	475	0.29	3.79E-12
375	0.44	1.18E-11	500	0.29	3.48E-12
400	0.44	1.09E-11	300	0.26	4.20E-12
425	0.44	1.06E-11	325	0.26	4.24E-12
450	0.44	1.12E-11	350	0.26	3.81E-12
475	0.44	9.85E-12	375	0.26	3.92E-12
500	0.44	8.62E-12	400	0.26	3.54E-12
300	0.41	1.02E-11	425	0.26	3.48E-12
325	0.41	1.04E-11	450	0.26	3.60E-12
350	0.41	9.39E-12	475	0.26	3.13E-12
375	0.41	9.81E-12	500	0.26	2.90E-12
400	0.41	9.01E-12	300	0.23	3.51E-12
425	0.41	8.79E-12	325	0.23	3.54E-12
450	0.41	9.24E-12	350	0.23	3.18E-12
475	0.41	8.14E-12	375	0.23	3.26E-12
500	0.41	7.19E-12	400	0.23	2.93E-12
300	0.38	8.54E-12	425	0.23	2.89E-12
325	0.38	8.67E-12	450	0.23	2.98E-12
350	0.38	7.84E-12	475	0.23	2.59E-12
375	0.38	8.16E-12	500	0.23	2.42E-12
400	0.38	7.47E-12	300	0.2	2.94E-12
425	0.38	7.30E-12	325	0.2	2.96E-12
450	0.38	7.65E-12	350	0.2	2.66E-12
475	0.38	6.72E-12	375	0.2	2.72E-12
500	0.38	6.00E-12	400	0.2	2.43E-12
300	0.35	7.15E-12	425	0.2	2.40E-12
325	0.35	7.25E-12	450	0.2	2.46E-12
350	0.35	6.55E-12	475	0.2	2.14E-12
375	0.35	6.80E-12	500	0.2	2.02E-12
400	0.35	6.20E-12			

The role of the silica fume, fly ash, and slag addition were also discussed in chapter 1 through equations 1.9, 1.12 and 1.13. The final equation for the reference chloride diffusion coefficient will be as follows:

$$D_{c,ref} = \left(-(1.55 \times 10^{-14})e^{1.834(w_c)} \times w_c \times Cem + 1.50 \times 10^{-12}e^{5.52(w_c)}\right) \times e^{-0.165.SF} \times \left(\frac{28}{t}\right)^{(0.2 + 0.4\left(\frac{FA}{50}+\frac{SG}{70}\right))} \quad (6.12)$$

where w_c is the water-cement ratio, Cem is the cement content, SF is the silica fume content, FA is the percentage of fly Ash, SG is the percentage of slag, and t is the age of concrete in days. This equation was developed based on literature review.

This reference chloride diffusion coefficient takes however the aggregate content that should be isolated so its presence would not be duplicated. The details of the aggregate properties used in all the literature review is unknown. For this reason, the following assumptions were made considering that the literature review has used standard materials complying with the international standards as follows:

- Average values for the materials finer than 75 microns, aggregate water absorption, and clay lumps and friable particles were taken equal to 1.5%.
- An average aggregate density of 2700kg/m^3 was selected.
- An average cement density of 3150kg/m^3 was selected
- An average cement surface area of 385 m^2/kg was selected
- Aggregate gradation complying with the requirements of ASTM C33 for nominal maximum aggregate size of 20 mm was selected.
- An average aggregate volume of 67% was selected.

Based on the above, the function f_4 will be equal to the following:

$$f_4(CA, Hy) = 0.23$$

The updated form of equation (6.2) will be as follows:

$$D_{c,ref} = \left(-(6.739 \times 10^{-14})e^{1.834(w_c)} \times w_c \times Cem + 6.522 \times 10^{-12}e^{5.52(w_c)}\right) \times e^{-0.165.SF} \times \left(\frac{28}{t}\right)^{(0.2 + 0.4\left(\frac{FA}{50}+\frac{SG}{70}\right))} \quad (6.13)$$

where w_c is the water-cement ratio, Cem is the cement content, SF is the silica fume content, FA is the percentage of fly Ash, SG is the percentage of slag, and t is the age of concrete in days. This equation was developed based on the literature review.

4. Calculation method and numerical example

The diffusion coefficient at each increment of time t in days is calculated using equation (6.1). Fick' second law is then applied to calculate the chloride ingress in concrete using the following method.

4.1. Solving Fick's differential equation in unidirectional problem using the finite difference method

In saturated conditions, the diffusion of chloride in concrete is considered to follow Fick's second Law. This is given by the following equation:

$$\frac{dC}{dt} = D\frac{d^2C}{dx^2} \tag{6.14}$$

where C is the concentration at a location x and a time t, and D is the diffusion coefficient.

In other terms, the equation can be written as:

$$C_t = DC_{xx} \tag{6.15}$$

The approximation of the left-hand side member of the equation by the Forward Euler method for time derivative implies the following:

$$\frac{dC}{dt} = \frac{C_i^{n+1} - C_i^n}{\Delta t} \tag{6.16}$$

The approximation of the right-hand side of the equation by the central difference method for spatial derivative implies the following:

$$\frac{d^2C}{dx^2} = \frac{C_{i+1}^n - 2C_i^n + C_{i-1}^n}{\Delta x^2} \tag{6.17}$$

It is to note that the index "n" is used for time and the index "i" is used for the position where the following applies:

$0 \leq x \leq I$ and $0 \leq t \leq T$; $\Delta t = \frac{T}{m}$ and $\Delta x = \frac{I}{p+1}$; $t^n = n\Delta t$ and $x_i = i\Delta x$; $0 \leq n \leq m$ and $0 \leq i \leq p+1$

Equation (6.14) becomes:

$$\frac{C_i^{n+1} - C_i^n}{\Delta t} = D\frac{C_{i+1}^n - 2C_i^n + C_{i-1}^n}{\Delta x^2} \tag{6.18}$$

The finite difference at any model in one dimension can be written therefore as:

$$C_i^{n+1} = C_i^n + 2s(C_{i-1}^n - 2C_i^n + C_{i+1}^n) \quad \text{Where} \quad s = \frac{D}{2}\frac{\Delta t}{\Delta x^2} \quad \text{This method is stable for } s < 1. \tag{6.19}$$

The method of crank Nicolson method is obtained by averaging the forward difference approximation and the backward difference approximation and demonstrated to be stable as follows:

$$\frac{C_i^{n+1} - C_i^n}{\Delta t} = \frac{D}{2}\left[\frac{C_{i+1}^n - 2C_i^n + C_{i-1}^n}{\Delta x^2} + \frac{C_{i+1}^{n+1} - 2C_i^{n+1} + C_{i-1}^{n+1}}{\Delta x^2}\right]$$

$$-sC_{i-1}^{n+1} + (1+2s)C_i^{n+1} - sC_{i+1}^{n+1} = sC_{i-1}^n + (1-2s)C_i^n + sC_{i+1}^n \qquad (6.20)$$

Putting the above equation in matrix form, the following implies:

$$[A]\{C^{n+1}\} = [B]\{C^n\} \qquad (6.21)$$

In other terms:

$$\{C^{n+1}\} = [A^{-1}][B]\{C^n\} \qquad (6.22)$$

Where A is a square matrix with (n+1) rows and (n+1) columns as follows:

A =

1	0	0	0	0	0	0	…
-s	1+2s	-s	0	0	0	0	…
0	-s	1+2s	-s	0	0	0	…
0	0	-s	1+2s	-s	0	0	…
0	0	0	-s	1+2s	-s	0	…
…	…	…	…	…	…	…	…

B=

1	0	0	0	0	0	0	…
s	1-2s	s	0	0	0	0	…
0	s	1-2s	s	0	0	0	…
0	0	s	1-2s	s	0	0	…
0	0	0	s	1-2s	s	0	…
…	…	…	…	…	…	…	…

C^{n+1} =

C_0^{n+1}
C_1^{n+1}
C_2^{n+1}
C_3^{n+1}
C_4^{n+1}
…
C_I^{n+1}

C^n =

C_0^n
C_1^n
C_2^n
C_3^n
C_4^n
…
C_I^n

4.2. Solving Fick's differential equation in bidirectional problems using the finite difference method

The same concept applies for bidirectional configuration except that the concentration should be expressed as: C(x,y,t). Similar matrices to the ones described in the unidirectional cases can be yielded whereas the two last matrices are equal to:

C^{n+1} =

$C_{0,0}^{n+1}$	$C_{0,1}^{n+1}$	…	$C_{0,J}^{n+1}$
$C_{1,0}^{n+1}$	$C_{1,1}^{n+1}$	…	$C_{1,J}^{n+1}$
$C_{2,0}^{n+1}$	$C_{2,1}^{n+1}$	…	$C_{2,J}^{n+1}$
$C_{3,0}^{n+1}$	$C_{3,1}^{n+1}$	…	$C_{3,J}^{n+1}$
$C_{4,0}^{n+1}$	$C_{4,1}^{n+1}$	…	$C_{4,J}^{n+1}$
…	…	…	…
$C_{I,0}^{n+1}$	$C_{I,1}^{n+1}$	…	$C_{I,J}^{n+1}$

C^{n} =

$C_{0,0}^{n}$	$C_{0,1}^{n}$	…	$C_{0,J}^{n}$
$C_{1,0}^{n}$	$C_{1,1}^{n}$	…	$C_{1,J}^{n}$
$C_{2,0}^{n}$	$C_{2,1}^{n}$	…	$C_{2,J}^{n}$
$C_{3,0}^{n}$	$C_{3,1}^{n}$	…	$C_{3,J}^{n}$
$C_{4,0}^{n}$	$C_{4,1}^{n}$	…	$C_{4,J}^{n}$
…	…	…	…
$C_{i,0}^{n}$	$C_{I,1}^{n}$	…	$C_{I,J}^{n}$

Taking into consideration the following equation:

$$\frac{dC}{dt} = D\left[\frac{d^2C}{dx^2} + \frac{d^2C}{dy^2}\right] \tag{6.23}$$

and

$$\frac{C_{i,j}^{n+1} - C_{i,j}^{n}}{\Delta t} = \frac{D}{2}\left[\frac{C_{i+1,j}^{n} - 2C_{i,j}^{n} + C_{i-1,j}^{n}}{\Delta x^2} + \frac{C_{i+1,j}^{n+1} - 2C_{i,j}^{n+1} + C_{i-1,j}^{n+1}}{\Delta x^2} + \frac{C_{i,j+1}^{n} - 2C_{i,j}^{n} + C_{i,j-1}^{n}}{\Delta y^2} + \frac{C_{i,j+1}^{n+1} - 2C_{i,j}^{n+1} + C_{i,j-1}^{n+1}}{\Delta y^2}\right] \tag{6.24}$$

4.3. Discretization example

The finite difference method explained in sections 4.1 and 4.2 are illustrated in figures 6.11 to 6.12 taking as example a beam with two layers or steel and different cracks perpendicular to the surface. The meshing in the direction perpendicular to the cracks should have an identical width to that considered in the testing campaign as explained in chapter 5; a mesh width of 94 mm should thus be considered.

At the cracks location and since the crack width will decrease from a maximum value at the surface to zero at the end of the cracks depth, the meshing in the direction parallel to the cracks can be divided to the level of requested accuracy, taking 6 layers as an example in figure 6.12, where each layer will have the diffusion coefficient attributed to the crack width. The red dots in figure 6.12 forms the nods of the discretization. The decrease in cracks width the maximum value to zero is taken linearly proportional following six value where the first value is the crack width at the surface and the sixth one is equal to zero. Additional layers of nods should be placed at the points of interest, which are the cover of the reinforcing steel.

At each time increments in days, the temperature profile on the nodes is calculated based on the ambient temperature and the heat transfer mechanism in concrete. The relative humidity in concrete follows in the same concept going from the ambient relative humidity. The chloride diffusion coefficient is then calculated at the specific time increment, at each node (x,y) using equation (6.1). The matrices [A] and [B] defined in section 4.2 are then concluded.

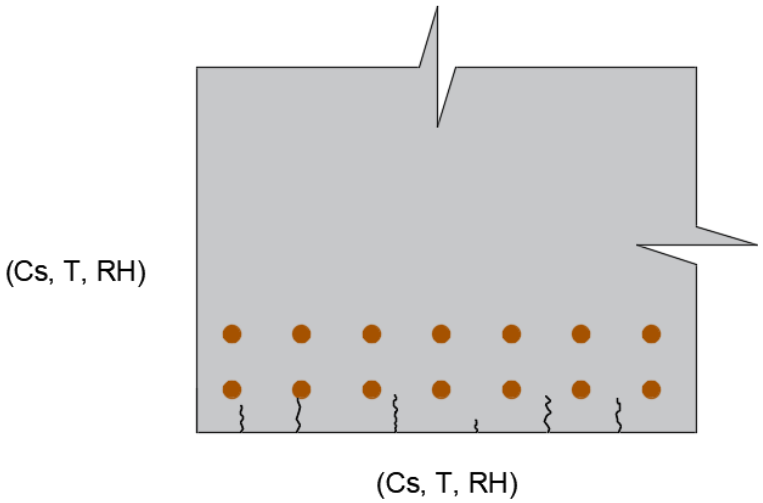

Figure 6.11 - Beam Subjected to a chloride concentration Cs, an ambient temperature T, and a relative humidity RH

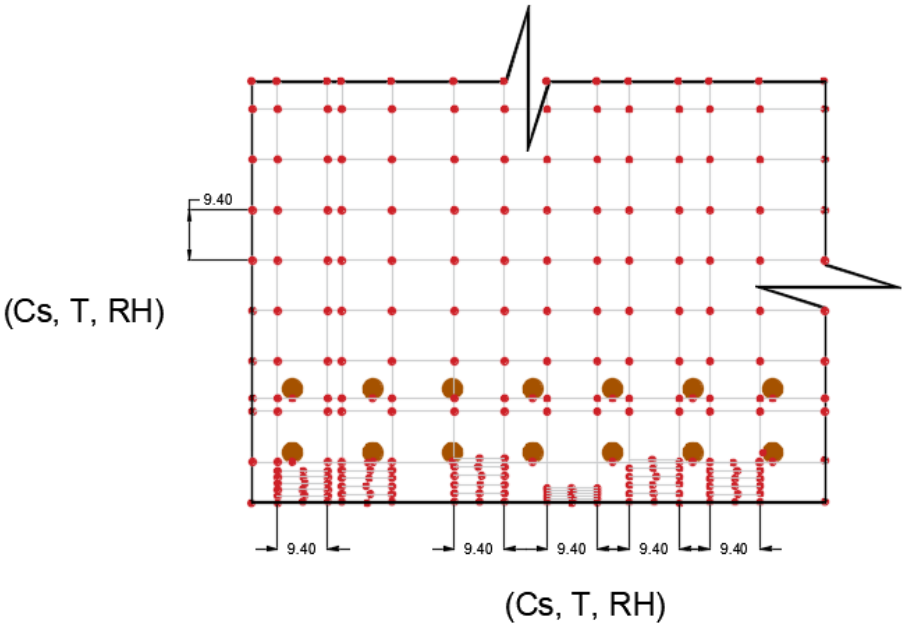

Figure 6.12 – Calculations nodes

The initial chloride concentration defined by the matrix $\{C^n\}$ is equal to the initial chloride concentration. The chloride concentration at the nodes at a time t defined by the matrix $\{C^{n+1}\}$ is then calculated at each time increment using equation (6.22). Figure 6.13 presents the steps explained in this paragraph.

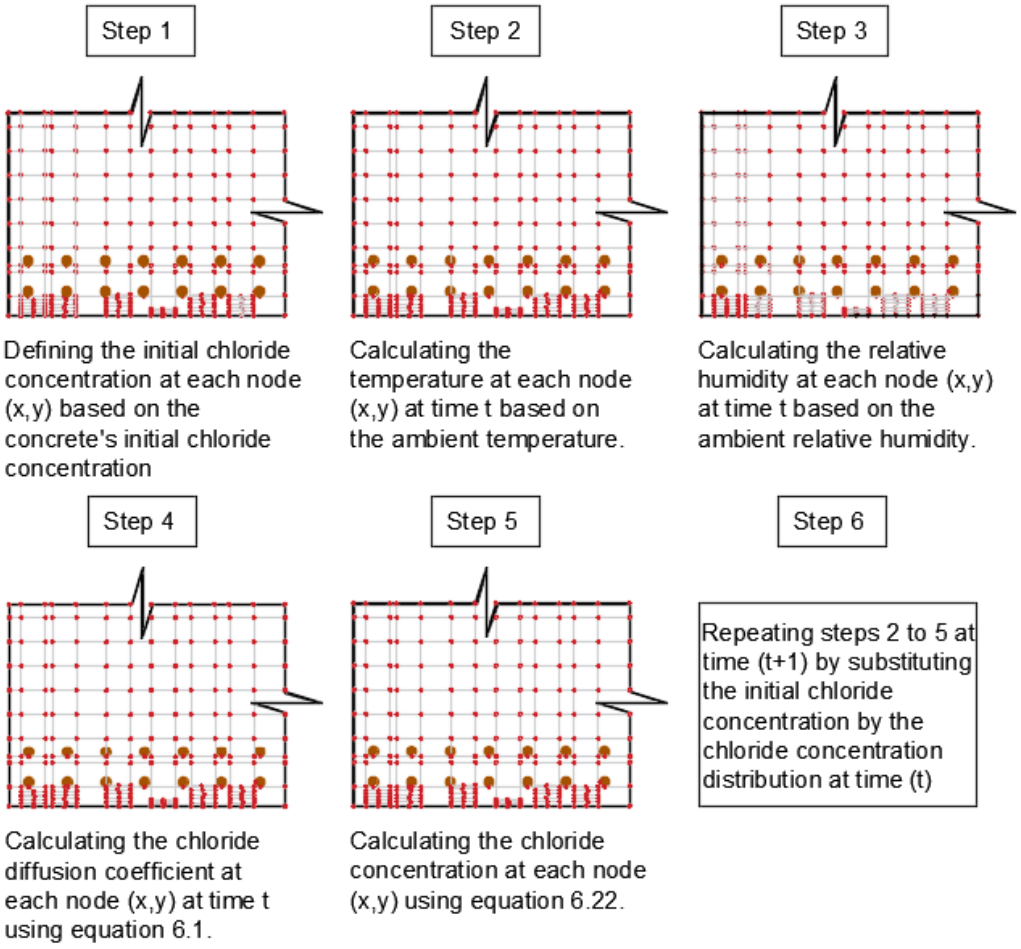

Figure 6.13 - Calculation Steps

5. Calculating the chloride diffusion coefficient – a numerical example

An Excel sheet was made to calculate the diffusion coefficient using equation (6.1) for the first 150 years with varying environmental conditions. Fick' second law is then used to calculate the chloride content at a certain depth at each increment t. The Microsoft Excel sheet format is attached as appendix 6.1. the following sections describe the input needed, computational methods, output graphs, sensitivity analysis, and comparison with the existing models.

5.1. Input parameters

The input parameters are illustrated in figures 6.14 and 6.15, they are divided into the four categories defined earlier as follows:

- Environmental parameters, including the chloride surface concentration, temperature and relative humidity.

- Concrete properties parameters, including the following: Concrete composition, cementitious materials properties, and aggregate properties. The interfacial transition zone's thickness is based on the literature review made in chapter 2, it is taken as 5 µm when silica fume is used and 50 µm otherwise.
- Workmanship parameters, including the curing time. The initial mixing time and the consolidation level were demonstrated to have no effect on the diffusion, there rather affect other chloride transportation properties. They were thus omitted from the input window.
- Post-placing parameters including the crack width and depth.

The critical chloride threshold that will initiate the reinforcing steel corrosion is also included as an input parameter that will be defined by the user. The reason goes back to the several available publications and literature that define this value. This value is still contradictory among the several researches as was initially the case for the chloride diffusion coefficient. Defining an accurate threshold that may initiate the reinforcing steel corrosion is out of this thesis's scope.

Chloride Diffusion Calculation

Input

Concrete Mix Design		**Aggregate Properties**					
Cement Content (kg/m3)	400	Aggregate Sieves Opening Sizes (mm)					
Silica Fume Content (kg/m3)	25	Aggregate Sieves		Percentage Retained Between the Seives (%)			
Fly Ash Content (kg/m3)	0	Larger Size	Smaller Size	Coarse Aggregate 1	Coarse Aggregate 2	Fine Aggregate 1	Fine Aggregate 2
Slag Content (kg/m3)	0						
Water Content (kg/m3)	160						
Quantity of Coarse Aggregate 1 (kg/m3)	947	100	90	0.00%	0.00%	0.00%	0.00%
Quantity of Coarse Aggregate 2 (kg/m3)	0	90	75	0.00%	0.00%	0.00%	0.00%
Quantity of Fine Aggregate 1 (kg/m3)	865	75	63	0.00%	0.00%	0.00%	0.00%
Quantity of Fine Aggregate 2 (kg/m3)	0	63	50	0.00%	0.00%	0.00%	0.00%
Admixture 1 (kg/m3)	2	50	37.5	0.00%	0.00%	0.00%	0.00%
Admixture 2 (kg/m3)	3	37.5	25	0.00%	0.00%	0.00%	0.00%
Admixture 3 (kg/m3)	4	25	19	0.00%	0.00%	0.00%	0.00%
Concrete Mix Design Properties		19	12.5	0.00%	0.00%	0.00%	0.00%
Water-Cement Ratio	0.38	12.5	9.5	6.80%	6.80%	0.00%	0.00%
Total Cementitious Materials Content (kg/m3)	425	9.5	4.75	83.10%	83.10%	4.00%	4.00%
Silica Fume Percentage from the total Cementitious Materials (%)	5.88%	4.75	2.36	9.40%	9.40%	15.00%	15.00%
Fly Ash Percentage from the total Cementitious Materials (%)	0.00%	2.36	1.18	0.10%	0.10%	22.00%	22.00%
Slag Percentage from the total Cementitious Materials (%)	0.00%	1.18	0.6	0.10%	0.10%	23.00%	23.00%
Cement Properties		0.6	0.3	0.10%	0.10%	20.00%	20.00%
ρc Density of Cement (kg/m3)	3150	0.3	0.15	0.10%	0.10%	12.00%	12.00%
Cement Actual Surface Area (m^2/kg)	385	0.15	0.075	0.10%	0.10%	1.80%	1.80%
Alite Percentage in Cement	63.00%	Pan		0.20%	0.20%	2.20%	2.20%
Belite Percentage in Cement	10.00%	Materials Finer than 75 Microns (%)					1.50%
Aluminate Percentage in Cement	5.00%	Aggregate Water Absorption (%)					1.50%
Ferrite Percentage in Cement	2.00%	Clay Lumps and Friable Particles in Aggregate (%)					1.50%

Aggregate Density							
Coarse Aggregate 1 (kg/m3):	2700	Coarse Aggregate 2 (kg/m3):	2700	Fine Aggregate 1 (kg/m3):	2700	Fine Aggregate 2 (kg/m3):	2700

Cover Conditions							
Surface Chloride Concentration (%)	5	Concrete Cover (mm):	25	Crack Width (mm):	0.12	Crack Depth(mm):	50
Concrete Initial Chloride Content (%)	0.02						
Initial Curing Time (Days)						7	
Studied Chloride Penetration Depth (mm)						25	
Critical Chloride Treshold (%)						5.00%	

Figure 6.14 - Input Parameters (Concrete Properties, Workmanship, and post-placing)

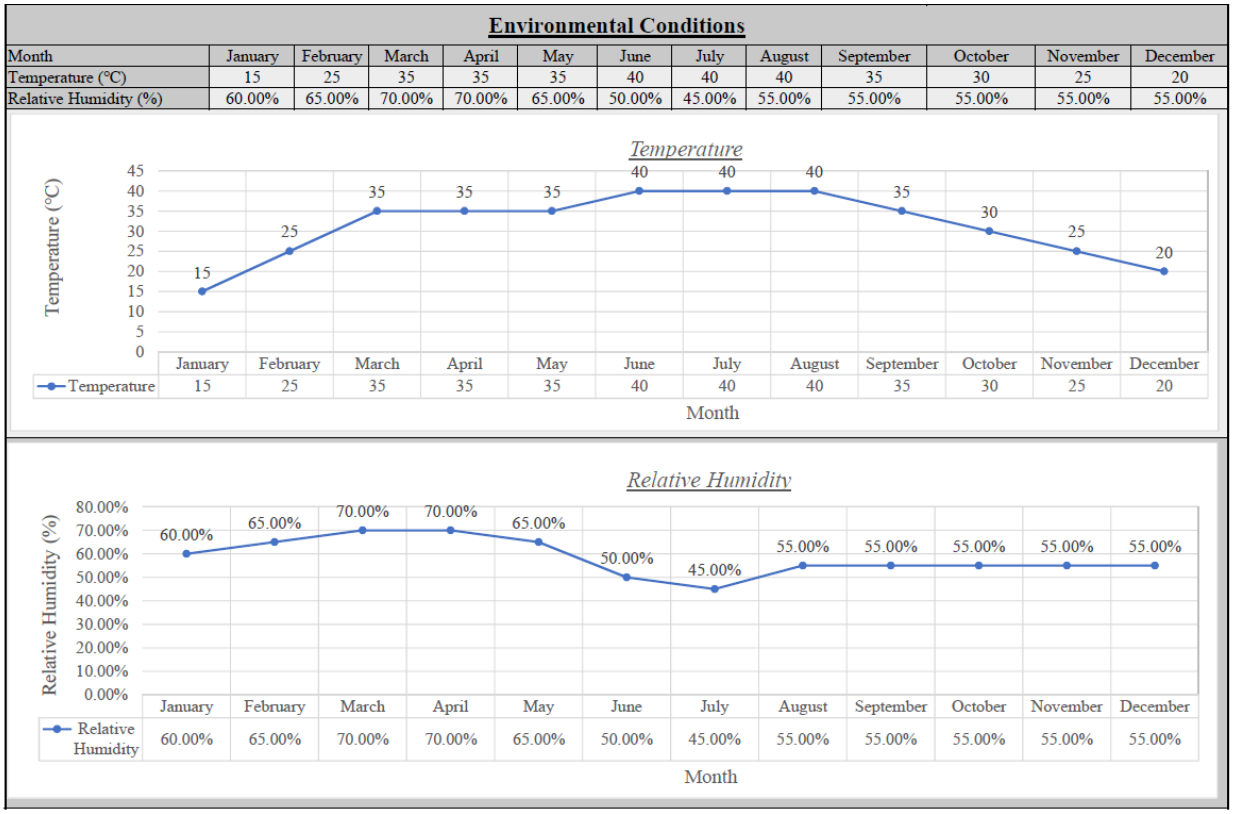

Figure 6.15 – Environmental input parameters

5.2. Computational method and output graphs

Once the input parameters are defined, and on a separate hidden Microsoft Excel sheet, illustrated in figure 6.16, the eight functions defined in paragraph 2 are calculated at each increment time t in days, as follows:

- The function $f_1(T)$ is calculated based on the temperature using equation (6.2).
- The function $f_2(h)$ is calculated using the corresponding relative humidity and equation (6.3).
- The function $f_3(x)$ is calculated at the depth x from the surface using equation (6.4).
- The calculations steps discussed in detail in chapter 2 are made separately to calculate the function $f_4(CA, Hy)$. This function changes at every time increment t since the hydration coefficient changes. This function takes into consideration, in addition to the defined aggregate properties, the cement characteristics.
- The tricalcium aluminate function is calculated using equation (6.5).
- Based on the water-cement ratio and the crack width values concluded from the input parameters, the function $f_8(cw, w_c)$ is calculated using equation (6.7). The function $f_6(Cs)$ and $f_7(Mi)$ are taken equal to 1 as concluded from chapter 4.
- The reference chloride diffusion coefficient is calculated based on the concrete's input parameters using equation (6.13).

The resulting chloride diffusion coefficient at a time t and a depth x will thus be equal to the product of the eight functions and the reference chloride diffusion coefficient.

As the crack width is maximum at the surface of concrete and equal to zero at the crack depth, the same calculation is made at a gradually decreasing crack width. The crack width is considered to linearly decrease from the crack width at the surface to zero at the crack depth. The chloride diffusion coefficient is thus an average of six values with gradually decreasing crack width.

The Microsoft Excel sheet will result in a chloride diffusion coefficient variation at a certain depth as illustrated in figure 6.17.

Output - Chloride Diffusion Calcualtion

time (t) in days	Depth (x) (mm)	Absolute Temperature (K)	Relative Humidity (%)	Crack Width (mm)	Weighted Cement Degree of Hydration α	f_1 (T)	f_2 (h)	f_3 (x)	f_4 (CA,Hy)	f_5 (C3A)	f_6 (Cs)	f_7 (Mi)	f_8 (CW,w/c)	Reference Chloride Diffusion Coefficient (m2/s)	Final Chloride Diffusion Coefficient (m2/s)
0.1	0	289.15	100.00%	0.12	0.016	0.69549	1	0.53	0.2339772	0.438357	1	1	1.45428	9.35E-11	5.142E-12
1	0	289.15	100.00%	0.12	0.053419098	0.69549	1	0.53	0.2339772	0.438357	1	1	1.45428	5.9E-11	3.244E-12
2	0	289.15	100.00%	0.12	0.454348806	0.69549	1	0.53	0.2339772	0.438357	1	1	1.45428	5.14E-11	2.824E-12
3	0	289.15	100.00%	0.12	0.515834907	0.69549	1	0.53	0.2339772	0.438357	1	1	1.45428	4.74E-11	2.604E-12
4	0	289.15	100.00%	0.12	0.543740014	0.69549	1	0.53	0.2339772	0.438357	1	1	1.45428	4.47E-11	2.459E-12
5	0	289.15	100.00%	0.12	0.563307313	0.69549	1	0.53	0.2339772	0.438357	1	1	1.45428	4.28E-11	2.351E-12
6	0	289.15	100.00%	0.12	0.578341816	0.69549	1	0.53	0.2339772	0.438357	1	1	1.45428	4.12E-11	2.267E-12
7	0	289.15	100.00%	0.12	0.590492983	0.69549	1	0.53	0.2339772	0.438357	1	1	1.45428	4E-11	2.198E-12
8	0	289.15	60.00%	0.12	0.600602437	0.69549	0.13239	0.53	0.2339772	0.438357	1	1	1.45428	3.89E-11	2.834E-13

Figure 6.16 - Chloride diffusion calculation

Chloride Diffusion Coefficient Development (m^2/s)

Year	Month											
	January	February	March	April	May	June	July	August	September	October	November	December
1	3.371E-13	7.63E-13	1.78E-12	1.68E-12	1.02E-12	3.52E-13	2.37E-13	4.9E-13	3.80548E-13	2.93826E-13	2.2575E-13	1.7225E-13
2	1.988E-13	5.11E-13	1.28E-12	1.27E-12	7.95E-13	2.82E-13	1.94E-13	4.08E-13	3.20857E-13	2.50764E-13	1.9463E-13	1.4987E-13
3	1.743E-13	4.51E-13	1.14E-12	1.13E-12	7.14E-13	2.54E-13	1.76E-13	3.71E-13	2.93033E-13	2.29803E-13	1.7891E-13	1.3817E-13
4	1.611E-13	4.18E-13	1.06E-12	1.05E-12	6.66E-13	2.38E-13	1.65E-13	3.48E-13	2.75368E-13	2.16298E-13	1.6864E-13	1.3043E-13
5	1.523E-13	3.96E-13	1E-12	1E-12	6.33E-13	2.26E-13	1.57E-13	3.32E-13	2.6263E-13	2.06486E-13	1.6114E-13	1.2473E-13
6	1.458E-13	3.79E-13	9.63E-13	9.6E-13	6.08E-13	2.17E-13	1.51E-13	3.19E-13	2.5277E-13	1.98855E-13	1.5527E-13	1.2026E-13
7	1.406E-13	3.66E-13	9.3E-13	9.28E-13	5.87E-13	2.1E-13	1.46E-13	3.09E-13	2.44783E-13	1.92656E-13	1.5049E-13	1.1661E-13
8	1.364E-13	3.55E-13	9.03E-13	9.01E-13	5.7E-13	2.04E-13	1.42E-13	3E-13	2.38105E-13	1.8746E-13	1.4648E-13	1.1353E-13
9	1.328E-13	3.46E-13	8.8E-13	8.78E-13	5.56E-13	1.99E-13	1.38E-13	2.93E-13	2.3239E-13	1.83006E-13	1.4303E-13	1.1089E-13
10	1.298E-13	3.38E-13	8.6E-13	8.58E-13	5.44E-13	1.95E-13	1.35E-13	2.87E-13	2.27411E-13	1.7912E-13	1.4002E-13	1.0857E-13
25	1.068E-13	2.78E-13	7.09E-13	7.08E-13	4.49E-13	1.61E-13	1.12E-13	2.38E-13	1.88737E-13	1.48815E-13	1.1645E-13	9.0388E-14
50	9.259E-14	2.41E-13	6.15E-13	6.15E-13	3.9E-13	1.4E-13	9.73E-14	2.07E-13	1.64134E-13	1.29461E-13	1.0134E-13	7.8685E-14
60	8.922E-14	2.33E-13	5.93E-13	5.93E-13	3.76E-13	1.35E-13	9.38E-14	1.99E-13	1.5823E-13	1.24811E-13	9.7701E-14	7.5867E-14
75	8.527E-14	2.22E-13	5.67E-13	5.67E-13	3.6E-13	1.29E-13	8.96E-14	1.9E-13	1.51297E-13	1.19349E-13	9.3431E-14	7.2556E-14
100	8.045E-14	2.1E-13	5.35E-13	5.35E-13	3.39E-13	1.22E-13	8.46E-14	1.8E-13	1.42813E-13	1.12663E-13	8.8202E-14	6.8499E-14
125	7.691E-14	2.01E-13	5.11E-13	5.11E-13	3.24E-13	1.16E-13	8.09E-14	1.72E-13	1.36566E-13	1.07738E-13	8.4349E-14	6.5509E-14
150	7.414E-14	1.93E-13	4.93E-13	4.93E-13	3.13E-13	1.12E-13	7.8E-14	1.66E-13	1.31667E-13	1.03876E-13	8.1327E-14	6.3163E-14

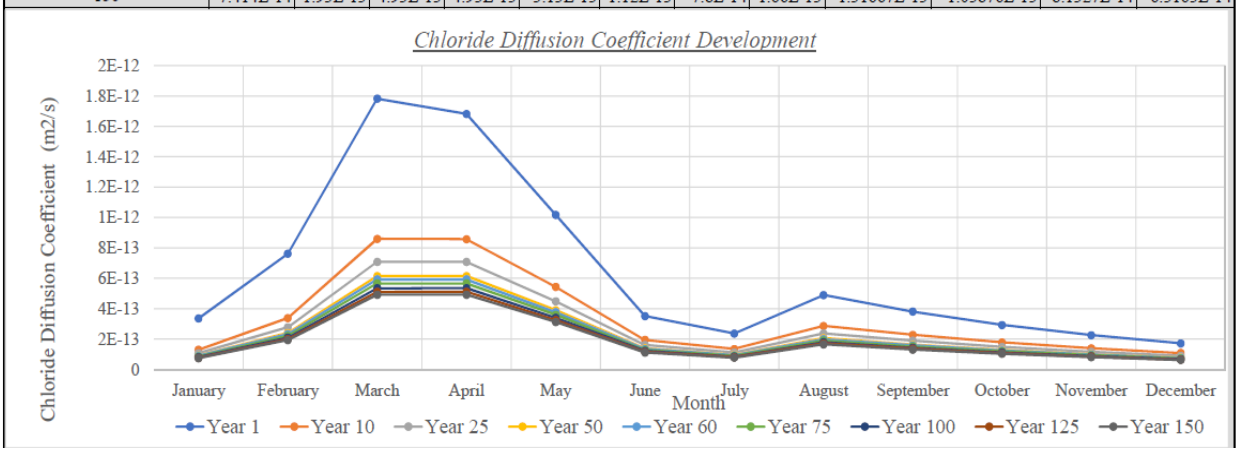

Figure 6.17 - Chloride diffusion coefficient development

Based on the chloride diffusion coefficient, the chloride surface concentration, and time t, the chloride content at a certain depth is calculated using Fick's second law. This output is illustrated in figure 6.18.

The chloride content is then compared to the critical chloride threshold that may initiate the reinforcing steel corrosion. This parameter is defined by the user. The end of the initiation phase is considered completed once the chloride content at the depth x reaches the critical chloride concentration. The propagation phase is considered equal to 6 years based on the literature made in chapter 1.

The Excel sheet thus gives the initiation phase period and the concrete service life which is equal to the initiate phase period and the propagation phase period. As the Excel sheet is limited to a calculation period of 150 years, when the initiation period exceeds this duration, the concrete service life will output "+150 years".

									Chloride Content at depth X(mm)		25	
Year	Month											
	January	February	March	April	May	June	July	August	September	October	November	December
1	0.020	0.020	0.020	0.020	0.020	0.020	0.020	0.020	0.020	0.020	0.020	0.020
2	0.023	0.024	0.029	0.034	0.039	0.040	0.042	0.045	0.047	0.049	0.050	0.052
3	0.097	0.103	0.119	0.135	0.146	0.149	0.152	0.158	0.163	0.167	0.169	0.172
4	0.276	0.284	0.304	0.323	0.336	0.341	0.344	0.351	0.356	0.360	0.363	0.366
5	0.510	0.517	0.537	0.556	0.568	0.572	0.575	0.582	0.587	0.591	0.594	0.596
6	0.759	0.765	0.783	0.799	0.810	0.814	0.816	0.822	0.826	0.830	0.832	0.834
7	1.002	1.008	1.022	1.036	1.045	1.049	1.051	1.056	1.059	1.062	1.064	1.066
8	1.231	1.235	1.248	1.259	1.267	1.270	1.271	1.275	1.279	1.281	1.283	1.284
9	1.442	1.445	1.456	1.465	1.472	1.474	1.476	1.479	1.481	1.484	1.485	1.486
10	1.634	1.637	1.646	1.654	1.660	1.661	1.663	1.666	1.668	1.669	1.671	1.672
25	3.177	3.178	3.179	3.180	3.181	3.181	3.181	3.181	3.182	3.182	3.182	3.182
50	3.957	3.957	3.957	3.957	3.957	3.957	3.957	3.957	3.957	3.957	3.957	3.958
60	4.105	4.105	4.105	4.106	4.106	4.106	4.106	4.106	4.106	4.106	4.106	4.106
75	4.261	4.261	4.261	4.261	4.261	4.261	4.261	4.261	4.261	4.261	4.261	4.261
100	4.424	4.424	4.424	4.424	4.424	4.424	4.424	4.424	4.424	4.424	4.424	4.424
125	4.526	4.526	4.526	4.526	4.526	4.526	4.526	4.526	4.526	4.526	4.526	4.526
150	4.596	4.596	4.596	4.596	4.596	4.596	4.596	4.596	4.596	4.596	4.596	4.596

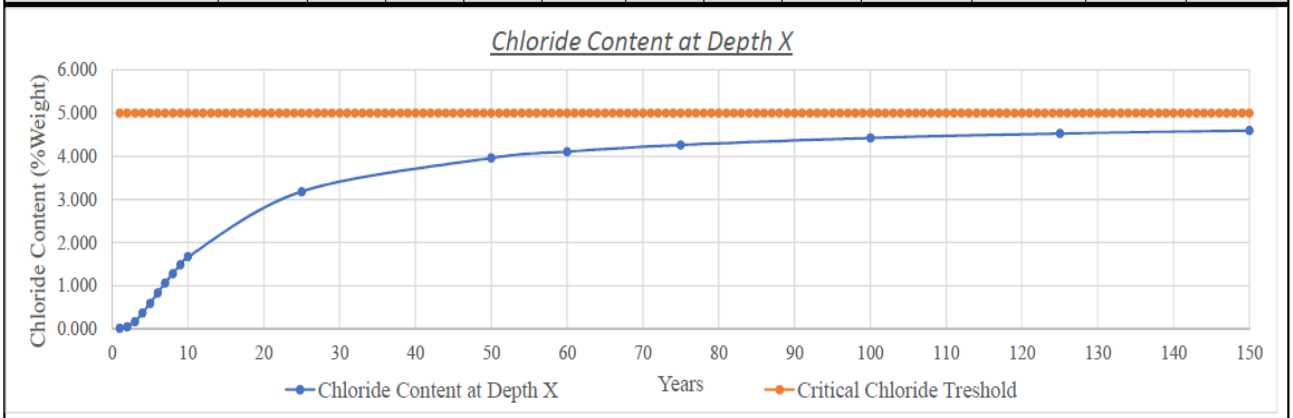

End of Initiation Phase (Years)	+150
Concrete Service Life (Years)	+150

Figure 6.18 - Chloride concentration at a depth *x*

5.3. Parametric analysis

A parametric analysis was made to assess the effect of each of the parameters on the concrete service life. A typical concrete mix design using type I cement (C3A content of 9%) was taken as example as illustrated in figure 6.19, selected parameters were changed, and the resulting concrete service life interpreted accordingly.

Chloride Diffusion Calculation

Input

Concrete Mix Design		Aggregate Properties					
Cement Content (kg/m3)	400	Aggregate Sieves Opening Sizes (mm)					
Silica Fume Content (kg/m3)	25	Aggregate Sieves		Percentage Retained Between the Seives (%)			
Fly Ash Content (kg/m3)	0	Larger Size	Smaller Size	Coarse Aggregate 1	Coarse Aggregate 2	Fine Aggregate 1	Fine Aggregate 2
Slag Content (kg/m3)	0						
Water Content (kg/m3)	160						
Quantity of Coarse Aggregate 1 (kg/m3)	947	100	90	0.00%	0.00%	0.00%	0.00%
Quantity of Coarse Aggregate 2 (kg/m3)	0	90	75	0.00%	0.00%	0.00%	0.00%
Quantity of Fine Aggregate 1 (kg/m3)	865	75	63	0.00%	0.00%	0.00%	0.00%
Quantity of Fine Aggregate 2 (kg/m3)	0	63	50	0.00%	0.00%	0.00%	0.00%
Admixture 1 (kg/m3)	2	50	37.5	0.00%	0.00%	0.00%	0.00%
Admixture 2 (kg/m3)	3	37.5	25	0.00%	0.00%	0.00%	0.00%
Admixture 3 (kg/m3)	4	25	19	0.00%	0.00%	0.00%	0.00%
Concrete Mix Design Properties		19	12.5	0.00%	0.00%	0.00%	0.00%
Water-Cement Ratio	0.38	12.5	9.5	6.80%	6.80%	0.00%	0.00%
Total Cementitious Materials Content (kg/m3)	425	9.5	4.75	83.10%	83.10%	4.00%	4.00%
Silica Fume Percentage from the total Cementitious Materials (%)	5.88%	4.75	2.36	9.40%	9.40%	15.00%	15.00%
Fly Ash Percentage from the total Cementitious Materials (%)	0.00%	2.36	1.18	0.10%	0.10%	22.00%	22.00%
Slag Percentage from the total Cementitious Materials (%)	0.00%	1.18	0.6	0.10%	0.10%	23.00%	23.00%
Cement Properties		0.6	0.3	0.10%	0.10%	20.00%	20.00%
ρc Density of Cement (kg/m3)	3150	0.3	0.15	0.10%	0.10%	12.00%	12.00%
Cement Actual Surface Area (m^2/kg)	385	0.15	0.075	0.10%	0.10%	1.80%	1.80%
Alite Percentage in Cement	63.00%	Pan		0.20%	0.20%	2.20%	2.20%
Belite Percentage in Cement	10.00%	Materials Finer than 75 Microns (%)					1.50%
Aluminate Percentage in Cement	9.00%	Aggregate Water Absorption (%)					1.50%
Ferrite Percentage in Cement	2.00%	Clay Lumps and Friable Particles in Aggregate (%)					1.50%

Aggregate Density

Coarse Aggregate 1 (kg/m3):	2700	Coarse Aggregate 2 (kg/m3):	2700	Fine Aggregate 1 (kg/m3):	2700	Fine Aggregate 2 (kg/m3):	2700

Cover Conditions

Surface Chloride Concentration (%)	3	Concrete Cover (mm):	50	Crack Width (mm):	0	Crack Depth(mm):	0.0
Concrete Initial Chloride Content (%)	0.02						
Initial Curing Time (Days)						7	
Studied Chloride Penetration Depth (mm)						50	
Critical Chloride Treshold (%)						1.20%	

Figure 6.19 - Example concrete Mix design used for sensitivity analysis

- Concrete temperature variations:

An average yearly concrete temperature was taken equal to 20°C then increased by five increments of 5°C each. Various other input parameters were kept constant with a relative humidity of 60%, using an uncracked concrete. The resulting chloride diffusion and concrete service life are given in table 6.4.

Going from a temperature of 20°C to 45°C, the chloride diffusion coefficient almost doubled for every 15°C increase in temperature. The resulting service life was almost half when comparing the corresponding values at the two ultimate temperature values.

Table 6.4 - Effect of temperature

Average Yearly Temperature (°C)	Chloride Diffusion Coefficient after 50 years (m^2/s)	Resulting Concrete Service Life (years)
20	1.10×10^{-14}	107
25	1.41×10^{-14}	94
30	1.81×10^{-14}	82
35	2.29×10^{-14}	73
40	2.88×10^{-14}	65
45	3.60×10^{-14}	58

- Concrete relative humidity variations:

The same exercise made in the previous paragraphs was made while keeping all the input parameters constant and varying the relative humidity from 50% to 100% based on 10% increments. The average yearly temperature was taken equal to 25°C. The resulting chloride diffusion coefficient and concrete service life are given in table 6.5.

The chloride diffusion coefficient increased drastically with increasing relative humidity; the resulting service life dropped as well by almost a factor of 4. The increase in relative humidity beyond 80% seems to have a smaller effect on the chloride diffusion in concrete.

Table 6.5 - Effect of relative humidity

Average Yearly Relative Humidity (%)	Chloride Diffusion Coefficient after 50 years (m^2/s)	Resulting Concrete Service Life (years)
50	6.29×10^{-15}	144
60	1.41×10^{-14}	94
70	3.48×10^{-14}	59
80	7.58×10^{-14}	40
90	1.04×10^{-13}	34
100	1.07×10^{-13}	34

- Aggregate content variations:

In order to conduct an aggregate content variation while keeping a total concrete volume of $1m^3$, the cementitious materials content should vary as well. A total of five concrete mixes were simulated using the Excel sheet generated, the weight of cementitious materials and aggregate were included in table 6.6 along with the corresponding variations in chloride diffusion coefficient and resulting service life. The same water cement ratio was used in the five mixes. The temperature was taken equal to 25°C and the relative humidity equal to 60%. Variation in aggregate quantity

may reduce the concrete service life by approximately 20% for an equivalent reduction in coarse aggregate. It is to note that the increase in cement for a fixed water-cement ratio has not contributed in an increased service life. The results below show that a concrete with an additional 250 kg/m^3 of cement will result in 23% less service life due to the decrease in aggregate quantity.

Table 6.6 - Effect of aggregate quantity

Cement quantity (kg/m^3)	Silica fume quantity (kg/m^3)	Total aggregate quantity (kg/m^3)	Chloride Diffusion Coefficient after 50 years (m^2/s)	Resulting Concrete Service Life (years)
300	25	1982	1.16×10^{-14}	104
350	25	1892	1.36×10^{-14}	96
400	25	1797	1.55×10^{-14}	89
450	25	1707	1.69×10^{-14}	85
500	25	1612	1.82×10^{-13}	82
550	25	1517	1.07×10^{-13}	80

- Materials finer than 75µm, aggregate absorption, and clay lumps and friable particle variations:

A reference concrete mix with various combinations of aggregate properties were considered and the corresponding chloride diffusion coefficient and concrete service life were calculated. The different combinations are given in table 6.7. Varying the aggregate properties in terms of Materials finer than 75µm, aggregate absorption, and clay lumps and friable particle, percentages, from 1 to 10% may reduce the concrete service life by approximately 20%. The results of these variations are included in table 6.5.

Table 6.7 - Effect of aggregate properties

Materials Finer than 75 µm (%)	Aggregate Absorption (%)	Clay Lumps and Friable Particles (%)	Chloride Diffusion Coefficient after 50 years (m^2/s)	Resulting Concrete Service Life (years)
1	1	1	1.46×10^{-14}	92
3	3	3	1.62×10^{-14}	87
5	5	5	1.78×10^{-14}	83
7	7	7	1.93×10^{-14}	79
9	9	9	2.09×10^{-14}	76
11	11	11	2.25×10^{-14}	73

- Tricalcium aluminate variations:

Various tricalcium aluminate content were considered in calculating the chloride diffusion coefficient and resulting service life of a refence concrete mix design as given in table 6.8. The results show the major effect of the tricalcium aluminate in binding the chloride ions and reducing

the resulting chloride diffusion coefficient and concrete service life. Varying the tricalcium aluminate content from 4 to 14% has increased the concrete service life almost 6 times.

Table 6.8 - Effect of Tricalcium Aluminate

Tricalcium Aluminate percentage (%)	Chloride Diffusion Coefficient after 50 years (m^2/s)	Resulting Concrete Service Life (years)
4	2.00×10^{-13}	25
6	6.80×10^{-14}	42
8	3.11×10^{-14}	62
10	1.68×10^{-14}	85
12	1.00×10^{-14}	112
14	6.46×10^{-15}	142

- Crack Width Variations:

A reference concrete mix design was simulated in different crack widths as tabulated in table 6.9. The different other parameters were kept constant. The crack depth was taken equal to the concrete cover of 50 mm. It is to note that the values given in table 6.9 are the crack width at the surface of the concrete that narrow down to 0 mm at the crack depth. Going from a crack width of 0 to 2mm, the chloride diffusion coefficient increases by more than 100 times and the resulting service life is reduced by approximately seven times.

Table 6.9 - Effect of Crack width

Crack width (mm)	Chloride Diffusion Coefficient after 50 years (m^2/s)	Resulting Concrete Service Life (years)
0.0	3.64×10^{-14}	57
0.1	4.32×10^{-14}	53
0.2	5.68×10^{-14}	48
0.3	6.25×10^{-14}	44
0.4	7.60×10^{-14}	40
0.6	1.16×10^{-13}	32
0.8	1.82×10^{-13}	26
1.0	2.94×10^{-13}	21
1.2	4.85×10^{-13}	17
1.4	8.18×10^{-13}	14
1.6	1.40×10^{-12}	12
1.8	2.43×10^{-12}	10
2.0	4.26×10^{-12}	9

5.4. Comparison with existing models

In order to compare the complete model with the existing ones, three mixes were considered, two at the extreme sides of the affecting parameters, and a third average mix. These mixes were considered in couples of cracked and uncracked concretes, considering a crack width of 0.5 mm. The mix parameters are given in table 6.10. Tables 6.11, 6.12, and 6.13 include the chloride diffusion coefficient resulting from the complete model and the thirteen existing model while excluding ClinConc and Duracrete which have different calculation concepts. The chloride diffusion coefficient for mixes 1 to 3 were replicated in three water-cement ratio values, while adjusting the fine aggregate quantity to yield a total volume of $1m^3$. The chloride diffusion coefficient was calculated at a relative humidity of 100%, a temperature of 23°C, and at an age of 28 days.

Table 6.10 – Concrete Mix Design Parameters

Parameter	Mix 1 Uncracked	Mix 2 Uncracked	Mix 3 Uncracked	Mix 1 Cracked	Mix 2 Cracked	Mix 3 Cracked
Crack width (mm)	0.0	0.0	0.0	0.5	0.5	0.5
Cement content (kg/m^3)	350	425	305	350	425	305
Silica Fume content (kg/m^3)	0	0	45	0	0	45
Fly Ash content (kg/m^3)	0	0	100	0	0	100
Slag content (kg/m^3)	0	0	150	0	0	150
Aggregate Content (kg/m^3)	1947	1810	1365	1947	1810	1365
Water Content (kg/m^3)	133	161.5	228	133	161.5	228
Water-cement ratio	0.38	0.38	0.38	0.38	0.38	0.38
Materials Finer than 75µm (%)	1	3	10	1	3	10
Aggregate Absorption (%)	1	2	10	1	2	10
Clay Lumps and Friable Particles (%)	1	1	10	1	1	10
Tricalcium aluminate (%)	12	8	5	12	8	5

Table 6.11 – Comparison of chloride diffusion coefficient model – w_c=0.38 – Uncracked Concrete

Model	Chloride diffusion coefficient for mix 1U (m^2/s)	Chloride diffusion coefficient for mix 2U (m^2/s)	Chloride diffusion coefficient for mix 3U (m^2/s)
LIFE365	7.11×10^{-12}	7.11×10^{-12}	2.06×10^{-12}
Concrete Works	8.92×10^{-12}	8.92×10^{-12}	2.54×10^{-12}
4SIGHT	2.75×10^{-12}	2.75×10^{-12}	2.75×10^{-12}
CHLODIF++	3.18×10^{-12}	3.18×10^{-12}	3.18×10^{-12}
HETEK	9.38×10^{-12}	9.38×10^{-12}	9.38×10^{-12}
Luciano and Miltenberger	2.89×10^{-12}	2.74×10^{-12}	8.77×10^{-13}
Riding	8.47×10^{-12}	8.47×10^{-12}	8.47×10^{-12}
Hobbs and Mattew	1.77×10^{-11}	1.77×10^{-11}	1.77×10^{-11}
Sague and Crank	1.00×10^{-11}	5.03×10^{-12}	Not Applicable
Malikakkal	7.2×10^{-12}	4.27×10^{-12}	3.10×10^{-12}
Papadakis	2.46×10^{-12}	2.87×10^{-12}	4.40×10^{-12}
Xi and Bazant	4.42×10^{-12}	4.42×10^{-12}	4.42×10^{-12}
Complete Model	1.14×10^{-13}	4.69×10^{-13}	3.97×10^{-12}

Table 6.12 – Comparison of chloride diffusion coefficient model – w_c =0.38 – Cracked Concrete

Model	Chloride diffusion coefficient for mix 1C (m^2/s)	Chloride diffusion coefficient for mix 2C (m^2/s)	Chloride diffusion coefficient for mix 3C (m^2/s)
LIFE365	7.11×10^{-12}	7.11×10^{-12}	2.06×10^{-12}
Concrete Works	8.92×10^{-12}	8.92×10^{-12}	2.54×10^{-12}
4SIGHT	2.75×10^{-12}	2.75×10^{-12}	2.75×10^{-12}
CHLODIF++	3.18×10^{-12}	3.18×10^{-12}	3.18×10^{-12}
HETEK	9.38×10^{-12}	9.38×10^{-12}	9.38×10^{-12}
Luciano and Miltenberger	2.89×10^{-12}	2.74×10^{-12}	8.77×10^{-13}
Riding	8.47×10^{-12}	8.47×10^{-12}	8.47×10^{-12}
Hobbs and Mattew	1.77×10^{-11}	1.77×10^{-11}	1.77×10^{-11}
Sague and Crank	1.00×10^{-11}	5.03×10^{-12}	Not Applicable
Malikakkal	7.2×10^{-12}	4.27×10^{-12}	3.10×10^{-12}
Papadakis	2.46×10^{-12}	2.87×10^{-12}	4.40×10^{-12}
Xi and Bazant	4.42×10^{-12}	4.42×10^{-12}	4.42×10^{-12}
Complete Model	4.70×10^{-13}	1.93×10^{-12}	1.63×10^{-11}

Table 6.13 – Comparison of chloride diffusion coefficient model – w_c =0.34 - Uncracked

Model	Chloride diffusion coefficient for mix 1U (m^2/s)	Chloride diffusion coefficient for mix 2U (m^2/s)	Chloride diffusion coefficient for mix 3U (m^2/s)
LIFE365	5.70×10^{-12}	5.70×10^{-12}	1.65×10^{-12}
Concrete Works	7.73×10^{-12}	7.73×10^{-12}	2.2×10^{-12}
4SIGHT	1.58×10^{-12}	1.58×10^{-12}	1.58×10^{-12}
CHLODIF++	2.62×10^{-12}	2.62×10^{-12}	2.62×10^{-12}
HETEK	6.99×10^{-12}	6.99×10^{-12}	6.99×10^{-12}
Luciano and Miltenberger	3.00×10^{-12}	2.85×10^{-12}	8.84×10^{-13}
Riding	7.34×10^{-12}	7.34×10^{-12}	7.34×10^{-12}
Hobbs and Mattew	1.59×10^{-11}	1.59×10^{-11}	1.58×10^{-11}
Sague and Crank	7.34×10^{-12}	3.69×10^{-12}	Not Applicable
Malikakkal	Not Applicable	4.94×10^{-12}	3.77×10^{-12}
Papadakis	7.23×10^{-13}	8.43×10^{-13}	1.30×10^{-12}
Xi and Bazant	2.13×10^{-12}	2.13×10^{-12}	2.13×10^{-12}
Complete Model	4.87×10^{-14}	2.05×10^{-13}	1.84×10^{-12}

Table 6.14 – Comparison of chloride diffusion coefficient model – w_c = 0.34 - Cracked

Model	Chloride diffusion coefficient for mix 1C (m^2/s)	Chloride diffusion coefficient for mix 2C (m^2/s)	Chloride diffusion coefficient for mix 3C (m^2/s)
LIFE365	5.70×10^{-12}	5.70×10^{-12}	1.65×10^{-12}
Concrete Works	7.73×10^{-12}	7.73×10^{-12}	2.2×10^{-12}
4SIGHT	1.58×10^{-12}	1.58×10^{-12}	1.58×10^{-12}
CHLODIF++	2.62×10^{-12}	2.62×10^{-12}	2.62×10^{-12}
HETEK	6.99×10^{-12}	6.99×10^{-12}	6.99×10^{-12}
Luciano and Miltenberger	3.00×10^{-12}	2.85×10^{-12}	8.84×10^{-13}
Riding	7.34×10^{-12}	7.34×10^{-12}	7.34×10^{-12}
Hobbs and Mattew	1.59×10^{-11}	1.59×10^{-11}	1.58×10^{-11}
Sague and Crank	7.34×10^{-12}	3.69×10^{-12}	Not Applicable
Malikakkal	Not Applicable	4.94×10^{-12}	3.77×10^{-12}
Papadakis	7.23×10^{-13}	8.43×10^{-13}	1.30×10^{-12}
Xi and Bazant	2.13×10^{-12}	2.13×10^{-12}	2.13×10^{-12}
Complete Model	1.80×10^{-13}	7.55×10^{-13}	6.80×10^{-12}

Table 6.15 – Comparison of chloride diffusion coefficient model – w_c = 0.30 - Uncracked

Model	Chloride diffusion coefficient for mix 1U (m^2/s)	Chloride diffusion coefficient for mix 2U (m^2/s)	Chloride diffusion coefficient for mix 3U (m^2/s)
LIFE365	4.57×10^{-12}	4.57×10^{-12}	1.33×10^{-12}
Concrete Works	6.70×10^{-12}	6.70×10^{-12}	1.91×10^{-12}
4SIGHT	9.12×10^{-13}	9.12×10^{-13}	9.12×10^{-13}
CHLODIF++	2.16×10^{-12}	2.16×10^{-12}	2.16×10^{-12}
HETEK	4.93×10^{-12}	4.93×10^{-12}	4.93×10^{-12}
Luciano and Miltenberger	3.14×10^{-12}	2.99×10^{-12}	9.06×10^{-13}
Riding	6.36×10^{-12}	6.36×10^{-12}	6.36×10^{-12}
Hobbs and Mattew	1.40×10^{-11}	1.40×10^{-11}	1.40×10^{-11}
Sague and Crank	4.67×10^{-12}	2.35×10^{-12}	Not Applicable
Malikakkal	Not Applicable	7.42×10^{-12}	6.26×10^{-12}
Papadakis	6.82×10^{-14}	8.24×10^{-14}	1.23×10^{-13}
Xi and Bazant	9.40×10^{-13}	9.40×10^{-13}	9.40×10^{-13}
Complete Model	1.44×10^{-14}	8.45×10^{-14}	7.89×10^{-13}

Table 6.16 – Comparison of chloride diffusion coefficient model – w_c = 0.30 - Cracked

Model	Chloride diffusion coefficient for mix 1C (m^2/s)	Chloride diffusion coefficient for mix 2C (m^2/s)	Chloride diffusion coefficient for mix 3C (m^2/s)
LIFE365	4.57×10^{-12}	4.57×10^{-12}	1.33×10^{-12}
Concrete Works	6.70×10^{-12}	6.70×10^{-12}	1.91×10^{-12}
4SIGHT	9.12×10^{-13}	9.12×10^{-13}	9.12×10^{-13}
CHLODIF++	2.16×10^{-12}	2.16×10^{-12}	2.16×10^{-12}
HETEK	4.93×10^{-12}	4.93×10^{-12}	4.93×10^{-12}
Luciano and Miltenberger	3.14×10^{-12}	2.99×10^{-12}	9.06×10^{-13}
Riding	6.36×10^{-12}	6.36×10^{-12}	6.36×10^{-12}
Hobbs and Mattew	1.40×10^{-11}	1.40×10^{-11}	1.40×10^{-11}
Sague and Crank	4.67×10^{-12}	2.35×10^{-12}	Not Applicable
Malikakkal	Not Applicable	7.42×10^{-12}	6.26×10^{-12}
Papadakis	6.82×10^{-14}	8.24×10^{-14}	1.23×10^{-13}
Xi and Bazant	9.40×10^{-13}	9.40×10^{-13}	9.40×10^{-13}
Complete Model	4.77×10^{-14}	2.80×10^{-13}	2.61×10^{-12}

Figure 6.20 illustrates the variations in chloride diffusion coefficient given by the various models. The following interpretations can be made:

- As the thirteen existing models do not take into consideration the crack width, the corresponding chloride diffusion coefficient values in the cracked and uncracked concrete were identical. The presence of cracks may increase the chloride diffusion coefficient by up to 100 times as demonstrated in the previous section. The complete model clearly differentiates the chloride diffusion coefficient values for cracked and uncracked concrete. It is to note that the example taken in this section includes a crack width of 0.5mm, higher crack widths will result in higher chloride diffusion coefficients.

- The various models have similar chloride diffusion coefficient for mixes 1 and 2 whereas a mix with much higher cementitious material quantity, lower tricalcium aluminate content, lower aggregate quality, and lower aggregate content should normally yield different chloride diffusion coefficient. The complete model distinguished this fact based on the inherent input parameters.

- The complete model seems to agree in a better way with the real-life prediction reflecting the different affecting parameters.

Figure 6.20 - Various models comparison versus the complete model

6. Conclusions

This chapter summarizes the works done reaching a final model that calculates the chloride diffusion coefficient. This model includes the product of a total of eight functions, that we defined in the previous chapters, with a reference chloride diffusion coefficient.

The reference chloride diffusion coefficient was based on available literature. A nonlinear regression analysis was made to conclude the final equation of the reference chloride diffusion coefficient as a function of the water-cement ratio, cementitious materials content and type. If the reference chloride diffusion coefficient will be furthermore refined, another 37 parameters should be investigated. This requires another large-scale testing campaign that requires a least 200

combination for an acceptable accuracy of the adjusted R-squared factor. Adding more parameters to the investigated 30 parameters is not however practical for construction used. The thirty parameters that were investigated are readily available and a prerequisite for the concrete mix design operation. This compromise in number of parameters forms and equilibrium between precision and complexity in calculating the chloride diffusion coefficient.

A Microsoft Excel sheet was made for the calculation of the chloride diffusion coefficient and corresponding chloride concentration in concrete for the first 150 years in unidirectional problems. The finite difference method that may be used for the chloride ingress calculations in unidirectional and bidirectional problems is also presented.

A numerical application and parametric analysis was made to identify the influence of each parameter. The crack width, relative, humidity, temperature, and tricalcium aluminate seem to have a significant effect on the chloride diffusion coefficient.

A comparison analysis was finally made to compare the complete model to the various available models. As these models do not take all the affecting parameters into consideration, it was normal to have similar diffusion coefficient values for different mixes. The complete model seems to agree in a better way with the real-life prediction reflecting the different affecting parameters.

Final Conclusions

The service life of concrete structures in chloride environment spans till the time when the degradation caused by the reinforcing steel corrosion are deemed to be unacceptable. It is defined by two phases: the initiation phase and the propagation phase. It is mostly controlled by the former due to its significant duration when compared to the propagation phase. The initiation phase is the duration where the chloride diffused in the concrete reaches a critical threshold in the vicinity of the reinforcement steel. The propagation phase starts as soon as the steel starts to corrode and ends by its degradation.

The modeling of this service life is basically a chloride diffusion in concrete, which is mainly governed by chloride diffusion coefficient, according to concrete properties.

Modeling the chloride diffusion coefficient as a function of the concrete properties was the quest of several researchers in the last decades. A literature review of the available models were found to rely mostly on the water-cement ratio, with few other models taking other properties into consideration. The available literature review also identified that many other parameters affect the value of the chloride diffusion coefficient. Among these parameters, the properties of the aggregate, the tricalcium aluminate content, the degree of consolidation, the concrete initial mixing time and the crack width were found to have a significant effect. The influence of these properties was studied in this thesis.

Regarding the aggregate properties, the study in chapter 2 shows that the chloride diffusion in concrete can be theoretically divided into three phases of diffusion; a diffusion that takes place in the aggregate, a diffusion that takes place in the interfacial transition zone between the aggregate and the cement paste, and the diffusion that takes place in the cement paste. The developed model includes two additional phases of affecting the diffusion: The aggregate surface condition and the impurities in aggregate. These two suggested phases can be quantified using simple laboratory tests including the following: Materials finer than 75 microns content, the Water absorption test, and the Clay lumps and friable particles content. The surface chloride concentration on the other side was found to be affected by the type of the aggregate material, the density and the soundness. It is also to note that the aggregate properties do not affect directly the chloride diffusion coefficient. These properties are rather dependent, and work in combination with, the concrete properties to affect the overall concrete chloride diffusion. It is thus necessary to consider these entities in combination when developing a function illustrating the effect of the aggregate properties on the total concrete chloride diffusion coefficient. The concrete properties that are part of the function illustrating the aggregate effect on the concrete chloride diffusion coefficient thus includes the following: Aggregate volume, Aggregate particle distribution and sizes, Aggregate materials finer than 75 microns, Aggregate absorption, Aggregate clay lumps and friable particles, Interfacial transition zone (ITZ) thickness, Cement content, Water-cement ratio, Cement composition (C3S, C2S, C3A, and C4AF), Cement fineness, Cement Density, Cement degree of hydration, Time after placing, Relative humidity, Temperature and Cement Activation Energy.

The role of the tricalcium aluminate was studied in chapter 3 where the corresponding influence function was generated. The main mechanism of influence is the binding that takes place between the tricalcium aluminate and the chloride that consequently affects the value of the chloride diffusion coefficient.

The concrete initial mixing time and degree of consolidation were found with no effect on the mechanism of diffusion, as shown in chapter 4. The main reason is attributed to the size of the pores created by these two parameters that were found to affect chloride ingress mechanisms other than the diffusion, namely the permeation. This fact exposes another very important fact proving that the chloride diffusion is not the main and most important chloride transportation in concrete. In specific instances, permeation may have a significant role in the chloride transportation. Considering therefore the chloride diffusion as a leading model of transportation may be erroneous. The two transportation mechanisms should be considered simultaneously for a better simulation of chloride ingress models. In another note, the quantity of chloride tested in concrete made with different consolidation levels varied significantly even for the same value of chloride diffusion coefficient. This is an item that should be considered while evaluating the chloride threshold causing the reinforcement corrosion.

As largely discussed in the literature, the cracks were found to decrease the concrete durability and to increase the chloride diffusion. Chapter 5 proposed an original testing protocol to quantify this effect through a large-scale testing campaign that simulates the accurate shape and width of the cracks. The study takes into consideration the effect of the autogenous healing and water-cement ratio, in addition to the crack width.

The final updated model was presented in chapter 6 where the additional parameters affecting the chloride diffusion coefficient was integrated in one equation. The calculation of the chloride ingress is made by calculating the diffusion coefficient at each increment of time t in days using this formula. Fick's second law is then applied to calculate the chloride ingress in concrete using finite difference method. The reference chloride diffusion coefficient taken in this formula was based on available literature, where the chloride diffusion coefficient is essentially modeled as a function of water-cement ratio. In addition, the cementitious material type and quantity was also taken into consideration.

As a result, an updated model for the chloride diffusion coefficient was developped as a function of eight influencing functions and a reference chloride diffusion coefficient. These functions include a total of thirty influencing parameters. This model provides a more accurate representation, in terms of the influencing parameters when compared to other models.

Although this model shows a significant progress in terms of parameters taken into consideration when modeling chloride diffusion coefficient, further studies can include more refinement of the model, such as:

- The thickness of Interfacial Transition Zone was taken equal to 5µm and 50µm for concrete containing and excluding microsilica, respectively. This value can be enhanced by defining the

corresponding accurate model and consequent thickness. The value of the ITZ was proved to be one of the diffusion zones, the relevant thickness plays an important role in its characterization.

- The chloride diffusion was demonstrated to be one of two important transportation mechanisms rather than the main chloride transportation mechanism. The permeation may also play an important role in some instance. The model should thus be updated to include the role of permeation simultaneously with the diffusion. Another new parameter, the water pressure will be included as part of this model.

- Cracks in concrete were considered in this model to have a maximum width at the surface, zero width at the bottom of the crack and with a linear progression in width. This fact was based on linear stress-strain relationship in service state. A more accurate cracking pattern based on the cause of cracks may be studied and identified. This study will enhance the crack width identification through the cracks and refine the chloride diffusion coefficient furthermore. The simultaneous permeation mechanism through cracked concrete should also be considered.

- For a more precise calculation of the reference chloride diffusion coefficient, another 37 parameters should be investigated. This requires another large-scale testing campaign that requires a least 200 combinations for an acceptable accuracy of the adjusted R-squared factor. This future work can significantly enhance the accuracy of the final model.

References

[1] Douglas F. Burke and Marc Wanagas, “Special Publication SP-NAVFAC ESC-CI-1201, Concrete Service Life Prediction Tools: Market Survey”, Naval Facilities Engineering Command – Engineering Service Center, California USA, 2012.

[2] Tang Luping, “Engineering expression of the ClinConc model for prediction of free and total chloride ingress in submerged marine concrete”, Cement and Concrete Research 38 (2008) 1092-1097

[3] L. Tang, “Chloride ingress in concrete exposed to marine environment — field data up to 10 years' exposure”, SP Report 2003:16, SP Swedish National Testing and Research Institute, Borås, Sweden, 2003.

[4] FIB Task Group 5.6, “ FIB Bulletin 34 - Model Code for Service Life Design”, FIB, 2006.

[5] Stanish, K., “Predicting the Diffusion Coefficient of Concrete from Mix Parameters,” University of Toronto Report, University of Toronto, ON, Canada, 2000

[6] Ralph Browne, “ConcreteWorks Version 2.0 - User’s Manual”, Texas Department of Transportation TxDOT project 4563, Concrete Durability Center, 2005.

[7] K.A. Snyder, “Validation and Modification of the 4SIGHT Computer Program”, NISTIR 6747, National Institute of Standards and Technology Gaithersburg, MD 20899 May 2001.

[8] Oslakovic I. S., Bjegovic, D. , Mikulic, D., & Krstic, V., “Development of Service Life model CHLODIF++, Computational modelling of Concrete structures. EURO C, 2010, 573-578.

[9] Oslakovic, I. S., Bjegovic, D., & Mikulic, D., “Evaluation of Serivce Life Design Models on Concrete Structures Exposed to marine environment”, Materials and Structures, 43 (10), 2010, 1397-1412

[10] Jens Mejer Frederisken, Henrik Ernhal Sorensen, Oskar Klinghoffer, “The Effect of the w/c Ratio on Chloride Transport into Concrete—Immersion, Migration and Resistivity Tests,” HETEK Report No. 54, Denemark Ministry of Transport, 1997.

[11] John Luciano, and Matthew Miltenberger, “Predicting Chloride Diffusion Coefficients from Concrete Mixture Proportions”, ACI Materials Journal, 96-M86, November – December 1999.

[12] Kyle A. Riding, Michael D. A. Thomas, and Kevin J. Folliard, “Apparent Diffusivity Model for Concrete Containing Supplementary Cementitious Materials”, ACI Materials Journal, 110-M65, November 2013

[13] Jens Mejer Frederisken, Henrik Ernhal Sorensen, Oskar Klinghoffer, “The Effect of the w/c Ratio on Chloride Transport into Concrete—Immersion, Migration and Resistivity Tests,” HETEK Report No. 54, Denemark Ministry of Transport, 1997

[14] Tang, L., and Sorenson, H. E., “Evaluation of the Rapid Test Methods for Measuring the Chloride Diffusion Coefficients of Concrete,” SP Report 1998:42, Nordtest Project No. 1388-98, 1998.

[15] Kyle Stanish, Michael Thomas, “The use of bulk diffusion tests to establish time-dependent concrete chloride diffusion coefficients”, Cement and Concrete Research 33 (2003) 55–62.

[16] Steen, P. E., “Chloride Penetration in Marine Environment Part 2: Results from Field Test on Coastal Bridges in Norway,” Proceedings of the Nordic Seminar in Lund: Corrosion of Reinforcement: Field and Laboratory Studies for Modeling and Service Life, 1995.

[17] Sandberg, P.; Pettersson, K.; and Jorgensen, O., “Field Studies of Chloride Transport into High Performance Concrete,” Proceedings of the Third CANMET/ACI International Conference

on the Performance of Concrete in a Marine Environment, SP-163, V. M. Malhotra, ed., American Concrete Institute, Farmington Hills, MI, 1996, pp. 233-254.
[18] Sandberg, P., and Tang, L., "A Field Study of the Penetration of Chlorides and Other Ions into a High Quality Concrete Marine Bridge Column," Proceedings of the Third CANMET/ACI International Conference on Durability of Concrete, SP-145, V. M. Malhotra, ed., American Concrete Institute, Farmington Hills, MI, 1994, pp. 557-571.
[19] Olga Garces Rodriguez, "Influence of Cracks on Chloride Ingress into Concrete", University of Toronto, 2001
[20] Smith, D., "The Development of a Rapid Test for Determining the Transport Properties of Concrete," MScE thesis, University of New Brunswick, Fredericton, NB, Canada, 2006.
[21] Kyle A. Riding, Michael D. A. Thomas, and Kevin J. Folliard, "Apparent Diffusivity Model for Concrete Containing Supplementary Cementitious Materials", ACI Materials Journal, 110-M65, November 2013.
[22] Obla, K. H.; Hill, R. L.; Thomas, M. D. A.; Shashiprakash, S. G.; and Perebatova, O., "Properties of Concrete Containing Ultra-Fine Fly Ash," ACI Materials Journal, V. 100, No. 5, Sept.-Oct. 2003, pp. 426-433.
[23] Hobbs DW, Matthews JD. Minimum requirements for concrete to resist deterioration due to chloride induced corrosion. In: Hobbs, D.W. (Ed.), Minimum Requirements for Durable Concrete. British Cement Association, Crowthorne, UK, 1998:43–89.
[24] Sagues AA, Kranc SC. Corrosion forecasting for 75-Year durability design of reinforced concrete, WPI# 0510805, Final Report to Florida Department of Transportation, University of South Florida, Tampa, FL, 2001.
[25] Malikakkal NC. Chloride diffusion in concrete/prediction of the onset of corrosion in reinforced concrete structures, M.Sc. thesis, King Fahad University of Petroleum & Minerls, 1994.
[26] Papadakis VG, Roumeliotis AP, Fardis MN, Vayenas CG, "Mathematical modelling of chloride effect of concrete durability and protection measures, concrete repair, rehabilitation and protection", UK: E & FN Spon; 1996. p. 165–74.
[27] Xi, Y. and Bazant, Z.P. (1999). " Modeling Chloride Penetration in Saturated Concrete." Journal of Materials in Civil Engineering, 11 (1), 58-65.
[28] Life 365 Consortium, "Life365 software User's Manual – Version 2.2.1", 2014
[29] Atiye Farahani, "Modeling of Chloride Diffusion in Concrete", INTECH, 2016 .
[30] Bamforth, P. B., "Spreadsheet Model for Reinforcement Corrosion in Structures Exposed to Chlorides," Concrete Under Severe Conditions 2, O. E. Gjørv, K. Sakai, and N. Banthia, eds., E&FN Spon, London, UK, 1998, pp. 64-75
[31] Kyle A. Riding, Michael D. A. Thomas, and Kevin J. Folliard, "Apparent Diffusivity Model for Concrete Containing Supplementary Cementitious Materials", ACI Materials Journal, 110-M65, November 2013
[32] A.V. Saetta, R.V. Scotta, R.V. Vitaliani, "Analysis of chloride diffusion into partially saturated concrete", ACI Mater. J. 90 (M47) (1993) 441 – 451.
[33] Z.P. Bazant, L.J. Najjar, Nonlinear Water Diffusion in nonsaturated concrete, Materiaux et Constructions, Volume 5, No. 25, 1972.
[34] Beatriz Martin Perez, "Service Life Modeling of R.C. Highway Structures Exposed to Chloride", A thesis submitted in conformity with the requirements for the degree of Doctor of Philosophy Graduate Department of Civil Engineering, University of Toronto, 1999.

[35] Jian-jun Zheng, Hong S. Wong, Nick R. Buenfeld, “Assessing the influence of ITZ on the steady-state chloride diffusivity of concrete using a numerical model”, Cement and Concrete Research 39 (2009) 805–813
[36] Hani H. Titi, Habib Tabatabai, “Effect of coarse aggregate type on chloride ion penetration in concrete”, Construction and Building Materials, 2018
[37] Rasheeduzzafar S.S. AI-Saadoun A.S. AI-Gahtani F.H. Dakhil, “Effect of Tricalcium Aluminate Content of Cement on Corrosion of Reinforcing Steel in Concrete”, Department of Civil Engineering King Fahd University of Petroleum & Minerals Dhahran 31261, Saudi Arabia, 1990, Cement And Concrete Research, Vol. 20. Pp. 723-738, 1990.
[38] G.K. Glass*, N.R. Buenfeld, “The influence of chloride binding on the chloride induced corrosion risk in reinforced concrete”, Department of Civil and Environmental Engineering, Imperial College, London SW7 2BU, UK, Corrosion Science, 1999.
[39] Sang-Hun Han, “Influence of diffusion coefficient on chloride ion penetration of concrete structure”, Coastal and Harbour Engineering Research Center, Korea Ocean Research and Development Institute, 1270 Sadong Ansan, Kyunggido 426-744, Republic of Korea, Construction and Building Materials, 2005.
[40] Paul Sandberg, “Studies of chloride binding in concrete exposed in a marine environment”, Cement and Concrete Research 29 (1999) 473–477.
[41] Shamsad Ahmad, “Reinforcement corrosion in concrete structures, its monitoring and service life prediction—a review”, Cement and Concrete Composites, Volume 25, Issues 4–5, May–July 2003, Pages 459-471
[42] Radhakrishna G. Pillai and Ashokreddy Annapareddy, “Service Life Prediction Models for Chloride-Laden Concrete structures: A review and Nomographs”, International Journal of 3R’s, Volume 4, No. 2, 2013, 563-580.
[43] Raj B., “India Loses 200,000 Cr Rs Yearly Through Corrosion”, WeeklyVoice, 2011
[44] Lieser, M. J. and Xu, J., “Composites and Future of Society: Preventing a legacy of Costly Corrosion with Modern materials. Owens Corning, OCV Reinforcements, 2013
[45] Gro Markeseta, Mahdi Kioumarsia, “Need for further development in service life modelling of concrete structures in chloride environment”, Procedia Engineering 00 (2017) 000–000, 2017
[46]American Concrete Institute, ACI standard 365.1, “Service Life Prediction”, 2000, page 2
[47] CIRIA report C577, “Guide to the Construction of Reinforced Concrete in the Arabian Peninsula”, Concrete Society Special Publication CS136, 2002, page 6
[48] EN 206-1, “Concrete - Part 1 Specification, performance, production and conformity”, European Norms, 2014, page 10
[49] Adam Neville, “Chloride Attack of Reinforced Concrete: An overview, Materials and Structures”, 1995, Page 1.
[50] V.M. Malhotra, Nicolas Carino, “Handbook of Nondestructive Testing of Concrete Second Edition”, CRC Press, 2004, Page 11.6
[51] Newman, J, Choo, B.S, “Advanced Concrete Technology, Testing and Quality”, Elsevier, 2003, p6/4
[52] K.D. Stanish, R.D. Hooton and M.D.A.,” Testing the Chloride Penetration Resistance of Concrete: A Literature Review”, Thomas Department of Civil Engineering University of Toronto Toronto, Ontario, Canada, 1997.

[53] American Society for Testing and Materials (ASTM) Committee C1202-12:" Standard Test Method for Electrical Indication of Concrete's Ability to Resist Chloride Ion Penetration, 2012.
[54] Matthew Sherman, P.E., F.ACI, NACE Conference, June 2017, New-York
[55] C.L. Page, N.R. Short, A. El Tarras, "Diffusion of Chloride Ions in Hardened Cement Pastes", Cement and Concrete Research, Volume 11, Issue 3, May 1981, page 395-406.
[56] L. Tang and L. O. Nilsson, "A Numerical Method for Prediction of Chloride Penetration Into Concrete Structures", Department of Building Materials Chalmers University of Technology S-412 96 Gothenburg, Sweden
[57] American Concrete Institute, ACI Committee 222, "Protection of Metals in Concrete Against Corrosion", 2001.
[58] American Concrete Institute, ACI Committee 201.2, "Guide to Durable Concrete", 2008.
[59]American Concrete Institute, ACI Committee 362.1, "Guide for the design of Durable Parking Structures", 1997.
[60] American Society for Testing and Materials (ASTM) Committee C31:" Standard Practice for Making and Curing Concrete Test Specimens in the Field", 2015.
[61] R. Feldman, G.W. Chan, R.J. Broussaeau, "Chloride ion diffusivity of blended cement mortars: A. C. impedance and pore structure parameters", Il Cemento 90 (4) (1993) 207–220.
[62] M.D.A. Thomas, S.J. Pantazopoulu, B. Martin-Perez, "Service Life Modeling of Concretes Exposed to Chlorides – A Literature Review", Prepared for the Ministry of Transportation, Ontario, at the University of Ontario, 1995.
[63] D.W. Hobbs, "Aggregate influence on chloride ion diffusion into concrete", British Cement Association (1999)
[64] T.C. Powers, L.E. Copeland, J.C. Hayes, H.M. Mann, "Permeability of Portland cement paste", Proc ACI 51 (1954) 285–298.
[65] Z. Hanshin, S. Shtrikman, "A variational approach to the theory of the elastic behaviour of multi-phase materials", J Mech Phys Solids 11 (1963) 127–140.
[66] Y.F. Houst, H. Sadouki, F.H. Wittmann, "Influence of aggregate concentration on the diffusion of CO2 and O2, in: Interface in Cementitious Composites", RILEM Proceedings, vol. 18, 1992, pp. 279-288.
[67] A. Princigallo, K. Breugel, G. Levita, "Influence of the aggregate on the electrical conductivity of Portland cement concretes", Cem. Concr. Res. 33 (2003) 1755-1763.
[68] B. Bourdette, E. Ringot, J.P. Ollivier, "Modelling of the transition zone porosity", Cem. Concr. Res. 25 (1995) 741–751.
[69] Z. Bajja, W. Dridi, A. Darquennes, R. Bennacer, P. Le Bescop, "Effect of aggregates on the diffusion properties and microstructure of cement with slurried silica fume based materials", Cement and Concrete Composites 70 (2016), 86-97
[70] D.N. Winslow, M.D. Cohen, D.P. Bentz, A. Snyder, E.J. Garbozci, "Percolation and pore structure in mortars and concrete", Cem. Concr. Res. 24 (1994) 25–37.
[71] Jian-jun Zheng, Hong S. Wong, Nick R. Buenfeld, "Assessing the influence of ITZ on the steady-state chloride diffusivity of concrete using a numerical model", Cement and Concrete Research 39 (2009) 805–813

[72] D.N. Winslow, M.D. Cohen, D.P. Bentz, A. Snyder, E.J. Garbozci, “Percolation and pore structure in mortars and concrete”, Cem. Concr. Res. 24 (1994) 25–37.
[73] J.-J. Zheng, X.-Z. Zhou, Y.-F. Wu, X.-Y. Jin, “A numerical method for the chloride diffusivity in concrete with aggregate shape effect”, Constr. Build. Mater. 31 (2012) 151–156.
[74] X.-Z. Zhou, J.-J. Zheng, Y.-Y. Liang, “Effect of aggregate shape on the chloride diffusivity of concrete”, Adv. Mater. Res. 450–451 (2012) 150–153.
[75] J.-J. Zheng, X.-Z. Zhou, X.-F. Huang, C.-Q. Fu, “Experimental and modeling of the effect of aggregate shape on the chloride diffusivity of concrete”, J. Mater. Civ. Eng. 26 (2014). 04014048-1-5.
[76] Jian-jun Zheng a,∗, Hong S. Wong b, Nick R. Buenfeld b, “Assessing the influence of ITZ on the steady-state chloride diffusivity of concrete using a numerical model”, Cement and Concrete Research 39 (2009) 805–813
[77] J.P. Olivier, J.C. Maso, and B. Bourdette, “Interfacial Transition Zone in Concrete”, Laboratoire Materiaux et Durabilite des Constructions, Toulouse, France.
[78] American Society of Testing Materials, Committee C117, "Standard Test Method for Materials Finer than 75-μm (No. 200) Sieve in Mineral Aggregates by Washing, 2013.
[79] John Newman, Ban Sen Choo, Advanced Concrete Technology – Constituent Materials, Elsevier, 2003, Page 8/12
[80] American Society of Testing Materials, Committee C33, "Standard Specification for Concrete Aggregate, 2013.
[81] Harrison, D.J. and Bloodworth, A.J. (1994) Construction Materials, Industrial Minerals Laboratory Manual. Technical Report WG/94/12, Nottingham.
[82] Hannah Nyambara Ngugi1, Raphael Ndisya Mutuku2, Zachary Abiero Gariy2, "Effects of Sand Quality on Compressive Strength of Concrete: A Case of Nairobi County and Its Environs, Kenya", Open Journal of Civil Engineering, 2014, 4, 255-273
[83] American Society of Testing Materials, Committee C127, " Standard Test Method for Density, Relative Density (Specific Gravity), and Absorption of Coarse Aggregate, 2012.
[84] American Society of Testing Materials, Committee C142, "Standard Test Method for Clay Lumps and Friable Particles in Aggregate", 2010.
[85] Breton, D.: Ollivier, J.P.; Ballivy, G. In Interfaces in cementitious Composites. Rilem Int. Conf. Toulouse. Maso, J.C. Ed.: 1992: pp 269-278
[86] Scrivener, K.L.: Bentur, A.: Pratt, P.L. Advances in Cement Research 1988, 1, 230-237
[87] A.K. Crumbie, Characterisation of the microstructure of concrete, PhD Thesis, Imperial College London, 1994.
[88] Jeffrey J. Thomas, Joseph J. Biernacki, Jeffrey W. Bullard, Shashank Bishnoi, Jorge S. Dolado, George W. Scherer, Andreas Luttge, Modeling and simulation of cement hydration kinetics and microstructure development, Cement and Concrete Research 41 (2011) 1257 - 1278
[89] L.J. Parrot, D.C. Killoh, Prediction of cement hydration, Br. Ceram. Proc. 35 (1984) 41–53.
[90] Schindler, A. K., and Folliard, K. J., “Heat of Hydration Models for Cementitious Materials,” ACI Materials Journal, V. 102, No. 1, Jan.-Feb., 2005, pp. 24-33.

[91] Pane, I., and Hansen, W., “Concrete Hydration and Mechanical Properties under Nonisothermal Conditions,” ACI Materials Journal, V. 99, No. 6, Nov.-Dec, 2002, pp. 534-542.
[92] Freiesleben Hansen, P., and Pedersen, E. J., “Maturity Computer for Controlling Curing and Hardening of Concrete,” Nordisk Betong, V. 1, No. 19, 1977, pp. 21-25.
[93] Jonathan L. Poole, Kyle A. Riding, Kevin J. Folliard, Maria C. G. Juenger, and Anton K. Schindler, Methods for Calculating Activation Energy for Portland Cement, ACI Materials Journal, January-February 2007
[94] Elakneswaran Yogarajah, Toyoharu Nawa, Eiji Owaki, “Prediction Of Hydration Products And Pore Solution Chemistry Of Fly Ash Cement”, Proceedings Of Academicsera International Conference, Milan, Italy, 6th-7th March 2018
[95] T.C. Powers, T.L. Brownyard, Studies of the physical properties of hardened Portland cement paste, Bull. 22, Res. Lab. of Portland Cement Association, Skokie, IL, USA, reprinted from J. Am. Concr. Inst. (Proc.) 43 (1947) 101–132, 249–336, 469–504, 549–602, 669–712, 845–880, 933–992.
[96] T.C. Hansen, Physical structure of hardened cement paste: a classical approach, Mater. Struct. 19 (6) (1986) 423–436
[97] J.J. Zheng, X.Z. Zhou, Analytical solution for the chloride diffusivity of hardened cement paste, J. Mater. Civ. Eng. 20 (5) (2008) 384–391.
[98] J.M.V.A. Koelman, A. de Kuijper, An effective medium model for the electric conductivity of an N-component anisotropic and percolating mixture, Physica A, 247 (1) (1997) 10–22.
[99] John Newman, Ban Sen Choo, Advanced Concrete Technology – Concrete Properties, Elsevier, 2003.
[100] Tayfun UYGUNOĞLU, Sevcan ÖZGÜVEN, "Kompozit Modellemeler ile Çelik Lifli Betonlarda Elastisite Modülü Tahmini", El-Cezerî Journal of Science and Engineering Vol: 1, No: 1, 2014 (19-28)
[101]American Concrete Institute, ACI Committee 318-14, “Building Code Requirements for Structural Concrete and Commentary”, 2014, page 321.
[102] Xianming Shi, Ning Xie, Keith Fortune, Jing Gong, “Durability of Steel reinforced concrete in chloride environments: An overview”, Construction and Building Materials, Volume 30, 2012, 125-138.
[103] Buenfeld NR, Glass GK, Hassanein AM, Zhang J-Z, “Chloride Transport in concrete subjected to an electric field”, Mater Civil Engineering 1998, 10(4), 220-8.
[104] Jingpei Li, Wei Shao, “The effect of chloride binding on the predicted service life of RC pipe piles exposed to marine environments”, Ocean Engineering 88 (2014) 55–62
[105] AASHTO M157 – “Standard Specification for Ready Mix Concrete”, American Association of State and Highway Transportation Officials, 2017.
[106] ACI 304-00 – “Guide for Measuring, Mixing, Transporting and Placing Concrete”, American Concrete Institute Committee number 304, 2000.
[107] ASTM C94 – “Standard Specification for Ready Mixed Concrete”, American Society for Testing and Materials, 2018.

[108] U.S. Department of Transportation - Federal Highway Administration Research and Technology, “Petrographic Methods of Examining Hardened Concrete: A petrographic Manual”, Publication Number FHWA-RD-97-146, 1997.
[109] Ameer Hilal, “Microstructures of Concrete”, Intechopen DOI: 10.5772/64574, 2015
[110] Junzhi Zhang, Fan Bian, Yurong Zhang, Zhaofeng Fang, Chuanqing Fu, Jie Guo, “Effect of pore structures on gas permeability and chloride diffusivity of concrete”, Construction and Building Materials 163 (402-413), 2018
[111] M.R. Nokkenm R.D. Hooton,” Using pore parameters to estimate permeability or conductivity of concrete, Materials and Strucutres, 2008
[112] Pavla Halamickova, Rachel J. Detwiler, Dale P. Bentz, Edward J.Garboczi, “Water permeability and chloride ion diffusion in portland cement mortars: Relationship to sand content and critical pore diameter”, Cement and Concrete Research, 1995
[113] Lapyote Prasittisopin And David Trejo, “Effects Of Mixing Variables On Hardened Characteristics Of Portland Cement Mortars”, Aci Materials Journal No. 112-M38, June 2015
[114] Jiameng Chen, “Influence of Transport Parameters on the Fresh and Hardened Characteristics of Ready-Mix Concrete”, Oregon State University (Thesis), 2014.
[115] Karol Urban, Alena Sicakova, “The Effect of Mixing Technique and Prolonged Mixing Time on Strength Characteristics of Concrete”, MDPI, 2018.
[116] D. Ravina, “ Effect of prolonged mixing on compressive strength of concrete with and without fly ash and/or chemical admixtures”, ACI Materials Journal 93(5):451-456, September 1996.
[117] American Petroleum Institute. 2002. “API SPEC 10A Specification for Cements and Materials for Well Cementing.” American Petroleum Institute, 2002.
[118] David Trejo, Jiaming Chen, “Effects of Extended Discharge Time and Revolution Counts for ready mixed Concrete”WSDOT Research Report, December 2014.
[119] Williams, D.A., A.W. Saak, and H.M. Jennings. 1999. “The Influence of Mixing on the Rheology of Fresh Cement Paste.” Cement and Concrete Research 29: 1491–96,1999.
[120] Rupnow, Tyson D., Vernon Ray Schaefer, Kejin Wang, and Benjamin L. Hermanson. 2007. Improving Portland Cement Concrete Mix Consistency and Production Rate Through Two-Stage Mixing. http://trid.trb.org/view.aspx?id=860066.
[121] Beitzel, H. 1981. “Effect of the Mixing Time on the Quality of the Mixing.” Precast Concrete 12 (9): 403–8, 1981.
[122] Waheeb Al-Khaja, Influence of temperature, cement type and level of concrete consolidation on chloride ingress in conventional and high-strength concretes, Construction and Building Materials, 1997.
[123] W Akili, “Field Investigtion of Chloride Diffusion in Concrete Using the Rapid Chloride Permeability Test”, Proceeding of the International Conference held at the University of Dundee, Scotland: Concrete Durability and Repair Technology, Scotland, UK, September 1999.
[124] Bruce, S.M., McCarten, P.S., Freitag S.A., Hasson, L.M., “Deterioration of prestressed concrete bridge beams”, Land Transport New Zealand Research Report 337, 2008.
[125] ASTM C642-13, Standard Test Method for Density, Absorption, and Voids in Hardened Concrete, American Society for Testing and Materials, 2013.

[126] Hugo Bohorquez, “Diffusion in Porous Media – A world of applications – Part 1“, Steemit.com, https://steemit.com/steemstem/@hugobohor/diffusion-in-porous-media-a-world-of-applications-part-1, 2018
[127] Welty, J. R.; Wicks, C. E. y Wilson, R. E., 1984. Fundamentos de transferencia de momento, calor y masa, Edit. Limusa, México D.C., México, pp. 533-733.
[128] Krasuk, J. H., 2002. Transferencia de masa por difusión, Ediciones MCA, Los Teques, Venezuela, pp. 1-175.
[129] Roberts D. (Concrete Society), “Autogenous Healing: Self Sealing of Fine Cracks”, Concrete Advice No. 09, Concrete Society, 2003.
[130] BS8007:1987, “Code of practice for design of concrete structures for retaining aqueous liquids”, British Standards, 1987 (replaced by BS EN1992-3:2006).
[131] Fagerlund, Göran; Hassanzadeh, Manouchehr, “Self- healing of cracks in concrete long-term exposed to different types of water : results after 1 year exposure”, Lund University, 2010.
[132] Mathias Maes, Didier Snoeck, Nele De Belie, “Chloride penetration in cracked mortar and the influence of autogenous crack healing”, Construction and Building Materials 115 (2016) 114–124, 2016.
[133] Clear, C. A., “The Effect of Autogenous Healing upon Leakage of Water through Cracks in Concrete,” Cement and Concrete Association, Wexham Springs, May 1985.
[134] Ripphausen, B., et al., “Zur Wasserdurchlässigkeit von Stahlbetonbauteilen mit Trennrissen (Water Permeability of Concrete Structures with Separation Cracks,” Beton und Stahlbetonbau, Berlin, 1989. (in German)
[135] Meichsner, H., “Über die Selbstdichtung von Trennrissen in Beton (Autogenous Healing of Cracks in Concrete),” Beton und Stahlbetonbau, Berlin, 1992. (in German)
[136] Guppy, R., “Autogenous Healing of Cracks in Concrete and Its Relevance to Radwaste Repositories,” Safety Studies, Nirex Radioactive Waste Disposal (NSS/R105), Harwell Laboratory, Ukaea, Mar. 1988.
[137] Carola Edvardsen, “Water Permeability and Autogenous Healing of Cracks in Concrete”, ACI Materials Journal, Title No. 96-M56, 1999.
[138] Amir Sidiq, Rebecca Gravina, Filippo Giustozzi, “Is concrete healing really efficient? A review”, Construction and Building Materials 205 (2019) 257–273, 2019.
[139] Kim Van Tittelboom, Elke Gruyaert, Hubert Rahier, Nele De Belie, “Influence of mix composition on the extent of autogenous crack healing by continued hydration or calcium carbonate formation”, Construction and Building Materials 37 (2012) 349–359, 2012.
[140] CIRIA C660 Early Age Thermal Cracking in Concrete
[141] P. Locogne, M. Massat, J.P. Ollivier, C. Richet, “Ion diffusion in microcracked concrete”, Cement and Concrete Research 22 (1992) 431–438, 1992.
[142] A. Konin, R. François, G. Arliguie, “Penetration of chlorides in relation to the microcracking state into reinforced ordinary and high strength concrete”, Materials and Structures 31 (1998) 310–316, 1998.
[143] R. François, G. Arliguie, Effect of microcracking and cracking on the development of corrosion in reinforced concrete members, Magazine of Concrete Research 51 (2) (1999) 143–150.
[144] B. Gérard, D. Breysse, A. Ammouche, O. Houdusse, O. Didry, “Cracking and Permeability of Concrete Under Tension, Materials and Structures 29 (1996) 141–151, 1996.

[145] Will D. Lindquist, David Darwin, JoAnn Browning, and Gerald G. Miller, “Effect of Cracking on Chloride Content in Concrete Bridge Decks, ACI Materials Journal No. 103-M52, 2006.
[146] P.P. Win, M. Watanabe, A. Machida, “Penetration Profile of Chloride Ion in Cracked Reinforced Concrete”, Cement and Concrete Research, 34 (2004) 1073–1079, 2004.
[147] Stefan Jacobsen, Jacques Marchand, and Luc Boisvert, “Effect of Cracking and Healing On Chloride Transport In OPC Concrete”, Cement and Concrete Research, Vol. 26, No. 6, pp. 869-881, 1996
[148] B. Gérard, J. Marchand, Influence of Cracking on The Diffusion Properties of Cement-Based Materials Part I: Influence of Continuous Cracks on The Steady-State Regime, Cement and Concrete Research 30 (2000) 37–43, 2000.
[149] E. Kato, Y. Kato, T. Uomoto, J., “Development of Simulation Model of Chloride Ion Transportation in Cracked Concrete”, Journal of Advanced Concrete Technology Volume 3, No.1, 85-94, 2005.
[150] Seung Yup Jang, Bo Sung Kim, Byung Hwan Oh, “Effect of crack width on chloride diffusion coefficients of concrete by steady-state migration tests”, Cement and Concrete Research 41 (2011) 9–19, 2011.
[151] A. Djerbi, S. Bonnet, A. Khelidj, V. Baroghel-bouny, Influence of traversing crack on chloride diffusion into concrete, Cement and Concrete Research 38 (2008) 877–883, 2008.
[152] M. Ismail, A. Toumi, R. François, R. Gagné, “Effect of crack opening on the local diffusion of chloride in cracked mortar samples, Cement and Concrete Research 38, 1106-1111, 2008.
[153] Sang-Soon Park a, Seung-Jun Kwon b,⇑, Sang Hwa Jung, “Analysis technique for chloride penetration in cracked concrete using equivalent diffusion and permeation”, Construction and Building Materials 29 (2012) 183‑192, 2012.
[154] Tang L., “Electrically Accelerated Methods for Determining Chloride Diffusivity in Concrete-Current Development”, Concrete Research, 48:173–9, 1996.
[155] Hai-Long Wang, Jian-Guo Dai, Xiao-Yan Sun, Xiao-Long Zhang, “Characteristics of concrete cracks and their influence on chloride Penetration”, Construction and Building Materials 107 (2016) 216‑225, 2016.
[156] NT BUILD 492, Concrete, mortar and cement-based repair materials: chloride migration coefficient from non-steady-state migration experiments, 1999.
[157] L. Marsavina, K. Audenaert, G. De Schutter, N. Faur, D. Marsavina, “Experimental and Numerical Determination of the Chloride Penetration in Cracked Concrete”, Construction and Building Materials 23 (2009) 264–274, 2009.
[158] Janina P. Kanjee, “Assessing the Influence of Crack Width on The Durability Potential of Cracked Concrete Using the Durability Index Approach”, University of Cape Town - Department of Civil Engineering Concrete Materials And Structural Integrity Research Unit (CoMSIRU), Thesis, 2015
[159] ASTM C1556 – 11, "Standard Test Method for Determining the Apparent Chloride Diffusion Coefficient of Cementitious Mixtures by Bulk Diffusion"
[160] Zhang Shao-Feng, Lu Chun-Hua, Liu Rong-Guic, “Experimental Determination of Chloride Penetration in Cracked Concrete Beams, Procedia Engineering 24 (2011) 380 – 384, 2011.
[161] Seung Jun Kwon, Ung Jin Na, Sang Soon Park, Sang Hwa Jung, “Service Life Prediction of Concrete Wharves With Early-Aged Crack: Probabilistic Approach for Chloride Diffusion”, Structural Safety 31 (2009) 75-83, 2009.

[162] AASHTO T260, " Standard Method of Test for Sampling and Testing for Chloride Ion in Concrete and Concrete Raw Materials", American Association of State Highway and Transportation Officials", 97 Edition, 2009
[163] Dale P. Bentz, Edward J. Garboczi, Yang Lu Nicos Martys, Aaron R. Sakulich, W. Jason Weiss, "Modeling of the Influence of Transverse Cracking on Chloride Penetration into Concrete", Cement and Concrete Composites, 38, 65-74, 2013
[164] Mills R, and Lobo VMM. Self-Diffusion in Electrolyte Solutions, Elsevier, Amsterdam, 1989, p. 317.
[165] Xiuli Du, Liu Jin, Renbo Zhang, Yue Li, "Effect of cracks on concrete diffusivity: A meso-scale numerical study", Ocean Engineering108(2015)539–551, 2015.
[166] Tetsuya Ishida, Prince O'Neill Iqbal, Ho Thi Lan Anh, Modeling of Chloride Diffusivity Coupled with Non-linear Binding Capacity in Sound and Cracked Concrete", Cement and Concrete Research 39 (2009) 913–923, 2009.
[167] K. Maekawa, R. Chaube, T. Kishi, Modeling of concrete performance, E & FN Spon, NY, 1999.
[168] T. Ishida, K. Maekawa, An integrated computational system for mass/energy generation, transport, and mechanics of materials and structures, Journal of JSCE (August 1999) No.627/V-44.
[169] K. Maekawa, T. Ishida, T. Kishi, Multi-scale modeling of concrete performance— integrated materials and structural mechanics, Journal of Advanced Concrete Technology, JCI 1 (July 2003) 91–126 No. 2.
[170] T. Ishida, S. Miyahara, T. Maruya, Chloride binding capacity of mortars made with various Portland cements and mineral admixtures, Journal of Advanced Concrete Technology 6 (2) (2008) 287–301, 2008.
[171] Branko Šavija, Jose Pacheco, Erik Schlangen, "Lattice Modeling of Chloride Diffusion in Sound and Cracked Concrete", Cement & Concrete Composites 42 (2013) 30‑40, 2013.
[172] M. Otieno, H. Beushausen, M. Alexander, "Chloride-induced corrosion of steel in cracked concrete – Part I: Experimental studies under accelerated and natural marine environments", Cement and Concrete Research 79 (2016) 373–385, 2016.
[173] ASTM 496-17, "Standard Test Method for Splitting Tensile Strength of Cylindrical Concrete Specimens", American Society of Testing and Materials, 2017.
[174] ASTM C39-18, " Standard Test Method for Compressive Strength of Cylindrical Concrete Specimens", American Society for Testing and Materials, 2018.